MOLECULAR AND FUNCTIONAL STUDIES OF PARTHENOGENETIC EMBRYONIC STEM CELLS

Ву

Neli Petrova Ragina

A DISSERTATION

Submitted to
Michigan State University
in partial fulfillment of the requirements
for the degree of

DOCTOR OF PHILOSOPHY

Genetics

2011

ABSTRACT

MOLECULAR AND FUNCTIONAL STUDIES OF PARTHENOGENETIC EMBRYONIC STEM CELLS

By

Neli Ragina

Parthenogenetic Embryonic Stem Cells (P-ESCs) are derived from Parthenogenetically activated embryos (PgEs) at the blastocyst stage. PgEs are created without sperm contribution, followed by inhibition of the second polar body extrusion which renders the PqE genome diploid, consisting of duplication of only the maternal genomic complement. Due to their exclusively maternal genomic complement, PgEs cannot develop to term. However, P-ESCs can be successfully derived. P-ESCs are morphologically indistinguishable from normal fertilized biparental embryonic stem cell (B-ESCs), they are pluripotent, i.e. can be propagated in vitro for prolong period of time while still keeping their embryonic stem cells characteristics, and when differentiated in vivo can give rise to tissues from the three germ layers – ectoderm, endoderm and mesoderm. Despite their broad differentiation plasticity, P-ESCs, exhibit some limitations to contribute to endoderm and mesoderm muscle tissues. This phenomenon has been attributed to deregulation of imprinted genes. Imprinted genes are subset of genes which are differentially expressed from the maternal and paternal alleles. H19 is a paternally imprinted gene whose expression in P-ESCs is highly

upregulated. A great body of literature suggests that *H19* is critical for proper development of PgEs since parthenogenetic offspring has been successfully derived by deleting the *H19* coding region from one of the maternal chromosomes. *H19* has been found to play an important role for P-ESCs differentiation potential as well. Therefore we hypothesized that modulation of *H19* gene expression in P-ESCs by using a small hairpin RNA (shRNA) approach, will enhance the ability of these cells to give rise to endoderm and mesoderm-muscle derivatives in *in vivo* and *in vitro* assays.

Our study focuses on developing a model for stable and efficient downregulation of *H19* in human, primate and mouse P-ESCs. We further follow the differentiation potential of mouse P-ESCs using an *in vivo* teratoma formation assay and an *in vitro* study whereby the P-ESCs are induced to give rise to beating cardiomyocytes.

Our data revealed that P-ESCs with stable *H19* downregulation can be derived from human, primate and mouse P-ESCs. Moreover, we showed for the first time, to our knowledge that suppression of *H19* in P-ESCs resulted in an increased propensity of the cells to give rise to endoderm and mesoderm muscle derivatives *in vivo* as well as to higher incidence of beating embryo bodies in an *in vitro* differentiation assay.

In conclusion, our study provides further knowledge to the biology of P-ESCs and the effect of the imprinted genes, *H19* in particular. Future studies would elucidate the molecular mechanism through which *H19* exerts its effect and the potential applicability of P-ESCs for autologous stem cell therapy.

COPYRIGHT BY NELI PETROVA RAGINA 2011

ACKNOWLEDGMENTS

I would like to acknowledge my mentor Dr. Jose B. Cibelli (Cellular Reprogramming Laboratory, Department of Animal Science, Michigan State University, East Lansing, Michigan, USA) for the privilege to be his graduate student and for all his help and guidelines throughout my study. I would like to thank my committee members; Dr. Vilma Yuzbasiyan-Gurkan (Department of Microbiology and Molecular Genetics, Michigan State University, East Lansing, Michigan, USA), Dr. Laura McCabe (Department of Radiology, Michigan State University, East Lansing, Michigan, USA), Dr. Pamela Swiatek (Division of Biology and Medicine, Brown University, Providence, Rhode Island, USA) and Dr. Pat Venta (Department of Microbiology and Molecular Genetics, Michigan State University, East Lansing, Michigan, USA), who was appointed to my committee as a Genetic program representitative, for their valuable scientific input and support. I would like to thank the Genetic Program, and specifically Dr. Barbara Sears and Jeannine Lee for leading one of the best graduate programs that ensures that each student gets the best of knowledge and research opportunities necessary to build up a successful scientific career. I would like to also acknowledge Karianne Schlosser (Division of Hematology/Oncology, Children's Hospital, Boston, Massachusetts, USA), Dr. Jason G. Knott (Developmental Epigenetics Laboratory, Department of Animal Science, Michigan State University, East Lansing, Michigan, USA), Dr. Arif Kocabas (Yale School of Medicine, Connecticut, USA), Dr. Zeki Beyhan (Sher Institute for Reproductive Medicine, Nevada, USA), Dr. Patricia K. Senagore (Department of Physiology, Michigan State University, East Lansing, Michigan, USA), Dr. Eun Ah

Chang (Cellular Reprogramming Laboratory, Department of Animal Science, Michigan State University, East Lansing, Michigan, USA), Dr. Walid D. Fakhouri (Department of Microbiology and Molecular Genetics, Michigan State University, East Lansing, Michigan, USA), Dr. Brian C. Schutte (Department of Microbiology and Molecular Genetics, Michigan State University, East Lansing, Michigan, USA) and Dr. Matti Kiupel (Department of Pathobiology and Diagnostic Investigation, Michigan State University, East Lansing, Michigan, USA) for being great teachers, mentors and scientific advisors.

I would also like to acknowledge the HistoPathology Laboratory at Michigan State University and especially Amy S. Porter and Kathy A. Joseph for their help with processing my teratoma samples.

I would like to acknowledge Dr. Hasan H. Otu, (Harvard University, MA, USA) for his assistance with predicting mir675 target genes

I would like to acknowledge Dr. Juan Pedro Steibel, Animal Science Department, Michigan State University for his assistance with the statistical data.

I would like to acknowledge all past and present members of the Cellular Reprogramming Laboratory, Michigan State University.

I would also like to acknowledge the "Van Andel Institute", Grand Rapids, MI, for their cooperation.

I appreciate the support from the Michigan State University (MSU) Foundation, MSU's Vice President of Research, and the Michigan Agricultural Experiment Station (MAES), as well as the Naylor Family Foundation.

This study was funded in part by US National Institutes of Health grant DE13513 (B.C.S.).

TABLE OF CONTENTS

LIST OF TABLES	Х
LIST OF FIGURES	xi
KEY TO ABBREVIATIONS	XV
CHAPTER 1: LITERATURE REVIEW	
AbstractIntroduction	
Conclusion	
Figures and Tables	
References	50
CHAPTER 2: MODULATION OF H19 EXPRESSION IN PRIMATE (Cynomolgus macaque) PARTHENOGENETIC EMBRYONIC STEM CELLS (Cyno1 P-ESCs) USING	
H19shRNA	61
Abstract	
Introduction	
Materials and Methods	
Results and Discussion	
Conclusion	
Figures and Tables	
References	97

	APTER 3: H19 CONTROLS THE DIFFERENTENTIAL OF MOUSE P-ESCs UPON DIFFE	
	OOF WIOUSE P-ESCS UPON DIFFE	_
	stract	
Intr	oduction	117
Mat	terials and Methods	119
Res	sults and Discussion	131
Cor	nclusion	140
	ures and Tables	
Sup	oplemental Figures and Tables	175
Ref	ferences	197
	APTER 4: CONCLUSIONS, FUTURE DIRECT	
	sertation Conclusions	
	ure Directions	
Pre	eliminary results (Human P-ESCs)	216
	Aims	
B.	Materials and Methods	
C.	Results and Discussion	222
D.	Figures and Tables	228
E.	References	

LIST OF TABLES

Table 1.1 Diseases and syndromes resulting from abnormal imprinting mechanisms 38
Table 2.1 qRT-PCR Primers Table 95
Table 2.2 Summary of the Cyno1 oocyte donor (Buttercup) derived fibroblast cells at p4, Cyno1p47 and Cyno1p60 P-ESCs (Cell Line Genetics, WI, USA)96
Supplemental Table 3.1 Cytogenetic analysis of B-ESC, P-ESC, and transgenic P-ESC cell ines
Supplemental Table 3.2 Mouse PCR Primer Sequences
Supplemental Table 3.3 Mouse qRT-PCR Primer Sequences194
Supplemental Table 3.4 Bisulfate Sequencing Primers
Supplemental Table 3.5 H19 small hairpin RNA (shRNA) sequence information196
Table 4.1 Human qPCR Primers248

LIST OF FIGURES

Figure 1.1 Construction of diploid embryos with genomes derived from a single sex
Figure 1.2 Stem cell hierarchy42
Figure 1.3 Characterization of parthenogenetic Cyno-1 embryos and derived cell lines
Figure 1.4 <i>In vivo</i> differentiation of Cyno-1 cellsCells were injected i.p. (IntraPeritoneal) in severe combined immunodeficient mice
Figure 1.5 In vitro differentiation of primate Cyno-1 P-ESCs
Figure 1.6 Morphology, AP and Immonustaining of stem cell markers for human Parthenogenetic Embryonic Stem -1 (hPES -1) cell line48
Figure 2.1 Experimental Outline (part of the figure was adopted from "Stem Cells: Scientific Progress http://stemcells.nih)
Figure 2.2 Derivation (A-B) and Immunocytochemical staining (C-E) of Cyno1 P-ESCs; Parthenogenetically activated Cyno1 oocytes
Figure 2.3 qRT-PCR Analysis of the expression levels of HcRed (A) and beta actin (B) and the maternally expressed <i>H19</i> (C) and paternally expressed <i>IGF2</i> (D,E) genes83
Figure 2.4 Teratomas from Cyno1 P-ESCs give rise to derivatives of all three germ layers- ectoderm, endoderm, and mesoderm (A-K)
Figure 2. 5 Downregulation of <i>H19</i> in Cyno1 P-ESCs. Cyno1 P-ESC colony stably transfected with <i>H19</i> shRNA expressing vector, 14days post Neomycin88

Figure 2.6 qRT-PCR Analysis of the expression levels of the maternally expressed <i>H19</i> and <i>P57</i> (Figure 5A and E respectively) and paternally expressed <i>IGF2</i> , <i>NDN</i> , <i>PEG10</i> and <i>SNRPN</i> (Figure 5B, C, D and F respectively) genes89
Figure 3.1 Alterations in H19/lgf2 expression and DMR methylation in P-ESCs147
Figure 3.2 Elevated levels of <i>H19</i> expression persist during P-ESCs differentiation <i>in vivo</i>
Figure 3.3 Lack of mesoderm muscle derivatives and downregulation of mesoderm specific transcripts in P-ESCs upon differentiation <i>in vivo</i>
Figure 3.4 Stable and efficient down-regulation of <i>H19</i> mRNA levels in mouse P-ESCs161
Figure 3.5 Downregulation of <i>H19</i> expression in P-ESCs promotes normal endoderm and mesoderm differentiation <i>in vivo</i>
Figure 3.6 Derivation of beating embryo bodies (EBs) from B-ESCs, Control P-ESCs, and Control vector (Con.vector) and <i>H19</i> shRNA P-ESCs
Supplemental Figure 3.1 Mouse Rosa 26 P-ESCs are morphologically indistinguishable from mouse Rosa 26 biparental ES (B-ESCs) cells (A and B) and stain positive for β -galactosidase expression (C and D)
Supplemental Figure 3.2 Mouse Rosa 26 P-ESCs and Rosa 26 B-ESCs express Oct4 and SSEA1 in mouse as shown by immunocytochemical analysis
Supplemental Figure 3.3 Hematoxylin-Eosin (H&E) staining of mouse B-ESCs and P-ESCs (P-ESCs 1 and P-ESCs 2) derived teratomas indicating the ability of these cells to give rise to all three germ layers when differentiated <i>in vivo</i>
Supplemental Figure 3.4 Immunohistochemical staining of teratoma sections derived from mouse Rosa 26 B-ESC and P-ESC lines confirming the identity of the germ layer derivatives.

Supplemental Figure 3.5 Laser Capture Microdisection (LCM)179
Supplemental Figure 3.6 Delta Np63 and TAp63 expression is indicative of germ layer commitment
Supplemental Figure 3.7 Immunohistochemical staining for delta Np63 of mouse B-ESCs derived teratomas using conjugated Alkaline Phosphates secondary antibody (red color) (A-C)
Supplemental Figure 3.8 Down-regulation of <i>H19</i> expression in Mouse Embryonic Fibroblasts (MEFs) infected with two different <i>H19</i> shRNA oligos (<i>H19</i> shRNA#1 and <i>H19</i> shRNA#2) by qRT-PCR
Supplemental Figure 3.9 Down-regulation of <i>H19</i> expression in mouse P-ESCs infected with two different H19 shRNA expressing pLenti-DEST/Hygro -EGFP shRNA expressing lentiviral and pMSCV-Hygro-EGFP shRNA expressing retroviral vectors
Supplemental Figure 3.10 Schematic representation of the mir675 region that is a perfect 11bp match to the TP63 Trans Activating (TA) domain and therefore may affect the transcription or regulate the translation of TP63 mRNA
Supplemental Figure 3.11 EGFP fluorescence (B) and bright field (A) of mouse PGES cells infected with pMSCV-Hygro-EGFP - <i>H19</i> shRNA retroviral vector190
Figure 4.1 Immunocytohemistry for the pluripotency markers NANOG (NAN), LIN28, SSEA4, SOX2, and OCT4 in human ES cells H1 and in human P-ESCS (LLC-6P)
Figure 4.2 Hematoxylin-Eosin (H&E) staining of human HES H1 derived teratomas indicating the ability of these cells to give rise to all three germ layers when differentiated <i>in vivo</i>
Figure 4.3 Hematoxylin-Eosin (H&E) staining of human LLC-6p cells derived teratomas indicating the ability of these cells to give rise to all three germ layers when differentiated <i>in vivo</i>

Figure 4.4 Quantification (%) of germ layer derivatives: ectoderm, endoderm and mesoderm in teratomas derived from wild type HES, H1 cells and in human P-ESCs (LLC-6p)
Figure 4.5 Fluorescent Activated Cell Sorting analysis (FACS) on the apoptotic rate of HES H1 and human LLC-6p cells measured by Annexin V expression
Figure 4.6 Quantification of mRNA abundance of the maternally expressed <i>H19</i> and <i>UBE3A</i> and the paternally expressed <i>IGF2</i> , <i>DIO3</i> and <i>NDN</i> in HES H1 and LLC-6p cells by qRT-PCR
Figure 4.7 Quantification of mRNA abundance of the maternally expressed <i>H19</i> (A, B), <i>UBE3A</i> (K, L) and the paternally expressed <i>IGF2</i> (C, D), <i>DIO3</i> (M, N), DNA Methyltransferase1 (<i>DNMT1</i>) (E, F), DNA Methyltransferase3A (<i>DNMT3A</i>) (G, H) and DNA Methyltransferase3B (<i>DNMT3B</i>) (I, J) in HES H1 and LLC-6p cells from different passages by qRT-PCR
Figure 4.8 Schematic representation of H19shRNA and H19asRNA expressing plasmid (A) and Retroviral (B-E) vector constructs
Figure 4.9 H19shRNA delivery in Hela cells
Figure 4.10 PCR-Agarose Gel Electrophoresis247

KEY TO ABBREVIATIONS

- Parthenogenetic Embryonic Stem Cells (P-ESCs)
- Androgenetic Embryonic Stem Cells (A-ESCs)
- Parthenogenetic Embryo (PgE)
- Androgenetic Embryo (AgE)
- Biparental Embryonic Stem Cells (B-ESCs)
- Inner Cell Mass (ICM)
- Maturation Promoting Factor (MPF)
- Cytostatic Factor (CSF)
- Days post fertilization (DPF)
- Days post activation (DPA)
- Wild type (wt)
- Fertilized embryos (FEs)
- Passage (p)
- Metaphase II (MII)
- Dimethylaminopurine (DMAP)
- IntraPeritoneal (i.p)
- Macaca fasciculatis /Cynomolgus macaque derived PGESCs(Cyno1 P-ESCs)
- Macaca fasciculatis /Cynomolgus macaque derived B-ESCs (CMK6)
- Cyno1 transfected with the H19shRNA expressing plasmid vector (Cyno1 H19shRNA cells)

- Cyno1 cells transfected with the empty control plasmid vector (Cyno1 Con.vector cells)
- Human Embryonic Stem Cells (HES cells)
- small hairpin RNA (shRNA)
- injection- human Chorionic Gonadotrophin (hCG)
- Mouse Embryonic Fibroblast (MEF)
- Messenger RNA (mRNA)
- Total RNA (tRNA)
- Laser Capture Microdissection (LCM)
- P-ESCs infected with H19shRNA expressing retroviral vector (H19shRNA cells)
- P-ESCs infected with the control viral vector (Con.vector cells)
- College of American Pathologists (CAP)
- Low Power Fields (LPFs)
- quantitative Real Time PCR (qRT-PCR)
- Differentially Methylated Region (DMR)
- Nuclear Transfer (NT)
- Wild Type B-ESCs (WT cells)
- Major Histocompatibility Complex antigens (MHC antigens)
- Embryoid Bodies (EB)
- micro RNA 675 (mir675)
- long non coding RNAs (ncRNA)
- Embryonic Stem Cells (ESCs)
- Human Parthenogenetic Embryonic Stem Cells (LLC 6p)

• Antisense RNA (asRNA)

DISSERTATION CHAPTER 1

TITLE LITERATURE REVIEW

ABSTRACT

Parthenogenesis is a naturally occurring process where the oocyte starts embryonic development without sperm contribution. In mammals, parthenogenetic embryos (PgE) cannot develop to term. The most commonly used method of artificially making diploid PgEs is via chemical activation of the egg and by preventing extrusion of the second polar body which renders the embryo genome diploid, having only maternal genetic material. Parthenogenetic Embryonic Stem cells (P-ESCs) are derived from the Inner Cell Mass (ICM) of parthenogenetic (PgE) embryo at the blastocyst stage. They are pluripotent i.e. they can differentiate into all three germ layers ecto-, meso- and endoderm and can be propagated as stem cells in culture for prolonged periods of time. However, P-ESCs have lower differentiation capacity in vivo (in chimeras and teratoma formation) and in vitro (embryo body formation); contributing poorly to muscle tissues and endoderm derivatives. P-ESCs have been derived from mouse, rabbit, monkey and human embryos. P-ESCs offer an easily obtainable pool of stem cells that can be used as a source of autologous tissues albeit limited to females in reproductive age. P-ESCs derivation does not require destruction of a viable embryo and therefore bypasses the ethical debates surrounding the use of naturally fertilized embryos.

INTRODUCTION

Parthenogenesis is the process by which the oocyte starts embryonic development without paternal contribution i.e the resulting PgE consists of only maternal genome complement. It is a natural way of reproduction in some lower organisms.

The opposite process is called Androgenesis, i.e. embryos having only paternal genome (AgE). In mammals, Parthenogenetic (PgE) and Androgenetic (AgE) embryos are not compatible with life and fail to thrive during the post-implantation stages [1].

Parthenogenetic fetuses exhibit severe growth and differentiation defects, failure to establish proper placental growth and die early in gestation. One of the major reasons for this phenomenon has been attributed to deregulation of imprinted genes [2],[3] (Figure 1.1).

Morphologically PgEs develop into normal embryo but fail to establish a functional placenta able to support embryo growth. In contrast AgEs extensively develop the extra embryonic membranes but lack proper formation of the embryo. These two phenomena reveal that genetic material derived from the opposite sexes exhibit differential effects on the offspring development and growth. In humans a subset of gestational trophoblastic diseases, found in women have been attributed to spontaneous parthenogenetic or androgenetic activation of the oocyte. For example it has been found that complete moles are androgenetic by origin. The tumor mass of such a mole represents a mixture of extra-embryonic membranes-like structures and the cytogenetic analysis confirmed that the cells in these lesions have only the paternal genomic

complement. In contrast to the complete moles, a specific subclass of benign ovarian teratomas, have been found to consist of parts of an embryo- hair, teeth, cartilage etc. Data showed that the genetic material of these teratomas is exclusively of maternal origin. How the complete moles and ovarian teratomas arise has been extensively studied. It has been suggested that activation of an enucleated oocyte by sperm entry may trigger the formation of these types of moles. Ovarian teratomas, on the other hand, may arise from activation of the oocyte by an enucleated sperm or by other environmental or age related stimuli. Regardless of the mechanism involved in the development of these two types of gestational trophoblastic diseases, these pathologies once again demonstrate the influence that the two parental genomes exert on embryo development and differentiation – the paternal genome driving placentation and the maternal genome-supporting the formation of the embryo proper [4].

Although parthenogenetic embryos are not viable, in mouse, P-ESCs derived from the ICM of parthenogenetically activated oocytes were able to give rise to viable animals, called chimeric animals, when inserted into a fertilized mouse blastocyst. The tissues and organs of such chimeric animals consist of mixture of cells derived from the injected P-ESCs and the cells of the host embryo. In primates, parthenogenetic stem cells (P-ESCs) have been derived *from Macaca Fascicularis* (called Cyno1 P-ESCs) and from *Rhesus* Monkey. However, their contribution to a chimeric embryo in non-human primates has not been tested due to ethical concerns.

In humans, parthenogenetic ES cells have also been successfully derived *in vitro* from human parthenogenetic blastocysts *[5]*, *[6-8]*. Moreover, a child whose peripheral blood leukocytes were entirely parthenogenetic by origin has been reported *[9]*. This

phenomenon indicates that although parthenogenetic development *in utero* is aborted and rarely detected, a chimeric individual can develop from a single zygote *[9-10]*.

PgEs can be artificially derived by chemical activation of the oocyte using different compounds which allow the oocyte to exit from Metaphase II (MII) arrest. The role of these compounds is to activate the oocyte by inactivating the activity of the maturation promoting factor (MPF) and cytostatic factor (CSF) directly or indirectly, by reducing protein synthesis and/or protein phosphorylation [11]. Depending on the protocol used, the extrusion of the second polar body can be prevented, rendering the embryonic genome diploid [12]. Since the parthenogenetic embryos are created without sperm contribution they only contain a duplication of the maternal genome. This is possible by preventing the extrusion of the second polar body using nontoxic microfilament inhibitors such as cytochalasin B and *Dimethylaminopurine* (DMAP) [13].

Parthenogenetic Embryonic Stem Cells (P-ESCs) are prone to chromosomal aberrations such as loss of one of the X-chromosomes which renders the cells aneuploid. This phenomenon is mostly due to the presence of two active XX chromosomes which is associated with global reduction of DNA methylation. In the P-ESCs as well as in normal fertilized female Biparental Embryonic Stem Cells (B-ESCs) there is a selective mechanism against loss of methylation which may provide the tendency of X-chromosome instability [14].

PARTHENOGENETIC EMBRYONIC STEM CELLS IN HUMAN AND NON-HUMAN PRIMATES

Non-human primates are the closest species to *Homo sapiens* in the tree of evolution

Derivation of human and primate PgEs and P-ESCs cells

and therefore are excellent model for studying human development and diseases. P-ESCs from non-human primate and human parthenogenetically activated oocytes have recently been derived [6-8]. These cells offer a valuable tool for studying the developmental, differentiation and functional potential of the P-ESCs in the context of their clinical application in organ and tissue transplantation in humans. Primate P-ESCs have been derived for the first time by Cibelli et al in 2002 from Macaca fascicularis PG embryos and are called Cyno-1 P-ESCs [15] (Figure 1.3). The protocol for derivation of primate PG embryos calls for the use of ionomycin for parthenogenetic activation of the oocyte followed by DMAP which prevents the extrusion of the second polar body. Primate P-ESCs are derived from the ICM of PG embryos at blastocyst stage. These cells exhibit normal ESC morphology i.e. small cytoplasmic/nuclear ratio, numerous nucleoli and cytoplasmic lipid bodies. They stain positive for markers for primate ESCs and express pluripotency markers such as OCT4. They exhibit high telomerase activity and are karyotypically normal (42XX) [16]. The capacity of the Cyno-1 P-ESCs to differentiate was tested in vivo by teratoma formation. Teratoma derived from Cyno-1 P-ESCs demonstrated these cells can give rise to cell derivatives from all three germ layers meso-, ecto- and endoderm. These include

cartilage, muscle and bone (mesoderm), neurons, melanocytes and hair follicles (ectoderm), and intestinal and respiratory epithelial (endoderm) with a preference towards ecto- and endoderm derivatives [15]. Teratomas derived from Cyno-1 P-ESCs consisted of mature differentiated tissues with a little contribution of mitotically dividing cells which indicates their benign origin (Figure 1.4). Cyno-1 P-ESCs were successfully differentiated in vitro into neurons and were capable of producing neural specific mediators such as dopamine and serotonin. Further characterization of Cyno-1 cells derived neurons demonstrate that these cells express tyrosine hydroxylase and are electrophysiologically active [16-17]. When dopamine neurons derived from Cyno-1 cells were transplanted *in vivo* in rodents and in primate models of Parkinson disease, they were able to maintain stable phenotype, express dopaminergic markers and show long term survival [17-18] (Figure 1.5).

Primate Parthenogenetic Stem cells have been also derived from *Rhesus Monkey* using the similar protocols. Briefly, these are protocols using electroporation as a method for oocyte activation and Cytochalasin B or Roscovitine for prevention of the second polar body extrusion *[11, 19]*. Similar to Cyno-1 cells, when injected into immuno-compromised mice, Rhesus P-ESCs were able to form teratomas also consisting of cell derivatives of all tree germ layers. The Rhesus monkey P-ESCs were morphologically similar to normal biparental stem cells derived from the same species. They expressed the key-pluripotency markers such as OCT4, SSEA-3 and -4, TRA-1-60, NANOG, SOX-2, TDGF, LEFTYA and TERT and were karyotypically normal *[19]*.

Genetic homozygosity is potentially one of the obstacles to potential implication of the P-ESCs for cell replacement therapy due to the possibility of immune rejection. However, Dighe et al. have demonstrated that diploid Rhesus Monkey P-ESCs restored heterozygosity at 64% of the examined loci on average in the five P-ESC cell lines analyzed by using a microsatellite analysis, also called Short Tandem Repeat analysis (STR) [19]. Moreover, the Rhesus Monkey P-ESCs demonstrated re-establishment of heterozygosity within 15 analyzed microsatellite markers of the Major Histocompatability Region (MHC) in three of the five Rhesus Monkey P-ESCs tested. This rendered the genotype of the MHC region of these three cell lines identical to the egg donors. The ability to generate isogenic MHC Rhesus Monkey P-ESCs suggests the potential application of these cells as a source of a patient's own MHC-matched cells for therapeutic cell replacement therapy. Dighe et al. have also genotyped one Cyno-1 P-ESC cell line for the 15 microsatellite markers of the MHC region. This Cyno-1 P-ESC cell line was homozygous for the MHC region STR markers [19]. Human parthenogenetic embryonic stem cells have been derived only recently in 2007

by International Stem Cell Corporation (ISCC) [6, 8]. The induction of PG development of human oocytes calls for 5 μ M Calcium Ionophore-A23187 (Sigma, St. Louis, MO) for 5 min followed by 10 μ g/mL puromycin (Sigma) or 1mM 6-DMAP (Sigma, St. Louis, MO) for 4 hours [6]. The human P-ESCs are then derived by mechanical slicing of the ICM and plating onto fresh feeder layers. The human P-ESCs stained positive for the major pluripotency markers such as SSEA-3, SSEA-4, TRA1-60, TRA1-81, and OCT4 similar to non-human primate P-ESCs and also exhibit similar morphology characterized by tightly packed colony with prominent nucleoli, and a small cytoplasm to nucleus ratio

(Figure 1.6). Upon induction of differentiation in vitro, the human P-ESCs give rise to derivatives of all three germ layers – ecto-, endo- and mesoderm [6]. DNA profiling of the human P-ESCs revealed that these cells can also give rise to MHC matched P-ESCs, isogenic to the oocyte donor [6]. Recently a derivation of new lines of human P-ESCs have been reported [20].

Despite the ability to produce karyotypically normal and donor-matched at the MHC loci, in human and non human P-ESCs, a major obstacle to a potential successful application of parthenogenetic stem cells in clinical trials is the deregulation of imprinted genes, which may render these cells prone to tumorogenesis and other abnormalities upon engraftment/transplantation.

Imprinting in Human and Primate Parthenogenetic Stem Cells

The phenomenon of imprinting refers to the differential expression of the maternally or paternally inherited alleles of specific genes (named imprinted genes) [21]. Thus a paternally imprinted gene is silenced when inherited from the paternal chromosome and expressed when inherited from the maternal chromosome and vice versa. The expression pattern changes do not occur as a result of changes of the underlying DNA sequence but as a result of different epigenetic modifications such as DNA methylation, histone modification, spreading of non-coding RNA molecules, small interfering RNAs, and other yet unidentified, factors [22]. The imprinting pattern of the genes is initially erased and then re-established during germ cell development in a parent-specific manner and is later maintained in all tissues and organs. The expression of the imprinted genes in most cases is under the control of an imprinting control region (ICR),

known also as the differentially methylated region (DMR), which is differentially methylated at Cytosin-5 in CpG dinucleotide repeats. Imprinted genes are usually found in clusters. In most cases, the differential methylation of the ICR can regulate the expression of an imprinted gene cluster both positively and negatively [23]. In humans, loss of imprinting of certain genes such as IGF2, H19, SNURF/SNRPN (small nuclear ribonucleoprotein polypeptide N/ SNRPN upstream reading frame), NDN (Necdin homolog) and others, can lead to the development of several congenital disorders and cancer (Table1.1). Parthenogenetic embryos and embryonic stem cells exhibit deregulation of imprinted genes due to their uni-parental origin, i.e. they lack the paternal set of the imprinted genes [24-26]. Loss of imprinting is one of the major causes for developmental failure in parthenogenetic embryos and for the limited differentiation potential of the parthenogenetic stem cell [3], [24-28]. Additional changes in imprinting can arise in the process of derivation of parthenogenetic embryos due to reasons that are yet to be determined. Loss of imprinting of the parthenogenetic stem cells can occur during culturing or manipulation of these cells in vitro. This holds true and is extensively investigated in primate P-ESCs and in normal primate biparental embryonic stem cells which are generated from a normally fertilized embryos [29]. The expression pattern and methylation status of two of the most extensively studied gene clusters —one on chromosome 11p15 and the other on chromosome 15p11 in primates and humans have been extensively investigated [29]. Chromosome 11p15.5 harbors *IGF2* and *H19* imprinted genes which expression is regulated by a common ICR, also called DMR that lies between the two genes. In the maternal allele the DMR is not methylated which allows an insulator protein to bind and prevent action of an enhancer

downstream of *H19* to stimulate *IGF2* expression and thus *H19* is expressed and *IGF2* is silenced. On the paternal allele DMR is methylated on the CpG dinucleotides, and the enhancer stimulates *IGF2* expression while *H19* is silenced.

The region on chromosomes 15q11-q13 is characterized with a set of oppositely imprinted genes the most studied of which are *SNURF/SNRPN*, UBE3A (Ubiquitin protein ligase E3A) and *NDN*. *NDN* is paternally expressed gene i.e. maternally imprinted. *SNURF/SNURPN* region is controlled by an imprinted center located at the 5' end of the SURF/SNURPN gene [30]. The *SNURF/SNURPN* gene is expressed from the paternal allele. *UBE3A* is maternally expressed gene i.e paternally imprinted in the opposite direction of *SNURF/SNURPN* gene and its imprinted expression is restricted to certain tissues [30].

Loss of Imprinting of *IGF2* and *H19* and other imprinted genes has been associated with multiple congenital disorders in humans such as Beckwith-Wiedemann syndrome [31] (*IGF2* and *H19*), Prader-Willi and Angelman syndromes [32] (*SNURF/SNRPN,UBE3Aand NDN*) and many others [33]. In parthenogenetic (PgEs) embryos and P-ESCs there is a severe deregulation of the imprinted genes with *H19* being expressed bi-allelically and therefore upregulated while *IGF2* is barely detectable [3, 34]. *H19* is a paternally imprinted gene (i.e. expressed form the maternal allele) and *IGF2* is maternally imprinted (i.e. expressed from the paternal allele) gene. The *H19* gene codes for an untranslated mRNA molecule. During embryogenesis *H19* mRNA transcription is activated in tissue specific manner at certain developmental periods such as in the extra-embryonic cell types at the time of implantation. Later in development, during mid-gestation, *H19* expression is observed in certain tissues and

cells most of which are derived from the endoderm and mesoderm germ layer such as the developing liver, gut, muscle, and kidney. In adult tissues, *H19* expression becomes predominantly restricted to the skeletal muscles, thymus, heart and lungs *[35]*.

Recently, *H19* has been implicated to be a part of the "Imprinted Genes Network (ING)" where any change of the expression levels of an imprinted gene in the network leads to changes in the expression levels of the connected genes [36-38]. It has been reported that *H19* can function as a long antisense RNA and as a micro RNA (miRNA) [39-40]. The miRNA originates from exon1 of the *H19* mRNA precursor and is referred to as mir675 [41-43].

The *IGF2* (insulin-like growth factor 2) gene encodes a member of the insulin family of polypeptide growth factors that is involved in development and growth. *IGF2* promotes differentiation and migration, inhibits apoptosis and is essential for proper embryo and placental growth *[44]*. *IGF2* is expressed by the embryo during early pregnancy and later becomes localized to the cytoplasm of the trophoblast cells, the cells that are going to contribute to the formation of the placenta and other extra-embryonic organs *[45]*. *IGF2* is also a potent mitogenic factor. *IGF2* is not only over expressed in a number of human neoplasms *[46]*, *[47]*, *[48]* but also, leads to malignant transformations, tumor development and hyperplasia when over expressed in mouse models *[49-51]*.

Due to deregulation of imprinted genes and *IGF2* and *H19* in particular, PG embryos are defective in ICM population maintenance and differentiation and in generation of multinucleated trophoblastic cells (syncitiotrophoblasts) leading to defective placentation and embryonic lethality *[25, 52]*.

It has been reported that biparental Rhesus monkey embryonic stem cells exhibit loss of imprinting of H19 and IGF2 due to aberrant methylation of the DMR region [53]. Mitalipov et al. took advantage of the availability of single nucleotide polymorphisms (SNPs) in the monkey to study the parental-specific methylation pattern of the H19/IGF2 and SNURF/SNRPN imprinted genes in biparental Rhesus monkey ESCs [53]. They performed methylation analysis on 17 Rhesus Monkey ESC lines for the methylation status of the DMR region by bisulfate sequencing and Southern blot using SNPs genotyping for defining the parent-of origin region. Mitalipov et al. found severe deregulation of the methylation of the DMR region which leads to bi-allelic expression of IGF2 and H19 [53]. The methylation status and imprinting expression of SNURF/SNRPN Imprinting Center (IC) was not affected. These results suggest that the imprinting status of genes is influenced and can be changed during in vitro culturing and that different genes have different degree of susceptibility to the epigenetic changes induced in culture. This is specifically critical and of great concern for the application and use of primate parthenogenetic - and all parthenogenetic stem cells in general - in clinics since, as stated, these cells lack the paternal imprints and additional imprinting defects can accumulate during cell culture. In a later report, the same group analyzed the imprinted pattern of Rhesus Monkey P-ESCS cell lines [19]. Expression levels of maternally expressed genes such as UBE3A and H19 and paternally expressed genes such as IGF2, PEG10, DIRAS3, SGCE, PEG3, MEST, ZIM2, PLAGL1, MAGEL2, MKRN3 and SNRPN were analyzed by reverse transcription-polymerase chain reaction (RT-PCR) and by Real Time PCR analyses. A significant expression of paternally expressed genes IGF2, SGCE and DIRAS3 were

detected in *Rhesus* monkey P-ESCS cells which normally are expected to be silenced. Moreover transcription from some of the other paternally expressed genes i.e. maternally imprinted was detected. To confirm the gene expression data, the methylation status of the H19/IGF2 and SNURF/SNURPN Imprinted Control (IC) regions was evaluated using a methylation-sensitive Southern Blot and Bisulfate Sequencing Analysis [19]. The methylation profiling of these two well defined imprinted centers demonstrated sporadic hypermethylation of the H19/IGF2 IC region which normally is expected to be hypomethylated on both maternal alleles and can explain the significant upregulation of IGF2 gene expression in Rhesus Monkey P-ESCS cells reported in this study. The methylation status of SNURF/SNURPN IC region was, as expected; both maternal alleles were completely methylated [19]. This data reinforces the notion that that multiple factors such as stem cell derivation, culture conditions and manipulation, combined with the intrinsic genetic instability that P-ESCS cells possess, may cause changes in the methylation status and inappropriate expression of imprinted genes.

The expression pattern of several of the imprinted genes such as *H19*, *IGF2*, *SNRPN*, *NDN*, *PEG10* and *P57* was analyzed in Cyno-1 cells as well by the means of Quantitative Real Time Polymerase Chain Reaction (qRT-PCR) on cDNA derived from total RNA (*Cibelli*, *unpublished*). As in *Rhesus* Monkey P-ESCS cells, *H19* mRNA expression levels were significantly higher in the Cyno-1 P-ESCS cells when compared to that of normal biparental *Macaca Fascicularis* embryonic stem cells. The expression of the paternally expressed gene *PEG10* was low but detectable while the expression of another set of paternally expressed genes –*SNRPN* and *NDN* was

undetectable, as expected according to their parent-of origin imprinting status. P57 is maternally expressed gene i.e. paternally imprinted and therefore high levels of P57 mRNA expression in Cyno-1 P-ESCS cells were detected compared to a normal biparental cell line (Cibelli, unpublished). Significant upregulation of IGF2 gene expression, normally imprinted on the maternal allele, was detected in Cyno-1 P-ESCS cells, similar to that observed in *Rhesus* monkey P-ESCS cells. An interesting observation was that upon downregulation of H19 in Cyno-1 P-ESCS cells by using a short hairpin RNA (shRNA), the mRNA levels of *IGF2* dropped significantly as well. The same phenomenon was observed upon downregulation of H19 in mouse P-ESCS cells. The causes of this unexpected observation are yet to be investigated. The expression patterns of H19, TSSC5, PEG1 and SNURPN have been analyzed in human P-ESCS cells [6]. The expression of PEG1 and SNRPN, two paternally expressed genes, was lower but detectable in human P-ESCS cells compared to the expression levels in normal biparental human embryonic stem cells. This data indicates that human P-ESCS cells also exhibit deregulation of some of the imprinted genes analyzed, similar to that observed in non-human primate P-ESCS cell. Another set of imprinted genes suggested of being important for development of parthenogenetically derived (PG) embryos and for proper differentiation of P-ESCS cells are the oppositely imprinted genes *DLK-DIO3* located on chromosome 14 in human and non-human primates. It was recently reported that parthenogenetic mice can develop to term when the H19 differentially methylated region (DMR) and Dlk1-*Dio3* intergenic germline -derived DMR region are deleted *[54]*.

Thus P-ESCS and ESCs derived from normally fertilized embryos exhibit aberrant expression of imprinted genes when cultured *in vitro*. This phenomenon raises a concerns and put into question the use of these cells in therapy since the majority of the imprinted genes control cell growth, division and proliferation and may be part of the development of tumors or disease phenotypes *[46],[47],[48], [49-51]*.

Nevertheless, In mouse models when P-ESCs were induced to differentiate or after manipulation of the ICR regions of key imprinted genes such as *H19, IGF2, DLK-DIO3*, these cells were able, by yet unknown mechanism, to give rise to terminally differentiated tissues or to viable animals capable of producing offspring (See below) *[27-28, 54-55]*.

Despite being important for the embryo development and differentiation, the role of *H19* and *Igf2* has been strongly implicated in the ethiology of tumor development. As mentioned above, *IGF2* is viewed as a potent mitogen and tumor promoter gene. The role of *H19* in malignant transformation has been controversial. It has been long believed that *H19* is a tumor suppressor and have negative effect on tumor growth [46, 50-51, 56-57]. The tumor suppressor role of *H19* comes mostly from mouse studies (see next chapter) and from clinical studies in patients with Beckwith-Wiedemann syndrome which is characterized by bi-allelic expression of *IGF2* and silencing of *H19* expression from the maternal allele. In these patients there is a high incidence of development of Willms tumors. These tumors have been also found to result from a mutation in the Wilms tumor gene 1 (WT1), another imprinted gene located in the same chromosome 11 where *H19* and *IGF2* genes reside. However, in a 1995 paper published by Dugimon *et al.* and in recent studies, it was reported that *H19* and/or its

product *mir675*, are over expressed in different types of cancers and they have been put forward as useful prognostic markers for tumor progression and metastasis [58-64]. In this context, a direct interaction between mir675, *Rb* and *C-Myc* in tumor development, growth and metastasis has been reported [59, 65].

Primate and Human Parthenogenetic Stem Cells – Future Applications and Concerns;

The rate of the organ transplantations performed in the United States is increasing [66]. In 2009 a record total of 28,465 organ transplant operations have been performed compared to 27,965 in year 2008 (New York Organ Donor Network). Despite the increasing number of organ transplantations, the pool of patients waiting for organ donations exceeds the supply [67]. There is a lack of awareness in the American population to the need to donate organs that must be addressed if this gap between supply and demand wants to be closed.

Even when the donors are available, a major issue in organ and tissue transplantation continues to be tissue matching. Engraftment of solid organs, tissues, and cells from unrelated donors carries a high risk of rejection due to lack of compatibility between the major histocompatible- complex (MHC) alleles of the recipient and donor. This obstacle can be surpassed by deriving tissues and organs from a cell pool that contains the patient's own genome. P-ESCS cells can be an alternative source of matched cells for women in reproductive age.

In the context of tissue transplantation, primate and human P-ESCS cells have not been extensively studied yet. More experiments are needed to determine the extent to which these cells can differentiate. Ideally chimeric primate and human P-ESCS embryos could be generated by injecting P-ESCS cells into a blastocyst of a fertilized embryo or more stringent yet, by aggregation of P-ESCS cells with tetraploid embryo (tetraploid complementation experiment) [68-69]. Due to their close relationship to human, non-human primate P-ESCS offer a valuable tool not only as a model to study human disease and epigenetic, but also as a model to study their potential to serve as a future source for cell replacement therapy.

There are two questions still to be answered regarding the plasticity of P-ESCS cells. If parthenogenesis does not lead to full-term development, due to failure to produce all organs and tissues of the embryo and the extra-embryonic membranes, how is it possible that ES cells derived from a parthenogenetic blastocyst can give rise to all embryonic germ layers? Recent data shows that one of the leading factors is epigenetic changes in the stem cell genome that occur during *in vitro* culture conditions [70]. Some of these culture–induced epigenetic changes may affect a sub-population of the P-ESCS cells and confer them with growth and/or differentiation advantages that are preferentially selected for in culture. Therefore, it is of great importance that terminal differentiation of these cells can be achieved before transplanting P-ESCS cells derivatives in order to ensure that no pluripotent, epigenetically abnormal P-ESCS cells exist in the graft that may lead to tumors and/or may have yet unknown consequences for the recipient.

Current efforts focus on optimizing the non-human primate and human P-ESCS growth conditions as to minimize the presence of animal proteins and other

contaminants in the growth media that have the potential to induce a severe immune response upon transplantation.

The use of feeder–free system for manipulation and propagation of the non-human primates and human P-ESCS cells will prevent contamination of the P-ESCS cells intended for clinical application with feeder layer cells or their metabolite products. This is another way to ensure the P-ESCS cell purity and thus ameliorate the risk of rejection upon engraftment into the recipient.

MOUSE PARTHENOGENETIC EMBRYONIC STEM CELLS

Derivation of mouse P-ESCS cells

The first mouse P-ESCS line was described by Kaufman and Robertson in 1983.

Initially, ethanol was used for parthenogenetic activation of the oocyte. This approach however led to derivation of haploid P-ESCs due to extrusion of the second polar body [11]. Currently the most efficient method for derivation of P-ESCs is a combination of strontium to activate the egg followed by treatment with cytochalasin B to prevent the extrusion of the second polar body. P-ESCS cells are later isolated from the ICM of the P-ESCs at blastocyst stage, and plated on mitotically inactivated feeder cells. Mouse P-ESCS cells and mouse P-ESCs represent a unique model for studying imprinting, embryo development and differentiation.

Mouse Parthenogenetic Embryo Development

The influence of the paternal genomes on the formation of the embryo studied using mouse P-ESCS cells and mouse P-ESCs. It was found that mouse P-ESCs cannot survive pass 10.5 days post activation (DPA). Surprisingly, Kono and colleagues succeeded, through series of modifications of the PgE genome, in generating a viable parthenogenetic offspring.

These modifications were done in the *H19/IGF2* DMR regions, and later combined with modifications of *Dlk1/Gtl2* imprinted region. That the imprinted genes are crucial for PgE development became clear after Kono's group observed an increase in the PgE survival after combining two maternal genomes, one coming from fully grown(fg) oocyte, where the maternal imprint was already established, with a genome from nongrowing (ng) oocyte, where the imprinting pattern was still not set up. These P-ESCs containing two maternal genomes one from fg and one from ng occyte, were able to develop until 13.5DPA. The development of PgE to term was allowed after 13kb deletion of the H19 coding region and the upstream differentially methylated region (DMR) which controls the coordinate expression of H19 and Igf2 by controlling the access of these two genes to a downstream enhancer element. Live-born offspring were obtained after the 13kb H19 and DMR deletion was combined with a deletion of Dlk1/Gt/2 imprinted control region. These results clearly demonstrated that the presence of the paternal genome complement is indispensable for proper embryo development in mammals and the mechanism by which the paternal genome influences the embryo development lies at the bases of the imprinted genes function, H19/Igf2 and Dlk1/Gt/2 genes in particular. Due to the use of mouse P-ESCs we know that the paternally expressed genes are critical for the proper embryo growth and

development of the extra-embryonic membranes, placenta in particular and muscle development. On the other hand the maternally expressed genes control for the proper development of the embryo proper. That the paternal genome is required for proper development of the extra-embryonic membranes is revealed by the inability of the P-ESCs to form functional placenta. It has been found [52] that P-ESCs exhibit a primary trophoblast formation which cannot be further developed due to defects in the proliferation and maintenance of trophoblast cells. The placental formation in mouse P-ESCs can be improved by addition of *Iqf2* or by serial nuclear transfers [71-72]. Both of these methods act trough supplementing the embryo with the missing paternally expressed gene (Igf2) [71] which is crucial for embryo growth or by down regulation of the maternally expressed genes, H19 and Peg10 in particular, which can occur through serial nuclear transfers [72]. Although in P-ESCs there is a silencing of the paternally expressed genes, in a study by Chao Li et al was reported that lgf2 transcript can be detected at 3.5DPA of development and later ceased by 9.5DPA [73]. In the same study it was revealed that at H19 was the most highly overexpressed maternal gene in all time points of PgE development. Also Le et al. found that from 3.5DPA to 9.5DPA the PgE genome is subjected to hypermethylation event which may explain the progressive loss of *Igf2* expression in P-ESCs at 9.5DPA [73]. Another evidence that the paternal genome is required for embryo growth comes from findings that P-ESCs exhibit lower weight compare to wild type (wt) embryos and that when introduced to form chimers with wt embryos, the weight of resulting offspring is inversely proportional to the P-ESCs that were introduced i.e. the greater the number of P-ESCs, the less is the weight of the newborn mice [74-75].

That the maternal genome is critical for embryo proper formation has been observed in androgenetic mouse embryos (AgE) – embryos that consist only of the paternal genome complement. In these embryos there is a proper formation of the extraembryonic membranes but failure in the embryo proper formation[76]. Another support of the aforementioned effect that the two opposite sexes confer on the offspring has been observed in ovarian malformations found in women known as gestational trophoblastic diseases and mentioned in the previous section.

Differentiation potential of mouse P-ESC cells

Mouse P-ESCs are an excellent model to study the differentiation potential of monoparental ESCs. There are five main approaches to study differentiation potential of embryonic stem cells and therefore their pluripotency; teratoma formation, embryo body formation, direct differentiation in culture dishes, chimera formation and tetraploid embryo complementation. The last two approaches, which also represent a test for ESCs pluripotency, are possible exclusively with mouse P-ESCs due to ethical issues associated with creating a chimera consisting of human or primate ESCs or P-ESCs. The generation of chimeric embryos calls for injection of the ESCs of interest into a host blastocyst or aggregation of the ES cells with host embryo [77]. If the ESCs of interest are pluripotent, they can be traced to all tissues and organs of the resulting offspring and if totipotent will be also passed through the germ line (Figure 1.2). The derivation of tetraploid embryos calls for aggregation of the ESCs of interest with a four-cell-stage tetraploid embryo. The last one generated by electro fusion of two-cell-stage (1.5DPF) embryos which were then left to cleave till four-cell-stage before

aggregation with host ESCs. In tetraploid embryo complementation experiment, the ESCs of interest, if totipotent, will give rise to all tissues and organs of the embryos including the germ line. The host cells, on the other hand, will give rise to the extra embryonic membranes [77].

The first report of P-ESCS-wt chimera was published in 1978 in Nature by Stevens [78]. Data from this first study clearly demonstrated that although complete PgE cannot develop to term, live chimeric animals can be produced when P-ESCS cells are aggregated with normal wt embryo. The ability of the P-ESCs to give rise to the embryo proper revealed that P-ESCs are viable and are capable to differentiate and give rise to all three germ layers- ecto, meso and endoderm and germ cells, in a chimeric animal. However, the P-ESCs-wt chimeras had significantly lower size than normal wt embryos and chimeras. Anderegg et al and Paldi et al. also found a negative correlation between embryo size and P-ESCs contribution into P-ESCs-wt chimeras [74-75]. Together with lower embryo size, Anderegg et al reported an increase in the number of the resorbing P-ESCs-wt embryos in the uterine horns of the recipient mice. Paldi et al attempted to quantify the percentage contribution of P-ESCs in the chimeric animals by quantifying the GPI isoenzyme intensity of staining in organs and tissues derived from P-ESCs-wt chimeras and normal fertilized embryos (fEs) [75]. They found that not only the P-ESCs –wt chimeric animals had lower weight but that there was a negative correlation between the weight of the chimeras and the P-ESC cell contribution (P-ESCs contribution to chimeric embryos ranged from 10-40%) i.e. the smaller the body size the more the P-ESCs were found to contribute to the embryo proper. The chimeric embryos that died soon after birth had the highest P-

ESCs cell contribution. It was also noticed that the P-ESCs-wt chimeras were only females. The surviving P-ESCs-wt female chimeric embryos were able to mate and passed the P-ESCs genotype through the germline and into the offspring as judged by their pigmented coat color [75]. That mouse P-ESCs are totipotent and that its genome can be transmitted through the germ line was also reported by Allen and Surani. They found that P-ESCs in P-ESCs-wt chimeras can contribute to the germ lineage and that this contribution did not depend on the passage number or the strain from which the P-ESCs were derived [76]. More striking was the observation that regardless of the strain, in chimeras with normal host cells, the P-ESCs exhibited restricted differentiation capacity consistent with that observed in PgEs i.e the P-ESCs were completely excluded or very low represented in the skeletal muscle tissues and testis. The chimerism varied from 40-80% in other organs tested such as brain, liver, and blood. Growth retardation was observed only in chimeric embryos derived by aggregation of PgE and wt embryo but not in P-ESCs-wt chimeras. Fundele and colleagues published in two separate studies a controversial data regarding the capacity of mouse P-ESCs to differentiate into all tissues and organs of the body when introduced into chimeric embryos. In the earlier publications the authors looked at adult and fetal chimeras [79-80]. It was found that by 13 DPA and 15DPA, the P-ESCs were progressively excluded from the skeletal muscle, pancreas and the liver and that they were completely excluded from the tongue right before the myoblast fusion occurs. Later study by Fundale et al reported that P-ESCs can contribute to all tissues of the chimeric animals with lower affinity to the colon, uterus,

duodenum and stomach with chimerism ranging from 0-21% [81]. They found that P-

ESCs contribute to the tongue tissue up to 23%. In 24 days old chimeras, it was found that the proliferation capacity of the P-ESCs in mesoderm derived mesenchymal cells of the colon and uterus and the endoderm derived duodenum is significantly lower than in wt control cells. Therefore the studies by Fundale and colleagues demonstrated again that P-ESCs are viable and pluripotent, they can give rise to derivatives of all germ layers and can be passed to the progeny through the germ cells but their differentiation potential may vary between chimeras and P-ESCs derived from different laboratories.

An exclusion of the P-ESCs from the endoderm germ lineage and stomach, in particular, has been reported by *Sturm et al* [82]. *Sturm et al* also analyzed the capability of P-ESCs to contribute to the hematopoietic stem cell lineage. They found, using FACS analysis, that in chimeras the P-ESCs contributed to the same extent to bone marrow and thymus hematopoietic cells as wt cells used to generate control chimeras. An interesting finding by *Sturm et al.* was that the chimeras with highest P-ESCs contribution, regardless of P-ESC cell line tested, were females [82]. However, the correlation between the P-ESCs contribution to P-ESCs –wt chimeras and the sex of the resulting offspring has been controversial since other groups have not reported such a gender preference [76, 83].

One possible explanation for the different contribution of the P-ESCs to the embryo proper of P-ESCs-wt chimers, as reported by the different scientific groups mentioned above, may be due to differences in P-ESCs culture conditions and propagation *in vitro*. For example it has been reported that *in vitro* culture conditions and passage number can alter the expression of the imprinted genes [73]. In this context, *Li et al* published data

on how passage number affects the differentiation potential of mouse P-ESCs when introduced into chimeras with wt embryos [73]. They found that the passage number of the P-ESCs used may have an effect on the contribution of these cells to tissues and organs of chimeric embryos. By using polymorphism markers to distinguish between the wt host cells and the P-ESCs, they found that when P-ESCs at early passage number five (p5) are introduced in chimeras, the P-ESCs are excluded from brain, lung, muscle, liver and kidney. The differentiation potential of the P-ESCs at later passage (p54) in chimeras was similar to that of the early passage P-ESCs (p5) with the exception of skin, heart and intestines where the P-ESCs contribution was very low. The highest contribution to chimeras was reported for P-ESCs at p21. The authors of this study tried to justify these findings by analyzing the methylation profile of a set of differentially methylated resgions (DMRs) controlling the expression of key imprinted genes; H19/Igf2DMR, Dlk1/Gtl2 DMR, Snrpn DMR, U2af1-rs1 and Peg1 promoter and exon1 region, in P-ESCs at the passages 5, 21 and 54. Li et al reported that there was no difference of the methylation profiles of the Snrpn DMR, U2af1-rs1 and Peg1 promoter and exon1 regions between P-ESCs at p5 and p54. The methylation of Snrpn DMR, U2af1-rs1 and Peg1 promoter and exon1 region at p21 was significantly decreased and correlated with over expression of the paternally expressed genes Snrpn, U2af1-rs1 and Peg1. Overexpression of the Snrpn, U2af1-rs1 and Peg1 genes was associated with the higher contribution of the P-ESCs to the embryo proper of chimeric animals. The expression of the maternally expressed gene *Dlk1* was also overexpressed in P-ESCs at p21. However the mRNA levels of *Dlk1* did not correlate with the methylation status of the Dlk1/Gtl2 DMR. This data demonstrated that the methylation of the imprinted genes DMR

regions is dynamic and may affect the expression of the imprinted genes. However, further studies are necessary to elucidate the exact mechanism through which the imprinted genes expression influence the differentiation potential of the P-ESCs [73]. In an attempt to improve the differentiation potential of mouse P-ESCs, Hikichi and colleagues used nuclear transfer method [84]. The original P-ESC cell nuclei were transferred into enucleated oocytes, and the resulting nuclear transfer (NT) embryos were used for establishment of a new NT-P-ESC cell line For this study they used two innovative strategies; instead of ethanol they activated the oocytes by using SrCl₂, a method that now is considered the most efficient in generating P-ESCs from mouse models. Second, instead of producing P-ESCs containing a duplication of only the oocyte genome, they combined the genomes of two oocytes. Third but not least, they introduced a green fluorescent protein (GFP) in the hybrid oocytes which allows them to follow the P-ESCs allocation into the chimeric animals. They found that the P-ESCs contribution to chimeric animals was very low-2-8% and especially low in mesoderm (heart and kidney) and endoderm (liver) derivatives and there was no germ line transmission. The low contribution to heart muscle and germ line was somehow controversial to the findings of the groups mentioned above [76, 78]. During three consecutive NT experiments the contribution of the P-ESCs was increased in the brain and intestines up to five fold compare to the initial P-ESC cell line. However, three consecutive rounds of NT were not able to reprogram the P-ESC genome in manner that will increase the P-ESCs propensity to contribute to heart and liver in P-ESCs-wt chimeras.

Another study on P-ESCs pluripotency by Onodega et al. reported significant differences in the potential of the P-ESC cell lines derived in his laboratory to contribute to the embryo proper in chimeras. Onodega et al. found high contribution of the P-ESCs to heart muscle and more than 30% P-ESCs contribution to liver of chimeric mice than Hikichi et al have reported before. The contribution of the P-ESCs to intestines, bone marrow, skeletal muscle and germ cells was from low to none. These discrepancies that arise between the different scientific groups in the ability to obtain germ line transmission of the parthenogenetic genome in P-ESCs –wt chimeras, Onodera and colleagues attributed to the instability of the P-ESC genome. That the P-ESCs exhibit unstable karyotype was reported in studies by multiple groups [84-87]. Tetraploid Embryo Complement (TEC) is considered to be the highest standard for totipotency [88-89]. None of the mouse P-ESCs studied so far has been able to generate TEC embryos. In a study by Allen and Surani, two P-ESCs were tested in P-ESCs-wt TEC experiment. One of the cells line used had the highest contribution to all tissues and organs of P-ESCs-WT chimeric embryos with no germ line transmission, and the second one had less potential of contributing to chimeras but allowed for gem line transmission and therefore was considered totipotent. However, when used in TEC experiment none of the two P-ESC cell lines was able to yield a viable embryo. The P-ESC cell line with the highest differentiation capability as judged by chimeric contribution, allowed for the embryos to develop passed day 13 of gestation. Despite the prolonged development, this embryo suffered an increase of the parts of the brain and was not compatible with life. TEC method was also not able to rescue PgE – wt aggregates. Moreover the phenotype of embryos derived by TEC with PgEs and P-

ESCs was indistinguishable. Therefore, this data suggested that whatever changes in the gene expression arise in the P-ESCs due to their manipulation and expansion in vitro, they have no effect on the capacity of the P-ESCs to differentiate *in vivo* at least as seen from the TEC experiments.[76]

Recently, a study by a Chinese group led by Chen et al, reported the first PgE embryo derived by TEC [90]. They injected 10-20 P-ESCs in tetraploid embryo at blastocyst stage. The tetraploid embryos were produced by electrical fusion of fertilized embryos at two cell stage. Only one PgE developed to term but died shortly after birth. The authors of the paper were not able to produce life parthenogenetic offspring and so far other groups have not been able to reproduce their results.

An alternative and more simplistic way to evaluate the differentiation potential of mouse P-ESCs *in vivo* is to inject the cells into immune compromised nude SCID mice. If the cells are pluripotent, after 4-8 weeks post injection they will develop teratomas consisting of derivatives of all three germ layers- ectoderm, mesoderm and endoderm.

Indeed it was found that teratomas derived from mouse P-ESCs comprise of tissues of all three germ layer [82-83, 86]. Allen *et al* studied differentiation potential of P-ESCs derived from two different strains of mice -CFLP and Rosa26, in teratomas. The teratomas were derived by injection of the P-ESCs into the kidney capsule of immune compromised NUDE-SCID mouse. Strikingly, they found that although the teratomas were composed of heterogeneous tissues and they were almost completely devoid of muscle tissue. The muscle was present only in few of the teratoma sections analyzed and was ranging from 5% of all tissue derivatives; compare to 20% in normal wild type

cells derived teratomas. In contrast teratomas derived from A-ESCs which possess a duplication of the paternal genomic complement without any maternal influence, consisted of predominantly muscle tissue [76]. In another study by Sturn *et al* it was reported that most of the P-ESCs derived teratomas (five out of seven) consist predominantly of neuro -ectoderm derived tissues and less mesoderm derived muscle tissue [82].

An alternative way to analyze the differentiation potential of ESCs and P-ESCs, in particular, is to induce them to differentiate, *in vitro*, into embryonic bodies (EB) upon withdrawal of Leukemia Inhibitory factor (LIF) and in the absence of mitotically inactivated feeder cells [91]. *In vitro* differentiation of mouse P-ESCs into Embryo bodies has revealed that, as in teratomas, multiple tissue derivatives can be observed. Park *et al* reported that in EBs derived from, P-ESCs, there is a restriction in the ability of the P-ESCs to give rise to endodermal derivatives [91].

Despite their restricted developmental potential mostly towards mesoderm muscle and endoderm tissues, P-ESCs can be successfully induced *in vitro* to give rise to mesoderm and muscle derivatives and to endoderm derived hepatocytes by using different combinations of growth factors and stimuli [84, 86].

Imprinting in Mouse Parthenogenetic Embryonic Stem Cells

Mouse PgEs and mouse P-ESCs have been invaluable model for studying imprinting and the role of *H19* and *Igf2*, in particular, in embryo development and cancerogenesis. In mouse, *H19* and *Igf2* are located on chromosome 7 and are coordinately regulated mainly by differentiation methylation of the DMR region located between the two genes.

H19 gene codes for an untranslated mRNA molecule. It has been reported that H19 can function as a long antisense RNA and as a micro RNA (miRNA 675) in humans and non-human primates [39-40]. Unlike humans, however, the mouse mir675 is presented by two isoforms: mmu-miR-675-3p and mmu-miR-675-5p. It was in mouse models where for the first time it was demonstrated that H19 may function as a tumor suppressor gene [56]. In this study the authors used H19Δ3 mice in which the maternal H19 allele and the upstream coding sequence was deleted and H19ΔEnh mice where the enhancer sequence downstream of H19 gene was deleted. It was found that upon grafting H19 Δ 3 and wild type control embryos at 6.5DPF and 6.5DPA, respectively, under the kidney capsule of syngenic mice, the resulted teratocarcinomas varied in weight between the two groups. The tumors derived from H19∆3 grafted embryos exhibit smaller weight compare to controls regardless if the IGF2 expression was paracrine or autocrine. When H19Δ3 mice were crossed with Apc mutant mice, the number of adenomas and the incidence of development of smaller polyps were significantly higher than in control mice with normal H19 expression [56]. However, as mentioned in the previous section, there is currently strong evidence that H19 and /or its product mir675 might be involved in the progression and pathogenesis of tumor development rather than tumor suppression [62-65].

The major reason for failure of the mouse PG embryos to develop to term, and the limited differentiation potential of P-ESCs, as in human and primate PgEs and P-ESCs, has been attributed to defects in establishing correct imprinting patterns of the imprinted genes (Allen, Barton et al. 1994; Park, Yoshida et al. 1998; Kono, Sotomaru et al. 2002;

Kono, Obata et al. 2004; Kono, Kawahara et al. 2006). Like primates, mouse PgEs and P-ESCs have a severe deregulation of the imprinted genes with *H19* being expressed bi-allelically and therefore upregulated while *Igf2* is barely detectable (Sotomaru, Kawase et al. 2001; Ogawa, Wu et al. 2006). Another study in uniparental mouse fetuses suggests that *H19* is over-expressed up to 400 times compared to mouse conceptuses that are normally fertilized (Sotomaru, Katsuzawa et al. 2002). Treatment of mouse parthenogenetic embryos with *Igf2* at pre- and post-implantation developmental stages could extend embryonic development up to the 50 somite stage (Platonov, Penkov et al. 2002).

Several studies analyzed the expression pattern and methylation status of imprinted genes in mouse P-ESCs upon differentiation *in vitro* and *in vivo* (Allen, Barton et al. 1994; Szabo and Mann 1994; McKarney, Overall et al. 1996; Barton, Arney et al. 2001; Sotomaru, Katsuzawa et al. 2002; Hernandez, Kozlov et al. 2003; Ogawa, Wu et al. 2006; Horii, Kimura et al. 2008; Li, Chen et al. 2009).

Most data suggests that the expression profile of the imprinted genes in P-ESCs changes during cell culture propagation and expansion [83]. Regardless of the method used for parthenogenetic oocyte activation, P-ESCs exhibit loss of imprinting of paternally and maternally imprinted genes such as *Igf2*, *Snrpn*, *Igf2r*, *peg1* and *U2af1-rs1* which may or may not coincide with the methylation status of their promoters or differentially methylated regions (DMR) known also as an imprinted control regions(ICR). In a study by Li et al it was reported that the expression of a set of paternally expressed genes; *Peg1*, *Peg3*, *Peg5*, *Peg10*, *Sgce*, *Snrpn*, *Zfp127*, *Lit1*, *Igf2*, *Zac1*, *U2af1-rs1*, *Dlk1*, *Ata3*, *Air* and *Impact* was detected in P-ESCs but not in the

PgEs from which the cells were derived [73]. Moreover the expression of the paternally expressed genes persisted in PgEs derived by tetraploid embryo complementation (TEC) between fertilized 4N embryo and P-ESCs with the exception of *Igf2* and *Dlk1* which expression was suppressed [73]. Another study by Jiang et al, also reported that a set of paternally imprinted genes tested, were detected in P-ESCs from earlier p10 and at later p20. These genes were Snrpn, U2af1-rs1, Peg3 Zfp127, Ndn, Impact and *Mest*. The most overexpressed maternally expressed gene was *H19* and the most highly overexpressed paternally expressed gene was *Peg3* at levels even higher than those of H19. The authors of this study surprisingly discovered that the re-activation of the maternally imprinted genes *Peg3*, *Snrpn* and *Mest* occurs in parthenogenetic blastocysts where the expression of these genes can be detected and then maintained into the P-ESCs derived [83]. It is worth mentioning an earlier study by Allen and Surani which observed a stable silencing of the paternally imprinted gene *lgf2* and over expression of the maternally expressed genes H19 and Igf2R in PgEs and P-ESCs from p2 to p8 derived from two different stain of mice CFLP and Rosa26 by using Northern analysis. However in this study the expression pattern of other paternally expressed genes, besides Igf2 was not analyzed. It would have been useful to look at the expression of imprinted genes at later passages in both, P-ESCs and PgEs. Analysis of the expression of imprinted genes in EBs has been also published by Szabo et al [92]. This group focused on analyzing the expression pattern of the maternally (H19, Igf2R) and paternally(Igf2 and Snrpn) expressed genes in EBs derived from mouse P-ESCs at different - late and early - passage and compare them to the

expression levels of the same genes in wild type biparental ES cells (B-ESCs) and in A-ESCs by Northern blot analysis.

P-ESCS cells from p8 and p12 were considered an early passage. P-ESCs at p27 and p32 were considered as old passage. Unfortunately, Szabo et al did not evaluate the expression pattern of these genes in P-ESCs, B-ESCs and A-ESCs prior to induction of EB differentiation. Szabo et al did show that P-ESCs give rise to, when differentiated in vitro for 14 days as EBs, tissues of all three germ layers. In P-ESCs from early passages, Igf2R was expressed later in EB differentiation around day 9 while in wild type derived EBs it was expressed at all time points peaking at days 9-14 of EB differentiation. Igf2R was expressed also in AG EBs but at low levels. Surprisingly, H19 was found to be expressed around day 9 in AG EBs and by day14 the H19 expression in AG EBs was significantly increased. The highest expression of H19 was however detected in P-ESCs derived EBs from day 9 to day 14 of EB formation. *Igf*2 expression was detected in EBs derived from all three cell lines- B-ESCs, P-ESCs and A-ESCs, and its expression became evident at day 9 and peaked at day 14 post fertilization for the B-ESCs and post activation for the P-ESCs and A-ESCs cell lines. Snrpn expression was detected in all three types of EBs; however its expression was highest at days 1-4 of AG EB formation. Analysis of the methylation status of the lgf 2 5' region, Igf2R intron II region and H19 promoter region were found to correlates with the mRNA expression of the imprinted genes Igf2, Igf2R and H19 respectively. Therefore, this data suggested that the expression of the imprinted genes in P-ESCs, B-ESCs and A-ESCs changes during different stages of EB differentiation and coincides with changes in the methylation status of their imprinted control regions.

Northern blot analysis on teratoma sections revealed that *H19* was highly expressed in P-ESCs and B-ESCs derived teratomas compare to A-ESCs derived ones. *Igf2* expression, on the other hand, was high in A-ESCs derived teratomas. *Igf2* expression was also detected in P-ESCs teratomas. No *Igf2* expression was found in B-ESCs teratomas.

The localization of *H19* and *Igf2* transcripts was detected by *in situ* hybridization. It was found that both *H19* and *Igf2* transcripts were co-expressed in striated muscle in P-ESCs, A-ESCs and B-ESCs derived teratomas and in cartilage from B-ESCs derived teratomas. In A-ESCs derived teratomas, *Igf2* was expressed in mature cartilage while *H19* transcript was detected in less differentiated cartilage regions. The expression of *H19* and *Igf2* in cartilage from P-ESCs cells derived teratomas has not been analyzed. In epithelial structures derived from B-ESCs and A-ESCs derived teratomas either *H19* or *Igf2* were expressed. There was a very low co-expression detected of *H19* and *Igf2* in the epithelium from B-ESCs and A-ESCs derived teratomas. In P-ESCs derived teratomas, *H19* was most highly expressed in epithelial layers and sub-epithelial stroma, while *Igf2* mRNA was more abundant in sub-epithelial stroma and smooth muscle[93]. These results revealed that both *H19* and *Igf2* were highly expressed in P-ESCs, A-ESCs and B-ESCs derived teratomas and in most instances their expression was co-localized to the same tissue derivatives analyzed.

CONCLUSION

P-ESCs cells are an invaluable tool for studying the effect of imprinting on development and disease as well as to study the potential application of P-ESCs for

cell replacement therapy in humans. Moreover, this source of cells is mitochondria and MHC- matched to the recipient which makes them valuable for transplantation therapy [5, 94-100]. Similar to the embryonic stem cells derived from fertilized embryos, P-ESCs stain positive for the major pluripotency markers such as SSEA-3, SSEA-4, TRA1-60, TRA1-81, and OCT4. P-ESCs morphology is indistinguishable from that of normal biparental ES cells. Unlike ES cells derived from normal biparental embryos, P-ESCs derivation does not require a destruction of a viable embryo and therefore bypass the ethical concerns that some members of the society possess. Unlike human and primate P-ESCs, whose in vivo differentiation potential can be tested only by teratoma formation, mouse P-ESCs are an excellent model to test the developmental behavior of the P-ESCs in vivo, directly, by introducing the P-ESCs into chimeras and TEC. These experimental in vivo studies indicated that although epigenetically instable, when injected into chimeras, mouse P-ESCs have been able to contribute to all tissues and organs of the embryo, to the germ line lineage and into the offspring. Moreover teratomas derived from mouse, primate and human P-ESCs revealed that these cells can differentiate into derivatives of all three germ layer and do not lead to any secondary teratomas besides the ones obtained at the site of injection. The results of the aforementioned studies indicate that P-ESCs are totipotent and are able to correct for the imprinting mis-expression upon induction of differentiation and generate terminally differentiated derivatives of ecto-, endo- and mesoderm origin.

Thus mouse, human and primate P-ESCs not only offer an unlimited source of pluripotent stem cells with a potential for cell replacement therapy but also represent a

valuable avenue for studying the molecular basis of human congenital disorders caused by deregulation of imprinting.

FIGURES AND TABLES

Table 1.1 Diseases and syndromes resulting from abnormal imprinting mechanisms [101] Swales and N.Spears; Reproduction (2005) 130 389 399, http://www.reproduction-online.org

Disorder	Affected genes	Phenotype
Angelman syndrome	Chromosome 15 – maternal copy, loss of SNRPN imprinting	Mental retardation, ataxic gait, seizures, sociable disposition
Autism	Unknown X-linked gene (not always connected to imprinting)	Impaired language development, problems with social and motor skills
Beckwith-Wiedemann syndrome	11p15 region – altered expression of IGF2, H19 and LIT1	Undescended testes, large newborn, seizures, abdominal wall defects
Cancer	Variable, e.g. IGF2 in lung cancer (not always connected to imprinting)	Tumours
ICF (immunodeficiency, centromeric region instability and facial anomalies syndrome)	DNMT3B	Immune problems, facial anomalies, growth retardation
Paraganglioma	Paternal mutations SDHA (PGL1) and PGL2	Glomus tumours of the parasympathetic ganglia mainly in the head and neck region, tend to be slow growing and benign
Prader-Willi Syndrome	Chromosome 15 – paternal copy	Undescended tests, mental retardation, short stature, obesity small hands and feet

Table 1.1 (cont'd)

+	 	100
Pre-eclampsia	Not yet defined	Serious complication of
		pregnancy
Pseudohypoparathyroidism	Imprinted GNAS cluster	Parathyroid horomone
type IA (Albright hereditary		resistance, short stature,
osteodystrophy)		round face and short hand
		bones
Pseudohypoparathyroidism	Imprinted GNAS cluster	Parathyroid hormone
type IB		resistance localized to renal
		system, causing
		hypocalcaemia and
		hyperphosphataemia
Rett syndrome	MeCP2	Childhood
		neurodevelopmental
		disorder mainly affecting
		females. Loss of motor
		function and mental
		retardation

Figure 1.1 Construction of diploid embryos with genomes derived from a single sex. In a fertilized egg, the male and female pronuclei can be removed before they fuse, and a diploid egg recreated by injection of another pronucleus. The development of these diploid eggs can then be followed *in vitro* by culturing or *in vivo* by transplantation to pseudopregnant mice. Parthenogenetic embryos can be created by the chemical activation of an unfertilized egg [102].

Lyle, R. Gametic imprinting in development and disease. J Endocrinol 155, 1-12 (1997), http://www.endocrinology-journals.org/

For interpretation of the references in color in this and all other figures, the reader is referred to the electronic version of the dissertation.

Figure 1.1 (cont'd)

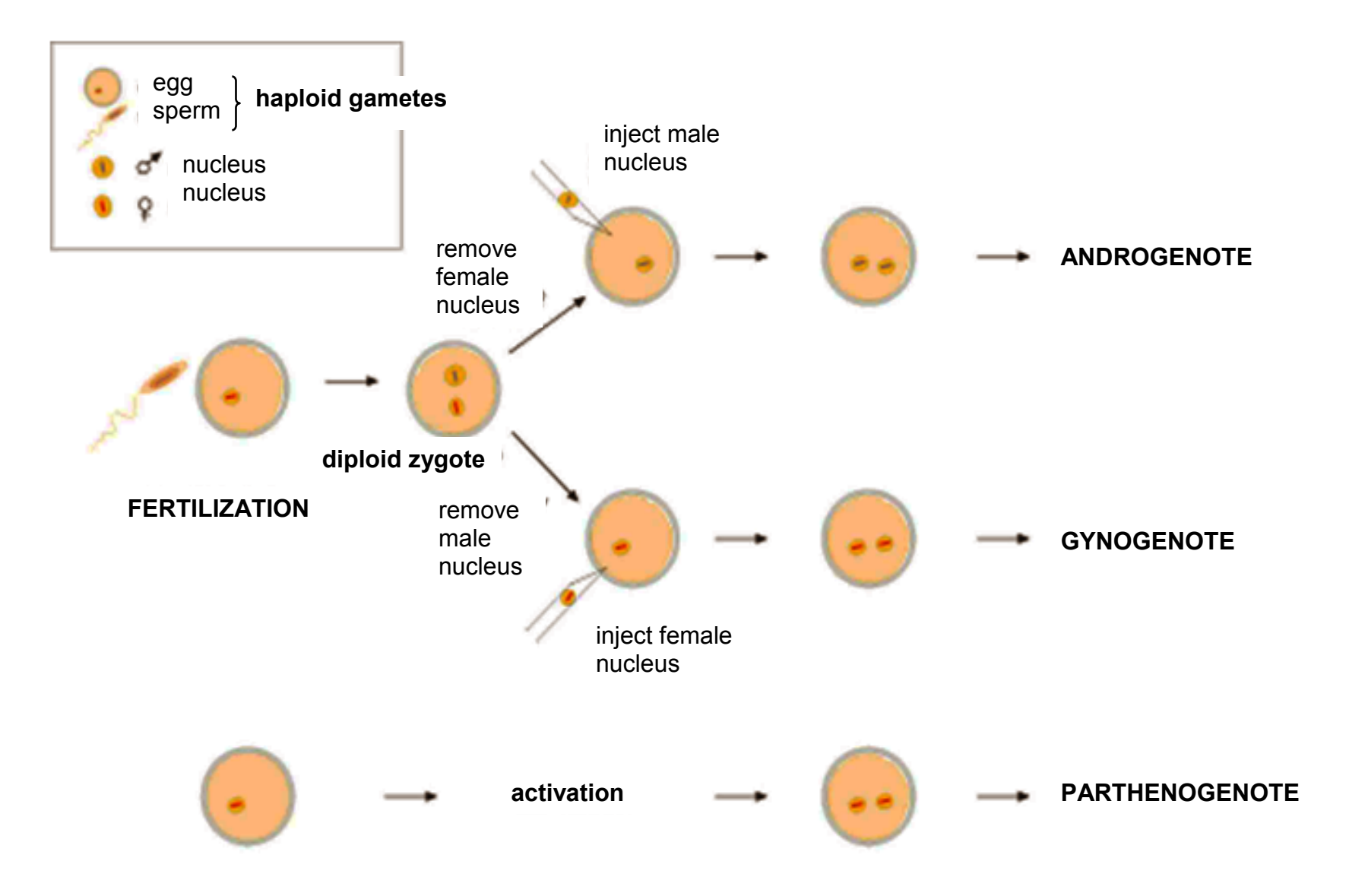


Figure 1.2 Stem cell hierarchy. Zygote and early cell division stages (blastomeres) to the morula stage are defined as totipotent, because they can generate a complex organism. At the blastocyst stage, only the cells of the inner cell mass (ICM) retain the capacity to derive all three primary germ layers, the endoderm, mesoderm, and ectoderm as well as the primordial germ cells (PGC), the founder cells of male and female gametes. In adult tissues, multipotent stem and progenitor cells exist in tissues and organs to replace lost or injured cells. At present, it is not known to what extent adult stem cells may also develop (transdifferentiate) into cells of other lineages or what factors could enhance their differentiation capability (dashed lines). Embryonic stem (ES) cells, derived from the ICM, have the developmental capacity to differentiate *in vitro* into cells of all somatic cell lineages as well as into male and female germ cells. *[103]*.

Wobus, et al, *Physiol Rev* 85:635-678, 2005, www.endocrinology.org & www.bioscientifica.com

Figure 1.2 Stem cell hierarchy (cont'd)

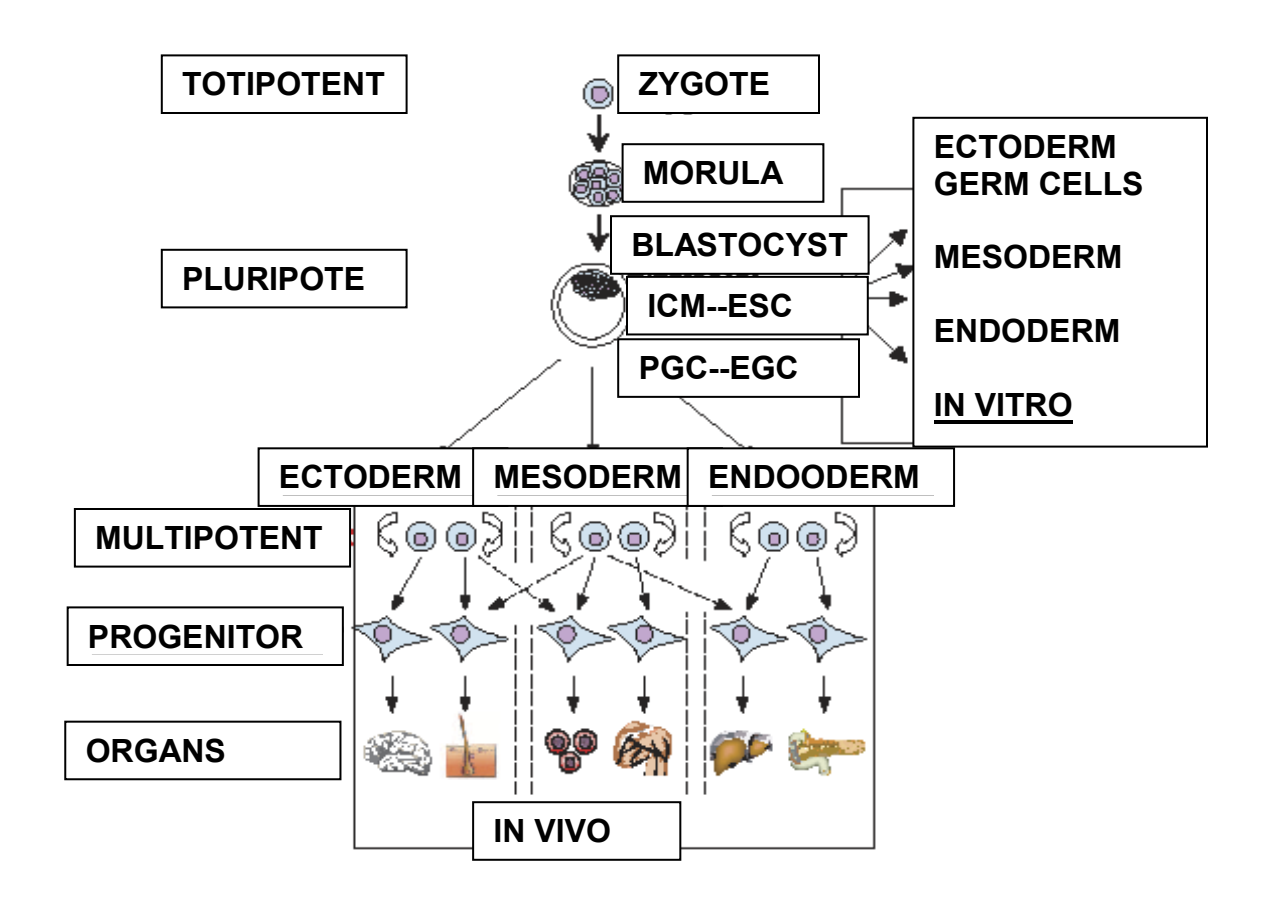


Figure 1.3 Characterization of parthenogenetic Cyno-1 embryos and derived cell lines. (A) Parthenogenetically activated eggs at day 8 of development before ICM isolation. (B) Phase contrast of Cyno-1 stem cells growing on top of mitotically inactivated mouse feeder layer (mef). (C) Alkaline phosphatase staining. (D) Stage-specific embryonic antigen 4. (E) Tumor rejection antigen 1-60. (F) Tumor rejection antigen 1-81 staining. (G) RT-PCR octamer-binding transcription factor 4 expression in undifferentiated Cyno-1 cells. (Scale bars = 50 μm in A, 10 μm in B and D–F, and 4 mm in C.) [16]. **Vrana et al**, *Proc.Natl.Acad.Sci USA.*, **2003 Sep 30; 100, http://www.pnas.org/**

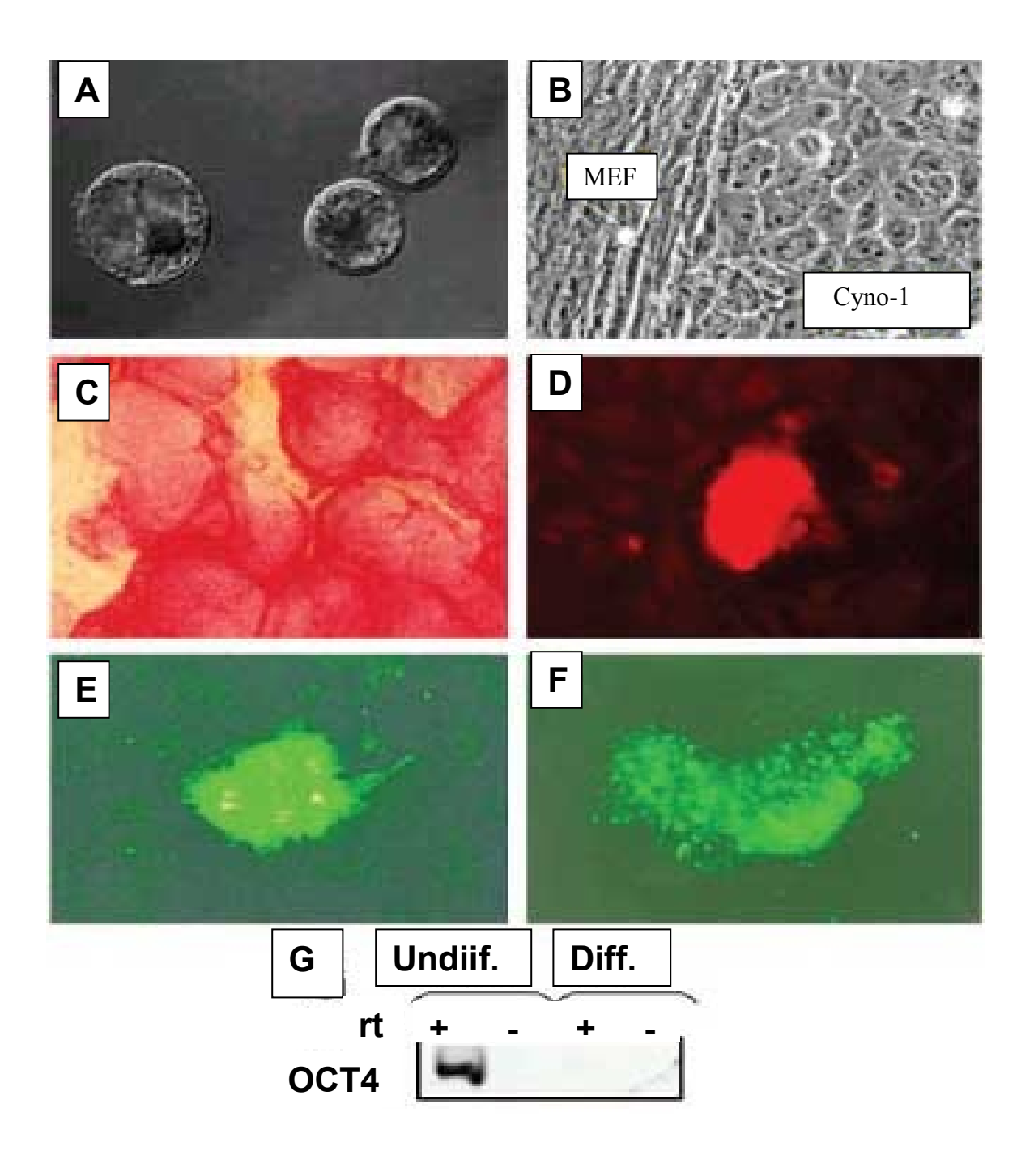


Figure 1.4 *In vivo* differentiation of Cyno-1 cells. Cells were injected i.p. (IntraPeritoneal) in severe combined immunodeficient mice. Eight and 15 weeks after injection, teratomas 12 and 30 mm in diameter, respectively, were isolated, fixed with 10% paraformaldehyde, and paraffin—embedded. Sections were stained with hematoxylin-eosin. The following complex structures were observed: gut (A), intestinal epithelium with typical goblet cells (gc) and smooth muscle (sm) (B), neuronal tissue with melanocytes (C), hair follicle complex with evident hair (h) and sebaceous gland (sg) (D), skin (E), cartilage (F), ganglion cells (G), and bone (H). (Scale bars = 40 μm in A, 10 μm in B and D–H, and 20 μm in C.) [16].

Vrana et al, Proc.Natl.Acad.Sci USA., 2003 Sep 30; 100, http://www.pnas.org/

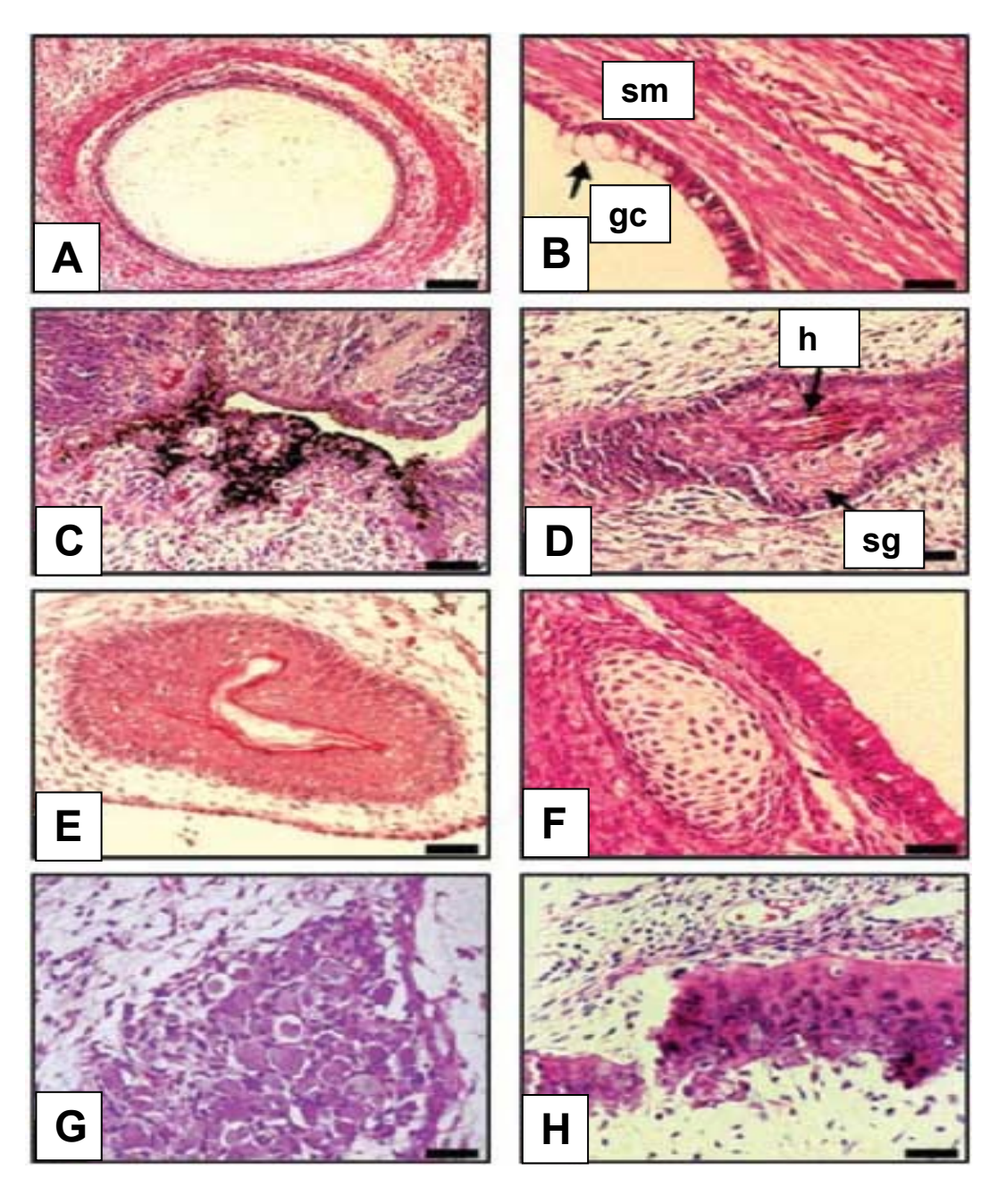


Figure 1.5 In vitro differentiation of primate Cyno-1 P-ESCs. (A): Schematic representation of the sequential steps designed to induce a dopamine neuronal phenotype from undifferentiated primate ES cells. ES cells are first grown in a coculture system on stromal feeders. At the rosette stage, these neuroepithelial structures are replated on coated dishes in a feeder-free system for differentiation. (B-D) Microscopic images illustrating the aspect of the colonies at each passage. Undifferentiated stage Cyno-1 cells grow in colonies and all cells (B) express the transcription factor Oct-4. (C) Soon after the first passage, cells are organized into typical neuroepithelial structures (rosettes, r); (D): At the differentiation stage neurons grow in clusters and extend out neurites and (E) express midbrain genes like Engrailed-1 (En1), which is colocalized in some neurons with TH. (F) TH neurons coexpressed the neuronal marker β-tubulin III (clone TuJ1) and (G) some coexpressed VMAT-2 (yellow coexpression). Scale bars = 100 µm (B–C), 150 µm (D), 75 µm (E), 50 μm (F), 35 μm (G) and inset in (E). Abbreviations: BDNF, brain-derived neurotropic factor; ES, embryonic stem; FGF8, fibroblast growth factor 8; GDNF, glial-derived neurotropic factor; TH, tyrosine hydroxylase; SHH, sonic hedgehog; TGFβ3, transforming growth factor β3; TH, tyrosine hydroxylase; VMAT, vesicular monoamine transporter; [17].

Sánchez-Pernaute, Studer, Ferrari et al; Stem Cells 2005 Aug; 23(7):914-22. Epub 2005 Jun; http://stemcells.alphamedpress.org

Figure 1.5 (cont'd)

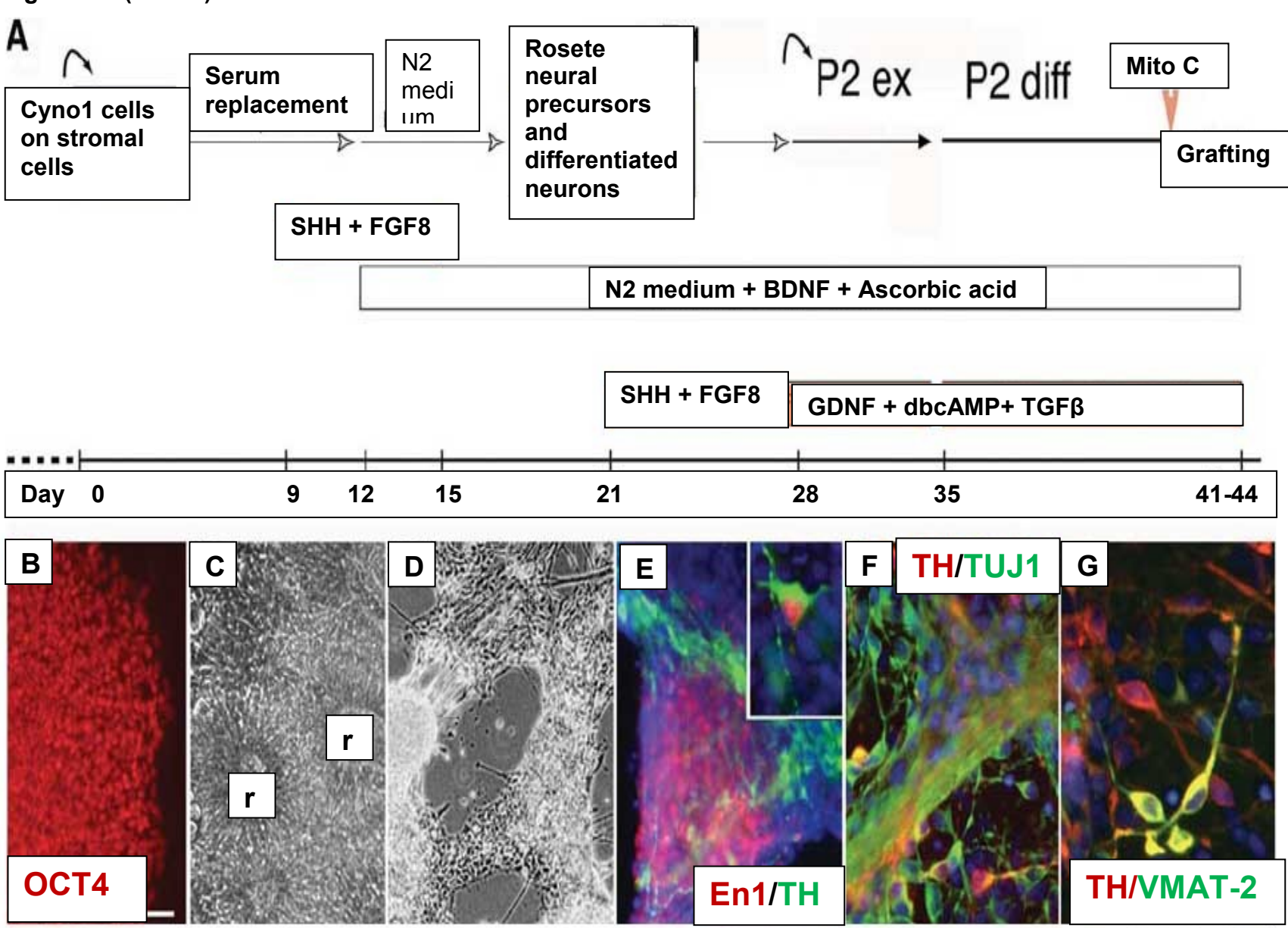
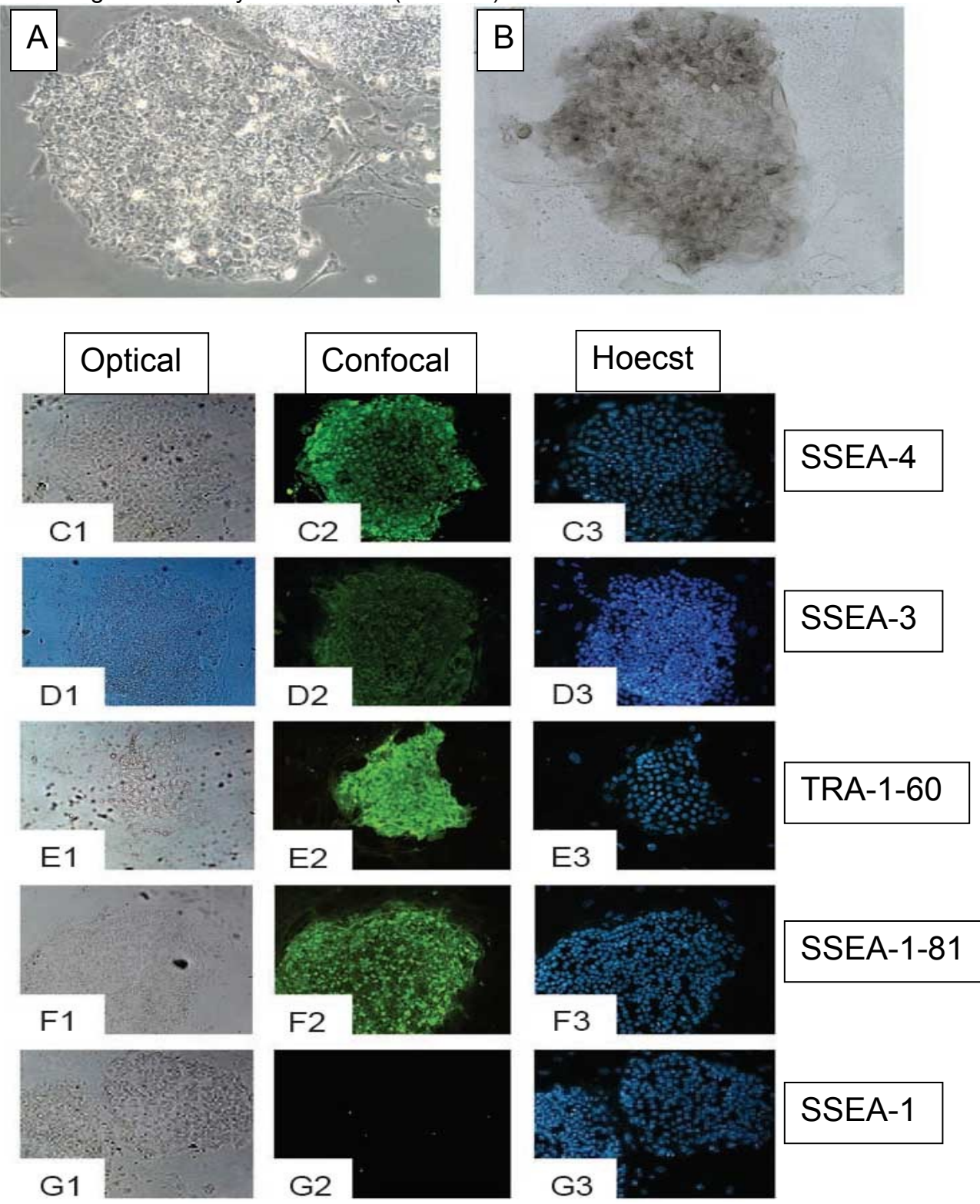


Figure 1.6 Morphology, AP and Immonustaining of stem cell markers for human Parthenogenetic Embryonic Stem -1 (hPES -1) cell line. (A) Morphology of hPES-1 colony under invert microscope; (B) AP staining of hPES-1; (C) SSEA4; (D) SSEA3; (E) TRA-1-60; (F) TRA-1-81; (G) SSEA1. (C-G) Listed are optical, confocal images and the corresponding Hoechst staining for the hPES-1 cells [8]. Qingyun Mai et al; Cell Research (2007) 17:1008-1019. http://www.nature.com/cr/index.html

Figure 1.6 Morphology, AP and Immonustaining of stem cell markers for human Parthenogenetic Embryonic Stem -1 (hPES -1) cell line.



REFERENCES

REFERENCES

- 1. Mutter, G.L., *Role of imprinting in abnormal human development.* Mutation Research/Fundamental and Molecular Mechanisms of Mutagenesis, 1997. 396(1-2): p. 141-147.
- 2. Sotomaru, Y., et al., *Unregulated Expression of the Imprinted Genes H19 and Igf2r in Mouse Uniparental Fetuses* J. Biol. Chem., 2002. 277(14): p. 12474-12478.
- 3. Ogawa, H., et al., *Disruption of parental-specific expression of imprinted genes in uniparental fetuses.* FEBS Letters, 2006. 580(22): p. 5377-5384.
- 4. Surti, U., et al., Genetics and biology of human ovarian teratomas. I. Cytogenetic analysis and mechanism of origin. Am J Hum Genet, 1990. 47(4): p. 635-43.
- 5. Revazova, E.S., et al., *Patient-Specific Stem Cell Lines Derived from Human Parthenogenetic Blastocysts.* Cloning Stem Cells, 2007. 9(3): p. 432-49.
- 6. Revazova, E.S., et al., *Patient-Specific Stem Cell Lines Derived from Human Parthenogenetic Blastocysts*. Cloning and Stem Cells, 2007. 9(3): p. 432.
- 7. Revazova, E.S., et al., *HLA Homozygous Stem Cell Lines Derived from Human Parthenogenetic Blastocysts*. p. 1-14.
- 8. Mai, Q., et al., *Derivation of human embryonic stem cell lines from parthenogenetic blastocysts*. Cell Res. 17(12): p. 1008-1019.
- 9. Strain, L., et al., *A human parthenogenetic chimaera*. Nat Genet, 1995. 11(2): p. 164-9.
- 10. Surani, M.A., *Parthenogenesis in man.* Nat Genet, 1995. 11(2): p. 111-3.
- 11. Cibelli, J.B., K. Cunniff, and K.E. Vrana, *Embryonic stem cells from parthenotes*. Methods Enzymol, 2006. 418: p. 117-35.

- 12. Mitalipov, S.M., K.D. Nusser, and D.P. Wolf, *Parthenogenetic Activation of Rhesus Monkey Oocytes and Reconstructed Embryos*. 2001. p. 253-259.
- 13. Cibelli, J.B., K. Cunniff, and K.E. Vrana, *Embryonic Stem Cells from Parthenotes*, in *Methods in Enzymology*, K. Irina and L. Robert, Editors. 2006, Academic Press. p. 117-135.
- 14. Zvetkova, I., et al., *Global hypomethylation of the genome in XX embryonic stem cells.* Nat Genet, 2005. 37(11): p. 1274-9.
- 15. Cibelli, J.B., et al., *Parthenogenetic stem cells in nonhuman primates.* Science, 2002. 295(5556): p. 819.
- 16. Vrana, K.E., et al., *Nonhuman primate parthenogenetic stem cells.* Proc Natl Acad Sci U S A, 2003. 100 Suppl 1: p. 11911-6.
- 17. Sanchez-Pernaute, R., et al., Long-Term Survival of Dopamine Neurons Derived from Parthenogenetic Primate Embryonic Stem Cells (Cyno-1) After Transplantation. 2005. p. 914-922.
- 18. Ferrari, D., et al., *Transplanted dopamine neurons derived from primate ES cells preferentially innervate DARPP-32 striatal progenitors within the graft.* 2006. p. 1885-1896.
- 19. Dighe, V., et al., *Heterozygous Embryonic Stem Cell Lines Derived from Nonhuman Primate Parthenotes*. 2008. p. 2007-0869.
- 20. Cheng, L., *More new lines of human parthenogenetic embryonic stem cells.* Cell Res. 18(2): p. 215-217.
- 21. Sapienza, C., Parental imprinting of genes. Sci Am, 1990. 263(4): p. 52-60.
- 22. Tang, W.-y. and S.-m. Ho, *Epigenetic reprogramming and imprinting in origins of disease*. Reviews in Endocrine & Metabolic Disorders.

- 23. Swales, A.K.E. and N. Spears, *Genomic imprinting and reproduction*. 2005. p. 389-399.
- 24. Fujimoto, A., et al., *Aberrant genomic imprinting in rhesus monkey embryonic stem cells*. Stem Cells, 2006. 24(3): p. 595-603.
- 25. Newman-Smith, E.D. and Z. Werb, *Stem cell defects in parthenogenetic peri-implantation embryos*. Development, 1995. 121(7): p. 2069-77.
- 26. Horii, T., et al., Loss of Genomic Imprinting in Mouse Parthenogenetic Embryonic Stem Cells. 2008. p. 79-88.
- 27. Kono, T., et al., *Birth of parthenogenetic mice that can develop to adulthood.* Nature, 2004. 428(6985): p. 860-4.
- 28. Kono, T., et al., Mouse parthenogenetic embryos with monoallelic H19 expression can develop to day 17.5 of gestation. Dev Biol, 2002. 243(2): p. 294-300.
- 29. Mitalipov, S., et al., *Methylation status of imprinting centers for H19/IGF2 and SNURF/SNRPN in primate embryonic stem cells.* Stem Cells, 2007. 25(3): p. 581-8.
- 30. Runte, M., et al., SNURF-SNRPN and UBE3A transcript levels in patients with Angelman syndrome. Human Genetics, 2004. 114(6): p. 553-561.
- 31. Reik, W. and E.R. Maher, *Imprinting in clusters: lessons from Beckwith-Wiedemann syndrome*. Trends Genet, 1997. 13(8): p. 330-4.
- 32. Nicholls, R.D., S. Saitoh, and B. Horsthemke, *Imprinting in Prader-Willi and Angelman syndromes*. Trends in Genetics, 1998. 14(5): p. 194-200.
- 33. Hurst, L.D. and G.T. McVean, *Growth effects of uniparental disomies and the conflict theory of genomic imprinting.* Trends Genet, 1997. 13(11): p. 436-43.

- 34. Sotomaru, Y., et al., *Disruption of imprinted expression of U2afbp-rs/U2af1-rs1 gene in mouse parthenogenetic fetuses.* J Biol Chem, 2001. 276(28): p. 26694-8.
- 35. Poirier, F., et al., *The murine H19 gene is activated during embryonic stem cell differentiation in vitro and at the time of implantation in the developing embryo.* 1991. p. 1105-1114.
- 36. Varrault, A., et al., Zac1 Regulates an Imprinted Gene Network Critically Involved in the Control of Embryonic Growth. Developmental Cell, 2006. 11(5): p. 711-722.
- 37. Gabory, A., et al., *H19 acts as a trans regulator of the imprinted gene network controlling growth in mice.* Development, 2009. 136(20): p. 3413-21.
- 38. Matsuda T, W.N., Genetics and molecular markers in gestational trophoblastic disease with special reference to their clinical application. Best Pract Res Clin Obstet Gynaecol, 2003. 17.(6): p. 827-36.
- 39. Schoenfelder, S., et al., *Non-coding transcripts in the H19 imprinting control region mediate gene silencing in transgenic Drosophila*. EMBO Rep, 2007. 8(11): p. 1068-73.
- 40. Berteaux, N., et al., A novel H19 antisense RNA overexpressed in breast cancer contributes to paternal IGF2 expression. Mol Cell Biol, 2008. 28(22): p. 6731-45.
- 41. Gabory, A., H. Jammes, and L. Dandolo, *The H19 locus: role of an imprinted non-coding RNA in growth and development.* Bioessays, 2010. 32(6): p. 473-80.
- 42. Gabory, A., et al., *The H19 gene: regulation and function of a non-coding RNA.* Cytogenet Genome Res, 2006. 113(1-4): p. 188-93.
- 43. Cullen, X.C.a.B.R., *The imprinted H19 noncoding RNA is a primary microRNA precursor.* RNA, 2007. 13: p. 313–316.

- 44. Han, V.K.M. and A.M. Carter, Spatial and Temporal Patterns of Expression of Messenger RNA for Insulin-Like Growth Factors and their Binding Proteins in the Placenta of Man and Laboratory Animals. Placenta, 2000. 21(4): p. 289-305.
- 45. Pringle, K.G. and C.T. Roberts, *New Light on Early Post-Implantation Pregnancy in the Mouse: Roles for Insulin-Like Growth Factor-II (IGF-II)?* Placenta, 2007. 28(4): p. 286-297.
- 46. Minniti, C.P., et al., *Insulin-like growth factor II overexpression in myoblasts induces phenotypic changes typical of the malignant phenotype*. 1995. p. 263-269.
- 47. Pacher, M., et al., *Impact of constitutive IGF1/IGF2 stimulation on the transcriptional program of human breast cancer cells*. 2007. p. 49-59.
- 48. Prelle, K., et al., Overexpression of insulin-like growth factor-II in mouse embryonic stem cells promotes myogenic differentiation. Biochem Biophys Res Commun, 2000. 277(3): p. 631-8.
- 49. Weber, M.M., et al., Postnatal Overexpression of Insulin-Like Growth Factor II in Transgenic Mice Is Associated with Adrenocortical Hyperplasia and Enhanced Steroidogenesis. 1999. p. 1537-1543.
- 50. Moorehead, R.A., et al., *Transgenic overexpression of IGF-II induces* spontaneous lung tumors: a model for human lung adenocarcinoma. Oncogene, 2003. 22(6): p. 853-7.
- 51. Petrik, J., et al., Overexpression of Insulin-Like Growth Factor-II in Transgenic Mice Is Associated with Pancreatic Islet Cell Hyperplasia. 1999. p. 2353-2363.
- 52. Newman-Smith, E. and Z. Werb, *Functional analysis of trophoblast giant cells in parthenogenetic mouse embryos.* Dev Genet, 1997. 20(1): p. 1-10.
- 53. Mitalipov, S., et al., Methylation Status of Imprinting Centers for H19/IGF2 and SNURF/SNRPN in Primate Embryonic Stem Cells
 10.1634/stemcells.2006-0120. Stem Cells, 2006: p. 2006-0120.

- 54. Kawahara, M., et al., *High-frequency generation of viable mice from engineered bi-maternal embryos.* Nat Biotechnol, 2007. 25(9): p. 1045-50.
- 55. Kono, T., et al., *Paternal dual barrier by Ifg2-H19 and Dlk1-Gtl2 to parthenogenesis in mice.* Ernst Schering Res Found Workshop, 2006(60): p. 23-33.
- 56. Yoshimizu, T., et al., *The H19 locus acts in vivo as a tumor suppressor.* Proc Natl Acad Sci U S A, 2008. 105(34): p. 12417-22.
- 57. Liou, J.-M., et al., Loss of imprinting of insulin-like growth factor II is associated with increased risk of proximal colon cancer. European Journal of Cancer. In Press, Corrected Proof.
- 58. Adriaenssens, E., et al., H19 Overexpression in Breast Adenocarcinoma Stromal Cells Is Associated with Tumor Values and Steroid Receptor Status but Independent of p53 and Ki-67 Expression. Am J Pathol, 1998. 153(5): p. 1597-1607.
- 59. Barsyte-Lovejoy, D., et al., *The c-Myc Oncogene Directly Induces the H19 Noncoding RNA by Allele-Specific Binding to Potentiate Tumorigenesis.* Cancer Research, 2006. 66(10): p. 5330-5337.
- 60. Berteaux, N., et al., *H19 mRNA-like Noncoding RNA Promotes Breast Cancer Cell Proliferation through Positive Control by E2F1.* Journal of Biological Chemistry, 2005. 280(33): p. 29625-29636.
- 61. Dugimont, T., et al., *The H19 gene is expressed within both epithelial and stromal components of human invasive adenocarcinomas.* Biology of the Cell, 1995. 85(2-3): p. 117-124.
- 62. Lottin, S., et al., Overexpression of an ectopic H19 gene enhances the tumorigenic properties of breast cancer cells. Carcinogenesis, 2002. 23(11): p. 1885-1895.

- 63. Lottin, S., et al., *Thioredoxin post-transcriptional regulation by H19 provides a new function to mRNA-like non-coding RNA*. Oncogene, 2002. 21(10): p. 1625-31.
- 64. Matouk, I.J., et al., *The oncofetal H19 RNA connection: Hypoxia, p53 and cancer.* Biochimica Et Biophysica Acta-Molecular Cell Research, 2010. 1803(4): p. 443-451.
- 65. Tsang, W.P., et al., *Oncofetal H19-derived miR-675 regulates tumor suppressor RB in human colorectal cancer.* Carcinogenesis, 2010. 31(3): p. 350-358.
- 66. Sheehy, E., et al., *Estimating the number of potential organ donors in the United States.* N Engl J Med, 2003. 349(7): p. 667-74.
- 67. Coombes, J.M. and J.F. Trotter, *Development of the allocation system for deceased donor liver transplantation*. Clin Med Res, 2005. 3(2): p. 87-92.
- 68. Nagy, A., et al., *Embryonic stem cells alone are able to support fetal development in the mouse.* 1990. p. 815-821.
- 69. Nagy, A., et al., *Derivation of Completely Cell Culture-Derived Mice from Early-Passage Embryonic Stem Cells.* 1993. p. 8424-8428.
- 70. Horii, T., et al., Loss of Genomic Imprinting in Mouse Parthenogenetic Embryonic Stem Cells. 2007. p. 2006-0635.
- 71. Platonov, E.S., L.I. Penkov, and D.A. New, [Effects of growth factors FGF2 and IGF2 on the development of parthenogenetic mouse embryos in utero and in vitro]. Ontogenez, 2002. 33(1): p. 60-7.
- 72. Hikichi, T., et al., Functional full-term placentas formed from parthenogenetic embryos using serial nuclear transfer. Development, 2010.
- 73. Li, C., et al., Correlation of expression and methylation of imprinted genes with pluripotency of parthenogenetic embryonic stem cells. Hum. Mol. Genet., 2009. 18(12): p. 2177-2187.

- 74. Anderegg, C. and C.L. Markert, Successful rescue of microsurgically produced homozygous uniparental mouse embryos via production of aggregation chimeras. Proc Natl Acad Sci U S A, 1986. 83(17): p. 6509-13.
- 75. Paldi, A., et al., *Postnatal development of parthenogenetic in equilibrium with fertilized mouse aggregation chimeras.* Development, 1989. 105(1): p. 115-8.
- 76. Allen, N., et al., *A functional analysis of imprinting in parthenogenetic embryonic stem cells.* Development, 1994. 120(6): p. 1473-1482.
- 77. Nagy A, G.M., Vintersten K, Behringer R, *Manipulating the Mouse Embryo, A Laboratory Manual*. Vol. Third Edition. 2003: Cold Spring Harbor Laboratory Press.
- 78. Stevens, L.C., *Totipotent cells of parthenogenetic origin in a chimaeric mouse*. Nature, 1978. 276(5685): p. 266-7.
- 79. Fundele, R.H., et al., *Temporal and spatial selection against parthenogenetic cells during development of fetal chimeras.* Development, 1990. 108(1): p. 203-211.
- 80. Fundele, R., et al., *Systematic elimination of parthenogenetic cells in mouse chimeras*. Development, 1989. 106(1): p. 29-35.
- 81. Jagerbauer, E.M., et al., *Parthenogenetic stem cells in postnatal mouse chimeras*. Development, 1992. 116(1): p. 95-102.
- 82. Sturm, K.S., et al., *Unrestricted lineage differentiation of parthenogenetic ES cells*. Development Genes and Evolution, 1997. 206(6): p. 377-388.
- 83. Jiang, H., et al., *Activation of paternally expressed imprinted genes in newly derived germline-competent mouse parthenogenetic embryonic stem cell lines.* Cell Res. 17(9): p. 792-803.
- 84. Hikichi, T., et al., *Differentiation Potential of Parthenogenetic Embryonic Stem Cells Is Improved by Nuclear Transfer.* Stem Cells, 2007. 25(1): p. 46-53.

- 85. Zvetkova, I., et al., *Global hypomethylation of the genome in XX embryonic stem cells*. Nat Genet, 2005. 37(11): p. 1274-1279.
- 86. Onodera, Y., et al., *Differentiation diversity of mouse parthenogenetic embryonic stem cells in chimeric mice.* Theriogenology, 2010. 74(1): p. 135-45.
- 87. Horii, T., et al., Loss of genomic imprinting in mouse parthenogenetic embryonic stem cells. Stem Cells, 2008. 26(1): p. 79-88.
- 88. Eggan, K., et al., *Hybrid vigor, fetal overgrowth, and viability of mice derived by nuclear cloning and tetraploid embryo complementation.* Proceedings of the National Academy of Sciences of the United States of America, 2001. 98(11): p. 6209-6214.
- 89. Eggan, K., et al., *Male and female mice derived from the same embryonic stem cell clone by tetraploid embryo complementation.* Nat Biotech, 2002. 20(5): p. 455-459.
- 90. Chen, Z., et al., *Birth of parthenote mice directly from parthenogenetic embryonic stem cells*. Stem Cells, 2009. 27(9): p. 2136-45.
- 91. Park, J.I., et al., *Differentiative potential of a mouse parthenogenetic embryonic stem cell line revealed by embryoid body formation in vitro*. Jpn J Vet Res, 1998. 46(1): p. 19-28.
- 92. Szabo, P. and J. Mann, Expression and methylation of imprinted genes during in vitro differentiation of mouse parthenogenetic and androgenetic embryonic stem cell lines. Development, 1994. 120(6): p. 1651-1660.
- 93. McKarney, L.A., M.L. Overall, and M. Dziadek, *Expression of H19 and Igf2 genes in uniparental mouse ES cells during in vitro and in vivo differentiation doi:10.1046/j.1432-0436.1996.6020075.x.* Differentiation, 1996. 60(2): p. 75-86.
- 94. Dighe, V., et al., *Heterozygous embryonic stem cell lines derived from nonhuman primate parthenotes.* Stem Cells, 2008. 26(3): p. 756-66.

- 95. Ferrari, D., et al., *Transplanted dopamine neurons derived from primate ES cells preferentially innervate DARPP-32 striatal progenitors within the graft.* Eur J Neurosci, 2006. 24(7): p. 1885-96.
- 96. Sanchez-Pernaute, R., et al., *Parthenogenetic dopamine neurons from primate embryonic stem cells restore function in experimental Parkinson's disease.* Brain, 2008. 131(Pt 8): p. 2127-39.
- 97. Sanchez-Pernaute, R., et al., Long-term survival of dopamine neurons derived from parthenogenetic primate embryonic stem cells (cyno-1) after transplantation. Stem Cells, 2005. 23(7): p. 914-22.
- 98. Kim, K., et al., *Histocompatible embryonic stem cells by parthenogenesis*. Science, 2007. 315(5811): p. 482-6.
- 99. Lengerke, C., et al., *Differentiation Potential of Histocompatible Parthenogenetic Embryonic Stem Cells*. Annals of the New York Academy of Sciences, 2007. 1106(1): p. 209-218.
- 100. Eckardt, S., et al., *Hematopoietic reconstitution with androgenetic and gynogenetic stem cells.* Genes Dev, 2007. 21(4): p. 409-19.
- 101. Swales, A.K.E. and N. Spears, *Genomic imprinting and reproduction*. 2005. p. 389-399.
- 102. Lyle, R., Gametic imprinting in development and disease. 1997. p. 1-12.
- 103. Wobus, A.M. and K.R. Boheler, *Embryonic Stem Cells: Prospects for Developmental Biology and Cell Therapy*. 2005. p. 635-678.

DISSERTATION CHAPTER 2

TITLE

MODULATION OF *H19* EXPRESSION IN PRIMATE

(*Cynomolgus macaque*) PARTHENOGENETIC

EMBRYONIC STEM CELLS (Cyno1 P-ESCs) USING *H19*shRNA

ABSTRACT

The non-human primate parthenogenetic embryonic stem cell line (Cyno1 P-ESC) was previously derived from a Macaca fasciculatis (also called Cynomolgus macaque) blastocyst created via artificial oocyte activation. A maternally derived parthenogenetic stem cell line does not require formation or destruction of a viable embryo, and therefore offers a valid alternative to the ethical and scientific challenges that bi-parental embryonic stem cells isolated from fertilized embryos pose to some members of society. However, the relative abundance of ectoderm tissues over mesoderm and endoderm in teratomas derived from parthenogenetically derived embryonic stem cells may limit their potential therapeutic applications. H19 is a paternally imprinted gene (i.e. maternally expressed) that encodes for an untranslated RNA linked to normal development whose expression in Cyno1 cells is upregulated. In addition, loss of H19 imprinting has been associated with several human diseases [104]. Thus, the objective of the present studies was to generate a transgenic Cyno1 cell line with suppressed H19 expression (Cyno1 H19shRNA), using the vector based shRNA system and use this cell line for comparisons of mRNA abundance of several known imprinted genes (H19, p57, IGF2, Peg10, and SNRPN) between transgenic Cyno1 H19shRNA cells, Cyno1 P-ESCs transfected with empty vector (Cyno1 Con.vector) and bi-parental Cyno1 cells (CMK6). We also aimed to determine the ability of the Cyno1 shRNA cells and control ones to differentiate in vivo, in teratomas, into derivatives of the three germ layers. expected, H19 mRNA levels in Cyno1 Con.vector cells were higher than in the biparental CMK6 cells. Knockdown of H19 mRNA in the Cyno1 H19shRNA cell line resulted in H19 mRNA expression similar to that observed in the biparental (CMK6) cell

line. A loss of imprinting of *IGF2* and *PEG10* in Cyno1 and Cyno1 H19shRNA cell lines was also observed. Future experiments are aimed towards investigating the differentiation potential of Cyno1 *H19*shRNA cells by teratoma formation. These experiments should help us elucidate the role of *H19* in differentiation of non-human primate parthenogenetic ES cells.

INTRODUCTION

A maternally derived primate parthenogenetic embryonic stem cell line (P-ESCs) does not require formation or destruction of a viable embryo, and therefore in the context of human embryonic stem (HES) cells, may offer a valid alternative to the ethical and scientific challenges that biparental embryonic stem cells (B-ESCs) isolated from fertilized embryos pose. Non-human primate P-ESCs have been derived from Macaca fascicularis (called Cyno1 P-ESCs) and from Rhesus Monkey- Rhesus P-ESCs [12, 15-16, 29, 94, 105]. When these cells are induced to differentiate they form cell derivatives from the three germ layers with a preference towards ectoderm and endoderm at the expense of mesoderm derivatives. This phenomenon is in part attributed to the monoparental origin of the cells. The lack of a paternal genome can contribute to a deregulation of imprinted genes. Deregulation of imprinted genes in mouse PgEs is viewed as the major barrier to parthenogenetic development to term and for the restricted developmental potential of the P-ESCs to mesoderm and endoderm derivatives. There are two major clusters of imprinted genes that have been extensively studied and primate P-ESCs. The first cluster is located on chromosome 11p15 and the other on chromosome 15p11-q13. H19 and IGF2, one of the most important genes for parthenogenetic development, are located on chromosome 11p15. As in mouse, in primates, H19 is a paternally imprinted gene (i.e. maternally expressed) that encodes for an untranslated mRNA linked to normal development and IGF2 is a paternally expressed (maternally imprinted gene).

SNURF/SNRPN, UBE3A and NDN are imprinted genes located on chromosome 15q11-q13 in primates and humans. SNURF/SNRPN and NDN are paternally expressed genes and UBE3A is a maternally expressed gene.

Mitalipov et al. and Dighe et al. have analyzed the expression patterns of H19 and IGF2 and SNURF/SNRPN genes and the methylation status of their imprinted control (ICR) regions in Rhesus monkey P-ESCs [29, 94]. Both groups reported significant upregulation of H19 gene in non-human primate P-ESCs tested. Moreover, IGF2 was also expressed in Rhesus Monkey P-ESCs which coincided with sporadic methylation pattern of the IGF2/H19 ICR region. The imprinting of SNURF/SNRPN gene was stably maintained and no expression was detected as expected for paternally expressed gene in bi-maternal genetic background. These results demonstrated that in vitro culture conditions and passaging can influence the epigenetic status of some of the imprinted genes such as H19 and IGF2. Nevertheless, despite their epigenetic instability, primate P-ESCs have been successfully differentiated into neuronal lineage in vitro, and upon transplantation into animal models, have exhibited lineage specific function and long term survival [17-18, 106]. Studies in mouse P-ESCs have revealed that in PGES cells both X-cromosomes are active which leads to genome wide hypomethylation. The genome wide hypomethylation can affect not only the imprinted genes expression but also can lead to aneuploidy due to extrusion of one of the X-chromosome. The loss of one of the X-cromosomes was reported as a natural attempt for dosage compensation [85]. The extent to which the imprinted genes and *H19*, in particular, can influence the differentiation potential of primate P-ESCs in embryo development in vivo, however, has not been extensively studied for several reasons. First the description of non human

primate P-ESCs has been relatively recent (Cibelli et al in 2001[15] and second, since the monkeys are the closest species to human, chimera experiments where primate P-ESCs are introduced into a primate embryo at early stage of development or chimeras between primate P-ESCs and embryo from other species have yet to be reported. Hence, teratoma formation is the readily available test, so far, to analyze the developmental potential of primate P-ESCs *in vivo*.

The main body of literature on the effect of imprinting on embryo development and parthenogenesis, in particular, come from studies of mouse uniparental fetuses. It was found that in mouse PgEs, the *H19* gene was over-expressed up to 400 times compared to biparental concepti [2, 71]. Moreover, deregulation of *H19* acts as a major barrier towards proper development of parthenogenetic embryos [2],[107],[108], [55]. Kono and co-workers showed that a 13 kb deletion encompassing the *H19* coding region and the upstream differentially methylated region (DMR) allows parthenogenetic embryos to develop to term [107]. The efficiency of full-term development significantly increases when the *H19/lgf2* DMR region together with the DMR region found within a second imprinted gene cluster *Dlk1/Dio3* on chromosome 12 are deleted [54, 109]. Most recently Hikichi *et al.* showed that the development of PG embryos can be extended following serial nuclear transfer and is associated with a decrease in *H19* expression [110].

Based on these findings in relation to the role of *H19* in PgE development and in mesoderm muscle differentiation, in particular, coming from mouse *in vivo* and *in vitro* studies [76, 79-80, 91, 111], we hypothesized that by modulating *H19* gene expression we could achieve a more homogeneous cell differentiation of Cyno1 P-ESCs into all 3

germ layers – ectoderm, mesoderm and endoderm, and muscle in particular, in a manner similar to their biparental counterparts.

To fulfill our goal, we developed a non-human primate parthenogenetic cell line from a Cynomolgus macaque blastocyst (Cyno1 P-ESCs). We sought to analyze the imprinted gene expression profile and the differentiation potential, in vivo, in teratomas, of wild type Cyno1 and in Cyno1 cells with suppressed H19 gene expression cells (Figure 2.6). Our data revealed re-activation of the paternally expressed gene PEG10 and IGF2. Consistent with previous reports in Rhesus P-ESCs, SNRPN expression in Cyno1 P-ESCs was not detected. The same was true for NDN gene expression, another paternally expressed gene. NDN was highly expressed in control CMK6 cells but not in Cyno1 cells. We also observed H19 to be overexpressed in Cyno1 P-ESCs. Teratomas from Cyno1 cells revealed high abundance of ectoderm germ layer followed by endoderm and mesoderm cartilage derivatives. However, no skeletal muscle development was observed (Figure 2.4). After downregulation of *H19* gene expression using a *H19* small hairpin (sh) RNA expressing vector system, we were able to achieve H19 mRNA expression levels, as measured by qRT-PCR, similar to that observed in control biparental (CMK6) cell line. Unfortunately, we were not able to proceed with using the Cyno1 cells with suppressed *H19* expression for further studies *in vivo*, in teratomas, due to high incidence of chromosomal aberration which rendered the cells karyotypically abnormal (Table 2.2). Nevertheless, the data provided here revealed that transgenic Cyno1 P-ESCs with stable down regulation of H19 can be generated in vitro. New lines of primate P-ESC Cyno1 or Rhesus monkey P-ESCs (Mitalipov[29, 94]) at lower passage

number will be used to test the effect of *H19* on the differentiation plasticity of primate P-ESCs *in vivo*.

MATERIALS AND METHODS

Cyno1 P-ESCs derivation and culturing

Monkey Parthenogenetic ES cells were derived from the inner cell mass (ICM) of a parthenogenetically activated embryos (PgEs) at blastocyst stage (Figure 2.2). The monkey oocyte donor was from Macaca fascicularis monkey also known as Cynomolgus monkey and therefore the P-ESCs derived were called Cyno1 P-ESCs. The protocol used for parthenogenetic oocyte activation and Cyno1 P-ESCs derivation was previously published by Cibelli et al in 2002 [15-16]. Briefly, the protocol for calls for the use of ionomycin for parthenogenetic activation of the oocyte followed by 6-DMAP which prevents the extrusion of the second polar body by inhibiting DNA synthesis and mitosis[112]. After removal of zona pellucida by brief pronase exposure, the PG blastocysts were cultured over mitotically inactivated mouse embryonic fibroblast (MEF) cells with DMEM F12 (Invitrogen) medium supplemented with 20% FBS-HI (Invitrogen, Carlsbad, CA), 2mM L-Glutamine (Invitrogen, Carlsbad, CA), 1% Non-essential Amino Acids (Invitrogen, Carlsbad, CA), 2-Mercaptoethanol (Sigma, St.Louis, MO), and 1x final volume of Penicillin-Streptomycin. After colonies appear (approximately after 2 weeks), they were mechanically removed and passed onto new MEF cells.

Human Embryonic Stem (HES) cells derivation and culture

HES were purchased from WiCell Research Institute (Madison, WI). HES cells were cultured over mitotically inactivated mouse embryonic fibroblast (MEF) cells with DMEM F12 (Invitrogen, Carlsbad, CA) medium supplemented with 20% Knock out Serum (Invitrogen, Carlsbad, CA), 2mM L-Glutamine (Invitrogen, Carlsbad, CA), 1%, Non-essential Amino Acids (Invitrogen, Carlsbad, CA), 4ng/ml FGF2 (Invitrogen, Carlsbad, CA), 2-Mercaptoethanol (Sigma, St.Louis, MO), Penicillin-Streptomycin, 1x final volume and cultured according to the manufacturer's recommendations. The human ES cells were mechanically passed onto new MEF cells during each passaging.

RNA isolation and cDNA synthesis

Total RNA from three biological replicates of wild type Cyno1, Cyno1 transfected with the H19shRNA expressing plasmid vector (Cyno1 H19shRNA) and Cyno1 cells transfected with the empty control plasmid vector (Cyno1 Con.vector) was extracted using Rneasy Kit (Qiagen, Valenica, CA) and residual genomic DNA was removed by DNAse I digestion, using the RNAse –Free DNAse Set (Qiagen, Valencia, CA) according to the manufacturer's instructions and observing strict RNAse and DNAse free procedures. Biparental Cyno1 (CMK6) cell lysed in Rneasy cell lysis buffer (Qiagen, Valencia, CA) were provided generously from Dr. Norio Nakatsuji (Institute for Frontier Medical Sciences, Kyoto University, Japan) and the RNA extraction was done following the manufacturer's recommendations. Additionally, following the same method as described above, we isolated total RNA from *Cynomolgus* monkey skin and testis and from teratoma derived from Cyno1 P-ESCs. Total RNA from all samples used was eluted from the purification column using 25 µl volume of nuclease free water (Ambion,

Austin, TX). Total mRNA amount was measured using Nanodrop. One ug of total RNA with OD260/280 > 2.1 was spiked with 1μl of 250fg/ μl of HcRed1 synthetic RNA as an exogenous control and then used for first strand cDNA synthesis. For first strand cDNA synthesis, Superscript II (Invitrogen, Carlsbad, CA) and anchored Oligo (dT₁₂₋₁₈) primers (Invitrogen, Carlsbad, CA) were used following the manufacturer's instructions in a final total volume of 20μl. For quantitative Real Time PCR (qRT-PCR), each Reverse Transcription (RT) reaction was then diluted with nuclease free water (Ambion, Austin, TX) to a final volume of 100μl.

In Vitro Transcription and RNA quantification

For synthesis of far-red fluorescent protein (HcRed1) cRNA, linear DNA templates having a SP6 promoter sequence at the 5'end and poly(T₁₈) tail on the 3'end were generated by polymerase chain reaction (PCR) from plasmid vector pHc-Red-Nuc (BD Bioscience, San Jose, CA). The conditions for cRNA synthesis are described elsewhere (Bettegowda et al, 2006, Molecular Reproduction and development). The RNA quality and quantity were estimated using an Agilent Bioanalyzer 2100 RNA 6000 nanochip (Agilent Technologies, Palo Alto, CA).

Absolute Quantitative Real –Time PCR

The quantification of all gene transcripts was performed by absolute real-time quantitative RT-PCR using SYBR Green PCR Master Mix (Applied Biosystems, Foster City, CA). Absolute quantification using this method is described elsewhere (Li and Wang, 2000; Whelan et al., 2003). Primers for absolute real time PCR were designed

using Primer Express program (Applied Biosystems, Foster City, CA) and derived from mouse sequences found in GeneBank. A primer matrix was performed for each gene tested to determine optimal concentrations. Each reaction mixture consisted of 2 μ l of cDNA, optimum concentration of each forward and reverse primer, nuclease free water, and 12.5 μ l of SYBR Green PCR Master Mix in a total reaction volume of 25 μ l (96well plates). Reactions were performed in duplicate for each sample using an ABI Prism 7000 Sequence Detection System (Applied Biosystems, Foster City, CA). The thermal cycle consisted of 40 cycles of 95°C for 15sec and 60 °C for 1min. Standard curves for each gene and controls were constructed using tenfold serial dilutions of corresponding plasmids and run on sample plates as standards. For gene expression, normalization the expression levels of beta actin (β -actin) were used. To monitor for the technical accuracy and reproducibility of our RNA extraction and qRT-PCR efficiency, HcRed expression levels were monitored.

Copies of HcRed 1 and b-actin RNA in each pool were determined using standard curves constructed from the plasmid pHc-Red1-Nuc and PCR2.1 plasmid (Invitrogen Life Technologies, Carlsbad, CA), containing the β -actin sequenced product. Real-time primer sequences for HcRed1 were designed elsewhere (Bettegowda et al, 2006). Partial cDNA sequences for *H19*, β -actin and other genes tested (Table2.1), were amplified from mouse Cyno1 ES cells cloned into pCR2.1 Topo vector (Invitrogen Life Technologies, Carlsbad, CA), and subjected to fluorescent dye primer sequencing to confirm identity. From the resulting plasmids were construct standard curves. Representative R² for *HcRed1*, *H19* and the rest of the genes will be estimated and only the one \geq 0.98 will be used. For each measurement, threshold lines will be adjusted to

intersect amplification lines in exponential portion of amplification curve (Bettegowda et al). For each sample amounts of mRNA (copies) for β -actin and HcRed1 were determined from their respective standard curves.

Plasmid shRNA delivery system

For the plasmid shRNA delivery, pRNAT- U6.1/Neo vector was used (GenScript, Piscataway, NJ). In this vector system the *H19* shRNA was expressed from U6 promoter and GFP and Neomycin expression were driven by CMV promoter. The pRNAT- U6.1/Neo *H19* shRNA vector was linearized by using a unique Scal (NEB, Ipswich, MA) restriction site and transformed into Cyno1 cell line by using Fugene6 transfection reagent (Roche, Basel Switzerland) according to the manufacturers' recommendations. Stable transgenic cell line was selected by using 100ug/ml of Neomycin for 14 days.

Teratoma formation

A suspension of approximately 2x10⁶ Cyno1 P-ESCs was injected subcutaneously into immune-deficient Nude mice, CD-1 (Charles River Laboratories, Wilmington, MA). Euthanasia was done following AAALAC's guidelines. One tumor was isolated and examined macroscopically. Diameter was recorder to be 0.8 cm. Subsequently, the tumor was fixed in paraformaldehyde, embedded in paraffin and stained with hematoxylin eosin. Contribution of the different tissue types in the tumor was determined under the microscope in 100 different fields.

We did not proceed to inject the Cyno1 H19shRNA or Cyno1 Con.vector cells due to their cytogenetic abnormalities which identified the cells as karyotypically unstable with multiple chromosomal aberrations (see Table2.2).

We also did not injected CMK6 cells since the lab that has established the CMK6 cell line, led by Dr. Norio Nakatsuji, agreed upon sending only lysed cells for RNA isolation and transcription analysis.

Immunocytochemistry

Cells were washed 3 times, each time 5 minutes with washing buffer (DPBS, 0.1% TX100 (Triton 100X) and incubated with Permeabilization Buffer (DPBS, 1% TX100) for 10 min. Subsequently, the cells were washed once more with washing buffer, then blocked with blocking buffer (DBPS + 0.1%TX100 + 1%BSA + 10%NGS) for 1-2 hours. Oct4 antibody (Santa Cruz Biotechnology, inc Santa, Cruz, CA.) in dilution 1:300, SSEA4 (R@D Systems, Minneapolis, MN) in dilution 1:500 and HuNu (Millipore, Billerica, MA) in 1:500 was added to the cells and incubated for 3 hours to overnight at 4C. Cells were washed 6 times each time 10minutes. Then secondary Ab (Abcam, Cambridge, MA) was added in 1:500 dilutions following the manufacturer's recommendations.

Immunohystochemical analysis of formalin fixed, paraffin embedded tumor sections

Hematoxylin-Eosin staining

Tissue samples previously fixed in 10% Neutral Buffered Formalin were processed embedded with the ThermoFisher HistoCentre III embedding station. The blocks were sectioned at 4-5 microns. Sections were stained with Hematoxylin and Eosin (H and E).

Statistics

qRT-PCR experimental data and teratoma quantification data were analyzed by analysis of variance (ANOVA) procedure using the mixed procedure of SAS (Cary, NC, USA). Differences of p < 0.05 were considered statistically significant

RESULTS AND DISCUSSION

Alteration of key imprinted genes in P-ESCs

For our initial experiments looking at *H19* and *IGF2* gene expression levels in Cyno1 PGES cells, we used HES cells as biparental control cell line. The reason was that at that time we did not have Cynomolgus macaque derived biparental cell line in our laboratory. The evolutionary proximity of the two species justified the use of human ESCs.

It has been reported that in mouse and Rhesus P-ESCs, *H19* is highly overexpressed. Consistent with these findings, our qPCR expression data revealed that in Cyno1 P-ESCs, *H19* mRNA levels were higher than that in the biparental HES cells (Figure 2.3). Our qPCR data also revealed *IGF2* to be also highly expressed in Cyno1 P-ESCs (Figure 2.3). We did not analyze further the mechanism of *IGF2* loss of imprinting, but data coming from the literature suggest that cell culture conditions and prolong passaging can alter the epigenetic status of the cells and lead to loss of imprinting [113].

We also looked at the expression pattern of *H19* and *IGF2* in cells derived from Cyno1 P-ESCs teratomas (Figure 2.3), Cyno1 skin and Cyno1 testis. We found that *H19* and *IGF2* were the most highly overexpressed in teratomas derived from Cyno1 P-ESCs. *IGF2* and *H19* expression was also detected in Cyno1 testis; however *IGF2* expression in testis was significantly higher than the expression of *H19* gene. Upon terminal differentiation into skin fibroblast, both mRNA abundance of *H19* and *IGF2* was very low but detectable.

The data presented above revealed *H19* to be highly overexpressed in Cyno1 P-ESCs and in cells derived from Cyno1 P-ESCs teratomas compare to control biparental HES cells, Cyno1 testis, and Cyno1 skin fibroblast cells (Figure2.3). *IGF2* was also highly expressed in Cyno1 P-ESCs, and Cyno1 derived teratomas followed by Cyno1 testis. As the cells proceed to terminal differentiation into skin, the expression levels of both *H19* and *IGF2* become barely detectable. The high expression levels of *H19* and *IGF2* in Cyno1 P-ESCs derived teratomas indicate that during differentiation *in vivo*, into teratomas, the expression pattern of *H19* and *IGF2* remain high as in the P-ESCs from which the teratomas were derived (see Figure2.3C-E)

Teratomas derived from P-ESCs give rise to a lower proportion of mesoderm derived muscle compared to tumors derived from B-ESCs

Cyno1 P-ESCs are pluripotent in that they stain positive for the pluripotency markers

Oct4 and SSEA4 (Figure2.2C-D). Staining of the cells with HuNu antibody to confirmed
the primate identity of the cells upon their derivation (Figure2.2E). Next we perform an
in vivo pluripotency assay by testing the ability of Cyno1 P-ESCs, upon teratoma

formation, to give rise to derivatives of all three germ layers –ectoderm, endoderm and mesoderm. We injected Cyno1 P-ESCs subcutaneously into immunodeficient Nude mice-CD-1 (see Materials and Methods). A teratoma was recovered, formalin fixed and paraffin embedded. The teratoma was then sectioned into 4-5 microns sections and H&E stained. Macroscopic examination of the teratoma sections revealed that morphologically it consisted of terminally differentiated tissues with very little contribution of mitotically dividing cells. There was a high abundance of ectoderm derived neural epithelium, followed by mesoderm derived cartilage and endoderm derived primitive glandular structures (Figure2.4). No mesoderm derived skeletal muscle was identified. Therefore, we concluded that Cyno1 P-ESCs are pluripotent and have the potential, when differentiated *in vivo*, into teratomas, to give rise to derivatives of all three germ layers ectoderm, endoderm and mesoderm. However, Cyno1 P-ESCs exhibit limited differentiation potential into mesoderm muscle derivatives.

Downregulation of H19 expression in Cyno1 ES cells

We designed an H19shRNA expressing vector system. The H19shRNA was expressed under the control of U6 promoter of pRNAT-U6.1 vector (GenScript Corporation). The pRNAT-U6.1 also encoded a green fluorescent protein (GFP) under the control of CMV promoter. This feature allowed us to monitor the transfection efficiency of the H19shRNA vector during the Neomycin selection for stable H19shRNA expressing cell line (Figure 2.5).

PCR and qRT-PCR data revealed that *H19* was stably downregulated in Cyno1 PGES cells transfected with the H19shRNA expressing vector (Cyno1 H19shRNA) compare to

Cyno1 PGES cells transfected with control empty vector (Cyno1 Con.vector)
(Figure2.5C and Figure2.6A). *H19* mRNA abundance in Cyno1 H19shRNA cells was similar to that of control biparental CMK6 cells (Figure2.6A). *IGF2* mRNA expression in Cyno1 H19shRNA cells was lower than in Cyno1 and CMK6 cells, but the level of *IGF2* mRNA in Cyno1 cells was significantly higher than that in the CMK6 cells. *PEG10* mRNA abundance in Cyno1 and Cyno1 H19shRNA cells was low but detectable compared to robust expression in CMK6 cells. *P57* mRNA abundance in Cyno1 H19shRNA cells was lower compared to Cyno1 and CMK6 cells, but the expression level of *P57* in Cyno1 cells was higher than that in the biparental CMK6 cells. *SNRPN* and *NDN* mRNA expression in Cyno1 Con.vector and Cyno1 H19shRNA cells was undetectable.

In conclusion, we were able to downregulate the *H19* levels in Cyno1 P-ESCs to levels similar to control biparental CMK6 Cyno1 cells.

Our data also indicated that with the exception of *IGF2*, the expression levels of the paternally expressed gene *SNRPN* were barely detectable while *PEG10* and *NDN* expression was not detected as expected according to their maternal imprinting status. The mRNA abundance of *P57*, a maternally expressed gene, was overexpressed in Cyno1 P-ESCs compare to that in biparental CMK6 cells, as expected, with or without suppressed *H19* gene expression.

CONCLUSION

Non-human primates are evolutionary the closest species to human and therefore, primate PGES cells offer an invaluable tool for studying the effect of imprinting on development and differentiation and the efficiency of engraftment and survival of P-ESC derived tissues.

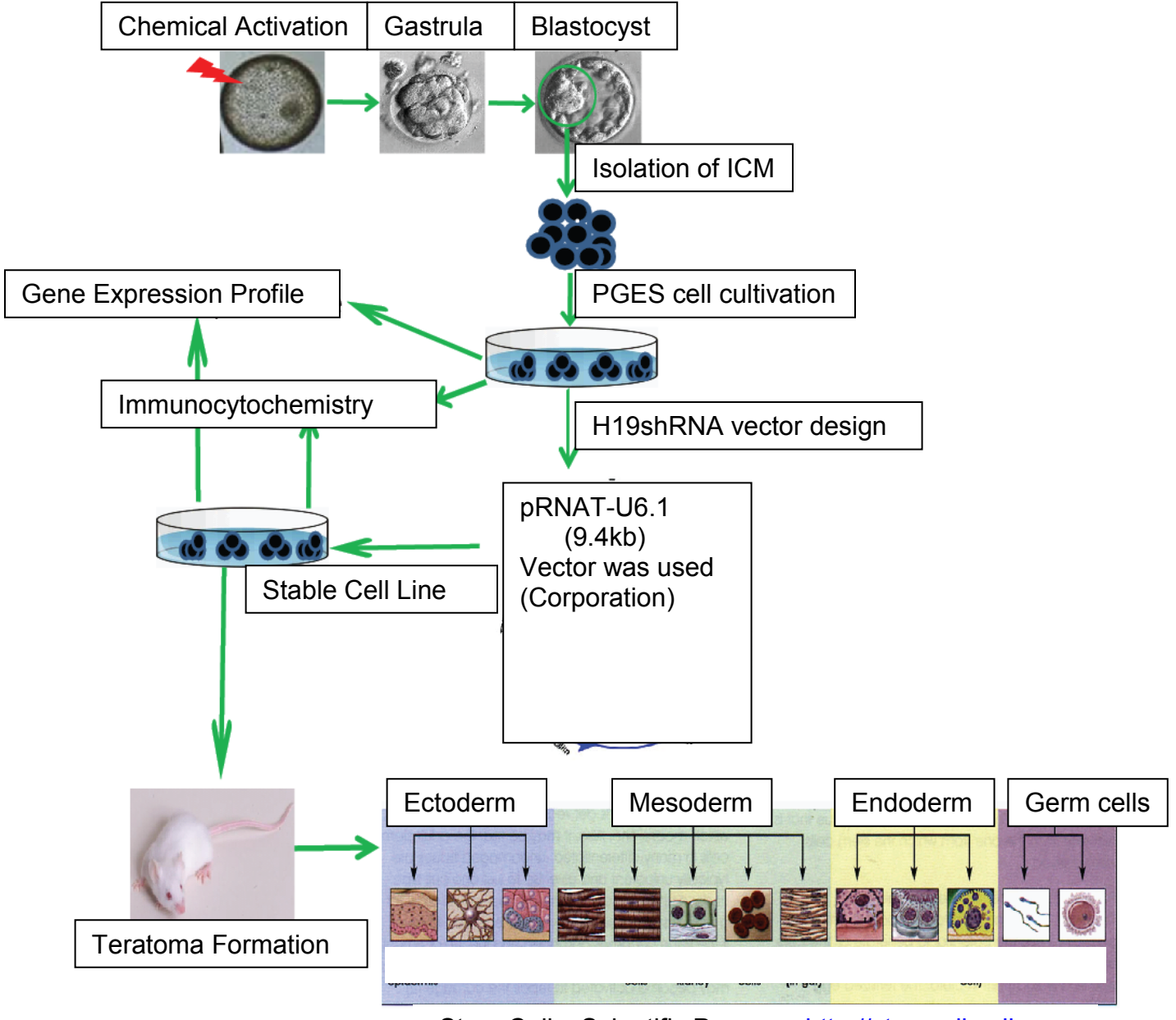
In our study we aimed to analyze the imprinted gene expression profile of IGF2 before and after suppression of H19 gene expression as well as the expression of P57, NDN, PEG10 and SNRPN in H19shRNA Cyno1 and Cyno1 Con.vector P-ESCs. H19 and P57 are maternally expressed (i.e paternally imprinted) genes and IGF2, NDN, PEG10 and SNRPN are paternally expressed (maternally imprinted) genes. Interestingly qRT-PCR data from Cyno1 PGES cells derived teratomas indicated that the expression of the imprinted genes is maintained during the differentiation of these cells in vivo. This data suggest that once established in the ES cell line, the imprinting status of some genes remains stable during differentiation, at least under the teratoma assay conditions. We also found that Cyno1 P-ESCs are pluripotent. They stained for the pluripotency markers OCT4, SSEA4 and upon differentiation in vivo, in teratomas, they give rise most exclusively to terminally differentiated tissues from all three germ layers – ectoderm, endoderm and mesoderm. These findings indicate their benign origin which emphasize on the feasibility of using Cyno1 P-ESCs for generation of terminally differentiated tissues for transplantation. Indeed, Cyno1 P-ESCs derived neurons were able, upon transplantation in vivo, to express dopamine and serotonin. They were also electrophysiologically active and exhibited long term survival upon transplantation into primate models of Parkinson disease [17-18, 106].

Scientific reports coming from mouse P-ESCs studies in vitro and in vivo have revealed that *H19* is the most over expressed gene in mouse PGES cells and PgEs. It has been also demonstrated that H19 is critical for PgE development to term since 13 kb deletion encompassing H19 coding and upstream DMR region allowed for parthenogenetic embryo to develop to term. When mouse P-ESCs are injected into wild type chimeras, their contribution to muscle tissue is restricted[79]. Moreover we and others have shown that teratomas derived from P-ESCs consist of predominantly ectoderm derivatives with very little muscle contribution around 5%, (Cibelli unpublished) compare to teratomas derived from biparental mouse P-ESCs -20% (Cibelli unpublished). We also showed that upon suppression of *H19* gene expression, mouse PGES cells exhibit increased differentiation potential to mesoderm muscle compare to wild type P-ESCs and more similar to normal biparental mouse P-ESCs controls (Cibelli unpublished). Consistent with these findings in mouse models, teratomas derived from our Cyno1 PGES cells did not exhibit muscle derivatives. In order to study the effect of the imprinted genes, and H19 in particular, on the mesoderm muscle development in primate Cyno1 P-ESCs, we derived a transgenic Cyno1 H19shRNA cell line with stable suppression of the H19 gene expression by using a shRNA expressing vector. Knockdown of H19 mRNA in the Cyno1 H19shRNA cell line resulted in H19 mRNA expression similar to that observed in the biparental CMK6 cell line. Unfortunately due to the multiple cytogenetic abnormalities of the Cyno1 P-ESCs we were unable to test the differentiation potential of the transgenic Cyno1 H19shRNA cell line in vivo. New Cyno1 cell lines, at lower passage number will be utilized in the future to fulfill this goal. We expect that downregulation of H19 will reverse the dearth of mesoderm derived muscle and will

allow for more complete differentiation potential of the Cyno1 P-ESCs similar to that of their normal biparental counterparts. This study will help elucidate the effect of imprinting on cellular differentiation in general and will increase the efficiency of primate Cyno1 P-ESCs for future application in the transplantation medicine.

FIGURES AND TABLES

Figure 2.1 Experimental Outline (part of the figure was adopted from "Stem Cells: Scientific Progress http://stemcells.nih).



Stem Cells: Scientific Progress http://stemcells.nih.gov
Germ Layers Derivation

Figure 2.2 Derivation (A-B) and Immunocytochemical staining (C-E) of Cyno1 P-ESCs; Parthenogenetically activated Cyno1 oocytes (A), Cyno1 P-ESCs morphology (B), OCT4 (C), SSEA4(D) and HuNu (E) Immunocytochemical staining.

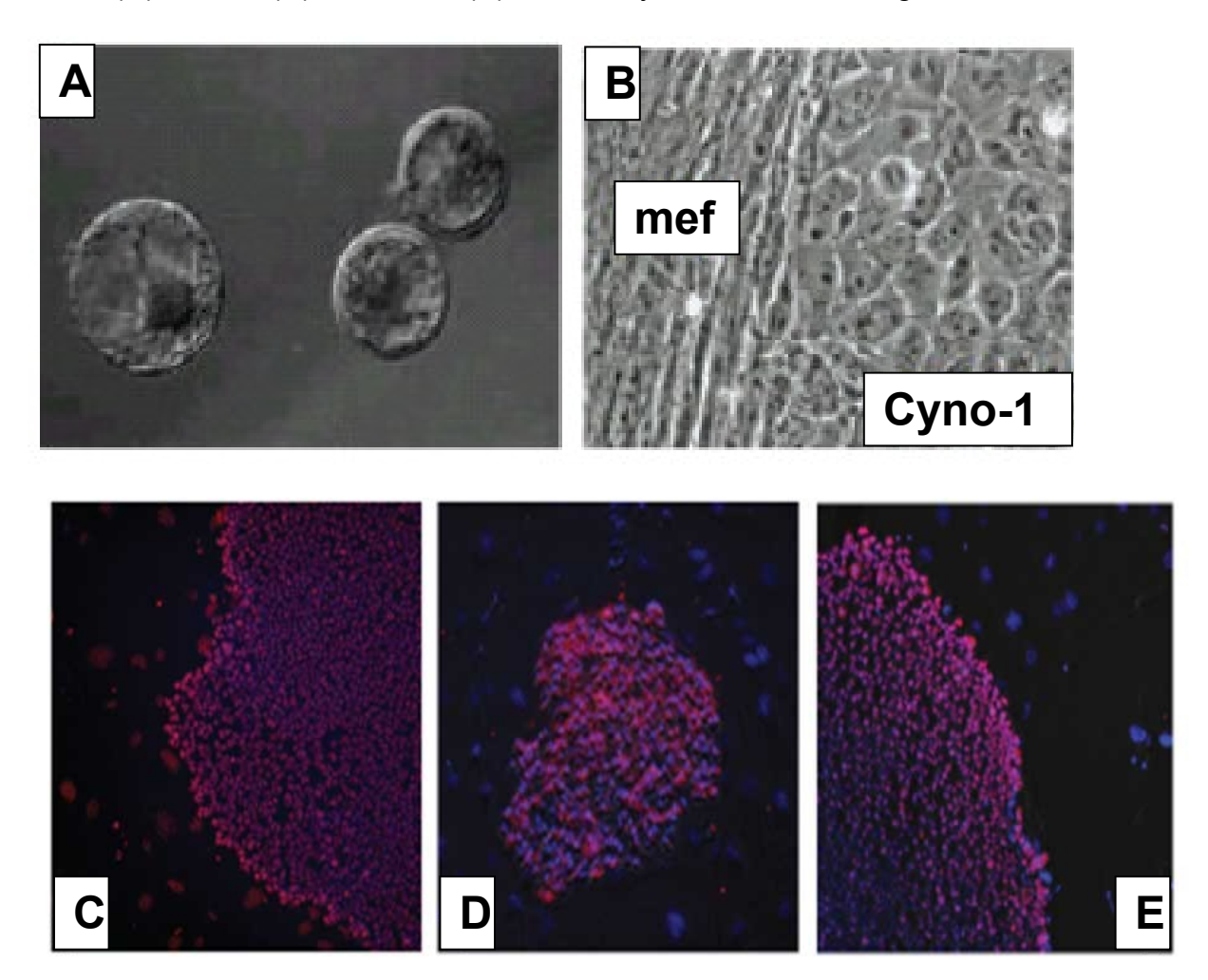


Figure 2.3 qRT-PCR Analysis of the expression levels of HcRed (A) and beta actin (B) and the maternally expressed *H19* (C) and paternally expressed *IGF2* (D,E) genes. The mRNA abundance of all the genes was normalized to beta actin control, n=3 (P<0.05). *HcRed* was used to assay for technical efficiency only. The bars represent stand error bars. All the letters above the error bars represent the difference between samples on the basis of standard error values (P<0.05).

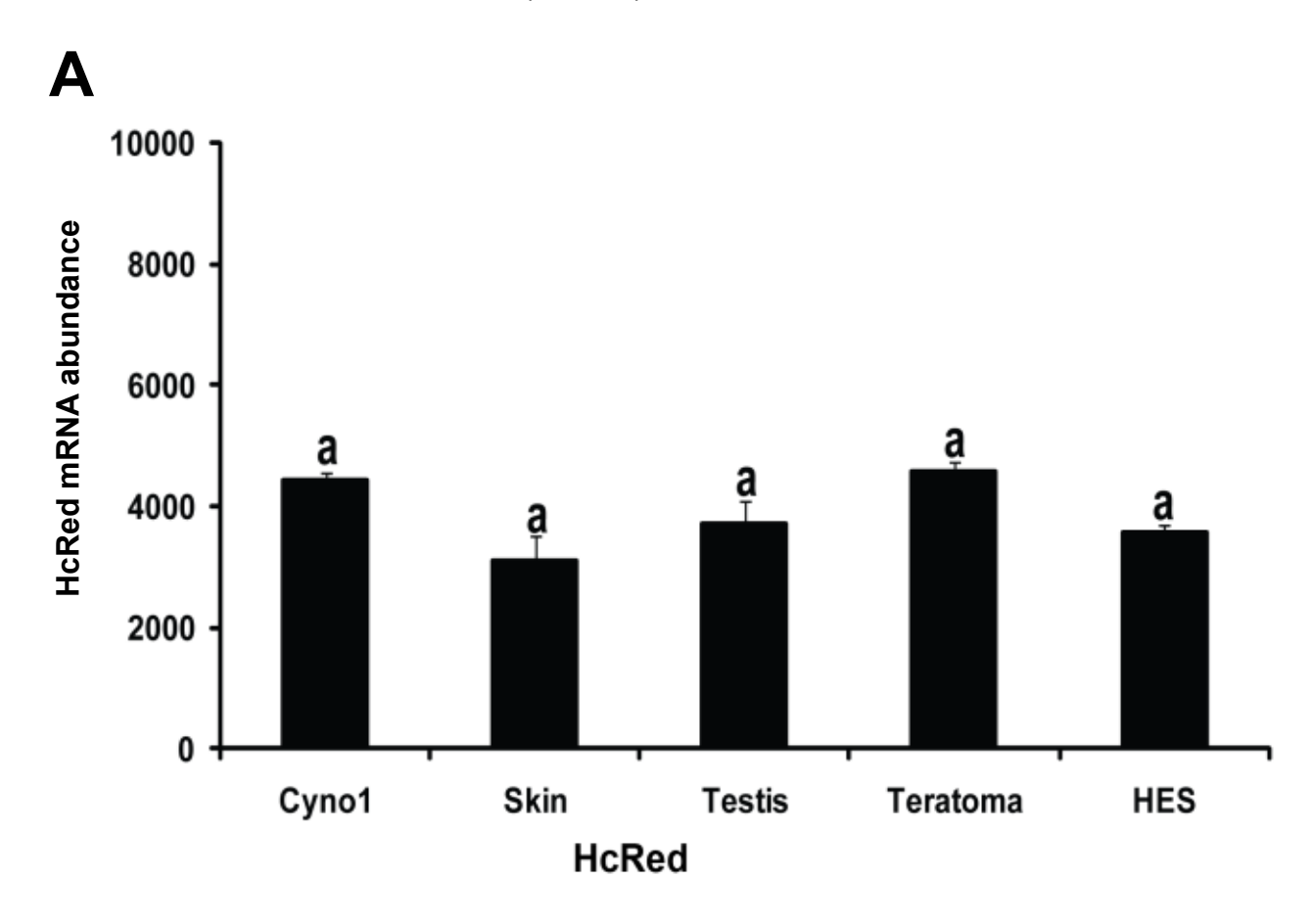


Figure 2.3 (cont'd)



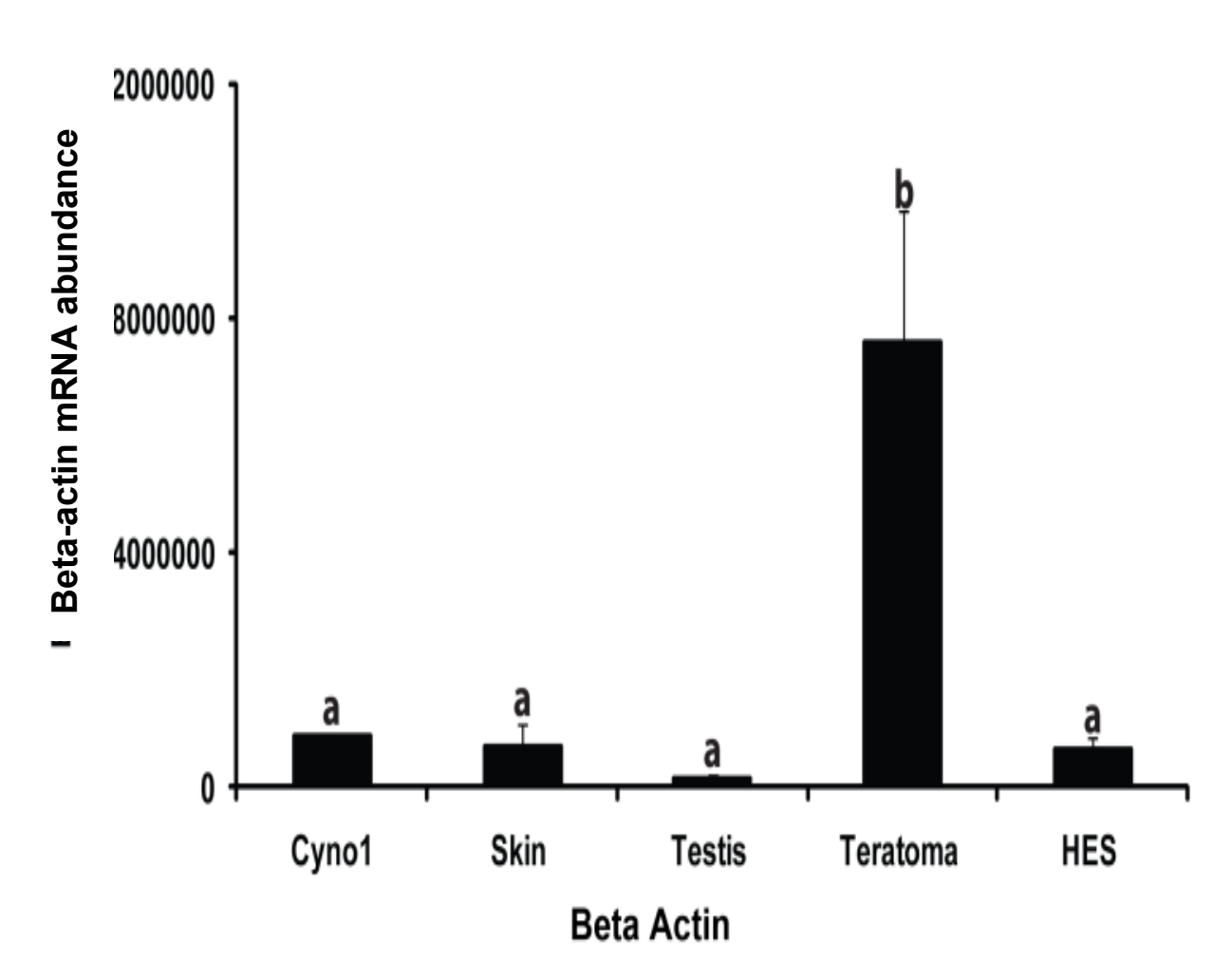
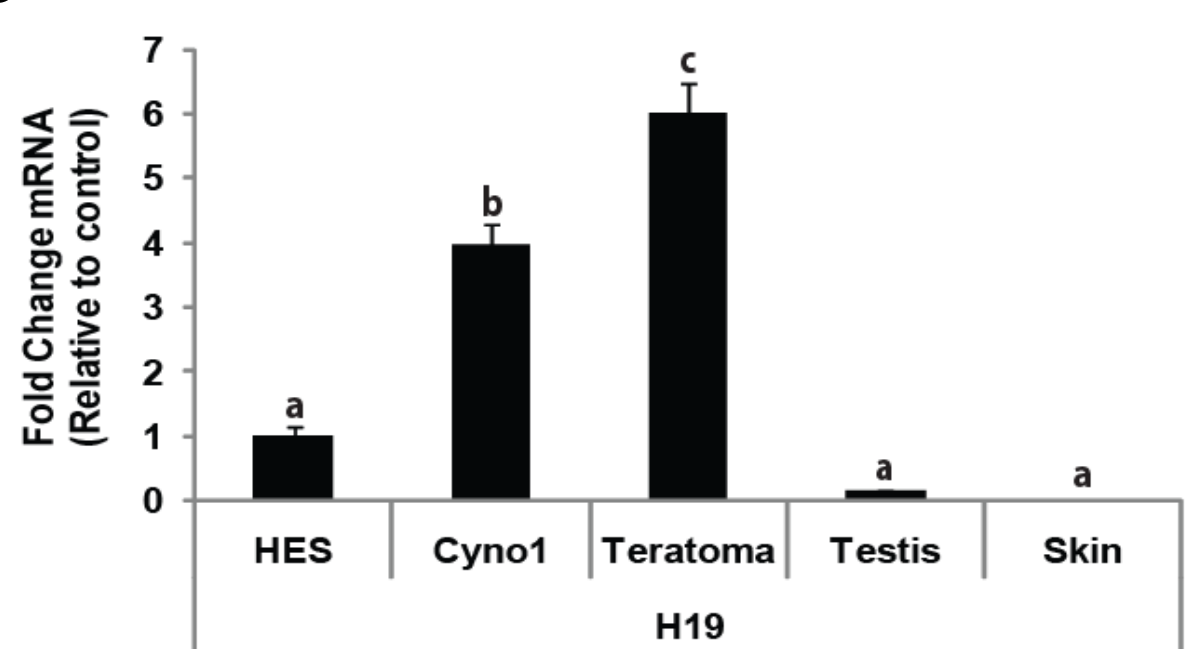


Figure 2.3 (cont'd)







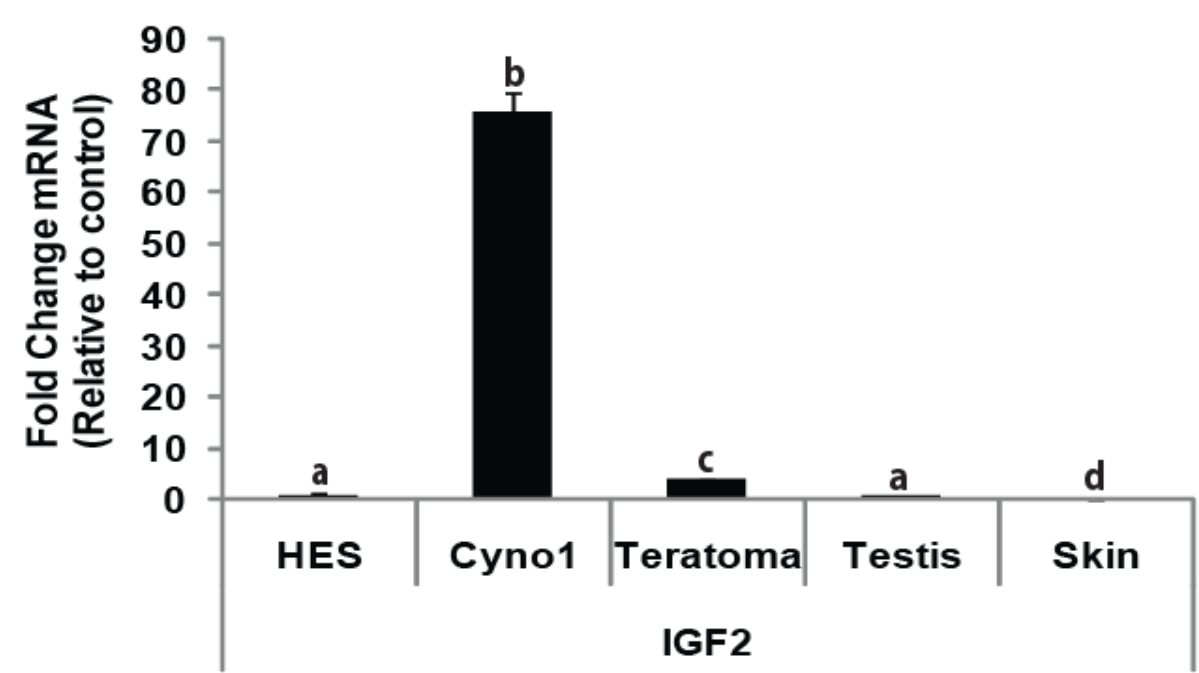


Figure 2.3 (cont'd)

Ε

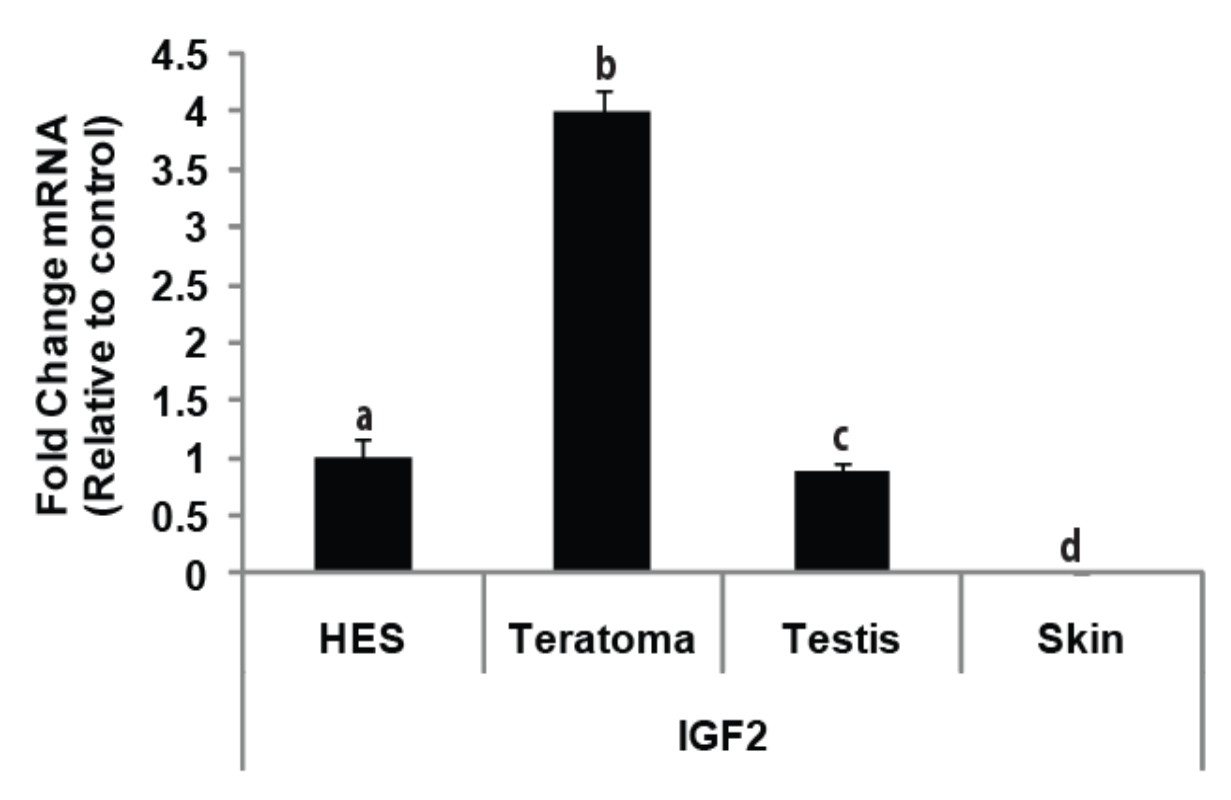


Figure 2.4 Teratomas from Cyno1 P-ESCs give rise to derivatives of all three germ layers- ectoderm, endoderm, and mesoderm (A-K); C -10X, A,B, D, E, F, G, J -20X, H, I, K-40X, ctr- cartilage, sm- smooth muscle, nt- neural tissue, gl- glandular structures, eps- ependymal papillary structures (ciliated epithelia).

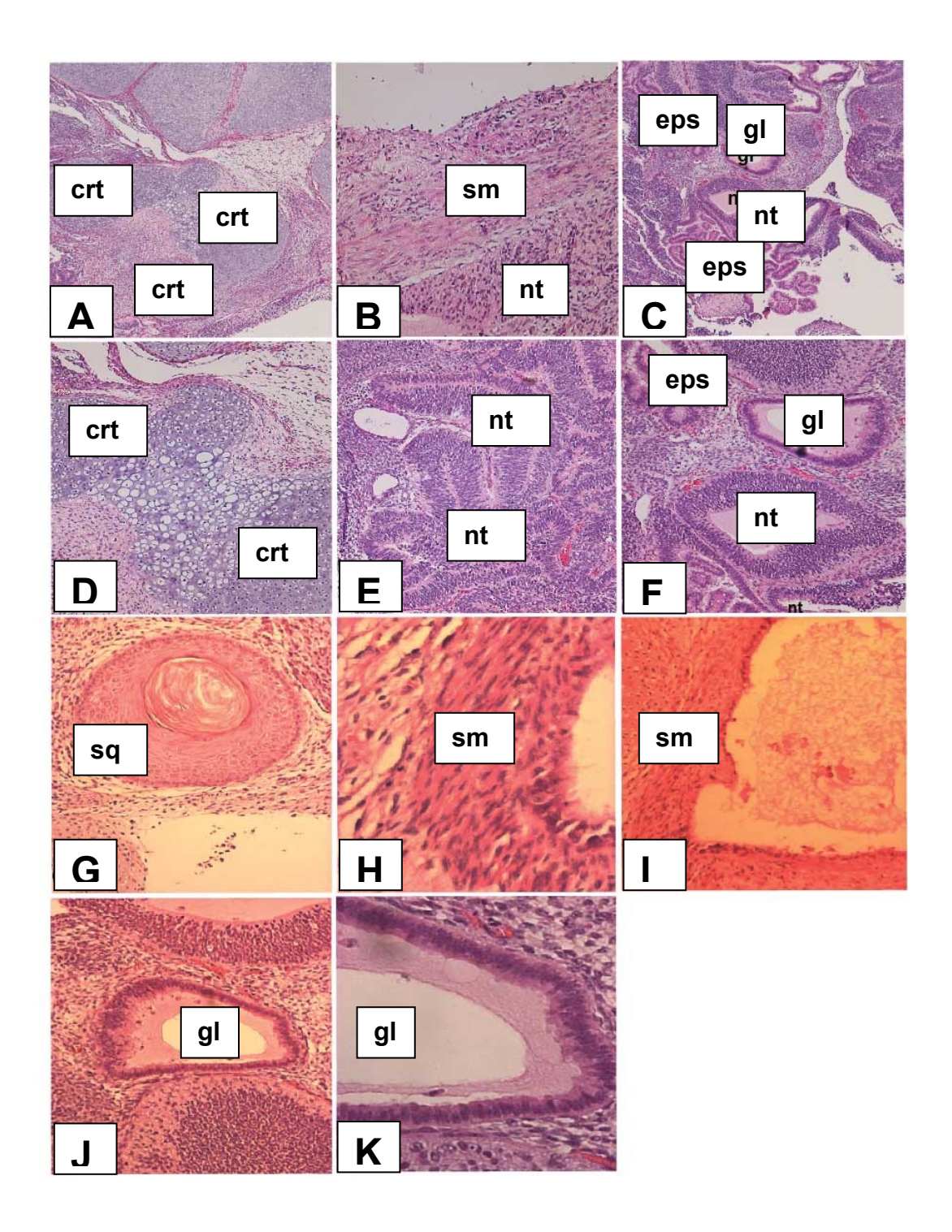
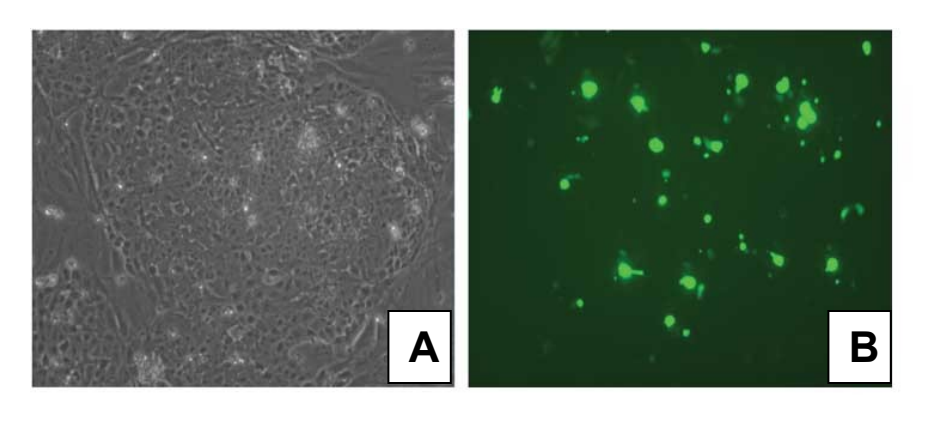


Figure 2.5 Downregulation of *H19* in Cyno1 P-ESCs. Cyno1 P-ESC colony stably transfected with *H19*shRNA expressing vector, 14days post Neomycin selection (A-B). A. Bright Field, B. Green Fulorescence expression from H19shRNA trasnfected plasmid vector. C. PCR gel electrophoresis for detection of *H19* expression (Lanes 1 and 4) using beat actin as control (Lanes 2 and 5). Lane 1 and 2- Cyno1 P-ESC Con.vector, Lane 4 and 5- H19shRNA Cyno1, Lane 7 Marker (M) -1 kb Plus DNA ladder.



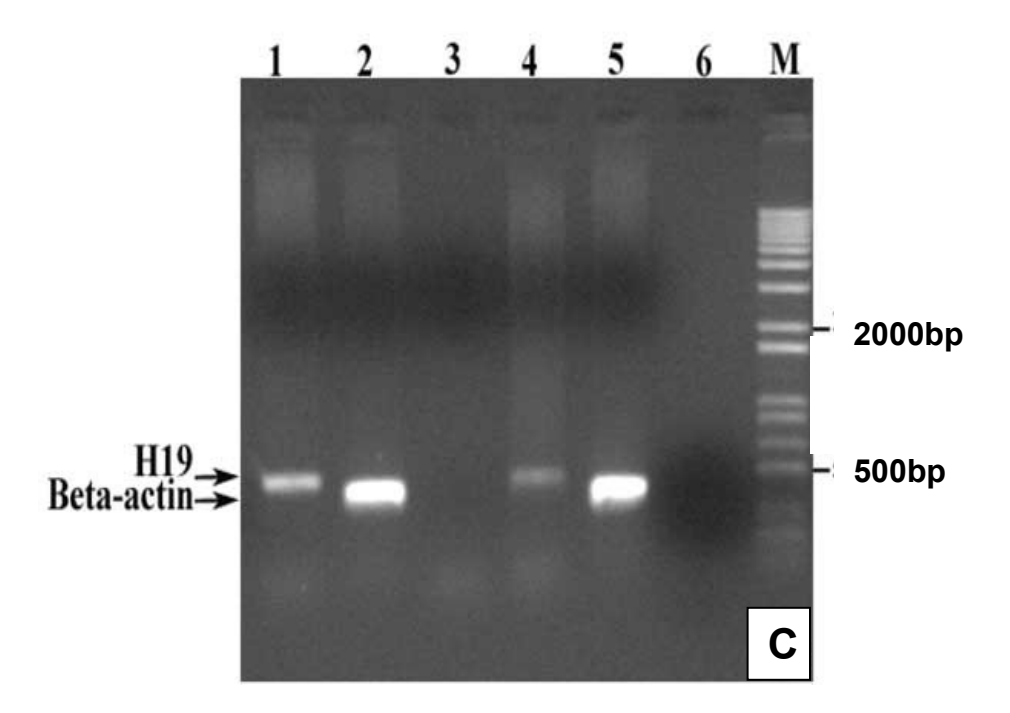


Figure 2.6 qRT-PCR Analysis of the expression levels of the maternally expressed *H19* and *P57* (Figure 2.5A and E respectively) and paternally expressed *IGF2*, *NDN*, *PEG10* and *SNRPN* (Figure 2.5B, C, D and F respectively) genes. The mRNA abundance of all the genes was normalized to beta actin control; for all runs n=3 (P<0.05). The bars represent stand error bars. All the letters above the error bars represent the difference between samples on the basis of standard error values (P<0.05).

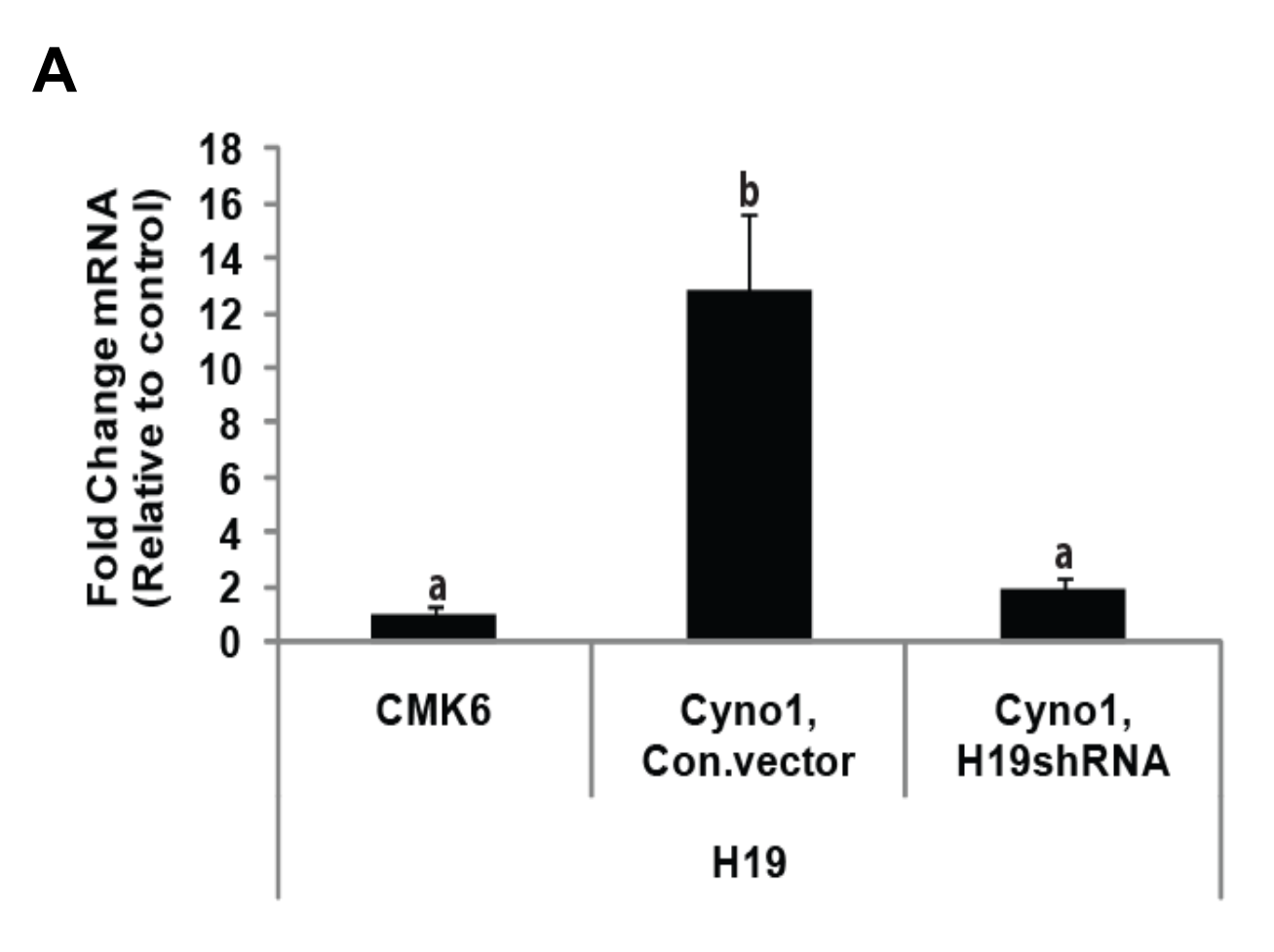


Figure 2.6 (cont'd)

В

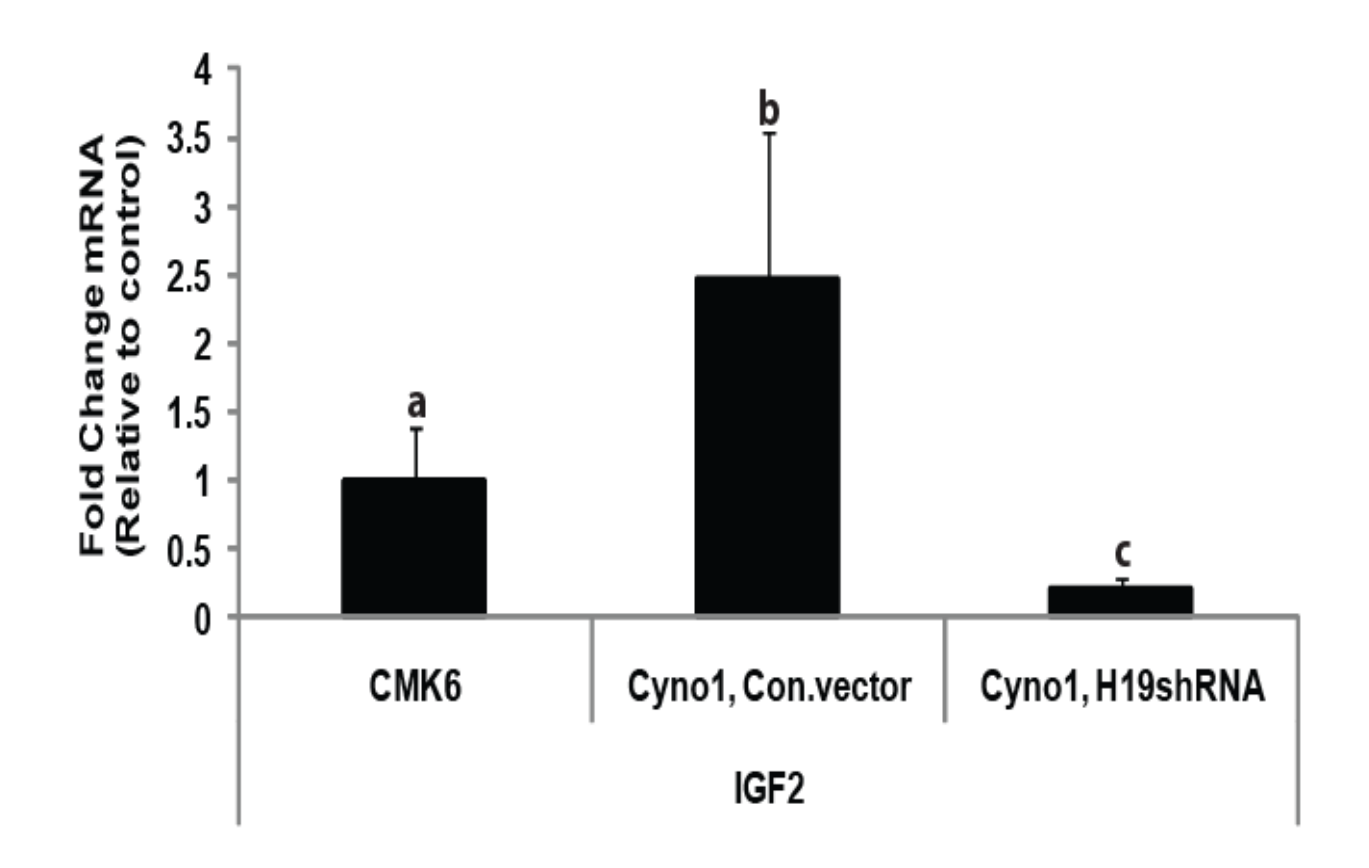


Figure 2.6 (cont'd)



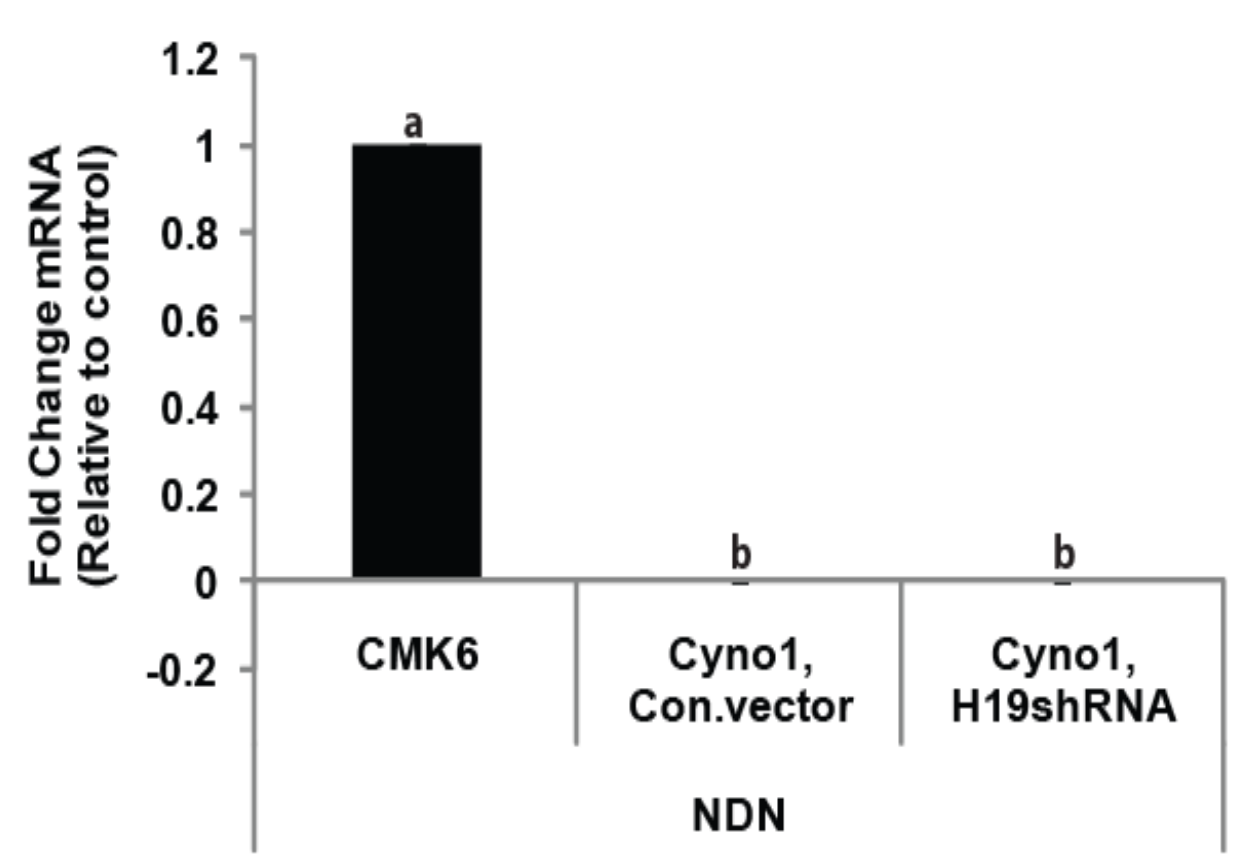


Figure 2.6 (cont'd)

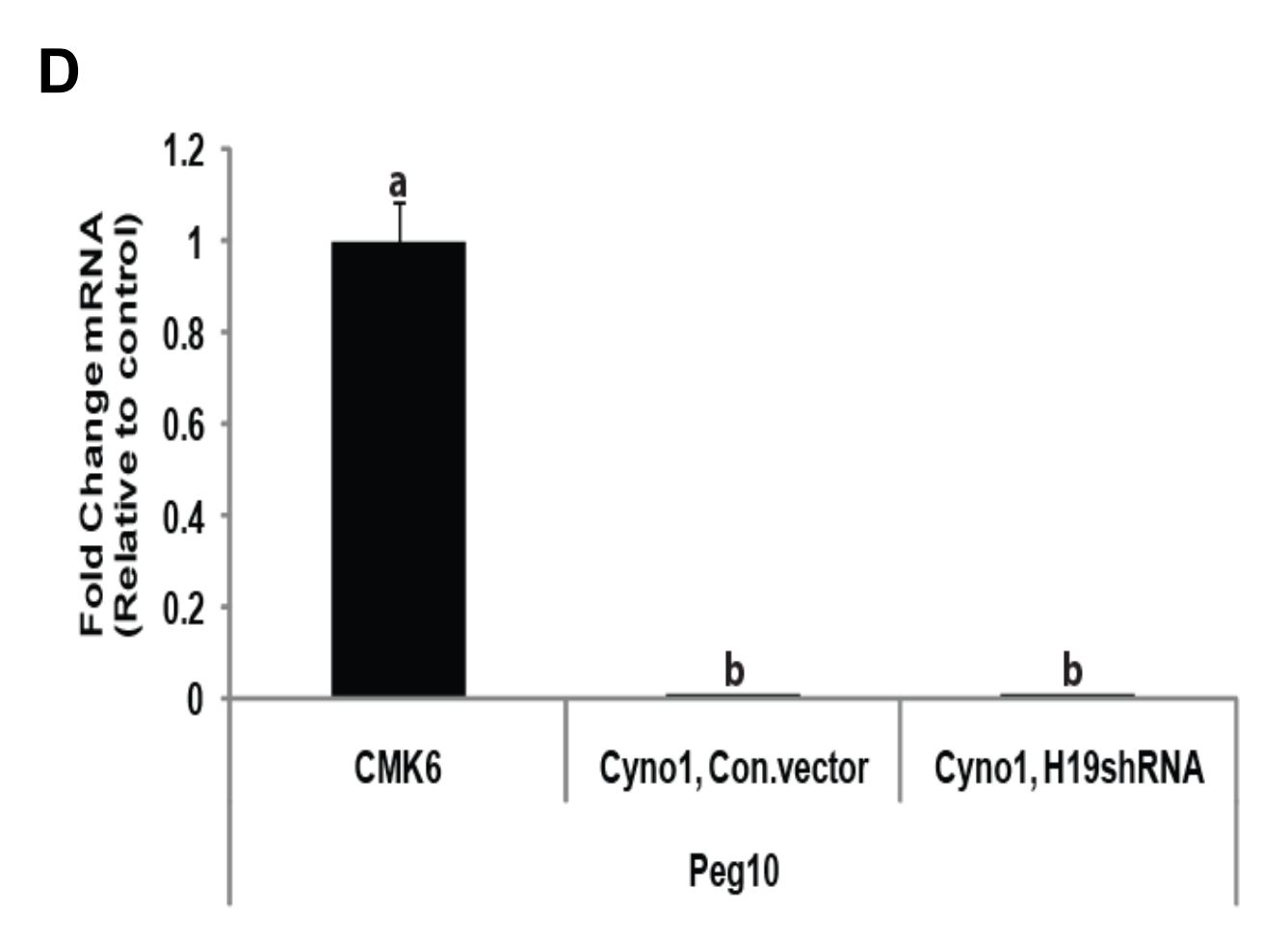


Figure 2.6 (cont'd)



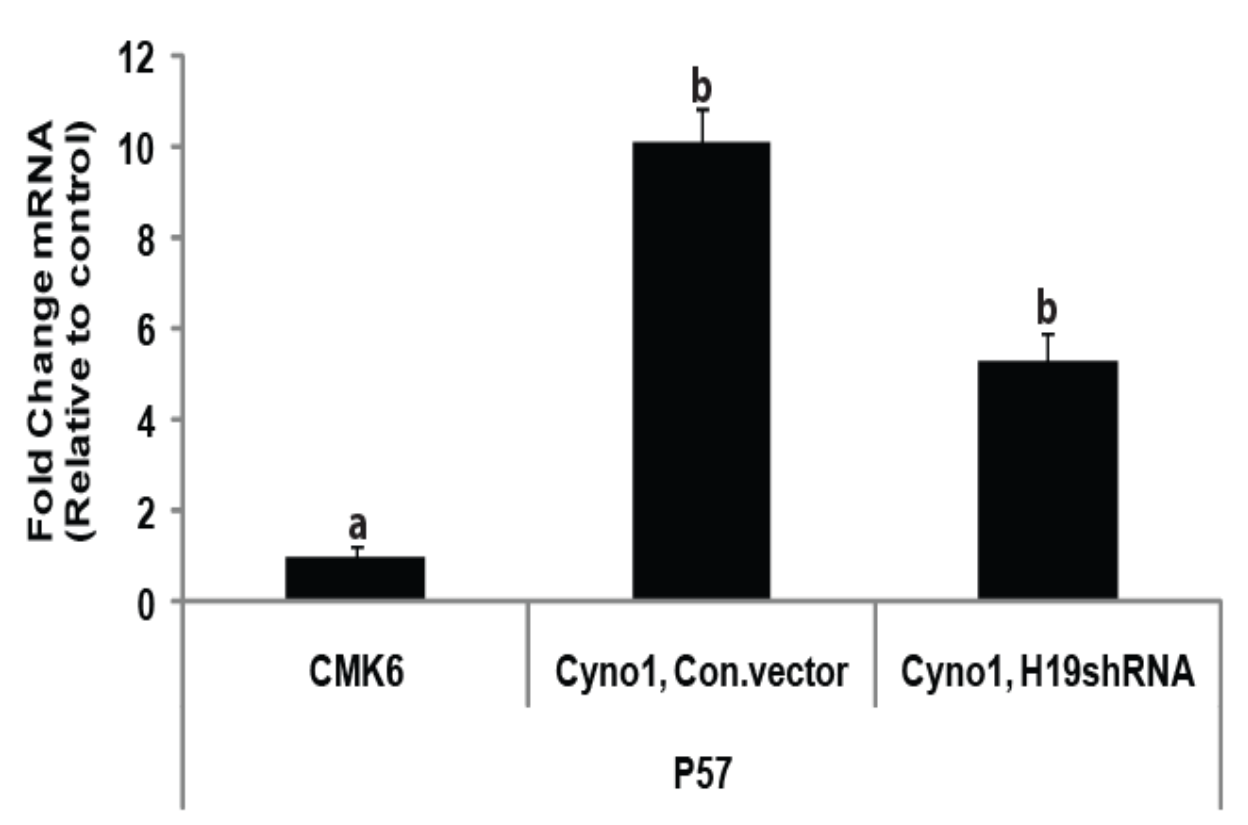


Figure 2.6 (cont'd)



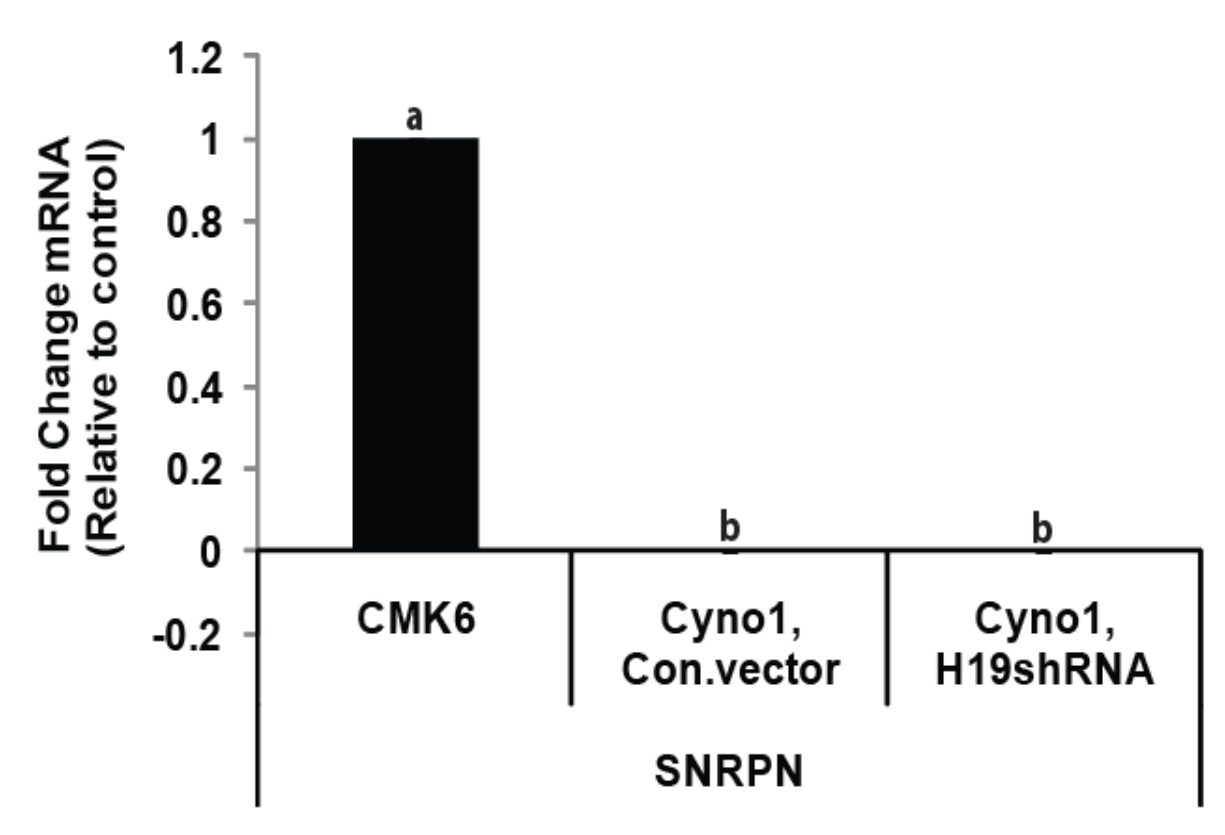


Table 2.1 qRT-PCR Primers Table

qRT-PCR primer name	Primer sequence	Accession number
H19 Forward	5'-CCCGTCCCTTCTGAATTTAATTT-3'	NR 002196.1
H19 Reverse	5'-CACTCGCACCGAGACTCAAG-3'	NR 002196.1
p57 Forward	GCGCGGCGATCAAGAA	NG_008022.1
p57 Reverse	ACATCGCCCGACGACTTC	NG_008022.1
IGF2 Forward	5'-CCGTGCTTCCGGACAACTT-3'	NM 000612.4
IGF2 Reverse	5'-TGGACTGCTTCCAGGTGTCA-3'	NM_000612.4
NDN Forward	CCGGCCTAACCAAGAAAAGTC	NM_001172102.1
NDN Reverse	ACTCCACGAGGGTGTTTTCTGT	NM_001172102.1
PEG10 Forward	TTGTCTGTAGCCCTGGCATGT	NM_001172427.1
PEG10 Reverse	GGGAACTTTTCCAGACTTTTGCT	NM_001172427.1
SNRPN Forward	GCAGAAGGACTGCCTCACTGA	XM_001106970.2
SNRPN Reverse	CAGGTACTTGCTGCTGAGA	XM_001106970.2
b-actin Forward b-actin Reverse	CATACTCCTGCTTGCTGATCCA GGATCGGCGGCTCCAT	NM 001101.3 NM 001101.3

Table 2.2 Summary of the Cyno1 oocyte donor (Buttercup) derived fibroblast cells at p4, Cyno1p47 and Cyno1p60 P-ESCs (Cell Line Genetics, WI, USA).

Cell Line ID	Passage #	Specimen Type	Results
Cyno1-Butter cup (Oocyte donor)	4	Monkey Fibroblast Culture	42,XX, inv(6) X2(20) Apparently normal monkey female karyotype
Cyno1 P-ESCs	47	Live ES culture	42,XX, inv(6q),inv.dup(6q), del(7p),del(18p) Abnormal female karyotype
Cyno1 P-ESCs	60	Live ES culture	42,XX, inv(6q),inv.dup(6q), del(7p),del(18p) Abnormal female karyotype

REFERENCES

REFERENCES

- 1. Mutter, G.L., *Role of imprinting in abnormal human development.* Mutation Research/Fundamental and Molecular Mechanisms of Mutagenesis, 1997. **396**(1-2): p. 141-147.
- 2. Sotomaru, Y., et al., *Unregulated Expression of the Imprinted Genes H19 and Igf2r in Mouse Uniparental Fetuses* J. Biol. Chem., 2002. **277**(14): p. 12474-12478.
- 3. Ogawa, H., et al., *Disruption of parental-specific expression of imprinted genes in uniparental fetuses.* FEBS Letters, 2006. **580**(22): p. 5377-5384.
- 4. Surti, U., et al., Genetics and biology of human ovarian teratomas. I. Cytogenetic analysis and mechanism of origin. Am J Hum Genet, 1990. **47**(4): p. 635-43.
- 5. Revazova, E.S., et al., *Patient-specific stem cell lines derived from human parthenogenetic blastocysts.* Cloning Stem Cells, 2007. **9**(3): p. 432-49.
- 6. Revazova, E.S., et al., *Patient-Specific Stem Cell Lines Derived from Human Parthenogenetic Blastocysts*. Cloning and Stem Cells, 2007. **9**(3): p. 432.
- 7. Revazova, E.S., et al., *HLA Homozygous Stem Cell Lines Derived from Human Parthenogenetic Blastocysts*. p. 1-14.
- 8. Mai, Q., et al., *Derivation of human embryonic stem cell lines from parthenogenetic blastocysts*. Cell Res. **17**(12): p. 1008-1019.
- 9. Strain, L., et al., *A human parthenogenetic chimaera*. Nat Genet, 1995. **11**(2): p. 164-9.
- 10. Surani, M.A., *Parthenogenesis in man.* Nat Genet, 1995. **11**(2): p. 111-3.
- 11. Cibelli, J.B., K. Cunniff, and K.E. Vrana, *Embryonic stem cells from parthenotes*. Methods Enzymol, 2006. **418**: p. 117-35.

- 12. Mitalipov, S.M., K.D. Nusser, and D.P. Wolf, *Parthenogenetic Activation of Rhesus Monkey Oocytes and Reconstructed Embryos*. 2001. p. 253-259.
- 13. Cibelli, J.B., K. Cunniff, and K.E. Vrana, *Embryonic Stem Cells from Parthenotes*, in *Methods in Enzymology*, K. Irina and L. Robert, Editors. 2006, Academic Press. p. 117-135.
- 14. Zvetkova, I., et al., *Global hypomethylation of the genome in XX embryonic stem cells*. Nat Genet, 2005. **37**(11): p. 1274-9.
- 15. Cibelli, J.B., et al., *Parthenogenetic stem cells in nonhuman primates.* Science, 2002. **295**(5556): p. 819.
- 16. Vrana, K.E., et al., *Nonhuman primate parthenogenetic stem cells.* Proc Natl Acad Sci U S A, 2003. **100 Suppl 1**: p. 11911-6.
- 17. Sanchez-Pernaute, R., et al., Long-Term Survival of Dopamine Neurons Derived from Parthenogenetic Primate Embryonic Stem Cells (Cyno-1) After Transplantation. 2005. p. 914-922.
- 18. Ferrari, D., et al., *Transplanted dopamine neurons derived from primate ES cells preferentially innervate DARPP-32 striatal progenitors within the graft.* 2006. p. 1885-1896.
- 19. Dighe, V., et al., *Heterozygous Embryonic Stem Cell Lines Derived from Nonhuman Primate Parthenotes*. 2008. p. 2007-0869.
- 20. Cheng, L., *More new lines of human parthenogenetic embryonic stem cells.* Cell Res. **18**(2): p. 215-217.
- 21. Sapienza, C., Parental imprinting of genes. Sci Am, 1990. 263(4): p. 52-60.
- 22. Tang, W.-y. and S.-m. Ho, *Epigenetic reprogramming and imprinting in origins of disease*. Reviews in Endocrine & Metabolic Disorders.

- 23. Swales, A.K.E. and N. Spears, *Genomic imprinting and reproduction*. 2005. p. 389-399.
- 24. Fujimoto, A., et al., *Aberrant genomic imprinting in rhesus monkey embryonic stem cells*. Stem Cells, 2006. **24**(3): p. 595-603.
- 25. Newman-Smith, E.D. and Z. Werb, *Stem cell defects in parthenogenetic peri-implantation embryos*. Development, 1995. **121**(7): p. 2069-77.
- 26. Horii, T., et al., Loss of Genomic Imprinting in Mouse Parthenogenetic Embryonic Stem Cells. 2008. p. 79-88.
- 27. Kono, T., et al., *Birth of parthenogenetic mice that can develop to adulthood.* Nature, 2004. **428**(6985): p. 860-4.
- 28. Kono, T., et al., *Mouse parthenogenetic embryos with monoallelic H19 expression can develop to day 17.5 of gestation.* Dev Biol, 2002. **243**(2): p. 294-300.
- 29. Mitalipov, S., et al., *Methylation status of imprinting centers for H19/IGF2 and SNURF/SNRPN in primate embryonic stem cells.* Stem Cells, 2007. **25**(3): p. 581-8.
- 30. Runte, M., et al., *SNURF-SNRPN* and *UBE3A* transcript levels in patients with Angelman syndrome. Human Genetics, 2004. **114**(6): p. 553-561.
- 31. Reik, W. and E.R. Maher, *Imprinting in clusters: lessons from Beckwith-Wiedemann syndrome*. Trends Genet, 1997. **13**(8): p. 330-4.
- 32. Nicholls, R.D., S. Saitoh, and B. Horsthemke, *Imprinting in Prader-Willi and Angelman syndromes*. Trends in Genetics, 1998. **14**(5): p. 194-200.
- 33. Hurst, L.D. and G.T. McVean, *Growth effects of uniparental disomies and the conflict theory of genomic imprinting.* Trends Genet, 1997. **13**(11): p. 436-43.

- 34. Sotomaru, Y., et al., *Disruption of imprinted expression of U2afbp-rs/U2af1-rs1 gene in mouse parthenogenetic fetuses.* J Biol Chem, 2001. **276**(28): p. 26694-8.
- 35. Poirier, F., et al., *The murine H19 gene is activated during embryonic stem cell differentiation in vitro and at the time of implantation in the developing embryo.* 1991. p. 1105-1114.
- 36. Varrault, A., et al., *Zac1 Regulates an Imprinted Gene Network Critically Involved in the Control of Embryonic Growth.* Developmental Cell, 2006. **11**(5): p. 711-722.
- 37. Gabory, A., et al., *H19 acts as a trans regulator of the imprinted gene network controlling growth in mice.* Development, 2009. **136**(20): p. 3413-21.
- 38. Matsuda T, W.N., Genetics and molecular markers in gestational trophoblastic disease with special reference to their clinical application. Best Pract Res Clin Obstet Gynaecol, 2003. **17.**(6): p. 827-36.
- 39. Schoenfelder, S., et al., *Non-coding transcripts in the H19 imprinting control region mediate gene silencing in transgenic Drosophila*. EMBO Rep, 2007. **8**(11): p. 1068-73.
- 40. Berteaux, N., et al., *A novel H19 antisense RNA overexpressed in breast cancer contributes to paternal IGF2 expression.* Mol Cell Biol, 2008. **28**(22): p. 6731-45.
- 41. Gabory, A., H. Jammes, and L. Dandolo, *The H19 locus: role of an imprinted non-coding RNA in growth and development.* Bioessays, 2010. **32**(6): p. 473-80.
- 42. Gabory, A., et al., *The H19 gene: regulation and function of a non-coding RNA.* Cytogenet Genome Res, 2006. **113**(1-4): p. 188-93.
- 43. Cullen, X.C.a.B.R., *The imprinted H19 noncoding RNA is a primary microRNA precursor.* RNA, 2007. **13**: p. 313–316.

- 44. Han, V.K.M. and A.M. Carter, Spatial and Temporal Patterns of Expression of Messenger RNA for Insulin-Like Growth Factors and their Binding Proteins in the Placenta of Man and Laboratory Animals. Placenta, 2000. **21**(4): p. 289-305.
- 45. Pringle, K.G. and C.T. Roberts, *New Light on Early Post-Implantation Pregnancy in the Mouse: Roles for Insulin-Like Growth Factor-II (IGF-II)?* Placenta, 2007. **28**(4): p. 286-297.
- 46. Minniti, C.P., et al., *Insulin-like growth factor II overexpression in myoblasts induces phenotypic changes typical of the malignant phenotype*. 1995. p. 263-269.
- 47. Pacher, M., et al., *Impact of constitutive IGF1/IGF2 stimulation on the transcriptional program of human breast cancer cells*. 2007. p. 49-59.
- 48. Prelle, K., et al., Overexpression of insulin-like growth factor-II in mouse embryonic stem cells promotes myogenic differentiation. Biochem Biophys Res Commun, 2000. **277**(3): p. 631-8.
- 49. Weber, M.M., et al., Postnatal Overexpression of Insulin-Like Growth Factor II in Transgenic Mice Is Associated with Adrenocortical Hyperplasia and Enhanced Steroidogenesis. 1999. p. 1537-1543.
- 50. Moorehead, R.A., et al., *Transgenic overexpression of IGF-II induces* spontaneous lung tumors: a model for human lung adenocarcinoma. Oncogene, 2003. **22**(6): p. 853-7.
- 51. Petrik, J., et al., Overexpression of Insulin-Like Growth Factor-II in Transgenic Mice Is Associated with Pancreatic Islet Cell Hyperplasia. 1999. p. 2353-2363.
- 52. Newman-Smith, E. and Z. Werb, *Functional analysis of trophoblast giant cells in parthenogenetic mouse embryos.* Dev Genet, 1997. **20**(1): p. 1-10.
- 53. Mitalipov, S., et al., Methylation Status of Imprinting Centers for H19/IGF2 and SNURF/SNRPN in Primate Embryonic Stem Cells
 10.1634/stemcells.2006-0120. Stem Cells, 2006: p. 2006-0120.

- 54. Kawahara, M., et al., *High-frequency generation of viable mice from engineered bi-maternal embryos.* Nat Biotechnol, 2007. **25**(9): p. 1045-50.
- 55. Kono, T., et al., *Paternal dual barrier by Ifg2-H19 and Dlk1-Gtl2 to parthenogenesis in mice.* Ernst Schering Res Found Workshop, 2006(60): p. 23-33.
- 56. Yoshimizu, T., et al., *The H19 locus acts in vivo as a tumor suppressor.* Proc Natl Acad Sci U S A, 2008. **105**(34): p. 12417-22.
- 57. Liou, J.-M., et al., Loss of imprinting of insulin-like growth factor II is associated with increased risk of proximal colon cancer. European Journal of Cancer. In Press, Corrected Proof.
- 58. Adriaenssens, E., et al., H19 Overexpression in Breast Adenocarcinoma Stromal Cells Is Associated with Tumor Values and Steroid Receptor Status but Independent of p53 and Ki-67 Expression. Am J Pathol, 1998. **153**(5): p. 1597-1607.
- 59. Barsyte-Lovejoy, D., et al., *The c-Myc Oncogene Directly Induces the H19 Noncoding RNA by Allele-Specific Binding to Potentiate Tumorigenesis.* Cancer Research, 2006. **66**(10): p. 5330-5337.
- 60. Berteaux, N., et al., *H19 mRNA-like Noncoding RNA Promotes Breast Cancer Cell Proliferation through Positive Control by E2F1.* Journal of Biological Chemistry, 2005. **280**(33): p. 29625-29636.
- 61. Dugimont, T., et al., *The H19 gene is expressed within both epithelial and stromal components of human invasive adenocarcinomas*. Biology of the Cell, 1995. **85**(2-3): p. 117-124.
- 62. Lottin, S., et al., Overexpression of an ectopic H19 gene enhances the tumorigenic properties of breast cancer cells. Carcinogenesis, 2002. **23**(11): p. 1885-1895.

- 63. Lottin, S., et al., *Thioredoxin post-transcriptional regulation by H19 provides a new function to mRNA-like non-coding RNA*. Oncogene, 2002. **21**(10): p. 1625-31.
- 64. Matouk, I.J., et al., *The oncofetal H19 RNA connection: Hypoxia, p53 and cancer.* Biochimica Et Biophysica Acta-Molecular Cell Research, 2010. **1803**(4): p. 443-451.
- 65. Tsang, W.P., et al., *Oncofetal H19-derived miR-675 regulates tumor suppressor RB in human colorectal cancer.* Carcinogenesis, 2010. **31**(3): p. 350-358.
- 66. Sheehy, E., et al., *Estimating the number of potential organ donors in the United States.* N Engl J Med, 2003. **349**(7): p. 667-74.
- 67. Coombes, J.M. and J.F. Trotter, *Development of the allocation system for deceased donor liver transplantation*. Clin Med Res, 2005. **3**(2): p. 87-92.
- 68. Nagy, A., et al., Embryonic stem cells alone are able to support fetal development in the mouse. 1990. p. 815-821.
- 69. Nagy, A., et al., *Derivation of Completely Cell Culture-Derived Mice from Early-Passage Embryonic Stem Cells.* 1993. p. 8424-8428.
- 70. Horii, T., et al., Loss of Genomic Imprinting in Mouse Parthenogenetic Embryonic Stem Cells. 2007. p. 2006-0635.
- 71. Platonov, E.S., L.I. Penkov, and D.A. New, [Effects of growth factors FGF2 and IGF2 on the development of parthenogenetic mouse embryos in utero and in vitro]. Ontogenez, 2002. **33**(1): p. 60-7.
- 72. Hikichi, T., et al., Functional full-term placentas formed from parthenogenetic embryos using serial nuclear transfer. Development, 2010.
- 73. Li, C., et al., Correlation of expression and methylation of imprinted genes with pluripotency of parthenogenetic embryonic stem cells. Hum. Mol. Genet., 2009. **18**(12): p. 2177-2187.

- 74. Anderegg, C. and C.L. Markert, Successful rescue of microsurgically produced homozygous uniparental mouse embryos via production of aggregation chimeras. Proc Natl Acad Sci U S A, 1986. **83**(17): p. 6509-13.
- 75. Paldi, A., et al., *Postnatal development of parthenogenetic in equilibrium with fertilized mouse aggregation chimeras.* Development, 1989. **105**(1): p. 115-8.
- 76. Allen, N., et al., *A functional analysis of imprinting in parthenogenetic embryonic stem cells.* Development, 1994. **120**(6): p. 1473-1482.
- 77. Nagy A, G.M., Vintersten K, Behringer R, *Manipulating the Mouse Embryo, A Laboratory Manual*. Vol. Third Edition. 2003: Cold Spring Harbor Laboratory Press.
- 78. Stevens, L.C., *Totipotent cells of parthenogenetic origin in a chimaeric mouse*. Nature, 1978. **276**(5685): p. 266-7.
- 79. Fundele, R.H., et al., *Temporal and spatial selection against parthenogenetic cells during development of fetal chimeras.* Development, 1990. **108**(1): p. 203-211.
- 80. Fundele, R., et al., *Systematic elimination of parthenogenetic cells in mouse chimeras*. Development, 1989. **106**(1): p. 29-35.
- 81. Jagerbauer, E.M., et al., *Parthenogenetic stem cells in postnatal mouse chimeras*. Development, 1992. **116**(1): p. 95-102.
- 82. Sturm, K.S., et al., *Unrestricted lineage differentiation of parthenogenetic ES cells.* Development Genes and Evolution, 1997. **206**(6): p. 377-388.
- 83. Jiang, H., et al., *Activation of paternally expressed imprinted genes in newly derived germline-competent mouse parthenogenetic embryonic stem cell lines.* Cell Res. **17**(9): p. 792-803.
- 84. Hikichi, T., et al., *Differentiation Potential of Parthenogenetic Embryonic Stem Cells Is Improved by Nuclear Transfer.* Stem Cells, 2007. **25**(1): p. 46-53.

- 85. Zvetkova, I., et al., *Global hypomethylation of the genome in XX embryonic stem cells*. Nat Genet, 2005. **37**(11): p. 1274-1279.
- 86. Onodera, Y., et al., *Differentiation diversity of mouse parthenogenetic embryonic stem cells in chimeric mice.* Theriogenology, 2010. **74**(1): p. 135-45.
- 87. Horii, T., et al., Loss of genomic imprinting in mouse parthenogenetic embryonic stem cells. Stem Cells, 2008. **26**(1): p. 79-88.
- 88. Eggan, K., et al., *Hybrid vigor, fetal overgrowth, and viability of mice derived by nuclear cloning and tetraploid embryo complementation.* Proceedings of the National Academy of Sciences of the United States of America, 2001. **98**(11): p. 6209-6214.
- 89. Eggan, K., et al., *Male and female mice derived from the same embryonic stem cell clone by tetraploid embryo complementation.* Nat Biotech, 2002. **20**(5): p. 455-459.
- 90. Chen, Z., et al., *Birth of parthenote mice directly from parthenogenetic embryonic stem cells*. Stem Cells, 2009. **27**(9): p. 2136-45.
- 91. Park, J.I., et al., *Differentiative potential of a mouse parthenogenetic embryonic stem cell line revealed by embryoid body formation in vitro*. Jpn J Vet Res, 1998. **46**(1): p. 19-28.
- 92. Szabo, P. and J. Mann, Expression and methylation of imprinted genes during in vitro differentiation of mouse parthenogenetic and androgenetic embryonic stem cell lines. Development, 1994. **120**(6): p. 1651-1660.
- 93. McKarney, L.A., M.L. Overall, and M. Dziadek, *Expression of H19 and Igf2 genes in uniparental mouse ES cells during in vitro and in vivo differentiation doi:10.1046/j.1432-0436.1996.6020075.x.* Differentiation, 1996. **60**(2): p. 75-86.
- 94. Dighe, V., et al., *Heterozygous embryonic stem cell lines derived from nonhuman primate parthenotes.* Stem Cells, 2008. **26**(3): p. 756-66.

- 95. Ferrari, D., et al., *Transplanted dopamine neurons derived from primate ES cells preferentially innervate DARPP-32 striatal progenitors within the graft.* Eur J Neurosci, 2006. **24**(7): p. 1885-96.
- 96. Sanchez-Pernaute, R., et al., *Parthenogenetic dopamine neurons from primate embryonic stem cells restore function in experimental Parkinson's disease.* Brain, 2008. **131**(Pt 8): p. 2127-39.
- 97. Sanchez-Pernaute, R., et al., Long-term survival of dopamine neurons derived from parthenogenetic primate embryonic stem cells (cyno-1) after transplantation. Stem Cells, 2005. **23**(7): p. 914-22.
- 98. Kim, K., et al., *Histocompatible embryonic stem cells by parthenogenesis*. Science, 2007. **315**(5811): p. 482-6.
- 99. Lengerke, C., et al., *Differentiation Potential of Histocompatible Parthenogenetic Embryonic Stem Cells*. Annals of the New York Academy of Sciences, 2007. **1106**(1): p. 209-218.
- 100. Eckardt, S., et al., *Hematopoietic reconstitution with androgenetic and gynogenetic stem cells.* Genes Dev, 2007. **21**(4): p. 409-19.
- 101. Swales, A.K.E. and N. Spears, *Genomic imprinting and reproduction*. 2005. p. 389-399.
- 102. Lyle, R., Gametic imprinting in development and disease. 1997. p. 1-12.
- 103. Wobus, A.M. and K.R. Boheler, *Embryonic Stem Cells: Prospects for Developmental Biology and Cell Therapy*. 2005. p. 635-678.
- 104. Lyle, R., *Gametic imprinting in development and disease.* J Endocrinol, 1997. **155**(1): p. 1-12.
- 105. Mitalipov, S.M., *Genomic imprinting in primate embryos and embryonic stem cells.* Reprod Fertil Dev, 2006. **18**(8): p. 817-21.

- 106. Sanchez-Pernaute, R., et al., *Parthenogenetic dopamine neurons from primate embryonic stem cells restore function in experimental Parkinson's disease*. 2008. p. 2127-2139.
- 107. Kono, T., et al., *Birth of parthenogenetic mice that can develop to adulthood.* Nature, 2004. **428**(6985): p. 860-864.
- 108. Kono, T., *Genomic imprinting is a barrier to parthenogenesis in mammals.* Cytogenet Genome Res, 2006. **113**(1-4): p. 31-5.
- 109. Wu, Q., et al., Regulated expression of two sets of paternally imprinted genes is necessary for mouse parthenogenetic development to term. Reproduction, 2006. **131**(3): p. 481-488.
- 110. Hikichi, T., et al., Functional full-term placentas formed from parthenogenetic embryos using serial nuclear transfer. Development, 2010. **137**(17): p. 2841-7.
- Lengerke, C., et al., Differentiation potential of histocompatible parthenogenetic embryonic stem cells. Annals of the New York Academy of Sciences, 2007. 1106(1): p. 209-18.
- 112. Simili, M., et al., 6DMAP inhibition of early cell cycle events and induction of mitotic abnormalities. Mutagenesis, 1997. **12**(5): p. 313-319.
- 113. Frost, J., et al., *The effects of culture on genomic imprinting profiles in human embryonic and fetal mesenchymal stem cells.* Epigenetics, 2011. **6**(1): p. 52-62.
- 114. Network, N.Y.O.D., http://www.donatelifeny.org/index.asp, 2010.
- 115. Sasazuki, T., et al., Effect of Matching of Class I HLA Alleles on Clinical Outcome after Transplantation of Hematopoietic Stem Cells from an Unrelated Donor. New England Journal of Medicine, 1998. **339**(17): p. 1177-1185.
- 116. Flomenberg, N., et al., Impact of HLA class I and class II high-resolution matching on outcomes of unrelated donor bone marrow transplantation: HLA-C

- mismatching is associated with a strong adverse effect on transplantation outcome. Blood, 2004. **104**(7): p. 1923-1930.
- 117. Petersdorf, E.W., et al., *Major-Histocompatibility-Complex Class I Alleles and Antigens in Hematopoietic-Cell Transplantation*. New England Journal of Medicine, 2001. **345**(25): p. 1794-1800.
- 118. Ishikawa, K., et al., *The innate immune system in host mice targets cells with allogenic mitochondrial DNA.* J Exp Med, 2010.
- 119. Petersdorf, E.W., et al., *Major-Histocompatibility-Complex Class I Alleles and Antigens in Hematopoietic-Cell Transplantation*. 2001. p. 1794-1800.
- 120. Hipp, J. and A. Atala, *Tissue engineering, stem cells, cloning, and parthenogenesis: new paradigms for therapy.* J Exp Clin Assist Reprod, 2004. **1**(1): p. 3.
- 121. Kaufman, M.H., et al., *Establishment of pluripotential cell lines from haploid mouse embryos*. J Embryol Exp Morphol, 1983. **73**(1): p. 249-261.
- 122. Robertson, E.J., M.J. Evans, and M.H. Kaufman, *X-chromosome instability in pluripotential stem cell lines derived from parthenogenetic embryos.* J Embryol Exp Morphol, 1983. **74**: p. 297-309.
- 123. Mitalipov, S.M., K.D. Nusser, and D.P. Wolf, *Parthenogenetic Activation of Rhesus Monkey Oocytes and Reconstructed Embryos.* Biology of Reproduction, 2001. **65**(1): p. 253-259.
- 124. Fang, Z.F., et al., *Rabbit embryonic stem cell lines derived from fertilized,* parthenogenetic or somatic cell nuclear transfer embryos. Exp Cell Res, 2006. **312**(18): p. 3669-82.
- 125. Kono, T., et al., *Epigenetic modifications during oocyte growth correlates with extended parthenogenetic development in the mouse.* Nat Genet, 1996. **13**(1): p. 91-4.

- 126. Barton, S.C., M.A.H. Surani, and M.L. Norris, *Role of paternal and maternal genomes in mouse development.* Nature, 1984. **311**(5984): p. 374-376.
- 127. Karin S. Sturm, M.L.F.R.A.P., *Abnormal development of embryonic and extraembryonic cell lineages in parthenogenetic mouse embryos.* Developmental Dynamics, 1994. **201**(1): p. 11-28.
- 128. Ogawa, H., et al., *Disruption of parental-specific expression of imprinted genes in uniparental fetuses.* FEBS Lett, 2006. **580**(22): p. 5377-84.
- 129. Liu, J.-H., et al., *Diploid parthenogenetic embryos adopt a maternal-type methylation pattern on both sets of maternal chromosomes*. Genomics, 2008. **91**(2): p. 121-8.
- 130. Zambrowicz, B.P., et al., Disruption of overlapping transcripts in the ROSA beta geo 26 gene trap strain leads to widespread expression of beta-galactosidase in mouse embryos and hematopoietic cells. Proc Natl Acad Sci U S A, 1997. **94**(8): p. 3789-94.
- 131. Kono, T., et al., A cell cycle-associated change in Ca2+ releasing activity leads to the generation of Ca2+ transients in mouse embryos during the first mitotic division. J Cell Biol, 1996. **132**(5): p. 915-23.
- 132. Abbondanzo, S.J., I. Gadi, and C.L. Stewart, *Derivation of embryonic stem cell lines*. Methods Enzymol, 1993. **225**: p. 803-23.
- 133. Bettegowda, A., et al., Quantitative analysis of messenger RNA abundance for ribosomal protein L-15, cyclophilin-A, phosphoglycerokinase, beta-glucuronidase, glyceraldehyde 3-phosphate dehydrogenase, beta-actin, and histone H2A during bovine oocyte maturation and early embryogenesis in vitro. Mol Reprod Dev, 2006. **73**(3): p. 267-78.
- 134. Whelan, J.A., N.B. Russell, and M.A. Whelan, *A method for the absolute quantification of cDNA using real-time PCR*. Journal of Immunological Methods, 2003. **278**(1-2): p. 261-269.

- 135. Li, X. and X. Wang, *Application of real-time polymerase chain reaction for the quantitation of interleukin-1[beta] mRNA upregulation in brain ischemic tolerance*. Brain Research Protocols, 2000. **5**(2): p. 211-217.
- 136. Norris, H.J., H.J. Zirkin, and W.L. Benson, *Immature (malignant) teratoma of the ovary: a clinical and pathologic study of 58 cases.* Cancer, 1976. **37**(5): p. 2359-72.
- 137. O'Connor, D.M. and H.J. Norris, *The influence of grade on the outcome of stage I ovarian immature (malignant) teratomas and the reproducibility of grading.* Int J Gynecol Pathol, 1994. **13**(4): p. 283-9.
- 138. Steeper, T.A. and K. Mukai, *Solid ovarian teratomas: an immunocytochemical study of thirteen cases with clinicopathologic correlation.* Pathol Annu, 1984. **19 Pt 1**: p. 81-92.
- 139. Lucifero, D., et al., *Methylation dynamics of imprinted genes in mouse germ cells.* Genomics, 2002. **79**(4): p. 530-8.
- 140. Friedman, R.C., et al., *Most mammalian mRNAs are conserved targets of microRNAs.* Genome Res, 2009. **19**(1): p. 92-105.
- 141. Yuasa, S., et al., *Transient inhibition of BMP signaling by Noggin induces cardiomyocyte differentiation of mouse embryonic stem cells.* Nat Biotechnol, 2005. **23**(5): p. 607-11.
- 142. Dean, W., et al., Altered imprinted gene methylation and expression in completely ES cell-derived mouse fetuses: association with aberrant phenotypes. Development, 1998. **125**(12): p. 2273-2282.
- 143. Bibikova, M., et al., *Human embryonic stem cells have a unique epigenetic signature*. Genome Res, 2006. **16**(9): p. 1075-83.
- 144. Sasaki, H., K. Ishihara, and R. Kato, *Mechanisms of Igf2/H19 imprinting: DNA methylation, chromatin and long-distance gene regulation.* J Biochem, 2000. **127**(5): p. 711-5.

- 145. Tsang, W.P., et al., Oncofetal H19-derived miR-675 regulates tumor suppressor RB in human colorectal cancer. Carcinogenesis, 2010. **31**(3): p. 350-358.
- 146. Onodera, Y., et al., *Differentiation diversity of mouse parthenogenetic embryonic stem cells in chimeric mice.* Theriogenology. **In Press, Corrected Proof**.
- 147. Milligan, L., et al., H19 gene expression is up-regulated exclusively by stabilization of the RNA during muscle cell differentiation. Oncogene, 2000. **19**(50): p. 5810-6.
- 148. Chung, S., et al., Analysis of different promoter systems for efficient transgene expression in mouse embryonic stem cell lines. Stem Cells, 2002. **20**(2): p. 139-45.
- 149. Thuan, N.V., S. Kishigami, and T. Wakayama, *How to improve the success rate of mouse cloning technology.* J Reprod Dev, 2010. **56**(1): p. 20-30.
- 150. Hao, J., et al., *Human parthenogenetic embryonic stem cells: one potential resource for cell therapy.* Sci China C Life Sci, 2009. **52**(7): p. 599-602.
- 151. Honeycutt, K.A., M.I. Koster, and D.R. Roop, *Genes involved in stem cell fate decisions and commitment to differentiation play a role in skin disease.* J Investig Dermatol Symp Proc, 2004. **9**(3): p. 261-8.
- 152. Senoo, M., et al., *p63 Is Essential for the Proliferative Potential of Stem Cells in Stratified Epithelia*. Cell, 2007. **129**(3): p. 523-536.
- 153. Yang, A., et al., *p63 is essential for regenerative proliferation in limb, craniofacial and epithelial development.* Nature, 1999. **398**(6729): p. 714-8.
- 154. Barrandon, C., B. Spiluttini, and O. Bensaude, *Non-coding RNAs regulating the transcriptional machinery*. Biol Cell, 2008. **100**(2): p. 83-95.
- 155. Koster MI, K.S., Mills AA, DeMayo FJ, Roop DR, *p63 is the molecular switch for initiation of an epithelial stratification program.* Genes Dev. , 2004 **18**(2): p. 126-31.

- 156. Roop, M.I.K.a.D.R., *Transgenic Mouse Models Provide New Insights into the Role of p63 in Epidermal Development*. CellCycle, 2004. **3**(4): p. 409 411.
- 157. Gaudet, F., et al., *Induction of tumors in mice by genomic hypomethylation*. Science, 2003. **300**(5618): p. 489-92.
- 158. Izadpanah, R., et al., Long-term in vitro expansion alters the biology of adult mesenchymal stem cells. Cancer Res, 2008. **68**(11): p. 4229-38.
- 159. Cimini, D. and F. Degrassi, *Aneuploidy: a matter of bad connections.* Trends Cell Biol, 2005. **15**(8): p. 442-51.
- 160. Cheng, L., *More new lines of human parthenogenetic embryonic stem cells.* Cell Res, 0000. **18**(2): p. 215-217.
- 161. Sun, X., et al., *Two active X Chromosomes and methylation of the imprinted gene in human parthenogenetic embryonic stem cell line*. Cell Res, 0000. **18**(S1): p. S35-S35.
- 162. Park JI, Y.I., Tada T, Takagi N, Takahashi Y, Kanagawa H., *Trisomy 8 does not affect differentiative potential in a murine parthenogenetic embryonic stem cell line.* Jpn J Vet Res., 1998 **46**(1): p. 29-35.
- 163. Epstein, C.J., *Mouse monosomies and trisomies as experimental systems for studying mammalian aneuploidy.* Trends in Genetics, 1985. **1**: p. 129-134.
- 164. Gropp, A., U. Kolbus, and D. Giers, *Systematic approach to the study of trisomy in the mouse. II.* Cytogenet Cell Genet, 1975. **14**(1): p. 42-62.
- 165. Gropp, A., et al., *Murine trisomy: developmental profiles of the embryo, and isolation of trisomic cellular systems.* J Exp Zool, 1983. **228**(2): p. 253-69.
- 166. Gropp, A., D. Giers, and U. Kolbus, *Trisomy in the fetal backcross progeny of male and female metacentric heterozygotes of the mouse. i.* Cytogenet Cell Genet, 1974. **13**(6): p. 511-35.

- Longo, L., et al., The chromosome make-up of mouse embryonic stem cells is predictive of somatic and germ cell chimaerism. Transgenic Research, 1997.
 6(5): p. 321-328.
- 168. Inoue, K., et al., *Sex-Reversed Somatic Cell Cloning in the Mouse.* The Journal of Reproduction and Development, 2009. **55**(5): p. 566-569.
- 169. Fauque, P., et al., *Modulation of imprinted gene network in placenta results in normal development of in vitro manipulated mouse embryos.* Hum Mol Genet, 2010. **19**(9): p. 1779-90.
- 170. Marina Bibikova, E.C., 1 Bonnie Wu,1 Lixin Zhou,1 Eliza Wickham Garcia,1 Ying Liu,2,12 Soojung Shin,2,12 Todd W. Plaia,3 Jonathan M. Auerbach,3 Dan E. Arking,4 Rodolfo Gonzalez,5 Jeremy Crook,6 Bruce Davidson,6 Thomas C. Schulz,7 Allan Robins,7 Aparna Khanna,8 Peter Sartipy,9 Johan Hyllner,9 Padmavathy Vanguri,10 Smita Savant-Bhonsale,10 Alan K. Smith,11 Aravinda Chakravarti,4 Anirban Maitra,4 Mahendra Rao,2,12 David L. Barker,1 Jeanne F. Loring,5 and Jian-Bing Fan1,13, *Human embryonic stem cells have a unique epigenetic signature*. Genome Research, 2006. **16**(9): p. 1075–1083.
- 171. Kim, K., et al., Recombination signatures distinguish embryonic stem cells derived by parthenogenesis and somatic cell nuclear transfer. Cell Stem Cell, 2007. **1**(3): p. 346-52.
- 172. Durbin, R.M., et al., *A map of human genome variation from population-scale sequencing*. Nature, 2010. **467**(7319): p. 1061-73.
- 173. Crespo, F.L., et al., *Mitochondrial reactive oxygen species mediate* cardiomyocyte formation from embryonic stem cells in high glucose. Stem Cells, 2010. **28**(7): p. 1132-42.
- 174. Zhu, D.Y., et al., *PPAR-beta facilitating maturation of hepatic-like tissue derived from mouse embryonic stem cells accompanied by mitochondriogenesis and membrane potential retention.* J Cell Biochem, 2010. 109(3): p. 498-508.

DISSERTATION CHAPTER 3

TITLE

H19 CONTROLS THE DIFFERENTIATION POTENTIAL OF MOUSE P-ESCs UPON DIFFERENTIATION IN VIVO

ABSTRACT

Parthenogenetic embryonic stem cells (P-ESCs) cells offer an alternative source of pluripotent cells, which hold great promise for autologous transplantation and regenerative medicine. P-ESCs have been successfully derived from blastocysts of several mammalian species. However, compared to biparental embryonic stem cells (B-ESCs), P-ESCs are limited in their ability to fully differentiate into all of the three germ layers. For example, it has been observed that there is a differentiation bias towards ectoderm derivatives at the expense of endoderm and mesoderm derivatives and muscle, in particular, in chimeric embryos, teratomas and embryoid bodies. The lack of paternal genome and inappropriate imprinting are thought to be major contributors to this limitation. In the present study we found that H19 was the most deregulated imprinted gene in P-ESCs with more than 6-fold over-expression compared to B-ESCs. Thus, we hypothesized that manipulation of the *H19* gene in P-ESCs would alleviate their limitations and allow them to function like B-ESCs. To test this we employed a small hairpin RNA (shRNA) approach to reduce the amount of H19 transcripts in mouse P-ESCs. We found, for the first time, that down-regulation of H19 led to an increase of mesoderm derived muscle and endoderm in P-ESCs teratomas similar to that observed in B-ESCs teratomas. This phenomenon coincided with upregulation of mesoderm specific genes such as *Myf5*, *Myf6* and *MyoD*. Moreover, *H19* down-regulated P-ESCs differentiated into a higher percentage of beating cardiomyocytes compared to control P-ESCs. Collectively, these results suggest that P-ESCs are amenable to molecular modifications that bring them functionally closer to true ES cells. In the future, such a

supply of cells may be useful as an alternative source of MHC matched stem cells for generation of organs and tissues from a female patients' own genome.

INTRODUCTION

The rate of organ transplantations performed in the United States is increasing [66]. In 2009 a record total of 28,465 organ transplant operations were performed compared to 27,965 in 2008 [114]. Despite the increasing number of organ transplantations, the pool of patients waiting for organ donations far exceeds the supply [67]. Another negative aspect of organ and tissue transplantation, even when a donor is available, is the failure of engraftment due to immune rejection. Engraftment of solid organs, tissues, and cells from unrelated donors has a very high risk of rejection due to lack of compatibility to the major histocompatible- complex (MHC) alleles and to the mitochondria of the recipient [115-118]. The risk of graft failure is increased even more when the donor is heterozygous and the patient is homozygous at the HLA locus [119]. The best alternative is the generation of autologous tissues and organs derived from a patient's own cells that express the same HLA antigens (MHC- matched cells). Parthenogenesis results when an oocyte is artificially activated and develops in the absence of a sperm [120]. ESCs derived from such embryos (P-ESCs) have been successfully derived from mouse [121-122], monkey [15, 123], rabbit [124], and human [5, 94]. Notably, P-ESCs are capable of giving rise to chimeric animals when injected into normal blastocysts [79, 81, 86]. However, mammalian parthenogenetic embryos per-se fail to develop past the early to mid stages of gestation [125-127], and are

deemed non-viable, alleviating many of the ethical concerns associated with destroying a fertilized embryo for ES cell derivation.

P-ESCs, like ES cells derived from fertilized embryos, can differentiate - in vitro as embryoid bodies and in vivo as teratomas – into cells from the three major germ layers ecto-, meso- and endoderm [82, 91]. Although these cells have the potential to differentiate in a manner similar to their biparental counterparts, a differentiation bias towards ectoderm derivatives at the expense of endoderm and mesoderm derivatives and muscle, in particular, has been observed in chimeric embryos, teratomas and embryonic bodies [76, 86, 127]. The major reason for failure of the PG embryos to develop to term, and the limited differentiation potential of P-ESCs in teratomas and embryo bodies, has been attributed to defects in establishing correct expression patterns of the imprinted genes [76],[91] [2, 107] [54, 128]. For example, the *H19* gene has been reported to be highly deregulated in PG embryos and P-ESCs [3, 128-129]. H19 is a maternally expressed (paternally imprinted) gene and codes for an untranslated mRNA. It has been reported that H19 can function as a long antisense RNA and as a micro RNA (mir675) [39-40]. In uniparental mouse fetuses the H19 gene was found to be over-expressed up to 400 times compared to biparental concepti [2, 71]. Moreover, deregulation of *H19* acts as a major barrier towards proper development of parthenogenetic embryos [2],[107],[108], [55]. Kono and co-workers showed that a 13 kb deletion encompassing the H19 coding region and the upstream differentially methylated region (DMR) allows parthenogenetic embryos to develop to term [107]. The efficiency of full-term development significantly increases when the H19/lgf2 DMR region together with the DMR region found within a second imprinted gene cluster

Dlk1/Dio3 on chromosome 12 are deleted [54, 109]. Most recently Hikichi *et al* showed that the development of PG embryos can be extended following serial nuclear transfer and is associated with a decrease in *H19* expression [110]. Altogether, these results suggest that the correct expression of *H19* is critical for normal embryonic development. The results of the aforementioned studies led us to hypothesize that correct expression of *H19* is required for proper differentiation of mouse P-ESCs into the three germ layers. To test this we utilized a retroviral-mediated shRNA approach to silence *H19* gene expression in mouse P-ESCs. Furthermore, we developed a method to quantify the abundance of the tissue derivatives of the three main germ layers in teratomas. We found that down-regulation of *H19* led to an increase of mesoderm derived muscle and endoderm in P-ESCs teratomas similar to that observed in B-ESCs teratomas. This phenomenon coincides with up regulation of the mesoderm specific genes such as *Myf5*, *Myf6* and *MyoD*. These results suggest that P-ESCs are amenable to molecular modifications that bring them functionally closer to true ES cells.

MATERIALS AND METHODS

Mouse ES cells derivation and culture

Mouse Parthenogenetic embryonic stem cells (P-ESCs) and biparental embryonic stem cells (B-ESCs) were derived from parthenogenetically activated and fertilized oocytes, respectively. P-ESCs and B-ESCs were derived from Rosa 26 (R26) strain of mice [130] expressing the β-galactosidase gene. Mouse R26 P-ESCs were produced by artificial activation of metaphase II (MII) eggs preventing the extrusion of second polar body [123, 131]. Briefly for P-ESCs derivation matured MII oocytes, were collected around

16hrs post hCG injection. The matured oocytes were activated by 5mM SrCl₂ in 2mM Ca²⁺ free mCZB medium in the presence of 5ug/ml cytochalasin B for 6hrs and cultured at 37 C in 5% CO₂ balance air up to 4 days in Ca²⁺ included mCZB medium [123]. Blastocysts were then treated with Tyrode's solution to remove the zona pellucida and placed in 96-multi well dishes coated with 90% confluent Mytomycin C inactivated MEFs until attachment [84]. From the plated embryos that exhibited sufficient ICM out-growth and colony formation, the colonies were manually cut, pipetted gently and replated onto fresh mytomycin C inactivated MEFs. The cells were sent for karyotyping at passage 4 to Cell Line Genetics (Madison, WI). All P-ESC and one B-ESC cell lines used in this study have been karyotyped, and found to have normal chromosome number 40XX and 40XY respectively. The cells were grown with complete medium consisting of KO DMEM (Invitrogen, Carlsbad, CA), Knockout Serum, 10% (Invitrogen, Carlsbad, CA), L-Glutamine 2mM (Invitrogen, Carlsbad, CA), Non Essential Amino Acids 1x solution (Invitrogen, Carlsbad, CA), FGF2, 4ng/ml, 2-Mercaptoethanol (Sigma, St. Louis, MO), Penicillin-Streptomycin, 1x final volume and 10³ Units of LIF(Millipore, Billerica, MA). Normal fertilized B-ESCs controls were derived from fertilized blastocysts at 3.5 dpc [132] and cultured under the same conditions as the mouse P-ESCs described above.

RNA isolation and cDNA synthesis from ES cells

A total mRNA form mouse P-ESCs and B-ESCs was isolated using the RNeasy Isolation Mini Kit (Qiagen, Valencia, CA) following the manufacturer's instructions and strict RNAse and DNAse free procedures. Total mRNA amount was measured using Nanodrop. One ug of total RNA with OD260/280 > 2.1 was used for first strand cDNA

synthesis. cDNA was synthesized with Superscript II (Invitrogen, Carlsbad, CA) using anchored Oligo (dT₁₂₋₁₈) primers (Invitrogen, Carlsbad, CA) and following the manufacturer's instructions.

RNA isolation and cDNA synthesis from formalin fixed paraffin embedded teratomas

RNA was isolated from ectoderm and endoderm derivatives and from whole teratoma sections following strict RNAse and DNAse free techniques. Ectoderm and endoderm derivatives were isolated by using Laser Capture Microdissection System (LCM) (Supplem. Figure3.5A and B). Total mRNA was extracted by using High Pure RNA paraffin Kit (Roche, Basel, Switzerland) following manufacturer's recommendations with the following modifications: after each RNA extraction procedure, the RNA was further purified by using NucleoSpin RNA II protocol for RNA purification (Machinery-Nagel, Bethlehem, PA) following the manufacturer instructions. Total RNA (tRNA) was measured by RNA picochip on Agilent 2100 *Bioanalyzer*. For the LCM obtained samples, one ng of total RNA (tRNA) was converted to cDNA using SuperScript II first strand cDNA kit (Invitrogen, Carlsbad, CA) using random oligo primers. For the tRNA extracted from whole sections, one µg was used for cDNA synthesis following the same protocol as mentioned above. A validation of this method has been published elsewhere [133].

Quantitative real time RT-PCR

The quantification of all gene transcripts was performed by reverse transcription of total RNA followed by absolute real-time quantitative RT-PCR using SYBR Green PCR Master Mix (Applied Biosystems, Foster City, CA). Absolute quantification using this method is described elsewhere [134-135]. Primers for PCR and absolute real time PCR were designed using Primer Express program (Applied Biosystems, Foster City, CA) and derived from mouse sequences found in GeneBank (Supplem. Table 3.2 and 3.3). A primer matrix was performed for each gene tested to determine optimal concentrations. Each reaction mixture consisted of 2 µl of cDNA, optimum concentration of each forward and reverse primer, nuclease free water, and 12.5 µl of SYBR Green PCR Master Mix in a total reaction volume of 25 µl (96well plates). Reactions were performed in triplicate for each sample using an ABI Prism 7000 Sequence Detection System (Applied Biosystems, Foster City, CA). The thermal cycle consisted of 40 cycles of 95°C for 15sec and 60 °C for 1min. Standard curves for each gene and controls were constructed using tenfold serial dilution and run on sample plates as standards. For gene expression normalization (except for the expression analysis done on the LCM obtained endoderm and ectoderm derivatives from fixed tumors) expression levels of β actin mRNA was used. For the normalization of gene expression in the LCM obtained endoderm and ectoderm derivatives from fixed tumors, Gapdh expression levels were used. Copies of β -actin and Gapdh RNA in each pool were determined using standard curves constructed from the plasmid PCR2.1 Topo containing partial β -actin and Gapdh cDNA sequences [133]. Partial cDNA sequences for β-actin, Gapdh H19, IGF2 and other genes tested, were amplified from mouse R26 P-ESCs, cloned into pCR2.1 Topo vector (Invitrogen, Carlsbad, CA), and subjected to fluorescent dye primer sequencing

to confirm identity. Resulting plasmids were used to construct standard curves. Representative R^2 for β -actin, Gapdh, H19 and the rest of the genes were estimated and only the one \geq 0.98 used. For each measurement, threshold lines were adjusted to intersect amplification lines in exponential portion of amplification curve [133].

Quantification of Endoderm, Ectoderm and Mesoderm derivatives in teratomas Teratomas from B-ESCs (BP), P-ESCs (PG1 and PG2), H19shRNA cells and P-ESCs infected with the control viral vector-Control (C), were derived by subcutaneous injection into immune-deficient Nude mice, CD-1 (Charles River Laboratories, Wilmington, MA). The teratomas were formalin fixed sectioned and embedded in paraffin blocks; each was entirely submitted for histological analysis. Initially one to three gross tissue samples per tumor was obtained for this study. The College of American Pathologists (CAP) guidelines for gross sampling of solid tumors state that one sample for each centimeter of tumor or three samples, whichever is greater, should be used for tumor grading. Histological grading was performed utilizing the modified Thurlbeck-Scully histological grading system for solid ovarian teratomas proposed by Norris et al. [136] and successfully implemented by O'Conner et al. [137] and Steeper and Mukai [138]. This system which is widely employed clinically, estimates percentage of neuro epithelium in the total tumor mass by counting the number of microscopic 10x Low Power Fields (LPFs) to differentiate between tumors grades I, II, and III. We estimated that from our teratoma samples about 12-16 LPFs could be evaluated per full tissue section on one glass microscopic slide and that 3 tissue sections would yield approximately 36-48 LPFs for examination, and thus comply with the modified

Thurlbeck-Scully histological grading system. However, in order to increase our quantification precision in an inherently heterogeneous tumor and adjust for variability in tumor size (0.8cm-1.2cm in diameter), we obtained consecutive additional deep level sections 15, 30 and 45µms apart from each tumor sample paraffin block. Thus the number of sections was increased to 10 -18 per tumor, the number of LPFs evaluated was increased to 120-288, and sections reflected whole tumor. The sections identity was hidden and the sections were also given to an independent histopathologist for evaluation.

Plasmid shRNA delivery system

For the plasmid shRNA delivery, pRNAT- U6.1/Neo vector was used (GenScript, Piscataway, NJ). In this vector system the *H19* shRNA was expressed from U6 promoter and GFP and Neomycin expression driven by CMV promoter. The pRNAT-U6.1/Neo *H19* shRNA vector was linearized by using a unique Scal (NEB, Ipswich, MA) restriction site and transformed into mouse R26 P-ESCs cell line by using Fugene6 transfection reagent (Roche, Basel, Switzerland) according to the manufacturers' recommendations. A stable transgenic cell line was selected using 100ug/ml of Neomycin for 14 days.

Lentiviral shRNA delivery system

For Lentiviral shRNA delivery pLenti-DEST-Block it TM lentiviral vector system was used (Invitrogen, Carlsbad, CA). In this system H1/TO promoter drives *H19* shRNA expression. The zeocin selectable marker is under the control of SV40 promoter. Due to

possible silencing of the SV40 promoter in mouse embryonic stem (MES) cells, pLenti-DEST-Block it TM vector was modified. The SV40 zeocin cassette was released by restriction digestion with Kpn1 and Xho1 (NEB, Ipswich, MA) and replaced with PGK promoter driving Hygromycin selectable marker cassette derived from plasmid pMSCV-Hygro (Clontech Laboratories, Inc. Mountain View, CA) by digesting with Clal and Xhol. This first construct was called pLenti-DEST-Block it/Hygro-H19 shRNA vector. For expression of fluorescent protein, chicken b- actin promoter driving EGFP expression was introduced downstream of the PGK-Hygromycine cassette by releasing it first from PCX-EGFP vector and subcloning it into pLenti-DEST-Block it/Hygro-H19 shRNA. The modified plasmid carrying both PGK-promoter driving Hygromycin selectable marker and EGFP expression cassette was called pLenti-DEST-Block it TM-CRL-H19 shRNA expression vector. The packaging and transduction of pLenti-DEST-Block it TM-CRL-H19 shRNA vector was done following the manufacturer's recommendations (Invitrogen, Carlsbad, CA) in mouse Rosa 26 P-ESC line. As a negative control, pLenti-DEST-Block it TM - CRL without the H19shRNA insert, was transduced into mouse Rosa 26 P-ESCs. The cells underwent Hygromycine selection two days post-viral infection. The Levels of *H19* downregulation was evaluated 10 to 14 days post infection with the H19shRNA lentiviral vector by Quantitative Real Time PCR as described above.

Retroviral shRNA delivery system

pMSCV-Hygro vector (Clontech Laboratories, Inc. Mountain View, CA) was used for H19 shRNA delivery into a mouse P-ESCs with the following modifications: Chicken bpromoter CMV-IE Enhancer fragment was derived from plasmid pCX-EGFP without PolyA signal by digestion with Sal-I and Bgl-II. The pMSCV-Hygro retroviral vector was digested with Sal1 and the Chicken b-promoter CMV-IE Enhancer-Intron-EGFP and introduced by T4 DNA ligation reaction into the Sal1 site. The cassette H1/TO promoter -H19 shRNA –Pol III termination site was released from plasmid pENTR/H1/TO plasmid (Invitrogen) by digestion with BamHI (NEB, Ipswich, MA) and cloned into unique Xho1 site of the pMSCV-Hygro retroviral vector. The so modified pMSCV-Hygro retroviral vector was called pMSCV-Hygro-EGFP-H19 shRNA retroviral vector.

The packaging and transduction of pMSCV-Hygro-EGFP-H19shRNA vector was done following the manufacturer's recommendations (Clontech, Mountain View, CA) in mouse R26 P-ESC cell line. For negative control, pMSCV-Hygro-EGFP-H19shRNA without the H19shRNA insert was transduced into mouse R26-P-ESCs. The cells were subjected to Hygromycin selection two days post-viral infection. The Levels of H19 downregulation was evaluated 10 to 14 days post infection with the H19shRNA Lentiviral vector by Quantitative Real Time PCR as described above.

Bisulfate sequencing analysis

Genomic DNA was isolated from mouse P-ESCs and B-ESCs using Dneasy Blood and Tissue Kit (Qiagen, Valencia, CA). Bisulfate conversion of genomic DNA (gDNA) from mouse P-ESCs and B-ESCs was performed by using EZ DNA Methylation -Direct[™] kit (ZymoResearch, Irvine, CA) and following the manufacturer's instructions. Bisulfate treated gDNA was then subjected to two rounds of PCR reaction. The primers for amplification of *H19/lgf2* DMR region and the amplification conditions are as described elsewhere (Supplem. Table3.4) [139].

Immunocytochemical analysis

A. β-galactosidase staining

Cells in a six-well plate were fixed with 1.5ml/well of 1% glutaraldehyde solution in PBS for 10min. The fixed cells were washed three times with PBS after which 1.5m/well of color substrate was added. The color substrate contains water, 10xPBS, 100X Ca²⁺ Mg²⁺, 0.5M K₃Fe (CN)₆, 0.5M K₄Fe (CN)₆, 1M MgCl₂ and X-gal. The cells were incubated with color substrate for 3 hours and washed three times with PBS

B. Oct4 and SSEA1 immunostaining

Cells were washed 3 times, each time 5minutes with washing buffer (DPBS, 0.1% TX100 (Triton 100X) and incubated with Permeabilization Buffer (DPBS, 1% TX100) for 10min. Subsequently, the cells were washed once more with washing buffer, then blocked with blocking buffer (DBPS + 0.1%TX100 + 1%BSA + 10%NGS) for 1-2 hours. Oct4 antibody (Abcam, Cambridge, MA) in dilution 1:75 and SSEA1 antibody (Santa Cruz biotechnology, Inc. Santa Cruz, CA) in 1:200 dilution was added to the cells and incubated for 3 hours to overnight at 4C. Cells were washed 6 times each time 10minutes. Then secondary Ab (Abcam, Cambridge, MA) was added in 1:500 dilutions following the manufacturer's recommendations.

C. Immunocytochemistry for muscle specific markers

Beating EBs were trypsinized and plated on day 10 of EB formation. The plated EB were immono-stained for muscle specific markers – Myf5 (Abcam, Cambridge, MA) 1:250 dilution, Sarcomeric α- actin (Abcam, Cambridge, MA) 1:100 dilution, and sarcomeric Myosin (Abcam, Cambridge, MA) 1:250 dilution and following the manufacturer's recommendations.

Immunohystochemical analysis of formalin fixed, paraffin embedded tumor sections

A. Hematoxylin-Eosin staining

Tissue samples previously fixed in 10% Neutral Buffered Formalin were processed embedded with the ThermoFisher HistoCentre III embedding station. The blocks were sectioned at 4-5 microns. Sections were stained with Hematoxylin and Eosin (H and E).

B. Beta Galactosidase, Alpha Fetoprotein, Beta Tubulin, and α - Smooth Muscle Actin staining.

Specimens were processed, embedded in paraffin and sectioned on a rotary microtome at 4 -5 µs. Sections were placed on slides coated with 3-Aminopropyltriethoxysilane and dried at 56°C overnight. The slides were subsequently deparafinized in Xylene. Following pretreatment standard avidin-biotin complex staining steps were performed at room temperature on the DAKO Autostainer. Slides were inset for two minutes between each staining step; after blocking for non-specific protein with Normal Horse Serum or Normal Goat Serum (Vector Labs, Burlingame, CA) for 30 minutes; sections were incubated with Avidin / Biotin blocking system for 15 minutes (Sigma, St. Louis, MO). Following subsequent rinsing in Tris Buffered Saline + Tween 20 (Scytek, Logan, UT) slides were incubated in the following primary antibodies: Polyclonal Rabbit anti-beta Galactosidase diluted (Abcam, Cambridge, MA); Polyclonal Rabbit anti-Alpha Fetoprotien (ThermoFisher Labvision, Hampton, NH); Monoclonal Mouse anti-beta Tubulin Isotype III Clone SDL (Sigma, St.Louis, MO); Monoclonal Mouse anti-Alpha Smooth Muscle Actin Clone (Dako North America). Upon completion of primary incubations, slides were incubated for 30 minutes with the corresponding biotinylated

secondary IgG (H+L) either Goat anti-Rabbit or Horse anti-Mouse (Vector) at a concentration of 11µg/ml. Samples were counterstained with Gill 2 Hematoxylin (ThermoFisher, Hampton, NH).

C. DeltaNp63 staining

Slides were stained using deltaNp63 primarily Antibody (Santa Cruz Biotechnology, Santa Cruz, CA) in 1:100 dilution and following the manufacturer's recommendations. Upon completion of primary incubations, slides were incubated for 40 minutes with the corresponding biotinylated secondary Goat anti-Rabbit at 1:136 dilutions. For visualization of the staining, Phospohatase labeled streptavidin (Kirkegaard & Perry Laboratories, Inc. Gaithersburg, Maryland) was used which upon addition of a vector red substrate (Kirkegaard & Perry Laboratories, Inc. Gaithersburg, Maryland) gave the brick red staining of the specimen.

Teratoma formation

For all teratoma experiments, a suspension of $5x10^5$ P-ESCs(PG1 and PG2) cells and control B-ESCs(BP) cells were injected subcutaneously (s.c.) into immunodeficient Nude mice-CD-1 (Charles River Laboratories, Wilmington, MA). Mice were euthanized around eight weeks after injection or when tumors had grown to about 1cm in diameter whichever came first. Tumors were then isolated, fixed in paraformaldehyde, embedded in paraffin and stained with hematoxilin eosin. Tumors were stained for β -galactosidase, to confirm their origin. The tumor sections were also stained for α -fetoprotein, α -smooth muscle and β -tubulin, markers of endoderm, mesoderm and ectoderm derivatives respectively.

Identification of Mier2 as a potential target of mir675

miRNA targets were found using TargetScan (Supplem. Figure 3.10) [140].

Derivation of beating embryo bodies (EB)

Beating EBs were derived from mouse ES cells as described by Yuasa *et al.* [141]. Briefly, mouse ES cells were cultured on gelatin-coated dishes for 3 days in α-MEM supplemented with 10% FBS (Invitrogen, Carlsbad, CA), 2mM L-glutamine (Invitrogen), 0.1mM nonessential amino acids (Invitrogen, Carlsbad, CA),1mM sodium pyruvate (Invitrogen, Carlsbad, CA), 0.1mM 2-mercaptoethanol, 2,000U/ml LIF (Chemicon, Billerica, MA) and 0.15μg/ml Noggin (R @D System Inc., Minneapolis, MN) for 3 days. The cell were then trypsinized and cultured to form spherical embryo bodies from 1,000 cells using tri-dimensional culture system in the same medium as above minus LIF and using 0.1μg/ml Noggin and round bottom low cell binding 96 well plates (Nunc, Roskilde, Denmark). The EBs were cultured until day 10 of EB formation. The incidence of EB beatings was recorded on days 8, 10 and 12 post EBs formation by us and by an independent researcher.

Pathogen testing

The mouse B-ESCs, wild type P-ESCs and P-ESCs infected with the retroviral H19shRNA expressing viral vector and the control ones were sent for IMPACT Profile I pathogen testing (www.radil.missouri.edu). The cells were identified as negative for all 22 pathogens tested such as: Mycoplasma spp., Sendai virus, Mouse hepatitis virus, Pneumonia virus of mice, Minute virus of mice, Mouse parvovirus (MPV1, MPV2,

MPV3), Theiler's murine encephalomyelitis virus, Murine norovirus, Reovirus 3, Mouse rotavirus, Ectromelia virus, Lymphocytic choriomeningitis virus, Polyoma virus, Lactate dehydrogenase-elevating virus, Mouse adenovirus (MAD1, MAD2), Mouse cytomegalovirus, K virus, Mouse thymic virus, Hantaan virus.

Statistics

qRT-PCR experimental data and teratoma quantification data were analyzed by analysis of variance (ANOVA) procedure using the mixed procedure of SAS (Cary, NC, USA). Differences of p < 0.05 were considered statistically significant.

RESULTS AND DISCUSSION

Generation of mouse P-ESCs and B-ESCs

Two mouse P-ESC lines (PG1 and PG2) and one B-ESC line were derived from parthenogenetic and biparental blastocysts of Rosa 26 strain of mice (see materials and methods). All three lines were found to possess a normal karyotype - 40XX and 40XY respectively when cultured under normal growth conditions (Supplem. Table3.1). Morphologically the P-ESCs and B-ESCs displayed small cytoplasmic/nuclear ratio and grew as small compact colonies with prominent nucleoli (Supplem. Figure 3.1A, B). These cells were extensively propagated *in vitro* while maintaining their ES cell morphology. The PG1, PG2 and B-ESCs stained positive for β-galactosidase (Supplem. Figure3.1C, D) and the pluripotency markers OCT4 and SSEA1 (Supplem. Figure3.2). Moreover, following injection into immunodeficient Nude mice-CD-1 both P-ESC lines were capable of forming teratomas (Supplem. Figure3.3).

Alteration of key imprinted genes in P-ESCs

It has been shown that in vitro culture of B-ESCs and P-ESCs can lead to alterations in DNA methylation and covalent modifications on histones such as histone acetylation and methylation [76, 83, 87, 110, 142-143]. Moreover, it has been reported that in P-ESCs the expression of several imprinted genes is altered due to absence of a paternal chromosomal complement [76, 83, 87]. We analyzed the expression profile of the paternally imprinted gene H19 and the maternally imprinted gene Igf2. Both H19 and Igf2 share the same differentially methylated region (DMR) as the main regulator of their expression (55). We found that expression levels of the paternally imprinted gene (i.e. maternally expressed gene) H19 was upregulated greater than 6-fold in P-ESCs compared to control B-ESCs (P<0.05; Figure 3.1A). Contrary to its maternal imprinted status there were significantly higher levels of *Igf2* in P-ESCs compared to B-ESCs (P<0.05; Figure 3.1A). We also evaluated the expression levels of other maternally (P57, Igf2R) paternally (Mest1, Mkrn) expressed genes (P<0.05; Figure3.1D), and the pluripotency marker Nanog (P<0.05; Figure 3.1E). The expression pattern of P57, Igf2R and Mkrn was also unexpected according to their imprinting status i.e. there was no statistical significant difference in the P57 and Igf2R expression between P-ESCs and B-ESCs and the expression of the paternally expressed gene *Mkrn* was low but detectable. The *Mest1* gene expression, however, remained faithful to the parent of origin expression, and was over-expressed in B-ESCs compare to P-ESCs (P<0.05; Figure 3.1D). We also analyzed the mRNA levels of *Nanog*, a key pluripotency gene (Figure 3.1E). We observed more than eight folds over-expression of *Nanog* in B-ESCs compare to P-ESCs (P<0.05; Figure 3.1E).

These results demonstrate that the expression of key imprinted genes such as *H19*, *Igf2*, *P57*, *Igf2R* and *Mkrn* is deregulated in P-ESCs.

Partial CpG methylation of the H19/Igf2 DMR region in P-ESCs

The methylation status of the H19/lgf2 DMR has been viewed as the main regulator of H19 and Igf2 gene expression (Figure 3.1B). On the maternal allele the CpG dinucleotides are not methylated which allows for a CTCF insulator protein to bind, preventing the enhancer downstream of H19 to reach Igf2 gene [144]. This leads to H19 being expressed on the maternal allele and *lgf2* silenced. On the paternal allele the DMR region is methylated which inhibits binding of the CTCF insulator protein and allows for the expression of *Igf2* from the paternal allele while *H19* remains silenced. Since we were able to detect expression of *Igf2* in our P-ESCs, and the expression of H19 and Igf2 is coordinately regulated, we decided to analyze the methylation status of the H19/IGF2 DMR region. It has been previously reported that this region in CD-1 mice contains 16 critical CpGs sites important for CTCF binding [139]. After bisulfite sequencing analysis we found that in the Rosa26 strain of mice there are 15 CpG sites, the fourth of which seems not to be methylated in normal fertilized B-ESCs (Figure 3.1C). The DMR methylation status in the two P-ESC lines (PG1 and PG2) revealed a partial methylation of the CpG sites analyzed with PG1 and PG2 having 7.3% and 19.3% methylation, respectively (Figure 3.1C). These results demonstrate that the DMR of the H19/lgf2 genes is not completely demethylated and that this may account for the elevated levels of *Igf*2 expression in mouse P-ESCs.

Elevated levels of *H19* persist throughout P-ESCs differentiation *in vivo* Next we wanted to determine the expression status of the *H19* gene throughout differentiation in vivo. We hypothesized that expression levels of H19 remained higher in teratomas derived from P-ESCs compared to B-ESCs. To test this we injected P-ESCs and B-ESCs subcutaneously into immune-deficient Nude mice-CD1. Teratomas were recovered and stained for β-galactosidase expression confirming that the teratomas originated from the injected cells (Supplem. Figure 3.4A). The ectoderm, endoderm and mesoderm derivatives were also stained for α- fetoprotein, β- tubulin and α-smooth muscle actin indicating the identity of the morphologically observed structures (Supplem. Figure 3.4B). qRT-PCR data indicated that the expression levels of H19 in ectoderm and endoderm derivatives and in whole teratoma sections from P-ESCs teratomas was significantly higher than in controls (P<0.05; Figure 3.2A-C). We also evaluated the expression levels of *lgf2* in teratomas. *lgf2* expression in ectoderm and endoderm derivatives did not differ between P-ESCs and B-ESCs derived structures (Figure 3.2B). The same expression pattern (no difference) was observed for *Igf* 2 mRNA expression between B-ESCs and P-ESCs from which the teratomas were derived (P<0.05; Figure 3.1A). However, when total RNA from whole teratoma sections was analyzed for Igf2 mRNA transcript abundance, there was a significant downregulation of Igf2 expression in P-ESCs teratomas compare to B-ESCs teratomas (P<0.05; Figure 3.2C). We also analyzed the Retinoblastoma gene (Rb) mRNA abundance in whole teratoma sections. It has been reported that mir675, a product of H19 gene, targets the 3'UTR region of the Rb mRNA and therefore affects the Rb mRNA levels [145]. Rb mRNA abundance in the P-ESCs derived teratomas was lower

than in B-ESCs derived ones; however, this difference was not statistically significant (P<0.05; Figure 3.2D).

Therefore, upon *in vivo* differentiation, the expression pattern of the imprinted gene *H19* and *Igf2* remains faithful to the origin of the P-ESCs from which the teratomas were derived.

Teratomas derived from P-ESCs give rise to a lower proportion of mesoderm derived muscle compared to tumors derived from B-ESCs

Results of previous studies suggest that there is a differentiation bias of P-ESCs towards ectoderm derivatives at the expense of endoderm and mesoderm derivatives and muscle in chimeric embryos, teratomas and embryonic bodies [76, 81, 146]. We hypothesized that correct expression of *H19* is required for normal germ layer formation *in vivo*. We quantified the percentage of ecto-, endo- and mesoderm derivatives in teratomas derived from our P-ESCs (PG1 and PG2) and B-ESCs (BP) by using our modified Thurlbeck-Scully grading system (see materials and Methods). We found that in teratomas derived from P-ESCs consisted of predominantly ectoderm derivatives (70%) (Figure3.3A) compared to B-ESCs ones (50%). There was less endoderm (20%) in P-ESC derived teratomas compared to B-ESC ones (30%). Interestingly, we found that P-ESCs give rise to less mesoderm derived muscle (5%) compared to B-ESC teratomas (20%) (Figure3.3A).

We also performed qRT-PCR to analyze the expression pattern of genes specific to ectoderm (*Vimentin* and *Nestin*), endoderm (α - feto protein (Afp) and Gata4) and

mesoderm (Myf5, Myf6, MyoD) germ layers in these teratomas (Figure 3.3B). In addition, we analyzed the expression pattern of *Mier2* gene. *Mier2* is an early mesoderm promoting gene that we identified as a target of mir675 by performing miRNA targets were found using TargetScan (see Materials and Methods). gRT-PCR data indicated that there was no difference in expression of ectoderm and endoderm specific transcript in P-ESCs and B-ESCs derived teratomas. In contrast there was a significant decrease in the expression of Myf5, Myf6 and MyoD in P-ESCs teratomas compared to B-ESCs ones (P<0.05; Figure 3.3B). The expression of *Mier2* was also lower in P-ESCs compared to B-ESCs teratomas (Figure 3.3B) and coincided with high levels of H19 gene expression (P<0.05; see Figure 3.2A and B). These results suggest that upon differentiation in vivo P-ESCs exhibit limited developmental potential towards endoderm and mesoderm germ layer, muscle in particular. This phenotype coincides with overexpression of H19 and downregulation of the muscle and mesoderm promoting genes - Myf5, Myf6, MyoD, and Mier2 in P-ESCs derived teratomas compare to B-ESC controls.

Downregulation of H19 expression in P-ESCs promotes normal mesoderm differentiation in vivo

Proper *H19* regulation is central to normal development of PG embryos [27-28]. Moreover, *H19* may be important for proper muscle cell differentiation [79, 147]. For example chimeras between wild type and P-ESCs result in restricted contribution of P-ESCs to muscle tissues in chimeric embryos [79]. Another study by Milligan *et al.* found a connection between *H19* and muscle differentiation *in vitro* [147]. In this study it was

elegantly shown that H19 ncRNA is stabilized in C2C12 myoblastic cells during muscle differentiation and inhibition of protein synthesis leads to H19 ncRNA destabilization [147]. Because we found that teratomas derived from P-ESCs are composed of a very limited amount of muscle tissue (Figure 3.3A), we hypothesized that deregulation of H19 expression in P-ESCs is responsible for the decreased differentiation potential of these cells into muscle. To test this hypothesis we employed an H19 shRNA expressing plasmid, lentiviral and retroviral vector systems to chronically suppress H19 gene expression in P-ESCs. The lentiviral and retroviral shRNA delivery vectors were modified to express fluorescent protein (EGFP) under the control of strong mouse ES cells promoter, such as CAG promoter [148]. The plasmid vector pRNAT-U6.1/Neo was used for preliminary study to test two different H19 shRNA oligos (Supplem. Table3.5). The pRNAT-U6.1/Neo expressing two H19shRNAs (Supplem. Table3.5) was transfected into mouse embryonic fibroblast (MEF) cells (Supplem. Figure 3.8). In this preliminary study we identified that H19shRNA#2 was more efficient in suppressing H19 gene expression (almost 4 fold downregulation of H19 levels) compare to H19shRNA#1 (two fold downregulation of *H19* expression) (P<0.05; Supplem. Figure 3.8). Therefore, we used H19shRNA#2 for all our further experiments. The H19shRNA#2 was introduced into the modified lentiviral and retroviral vectors. P-ESCs infected with the H19shRNA viral vectors exhibit reduced expression of H19 mRNA (P<0.05; Supplem. Figure 3.9).

Because the retroviral *H19*shRNA vector had a better expression of the introduced EGFP fluorescent protein, we have proceeded using the retroviral *H19*shRNA vector for all our experiments (Supplem. Figure 3.11).

We infected P-ESCs with an H19 shRNA retroviral vector or control vector and selected with Hygromycin for 14 days and selected for clonal cell lines (Figure 3.4A). gRT-PCR analysis revealed that H19 was stably and efficiently down-regulated in the H19shRNA cell line compare to the control P-ESC lines (P<0.05; Figure 3.4A). Moreover, low levels of H19 transcripts were faithfully maintained in teratomas derived from H19shRNA P-ESCs (P<0.05; Figure 3.5A). We also analyzed the maternally (P57, Igf2R, Grb10) and the paternally (Igf2, Mest1 and Mkrn) expressed genes between cells infected with the H19shRNA and the control retroviral vector (Figure 3.4B). Mkrn mRNA expression was very low but detectable. Igf2 expression was upregulated in P-ESCs with suppressed H19 (P<0.05; Figure 3.4B) and this expression pattern was maintained in the teratomas (P<0.05; Figure 3. 5D). Mest 1 mRNA levels were six folds upregulated in H19 downregulated P-ESCs (P<0.05; Figure 3.4B). This can phenomenon can be explained by the recently reported Imprinted Gene Network (IGN) [36]. In the IGN any change of imprinted genes directly connected in the hub lead to alteration of the neighboring gene. In this context H19 may influence the expression of Igf2 and Mest1 probably trough it antisense mRNA gene product.

We also analyzed the expression pattern of *Mier2* and *Rb* genes and found no statistically significant differences in *Mier2* gene expression between *H19* downregulated P-ESCs and Control ones (P<0.05; Figure3.4D). However, downregulation of *H19* coincided with significant upregulation of the *Rb* mRNA abundance in P-ESCs (P<0.05; Figure3.4C) and this tendency persisted in the P-ESCs derived teratomas (P<0.05; Figure3.5E).

To determine whether down-regulation of *H19* expression improved the differentiation potential of P-ESCs *in vivo*, we used our modified Thurlbeck-Scully grading system to quantify the percentage of ecto-, endo- and mesoderm derivatives in teratomas. We found that there was a significant increase in endoderm (15%) and mesoderm-muscle derivatives (11%) in H19shRNA derived teratomas compared to control P-ESCs (P<0.05; Figure3.5B). This increase was similar to the percentage of endoderm and muscle derivatives in teratomas derived from B-ESCs (P<0.05).

To further confirm our findings, we performed qRT-PCR analysis of mesoderm specific transcripts – *MyoD*, *Myf6* and *Mier2* whose transcription levels were significantly altered in teratomas derived from wild type P-ESCs (see Figure3.3B). We found that upon downregulation of *H19*, the levels of *MyoD*, *Myf6* and *Mier2* were significantly upregulated in *H19*shRNA derived teratomas compared to control ones (P<0.05; Figure 3.5C). Such results suggest that the increased propensity of the *H19*shRNA cells to differentiate into the mesoderm lineage is dependent upon the downregulation of *H19* expression and the upregulation of the mesoderm specific markers (*MyoD*, *Myf6* and *Mier2*) (P<0.05; Figure 3.5A-C).

Induction of beating Embryoid Bodies (EBs) from *H19* down-regulated P-ESCs
In order to further compare and analyze the differential potential of PG1, PG2 and *H19*shRNA cell lines, we employed an embryoid body (EB) assay to examine
cardiomyocyte formation. We adopted a protocol for derivation of beating
cardiomyocytes by Shinsuke Yuasa *et al.* [141] . The incidence of beating EBs was

recorded at days 8, 10 and 12 of EB formation. Then the beating EBs were dissociated and plated on gelatin coated dishes and stained for cardiomyocyte specific markers. All the cardiomyocyte cells stained positive for α -sarcomeric actin, α -sarcomeric myosin and *Myf5* (Figure3.6A) and express the cardiomyocyte specific marker; α -cardiac actin (Figure3.6C). The cardyomyocyte contractions were inhibited upon addition of $10\mu M$ Verapamil which acts by specifically blocking L-type Ca^{2+} channels in smooth and cardiac muscle (Supplem. movie 1). Our data indicated that P-ESCs and control vector P-ESCs have a lower potential to give rise to beating EBs compared to control B-ESCs. Remarkably, upon downregulation of *H19*, this phenotype was completely reversed (Figure3.6B). The incidence of beating cardiomyocytes was similar between EBs derived from H19shRNA P-ESCs and B-ESCs (p>0.05). In summary, downregulation of *H19* gene expression increases the differentiation potential of P-ESCs into cardiomyocytes and beating EBs in a manner similar to that of normal B-ESCs.

CONCLUSION

P-ESCs: an alternative source of pluripotent stem cells in regenerative medicine
In light of an increased need for cell and tissue replacement therapy, a number of
different strategies have been implemented to obtain a pluripotent source of stem cells.
P-ESCs represent a unique source of pluripotent cells that can potentially overcome the
current limitations that destruction of viable embryos (during the derivation of stem cells
from fertilized and nuclear transfer derived embryos) or the viral integration of
oncogenes expressing vectors (used in iPS cell production) represent. The efficiency of
derivation of P-ESCs is higher than the efficiency for derivation of ES cells from Nuclear

Transfer (NT) [98, 111, 149-150]. Moreover, MHC matched to the major histocompatible complex human P-ESCs have been derived with high efficiency. Such cells can be used to treat not only the oocyte donor's but also her siblings and perhaps, other individuals that share their HLA types [94, 98, 111, 150].

The results reported in this study strongly suggest that *H19* plays an important role for the parthenogenetic ES cell development towards mesoderm germ layer, muscle in particular. We used teratomas as an experimental model for evaluating the differentiation potential of the P-ESCs instead of chimeras. In a chimeric embryo the P-ESCs form aggregates with the wild type host cells and are under the influence of host cell's environment. Therefore, during embryo development the P-ESCs, in P-ESCs-WT cells chimeras, are in constant cross-talk and can exchange biochemical and protein signaling with the host cells that may influence their developmental potential. Thus, in order to evaluate the intrinsic differentiation potential of our mouse P-ESCs we used teratoma formation and cardiomyocyte differentiation assays to analyze the sole ability of these cells to give rise to derivatives of all three germ layers- ectoderm, endoderm and mesoderm and to beating embryo bodies. Our results demonstrated for the first time, that downregulation of a single imprinted gene can increase the differentiation potential of P-ESCs towards mesoderm development and beating EBs and that this phenotype coincides with an up –regulation of the expression of mesoderm specific genes – MyoD, Myf6 and Mier2. These findings are consistent with reported studies by Surani and Kono's groups revealing the significance of H19 in development and differentiation of parthenogenetic embryos and P-ESCs [55, 79, 108]. Future studies are necessary in order to reveal the exact mechanism through which *H19* exerts its role in the P-ESCs differentiation potential. One suggestive mechanism could be that *H19* through its product mir675 regulates the expression of *MyoD*, *Myf6* and *Mier2*. We already have identified *Mier2* as potential targets of mir675 based on miRNA TargetScan [140].

We also found the expression of *deltaNp63* to be 250 fold overexpressed in P-ESCs compared to control B-ESCs (P<0.05; Supplem. Figure 3.6A). DeltaNp63 is a product of the Tumor Protein 63 gene (TP63) and is involved in stem cell maintenance and commitment to ectoderm lineages [151-152]. TP63 mRNA is transcribed from two alternative promoters which give rise to two different TP63 isoforms – deltaNp63 and TAp63. Disruption of deltaNp63 in mice results in failure of proper ectoderm development [153]. Overexpression of deltaNp63 may induce the P-ESCs, when differentiated in vivo, to give rise to mostly ectodermal derivatives. Moreover, we found that suppression of H19 gene expression in P-ESCs results in significant downregulation of the deltaNp63 which coincides with less propensity of these cells to differentiate to ectoderm lineage (P<0.05;Supplem. Figure 3.6D). The aforementioned findings may explain the high prevalence of ectoderm derivatives in teratomas derived from P-ESCs (see Figure 3.3A) and the decrease of ectoderm contribution to teratomas derived from P-ESCs with downregulated H19 expression. Unlike the expression in ES cells, the expression of *deltaNp63* in teratomas was inconclusive (Supplem. Figure 3.6C, D). However, since teratomas consist of heterogenous population of germ layer

derivatives, it is logical to conclude that the detection of the deltaNp63 in teratomas will vary depending on the prevalence of structures that express it (Supplem. Figure 3.7). We have also analyzed the mRNA abundance of the second major isoform of TP63 gene -TAp63. TAp63 expression is negatively regulated by deltaNp63 during ectoderm development. For a proper ectoderm differentiation, TAp63 expression is downregulated which coincides with upregulation of *deltaNp63*. We found that *TAp63* was significantly downregulated in P-ESCs compare to B-ESCs which coincided with high levels of deltaNp63 (P<0.05; Figure 3.6A). Upon downregulation of H19 the TAp63 expression was increased. Interestingly this expression pattern was maintained upon in vivo differentiation of the P-ESCs and B-ESCs into teratomas (Supplem. Figure 3.6A-C). qRT-PCR for *TAp63* expression in teratomas derived from P-ESCs with suppressed H19 expression indicated that the TAp63 mRNA abundance was significantly increased (Supplem. Figure 3.6D). It is well known that long non coding RNAs (ncRNA), such as H19, are involved in transcriptional regulation of multiple gene targets [154]. Therefore, one possible mechanism for the high overexpression of *deltaNp63* in P-ESCs may involve the H19ncRNA. H19ncRNA may act as transcriptional activator of deltaNp63 expression and therefore suppression of H19 may result in decrease of deltaNp63 transcript. TAp63 expression pattern observed in P-ESCs and B-ESCs as well as in cells with downregulated *H19* might be a result of transcriptional repression by deltaNp63 as, a mechanism reported by many scientific groups [155-156]. Interestingly we found that mir675 has 11bp perfect match to the trans-activating (TA) domain of TP63 mRNA (Supplem. Figure 3.10) and may account for upregulation of TAp63 in ES cells and teratomas observed (P<0.05; Supplem. Figure 3.6A-D) upon down regulation

of *H19*. Another possible mechanism for regulation of *deltaNp63* and *TAp63* expression in P-ESCs and B-ESCs might be through other, yet unknown factors.

Parthenogenetic stem cells represent a unique source of stem cells. They are indistinguishable by morphology from normal B-ESCs and can be propagated in vitro for a long period of time while still keeping their pluripotency. Moreover, our study revealed that P-ESCs differentiation potential towards mesoderm and endoderm germ layers can be enhanced by modulating *H19* gene expression. The major obstacles of using mouse P-ESCs as a model is that longer culture propagation, evokes high frequency of aneuploidy 39XO and other chromosomal aberrations. This phenomenon has been very well studied and described in parthenogenetic and normal fertilized B-ESC lines by various groups [85, 122, 157-161]. Some of the chromosomal abnormalities can be affecting the stem cells properties of the ES cell and some may not. For example trisomy eight has been found to be a problem during prolong passaging of mouse B-ESCs, however it has no effect on differentiation potential of the mouse B-ESCs [162]. The same holds true also for trisomies 1, 2, 6, 7, 10, 12-14, 16, 18 and 19. Complete trisomic mice for aforementioned chromosomes can complete gastrulation stage (6.5-13.5 dpc) giving rise to all three main germ layers – ecto-, meso- and endo-derm [163-166]. We also found that P-ESCs at passage 9 already show an euploidy for the X chromosome (Supplem. Table3.1). This tendency escalates pass passage12 when other chromosome abnormalities may occur. It has been also reported that aneuploid cells are indistinguishable from normal cells in that they can contribute to all tissues and organs of a chimeric animal [167-168]. Therefore, due to high frequency of cytogenetic abnormalities in mouse B-ESCs and P-ESCs in culture, the number of clones without

chromosomal aberrations that can be derived after prolonged passaging, may be very limited. Despite the obstacles mentioned above, the embryonic stem cells properties do not change at least in term of their differentiation potential, even in the presence of certain trisomies.

In conclusion, these data demonstrate that suppression of *H19* in P-ESCs has a profound effect on the ability of these cells to give rise to mesoderm muscle derivatives. Our data together with others strongly enforce the rationale of using P-ESCs in the clinic. Studies in primate P-ESCs, the closest species to human, have already shown the differentiation plasticity of these cells to give rise to all three germ layers in teratomas and to functional neurons when differentiated *in vitro* and transplanted into animal models *[17, 95, 106]* Further studies of the role of the imprinted genes in modulating the developmental potential of human P-ESCs are needed to assess the safety and the efficiency of these cells to replace or regenerate the needed tissue *in vivo*.

FIGURES AND TABLES

Figure 3.1 Alterations in *H19/lgf2* expression and *DMR* methylation in P-ESCs. (A) Quantification of mRNA abundance of *H19* and *lgf2* imprinted gene expression in mouse B-ESCs and P-ESCs by qRT-PCR. (B) Schematic representation of the *H19/lgf2* DMR region. (C) Methylation profile of *H19/lgf2* DMR region in Rosa 26 strain of mice, on the bottom are indicated the CpG sites in nucleotides (nt), on the top is indicated the number of the CpG site. (D) Percent (%) methylation of the 15th CpG islands of the DMR region in Rosa26 strain of mice. (E) Quantification of mRNA abundance of the *P57*, *lgf2R*, *lgf2*, *Mest1* and *Mkrn* imprinted genes expression in mouse B-ESCs and P-ESCs by qRT-PCR. (F) Quantification of mRNA abundance of the pluripotency gene *Nanog* gene expression in mouse B-ESCs and P-ESCs by qRT-PCR. For all qRT-PCR experiments three biological replicates (n=3) in three technical replicates were used in each run and a P<0.05 has been considered as statistical significant, unless stated otherwise. The bars represent stand error bars. All the letters above the error bars represent the difference between samples on the basis of standard error values (P<0.05).



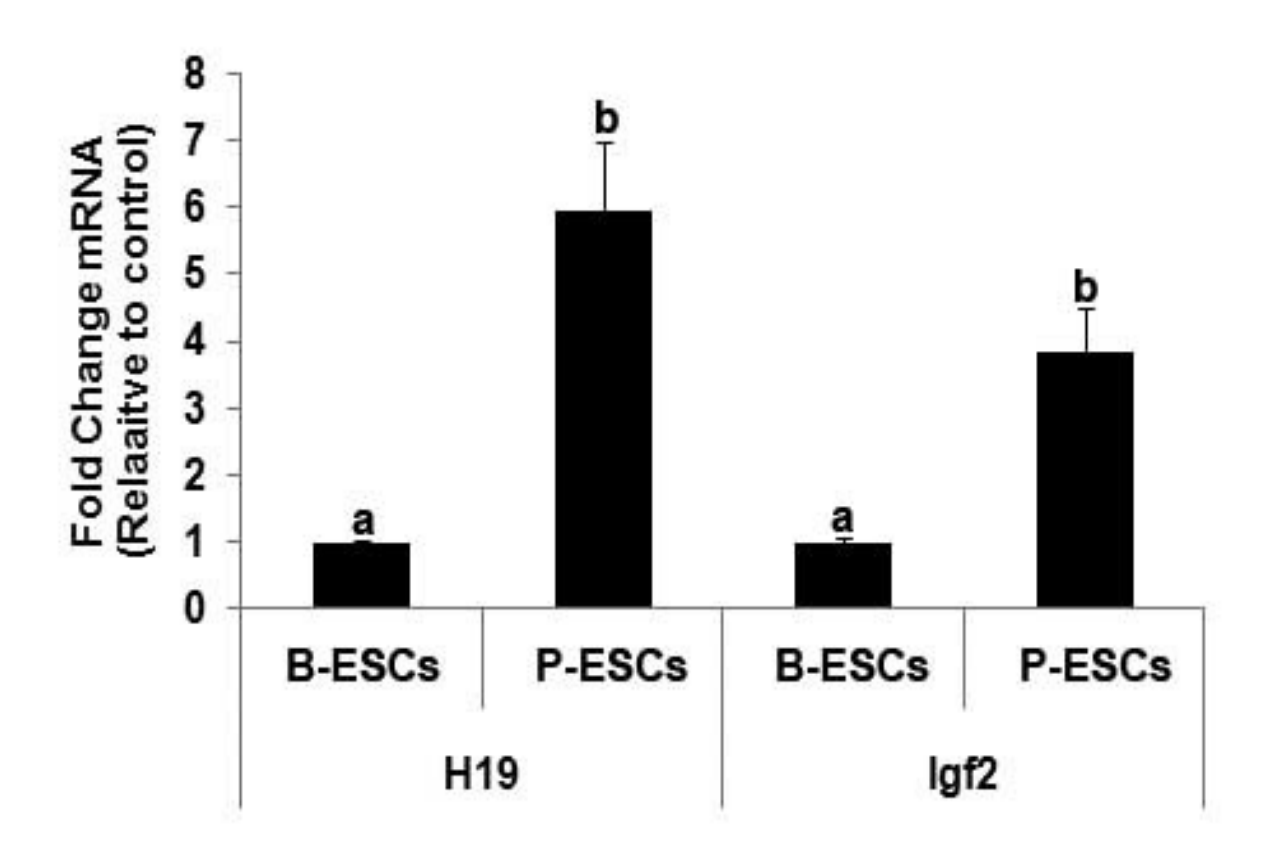


Figure 3.1 (cont'd)

B

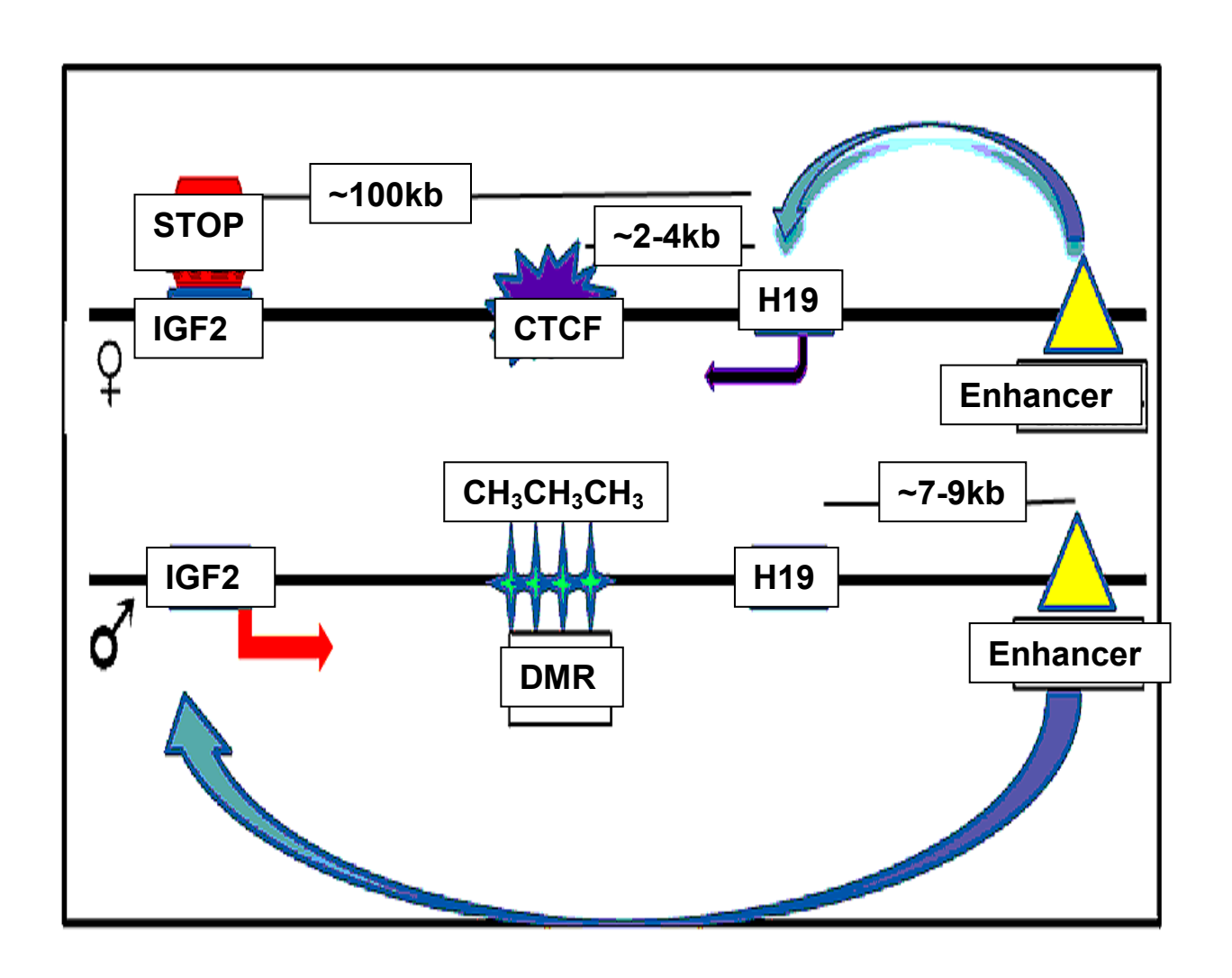


Figure 3.1 (cont'd)

C

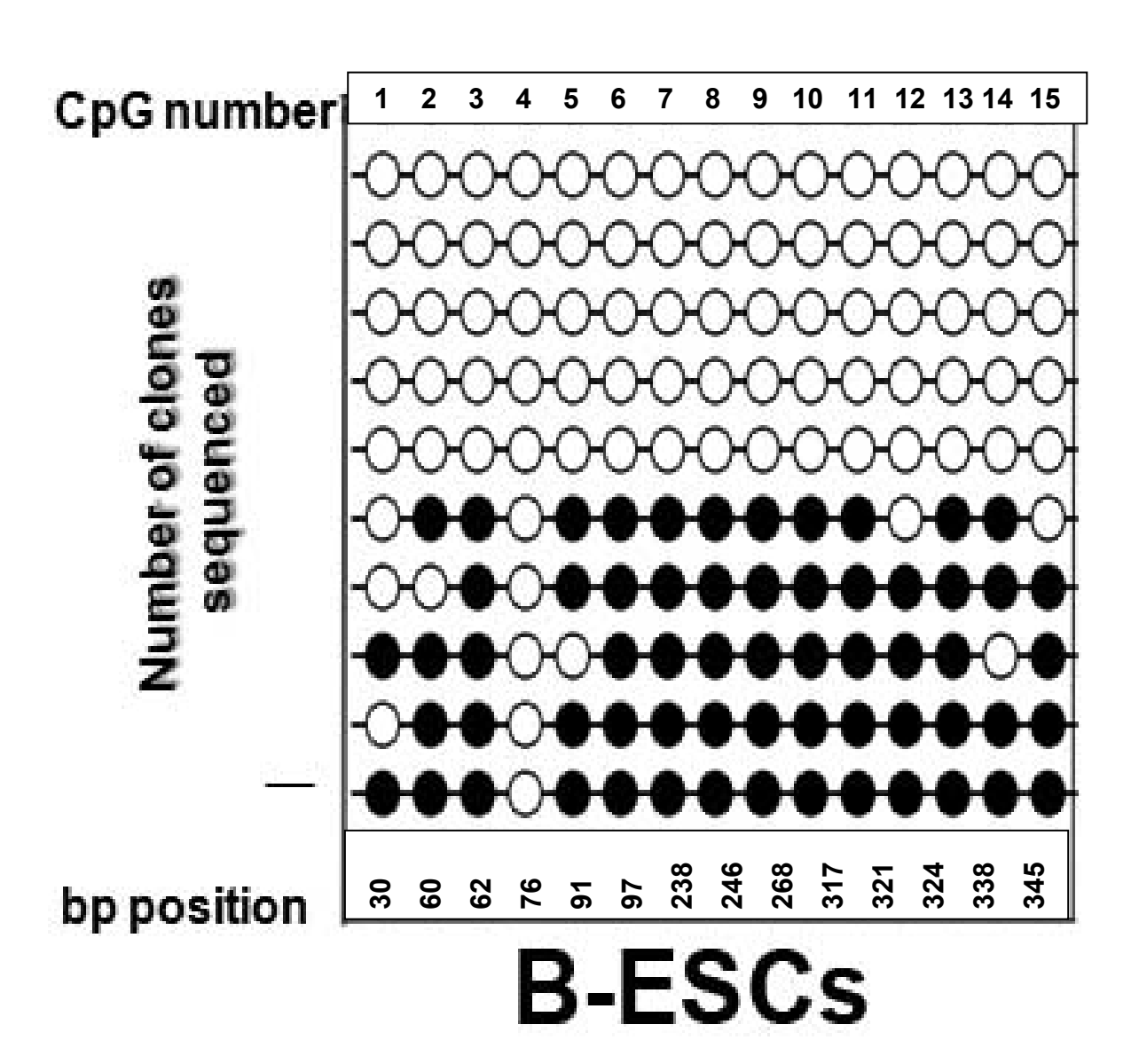
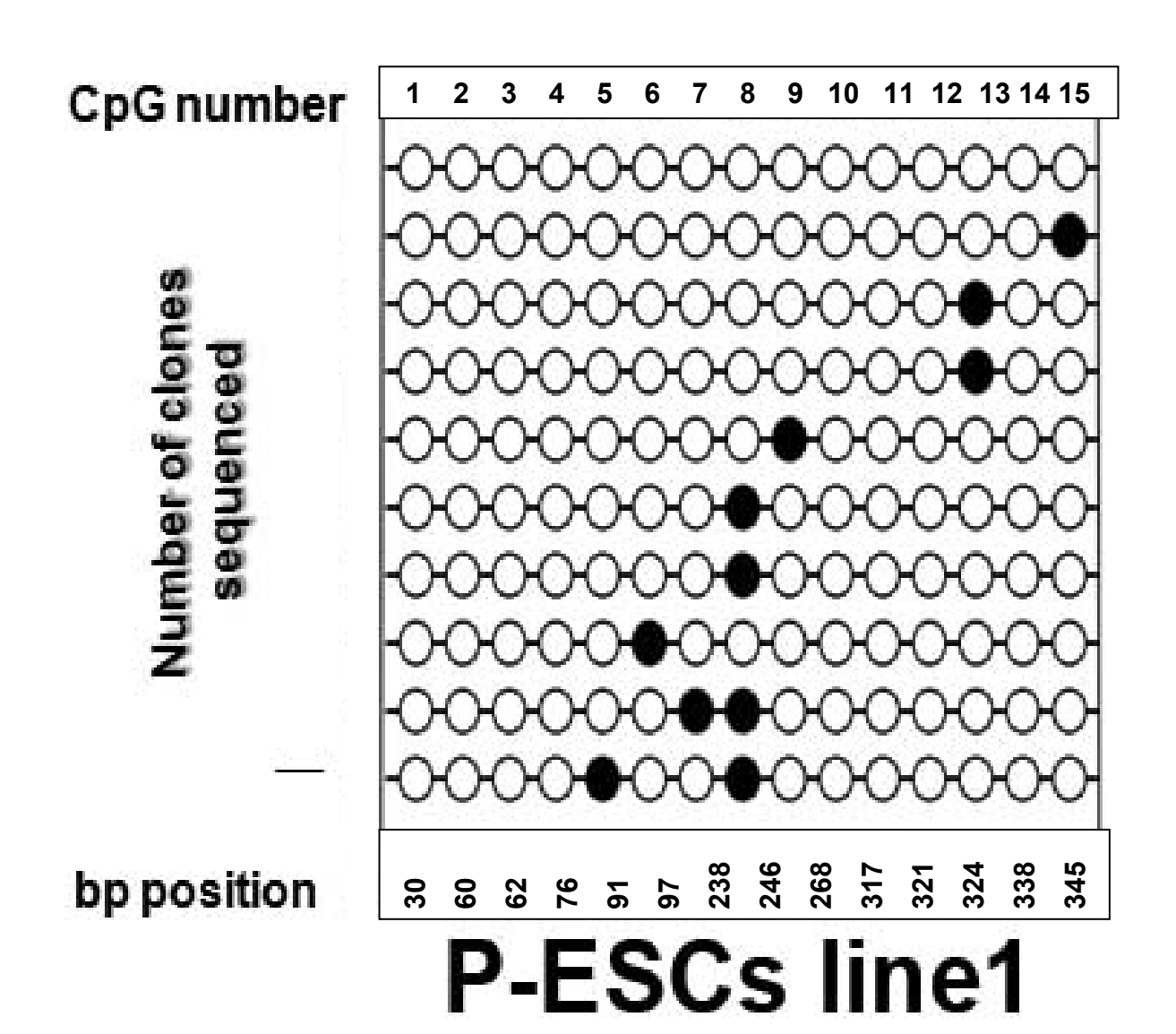


Figure 3.1 C (cont'd)



150

Figure 3.1 C (cont'd)

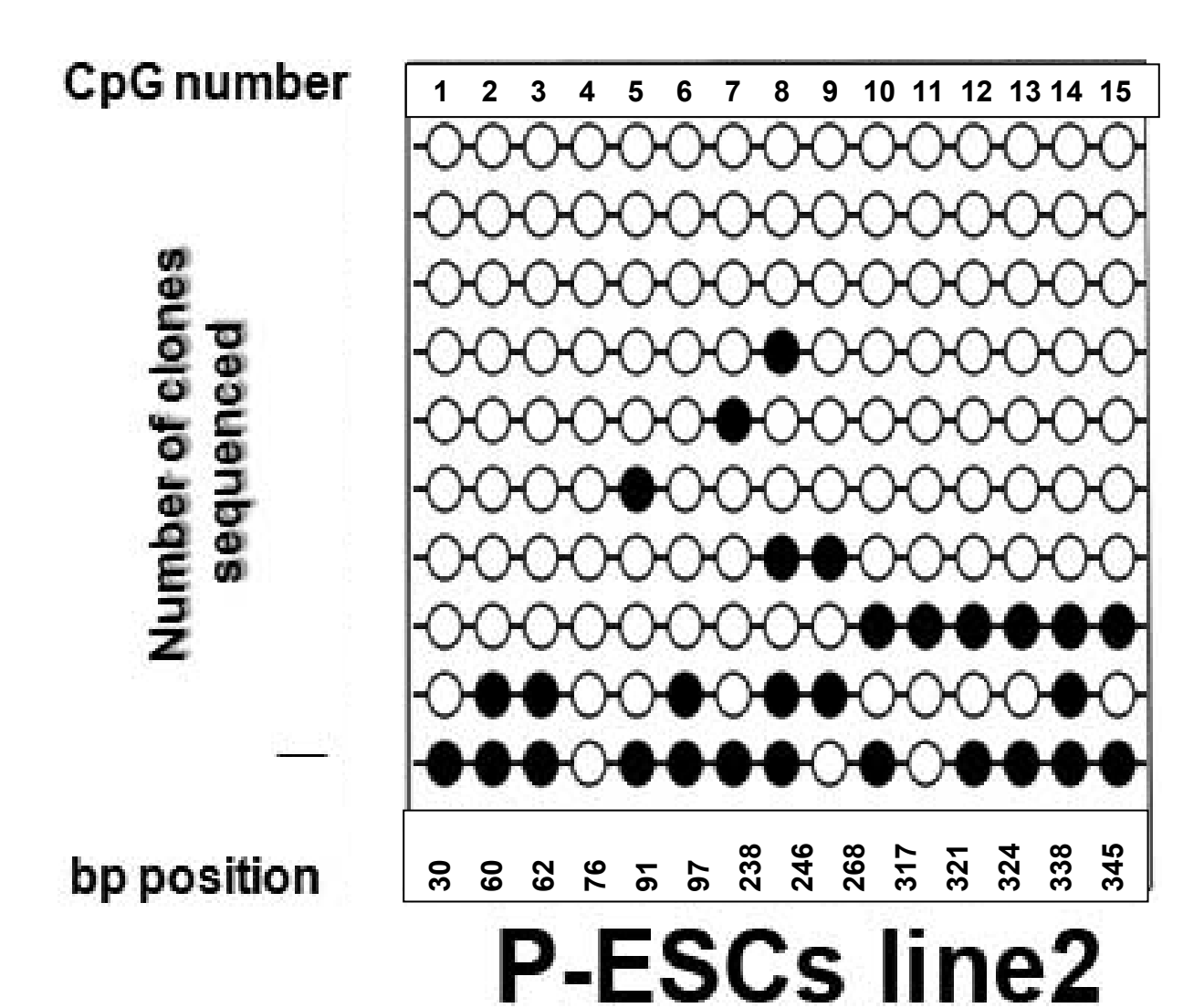


Figure 3.1 (cont'd)

D

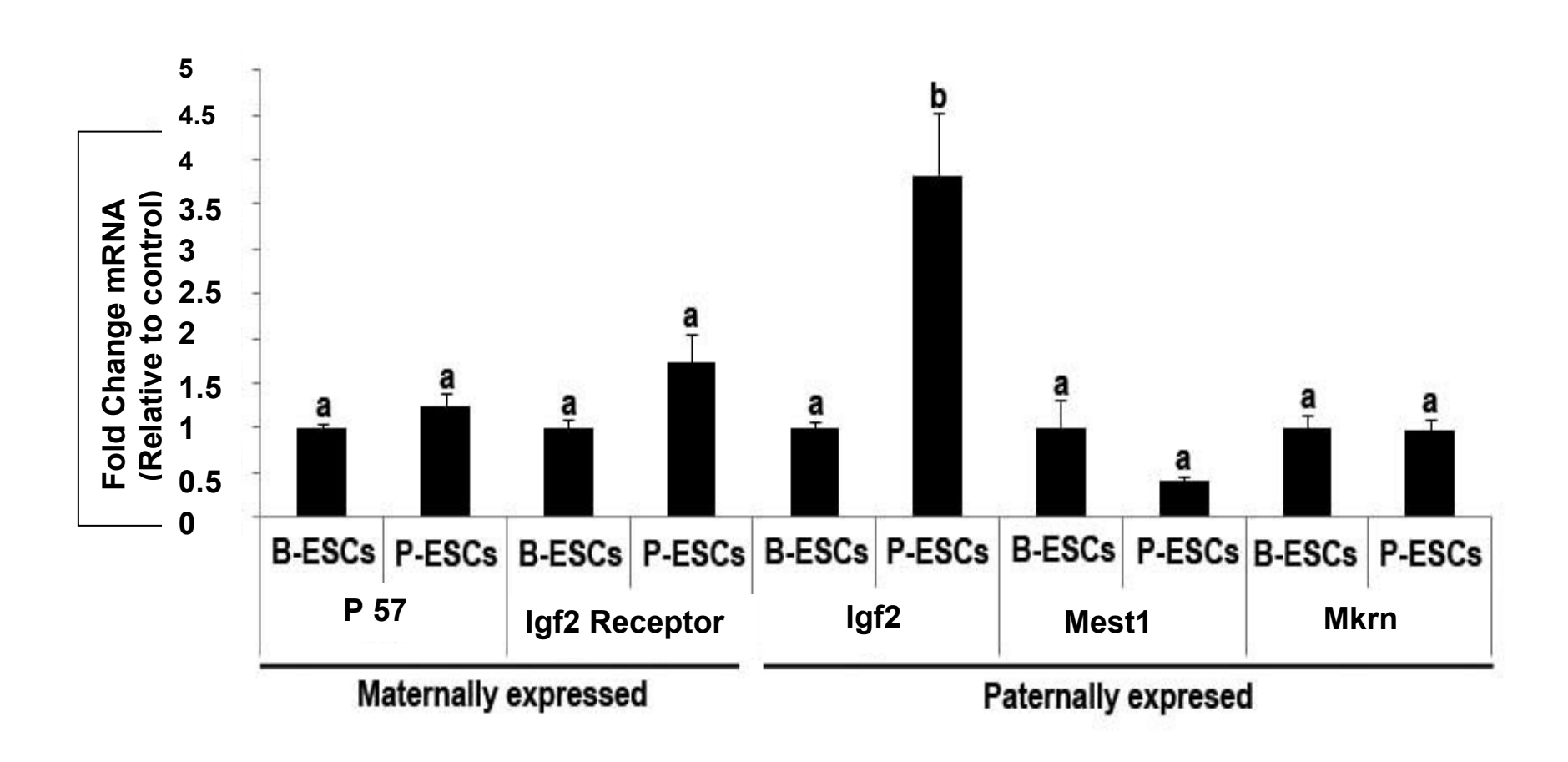


Figure 3.1 (cont'd)

E

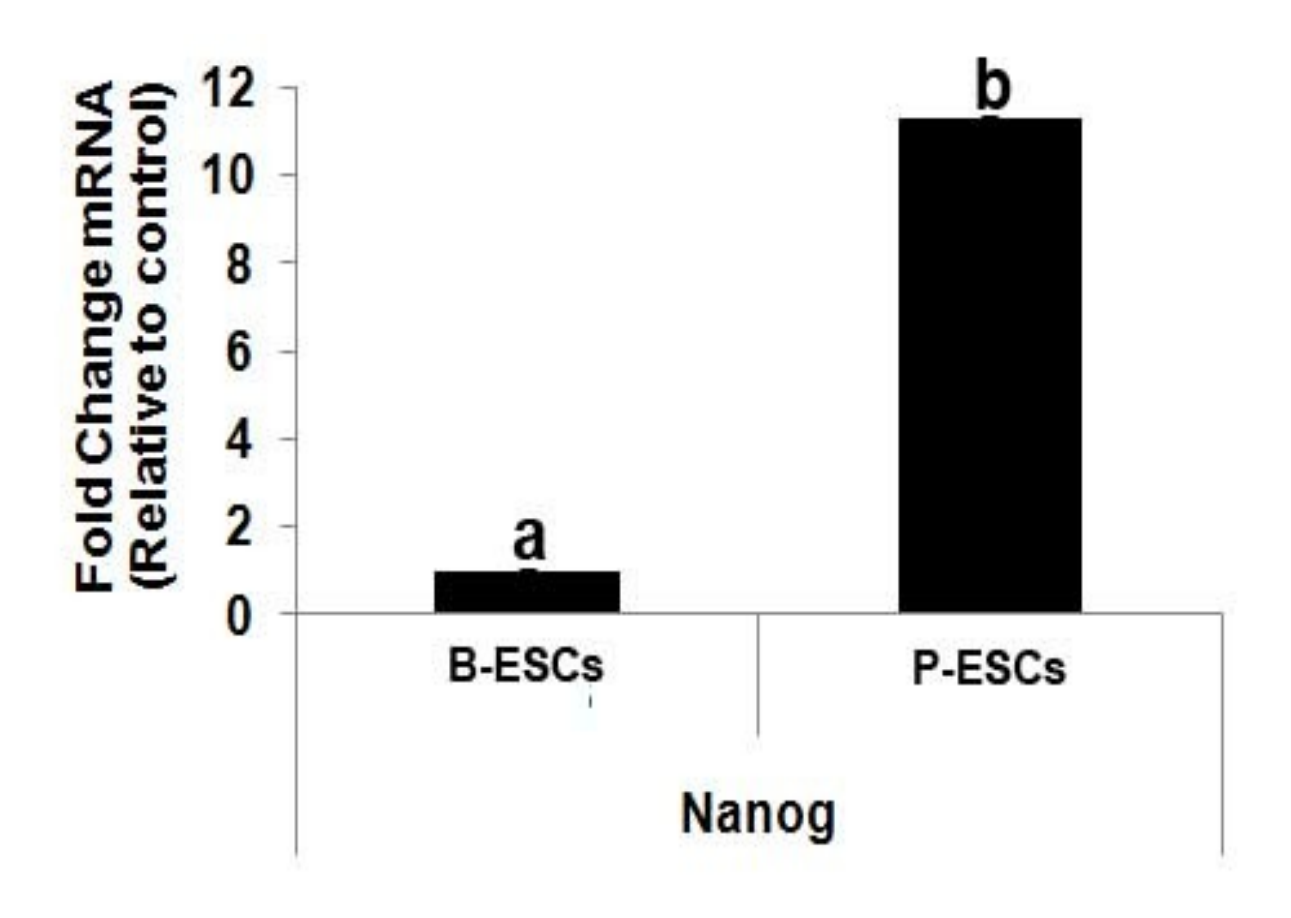


Figure 3.2 Elevated levels of *H19* expression persist during P-ESCs differentiation *in vivo*. Quantification of *H19* (A) and *Igf2* (B) from LCM obtained primitive glandular structures (Endoderm) and neural rosettes (Ectoderm) by qRT-PCR. (C-D) Quantification of *H19* and *Igf2*(C) *and Rb* (D) mRNA abundance in whole teratoma sections by qRT-PCR (P<0.05). For all qRT-PCR experiments three biological replicates (n=3) in three technical replicates were used in each run and a P<0.05 has been considered as statistical significant, unless stated otherwise. The bars represent standard error bars. All the letters above the error bars represent the difference between samples on the basis of standard error values (P<0.05).



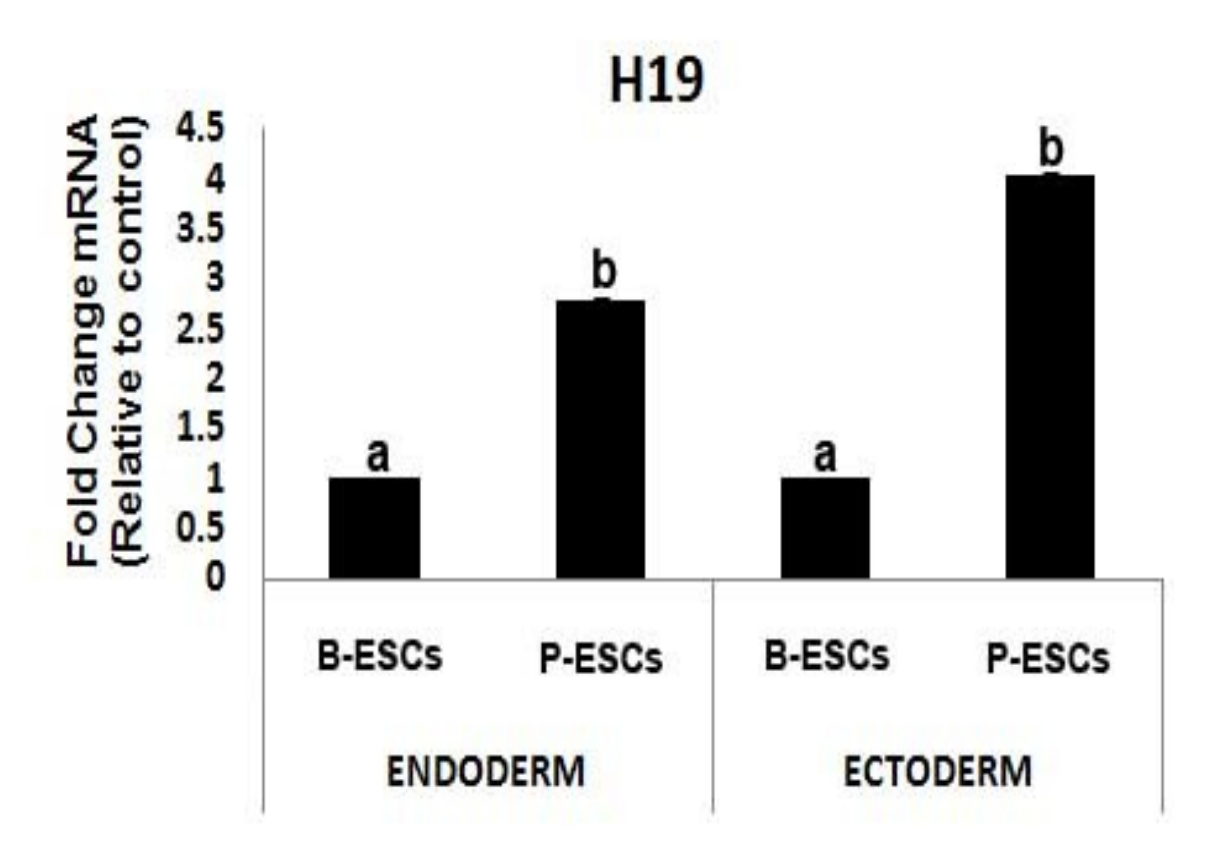


Figure 3.2 (cont'd)

B

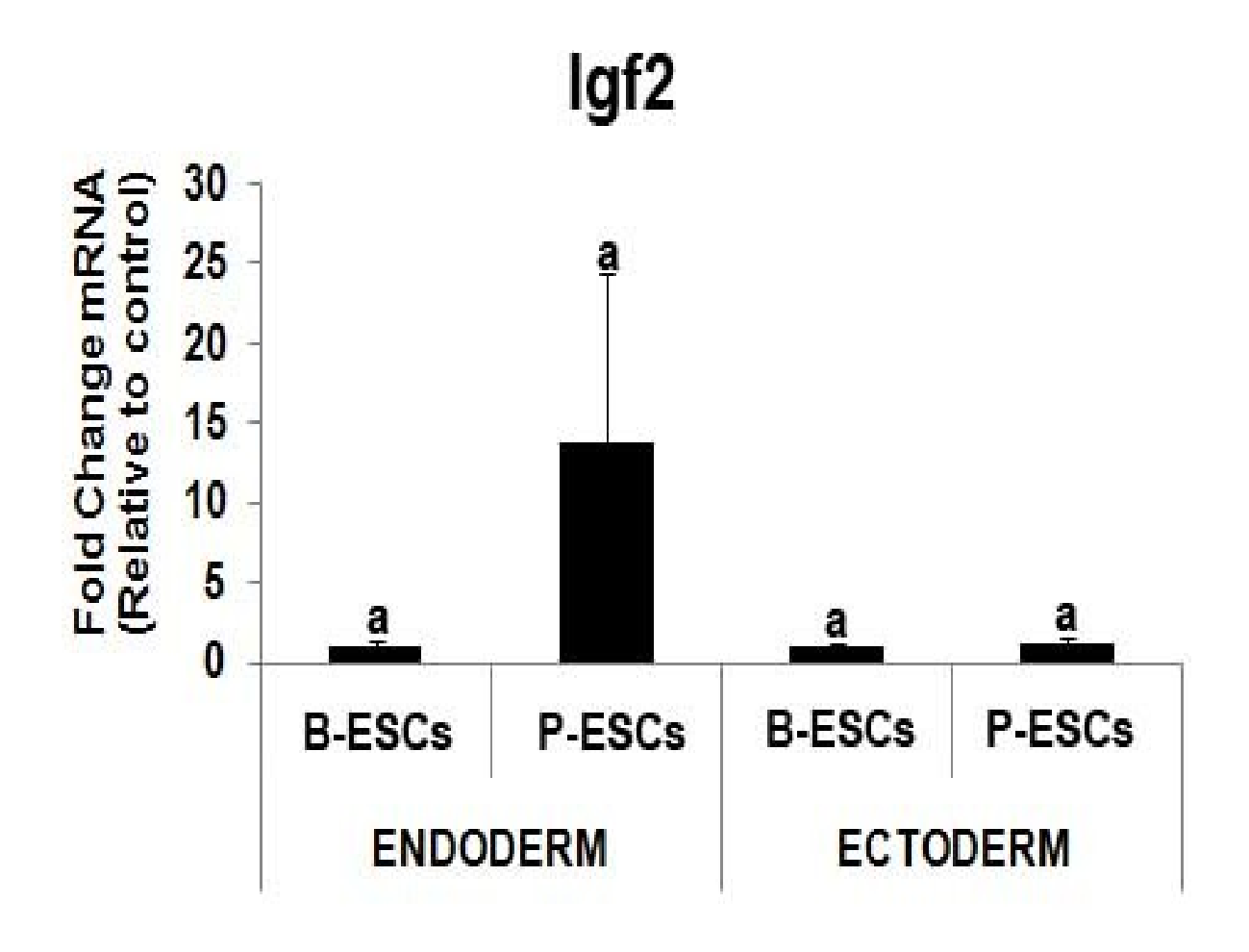


Figure 3.2 (cont'd)

C

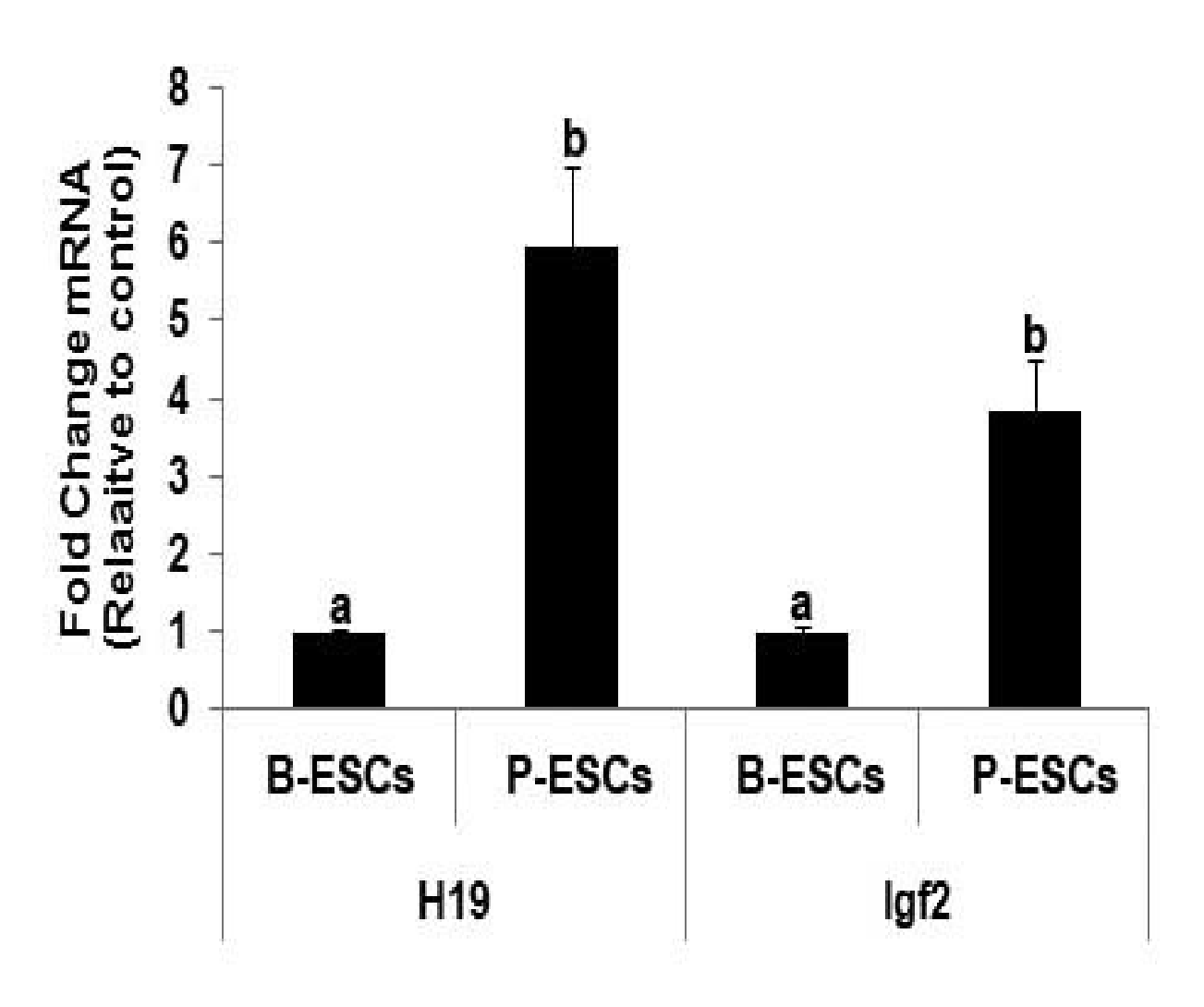


Figure 3.2 (cont'd)

D

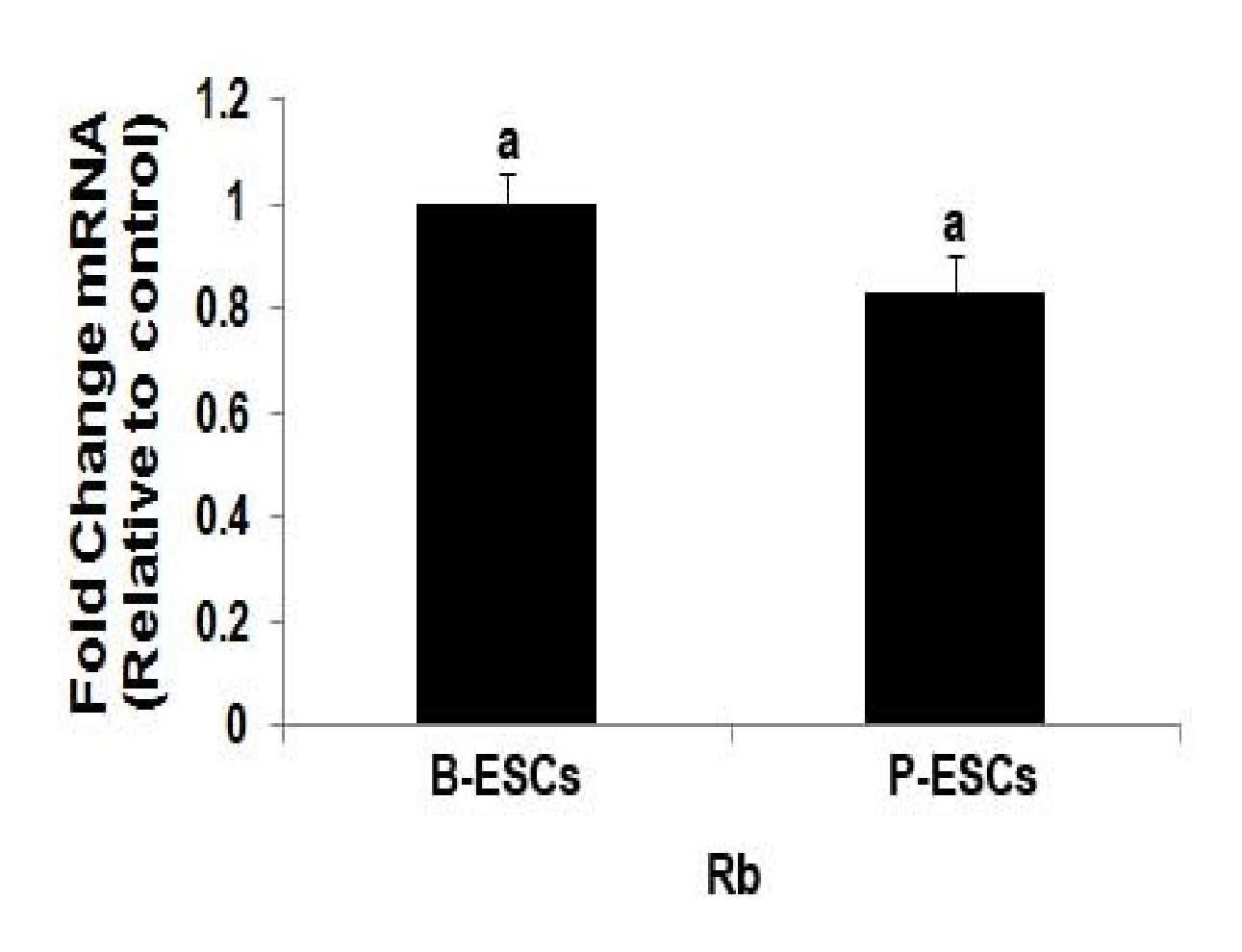


Figure 3.3 Lack of mesoderm muscle derivatives and downregulation of mesoderm specific transcripts in P-ESCs upon differentiation *in vivo*. (A) Quantification (%) of germ layer derivatives: ectoderm, endoderm and mesoderm; Three teratomas per sample have been evaluated (n=3). The bars represent stand error bars. All the letters above the error bars represent the difference between samples on the basis of standard error values (P<0.05). (B) qRT-PCR measuring the mRNA abundance of germ layer specific transcripts in P-ESCs and B-ESCs derived teratomas (P<0.05). For all qRT-PCR experiments three biological replicates (n=3) in three technical replicates were used in each run and a P<0.05 has been considered as statistical significant, unless stated otherwise. The bars represent stand error bars. All the letters above the error bars represent the difference between samples on the basis of standard error values (P<0.05).

Figure 3.3 (cont'd)

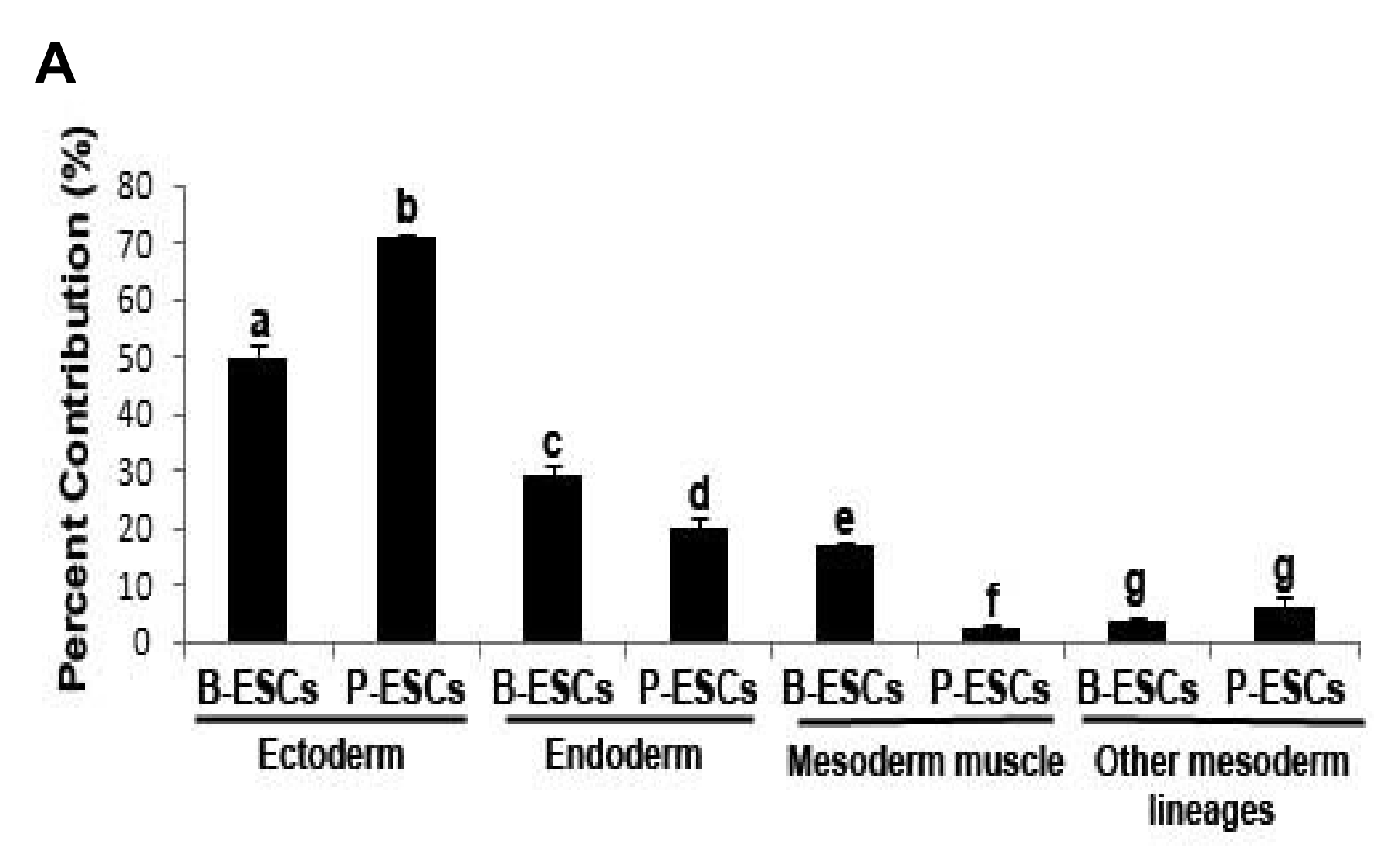


Figure 3.3 (cont'd)

B

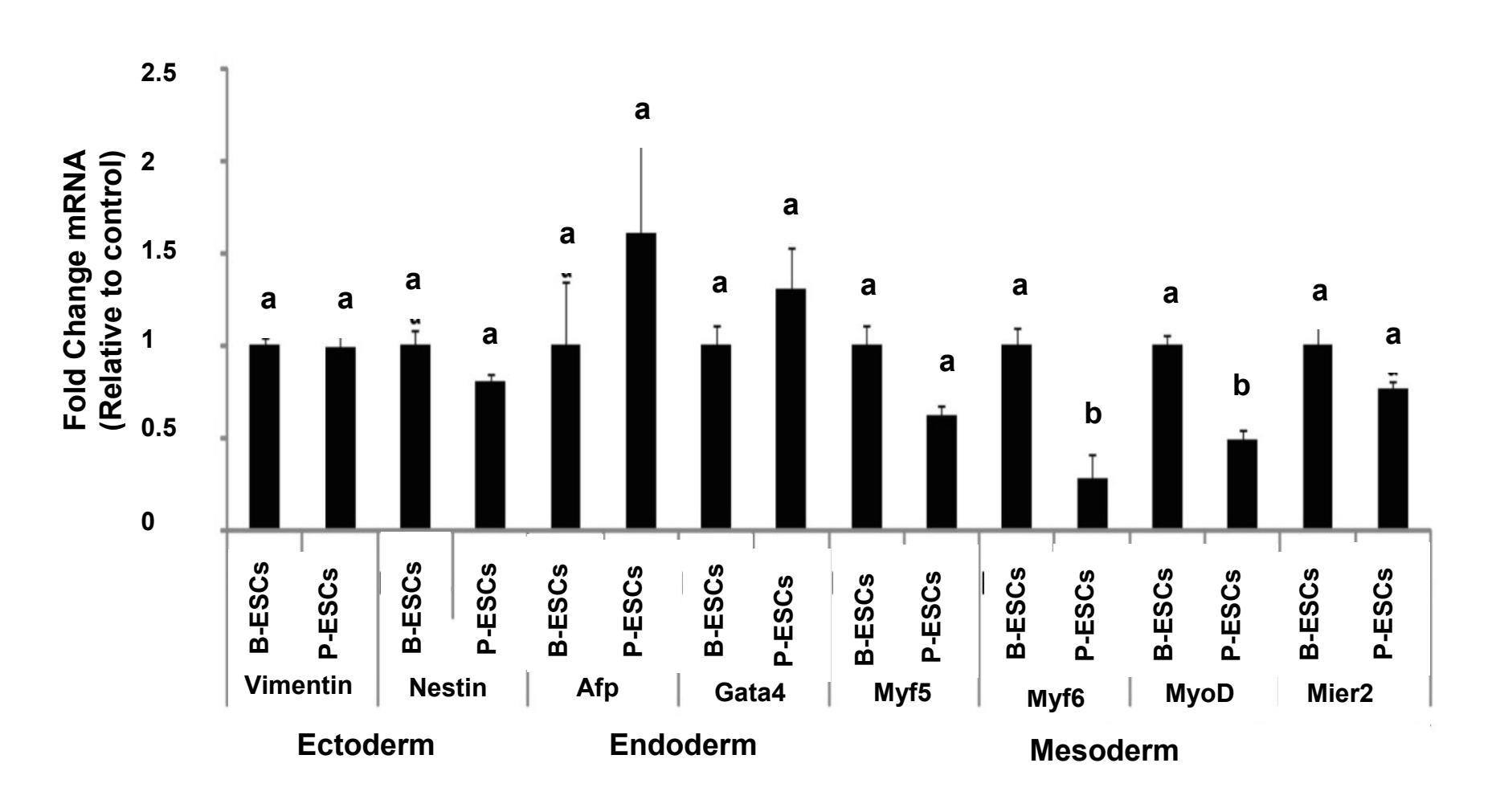


Figure 3.4 Stable and efficient down-regulation of *H19* mRNA levels in mouse P-ESCs; Quantification of the imprinted genes *H19* mRNA(A), *P57*, *Igf2R*, *Grb10*, *Igf2*, *Mest1* and *Mkrn* (B), *Rb* (C) and the early mesoderm promoter gene *Mier2* (D)abundance by qRT-PCR in *H19* down-regulated P-ESCs (shRNA) and in P-ESCs infected with the control retroviral vector (Con.vector) (P<0.05). For all qRT-PCR experiments three biological replicates (n=3) in three technical replicates were used in each run and a P<0.05 has been considered as statistical significant, unless stated otherwise. The bars represent stand error bars. All the letters above the error bars represent the difference between samples on the basis of standard error values (P<0.05).

Figure 3.4 (cont'd)



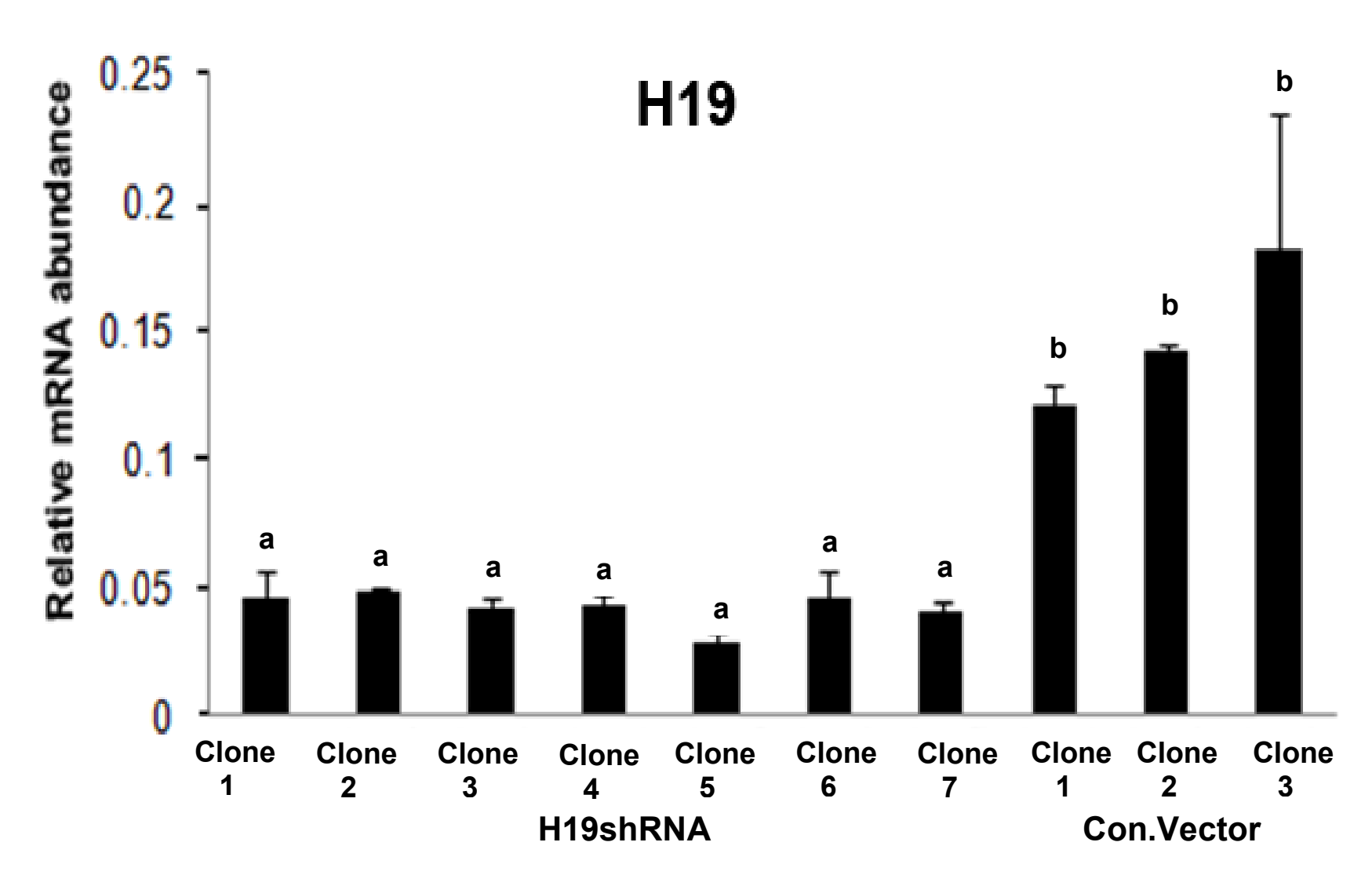
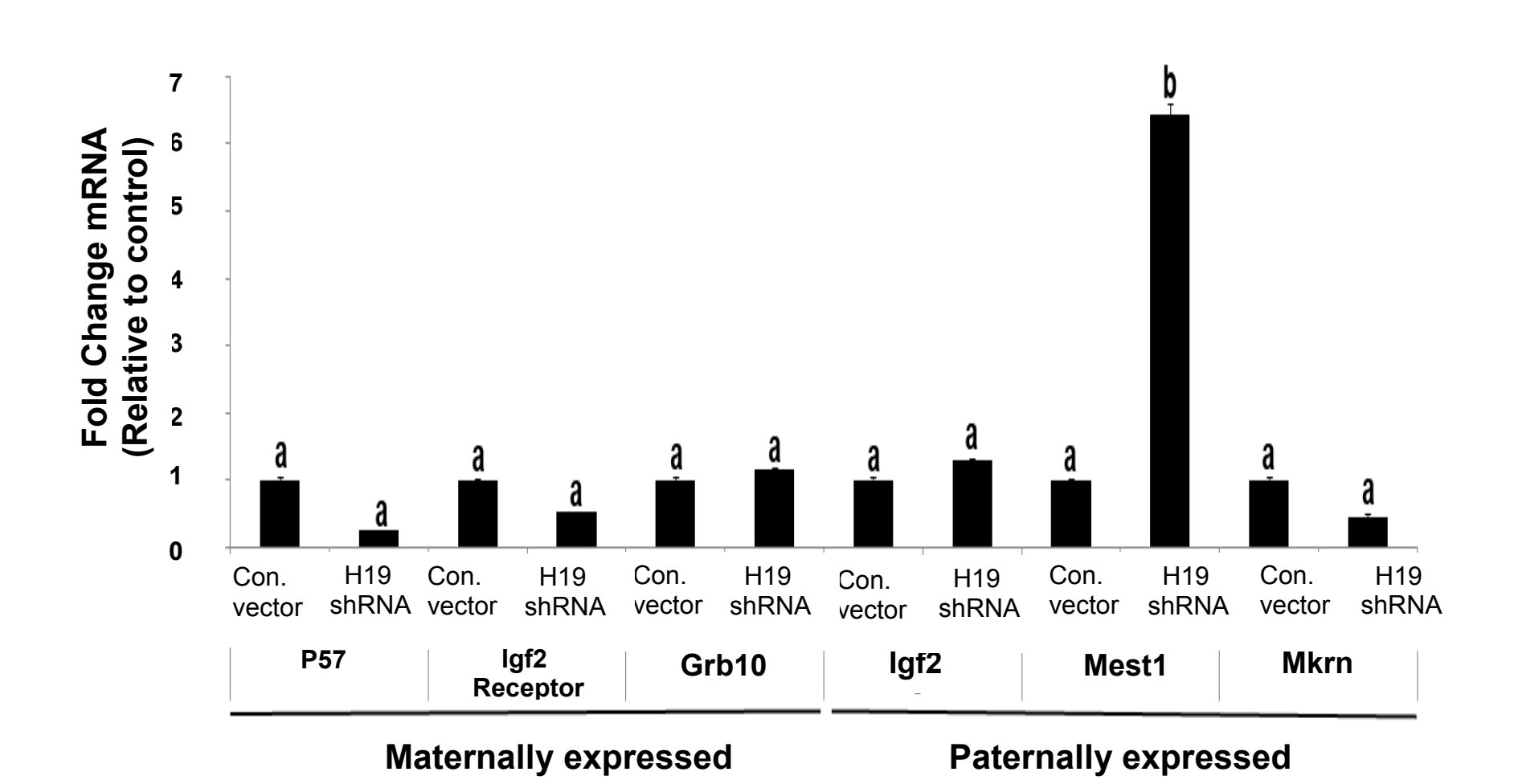


Figure 3.4 (cont'd)

B



163

Figure 3.4 (cont'd)

C

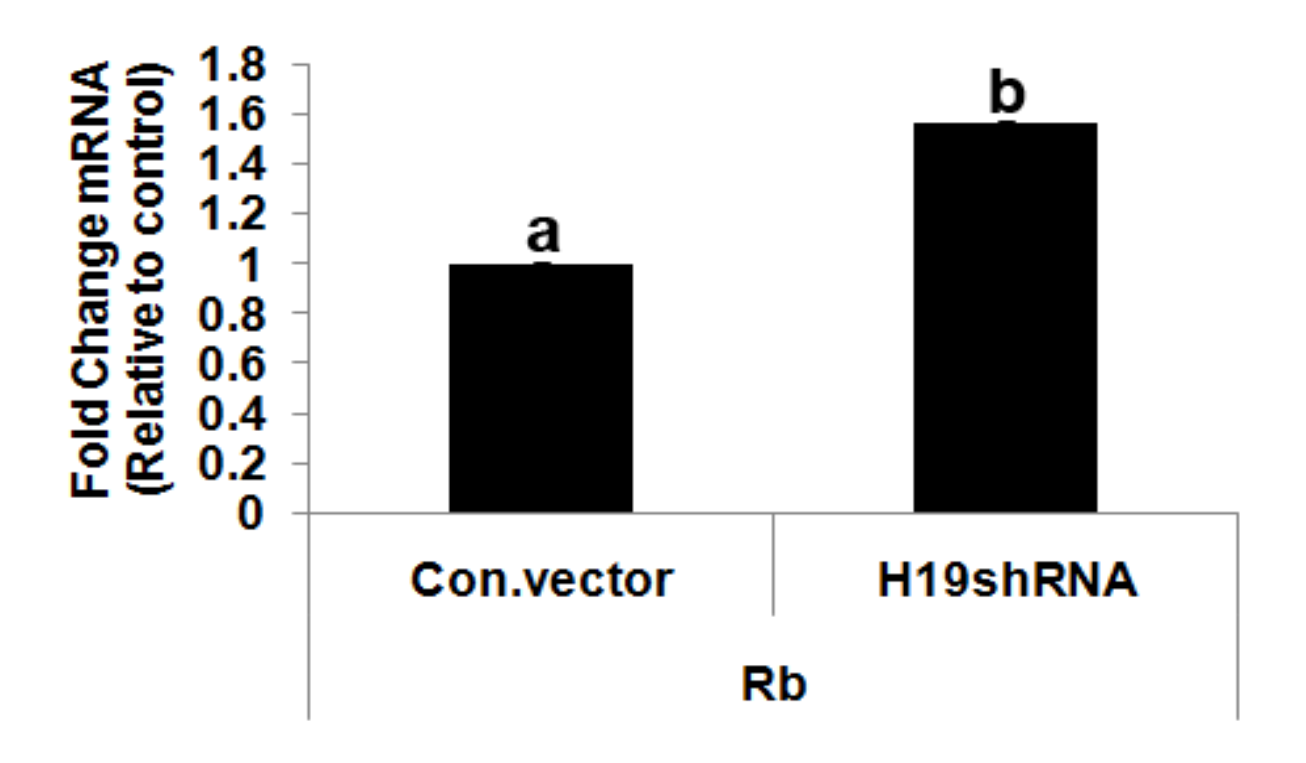


Figure 3.4 (cont'd)



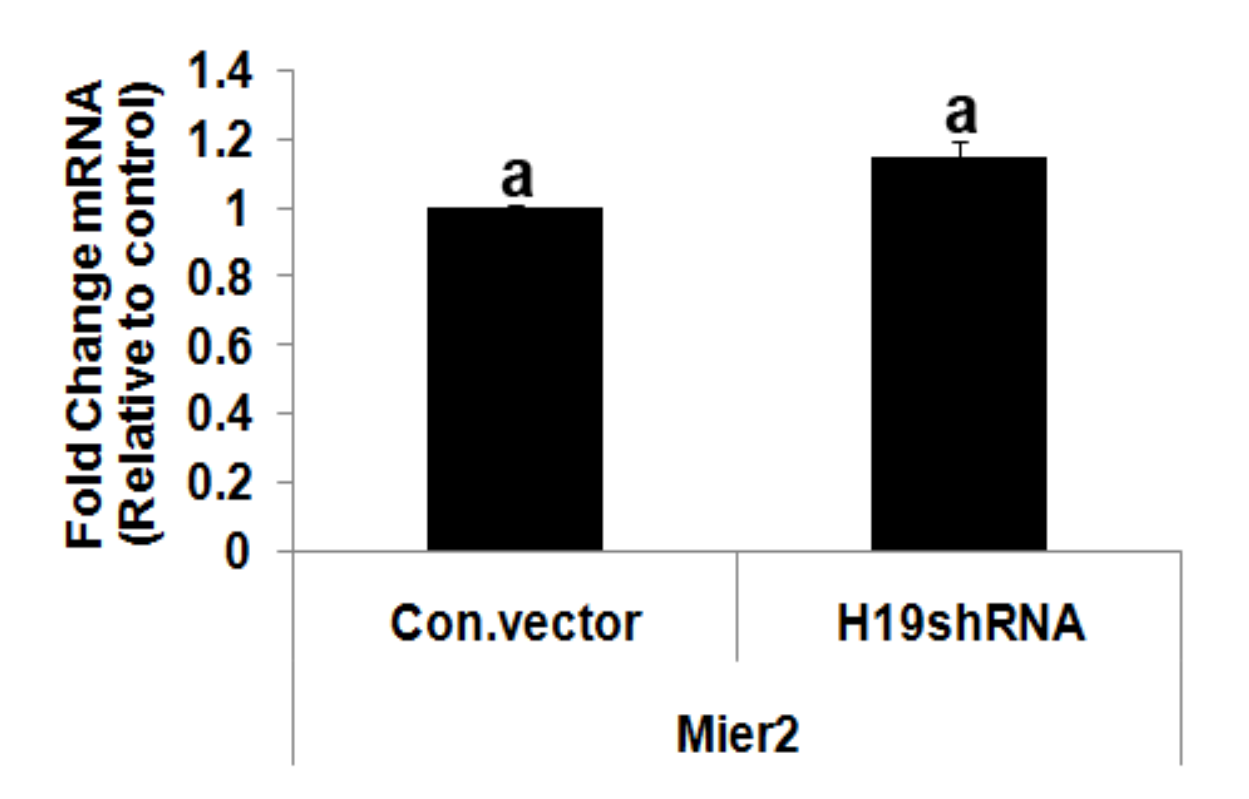


Figure 3.5 Downregulation of *H19* expression in P-ESCs promotes normal endoderm and mesoderm differentiation in vivo. (A) Quantification of H19 by gRT-PCR in samples derived from whole teratoma sections (P<0.05). For all qRT-PCR experiments three biological replicates (n=3) in three technical replicates were used in each run and a P<0.05 has been considered as statistical significant, unless stated otherwise. The bars represent stand error bars. All the letters above the error bars represent the difference between samples on the basis of standard error values (P<0.05). (B) Quantification (%) of germ layer derivatives; ectoderm, endoderm and mesoderm in teratomas derived from B-ESCs, H19 down-regulated P-ESCs (shRNA) and in P-ESCs infected with the control retroviral vector (Con.vector). Three teratomas per sample have been evaluated (n=3). The bars represent stand error bars. All the letters above the error bars represent the difference between samples on the basis of standard error values (P<0.05). (C) Quantification of mesoderm specific transcripts: MyoD, Myf6, Mier2 the paternally expressed gene Igf2 (D) and Rb (E) by qRT-PCR in samples derived from whole teratoma sections (P<0.05), n=3. The bars represent standard error bars. All the letters above the error bars represent the difference between samples on the basis of standard error values (P<0.05).

Figure 3.5 (cont'd)

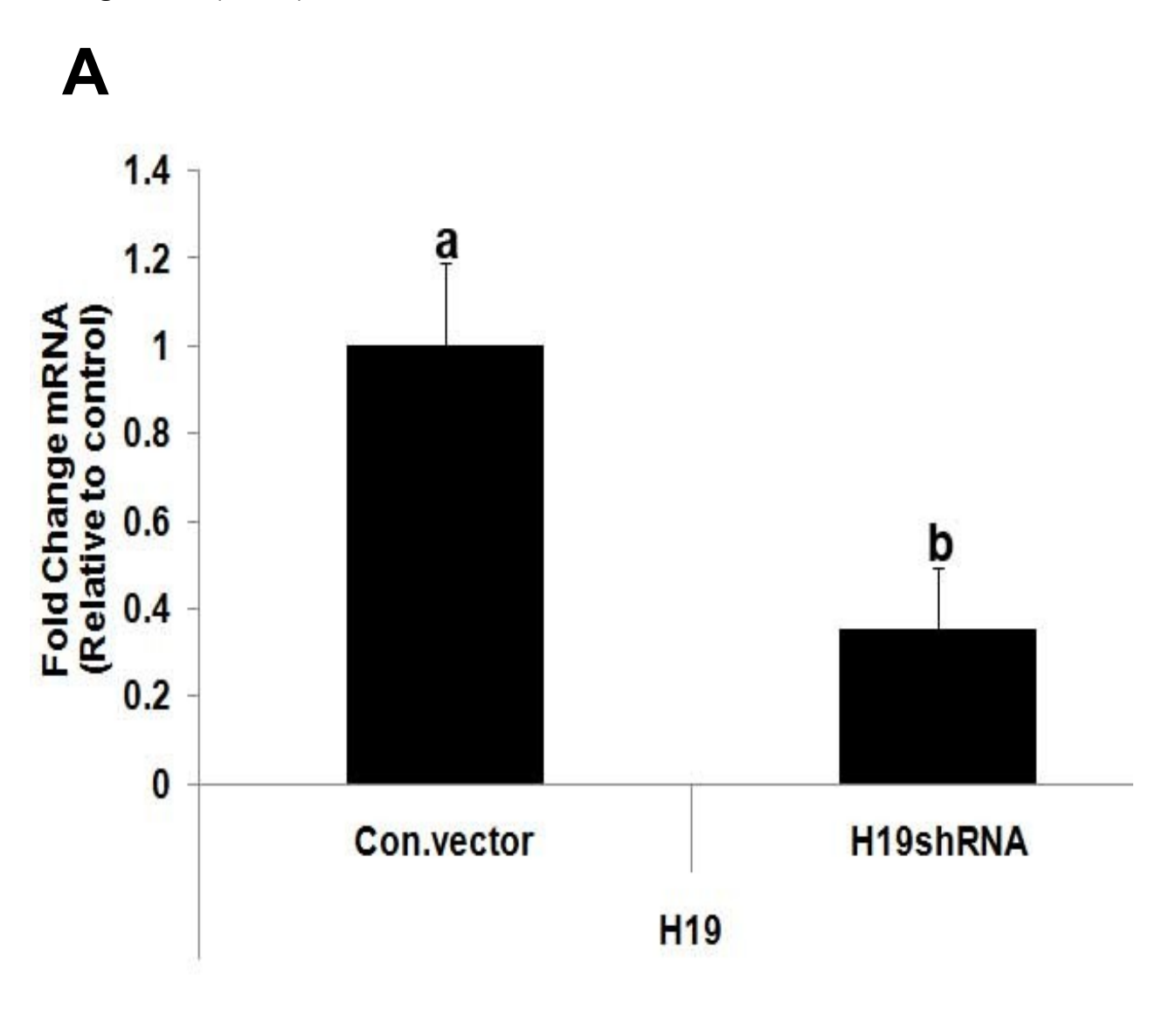


Figure 3.5 (cont'd)

B

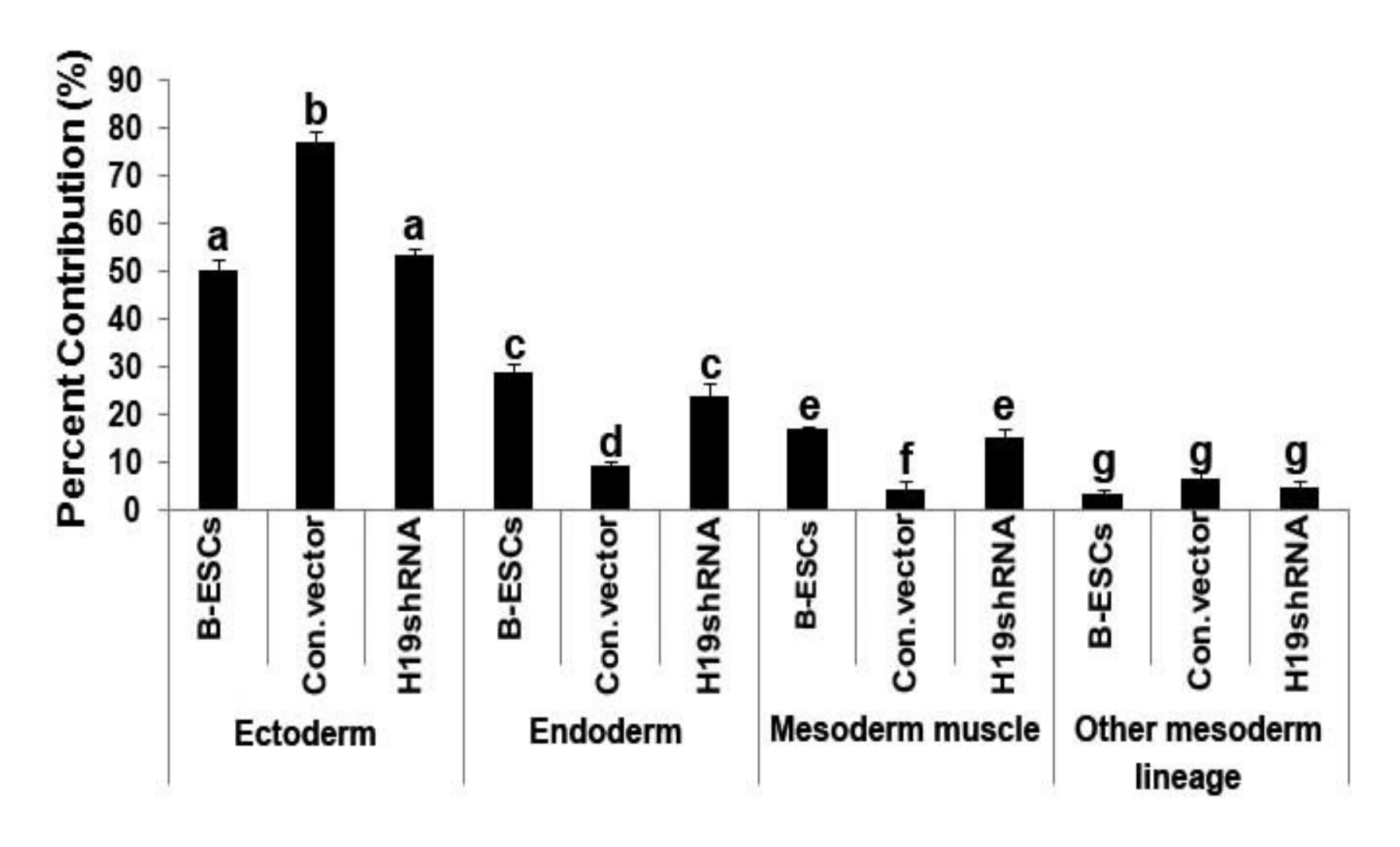


Figure 3.5 (cont'd)

C

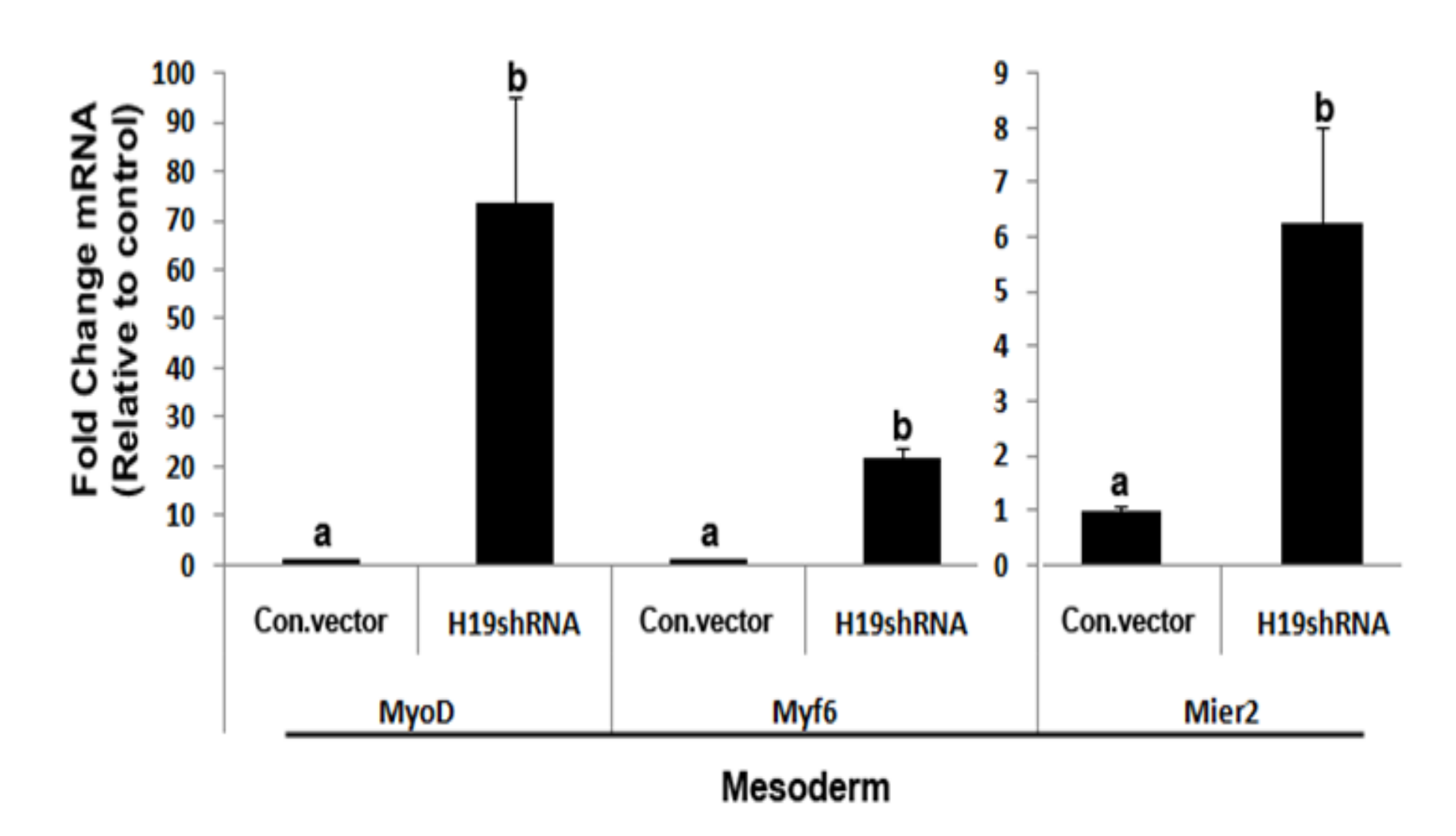


Figure 3.5 (cont'd)

D

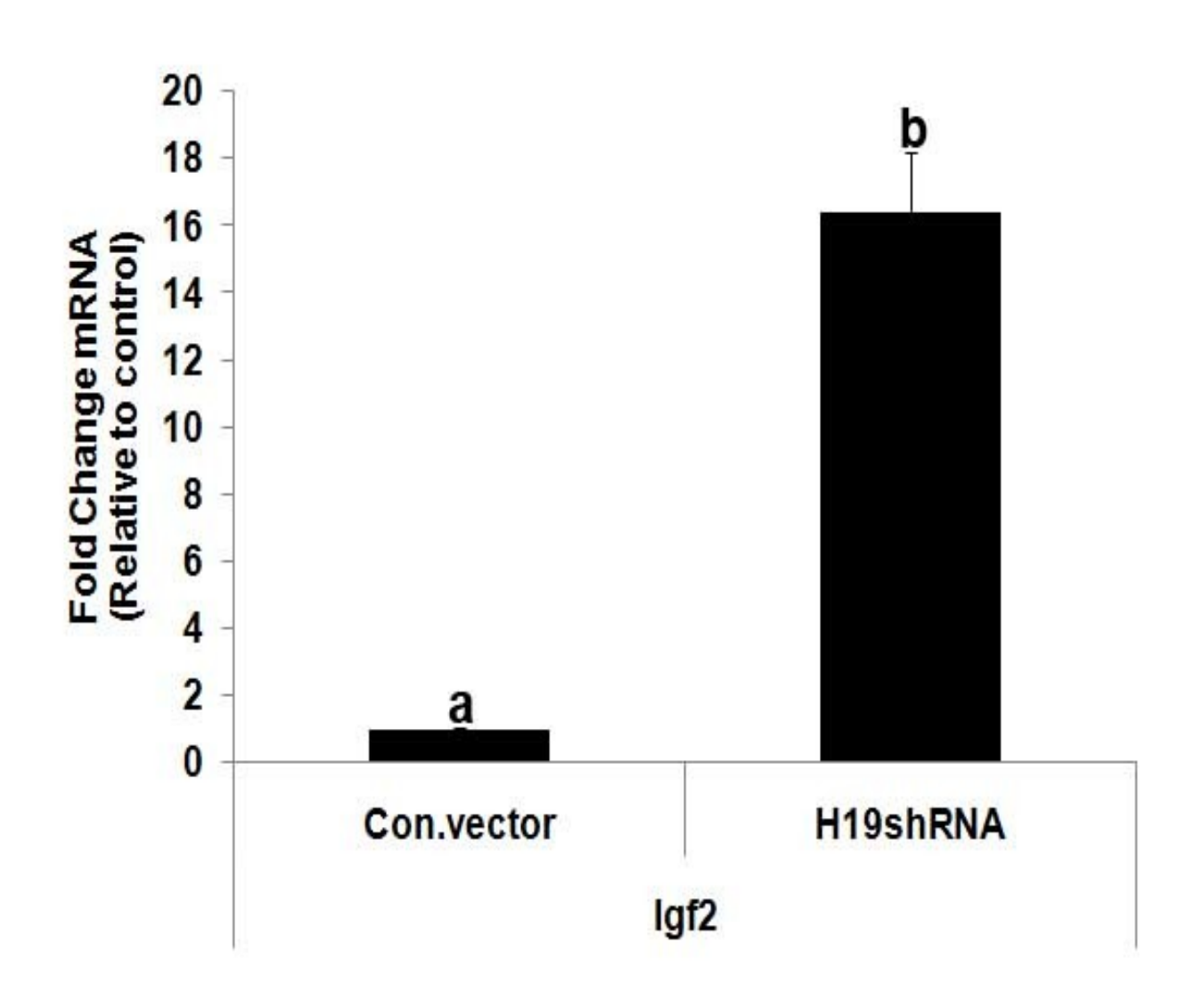


Figure 3.5 (cont'd)



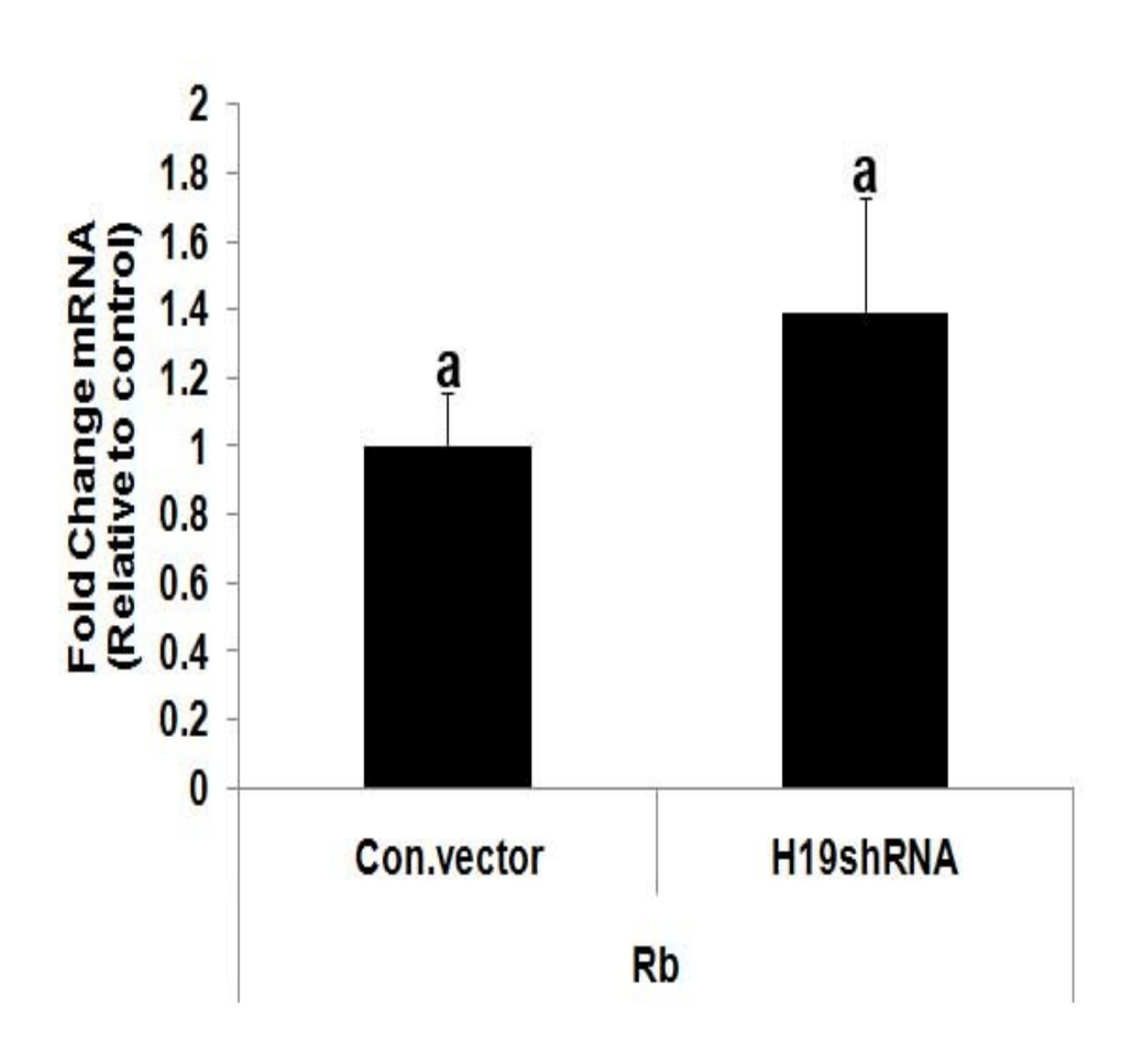


Figure 3.6 Derivation of beating embryo bodies (EBs) from B-ESCs, Control P-ESCs, and Control vector (Con.vector) and H19shRNA P-ESCs. (A) Immunostaining for cardiomyocyte specific markers: α-sarcomeric actin (αSM), α-sarcomeric myosin (αSM), and Myf5. (B). Incidence of derivation of beating EBs in percentage (%) on y-axis vs. days in culture on the x-axes. These experiments were repeated three times and total of 100 BPES, 176 Control P-ESCs, 140 H19shRNA P-ESCs and 224 Control vector (Con.vector) P-ESC derived embryo bodies (EB) were analyzed per experiment. (C) PCR for detection of alpha –cardiac actin in beating embryo bodies (EB). The bars represent stand error bars (P<0.05).

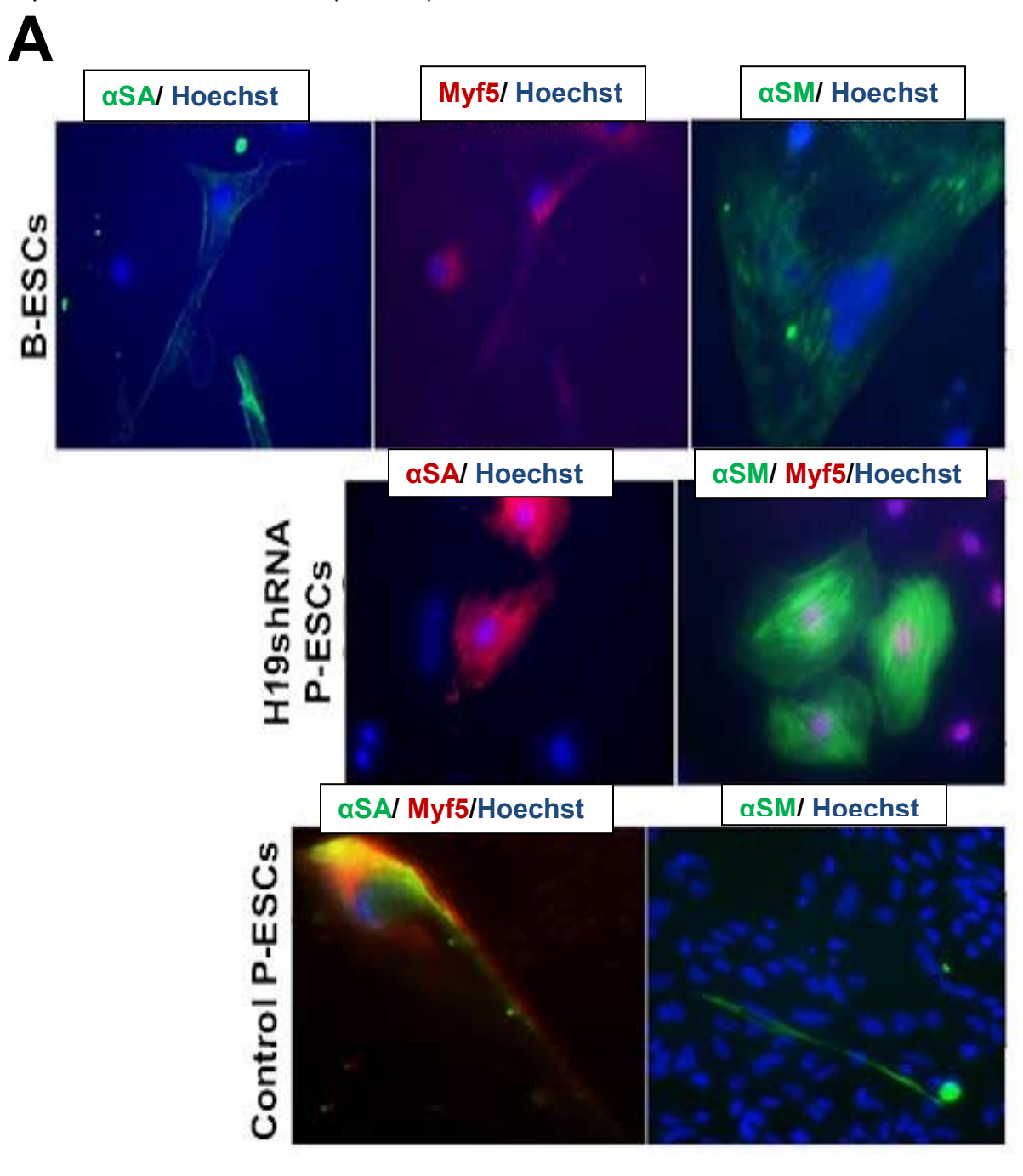


Figure 3.6 (cont'd)

B

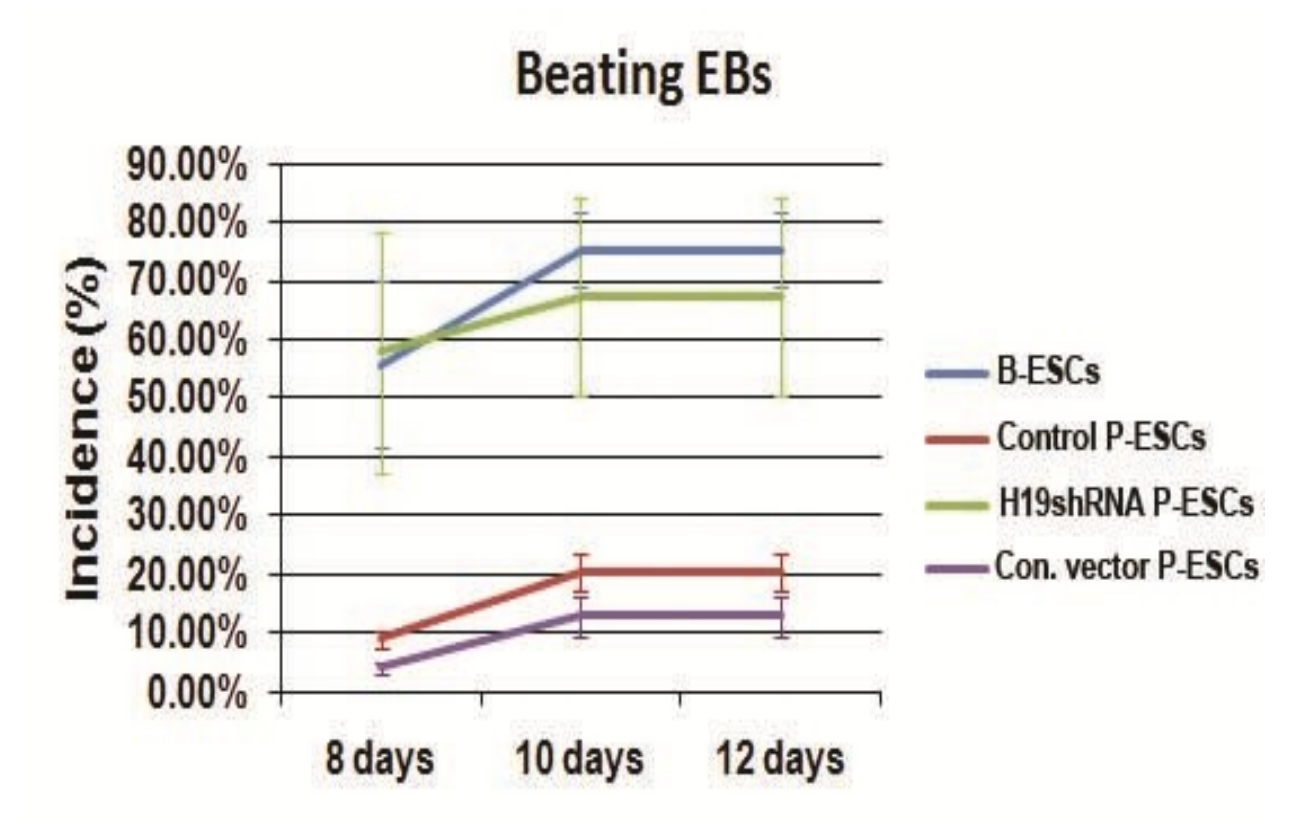
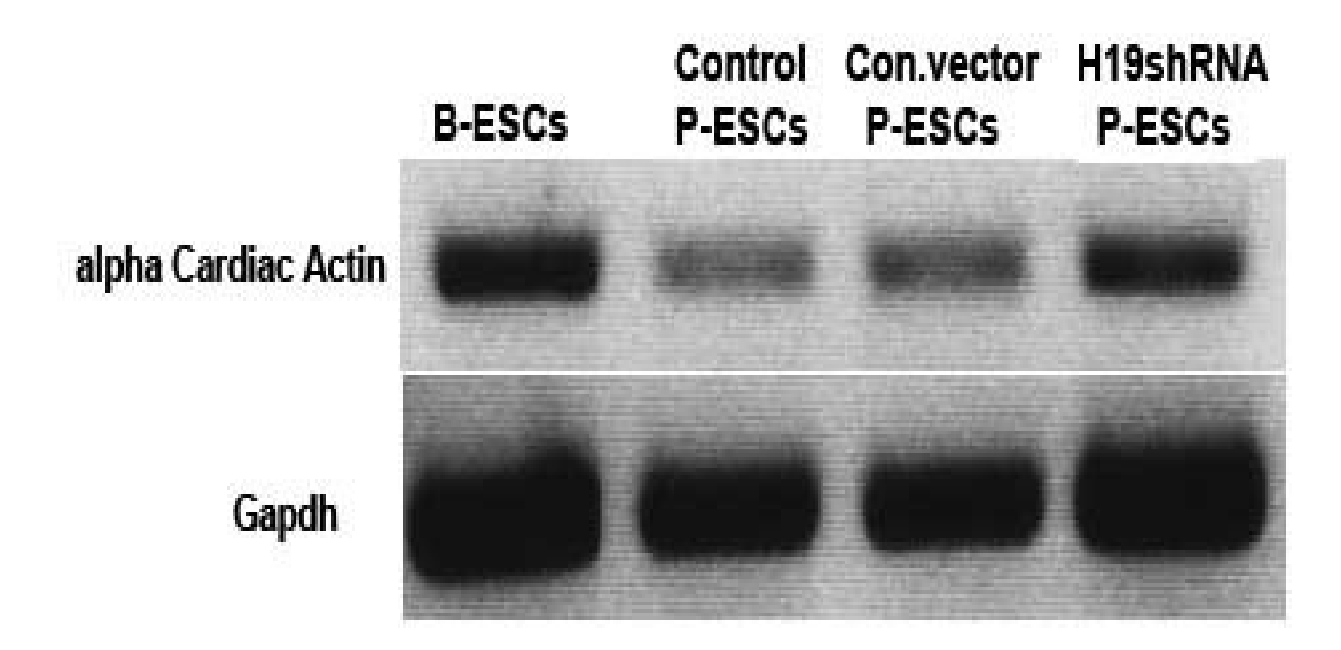


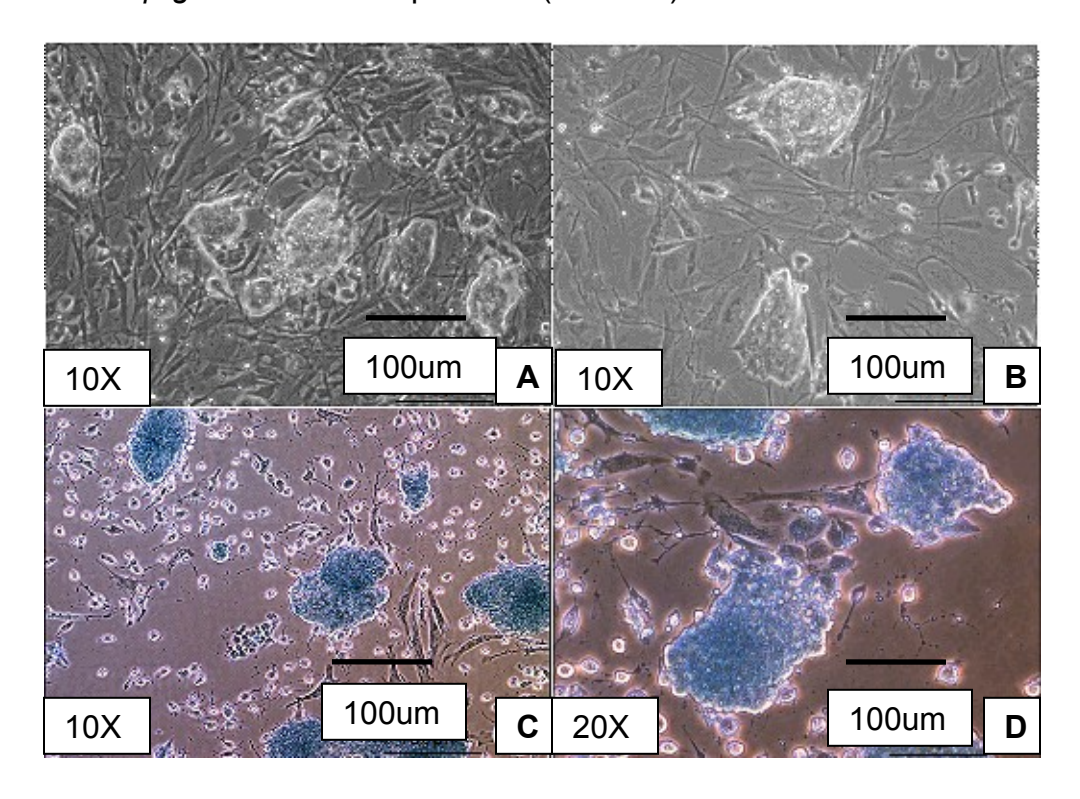
Figure 3.6 (cont'd)

C

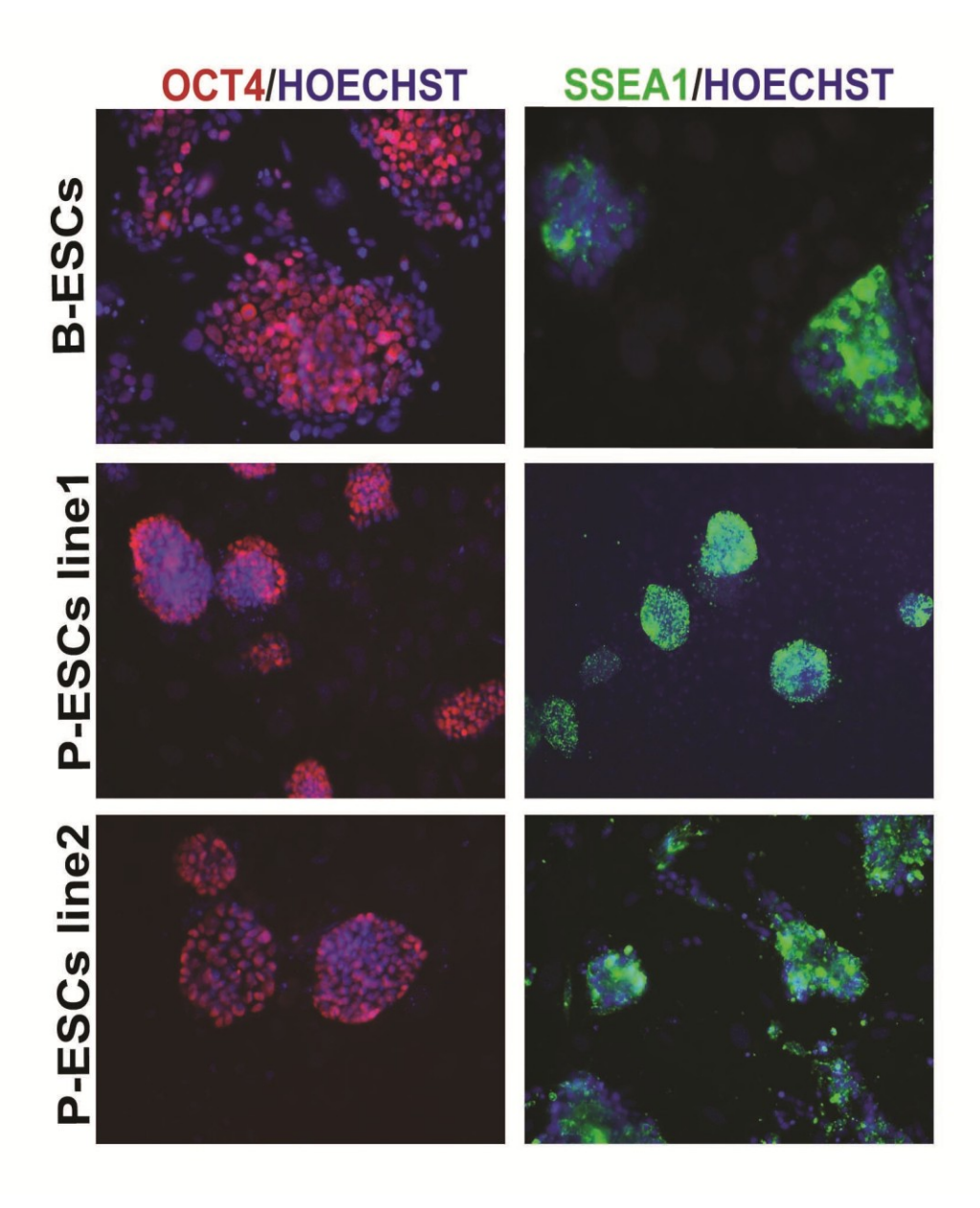


SUPPLEMENTAL FIGURES AND TABLES

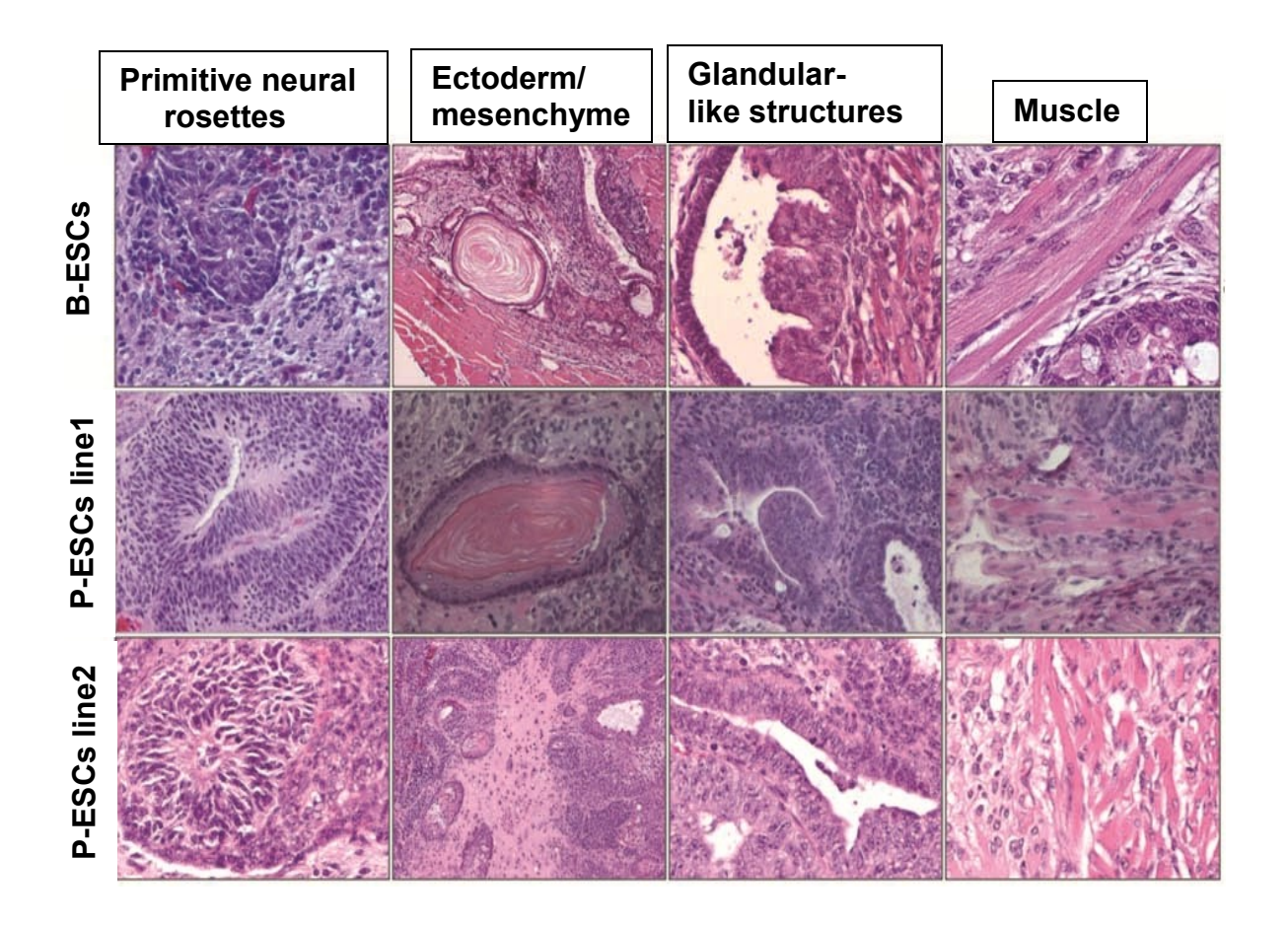
Supplemental Figure 3.1 Mouse Rosa 26 P-ESCs are morphologically indistinguishable from mouse Rosa 26 biparental ES (B-ESCs) cells (A and B) and stain positive *for* β -galactosidase expression (C and D).



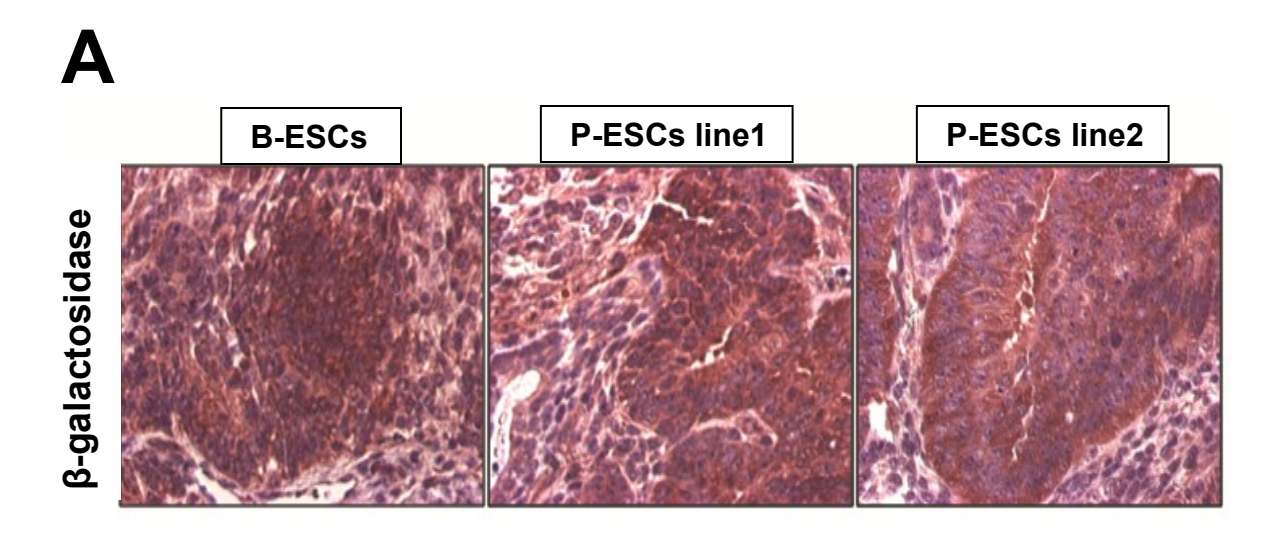
Supplemental Figure 3.2 Mouse Rosa 26 P-ESCs and Rosa 26 B-ESCs express Oct4 and SSEA1 in mouse as shown by immunocytochemical analysis.



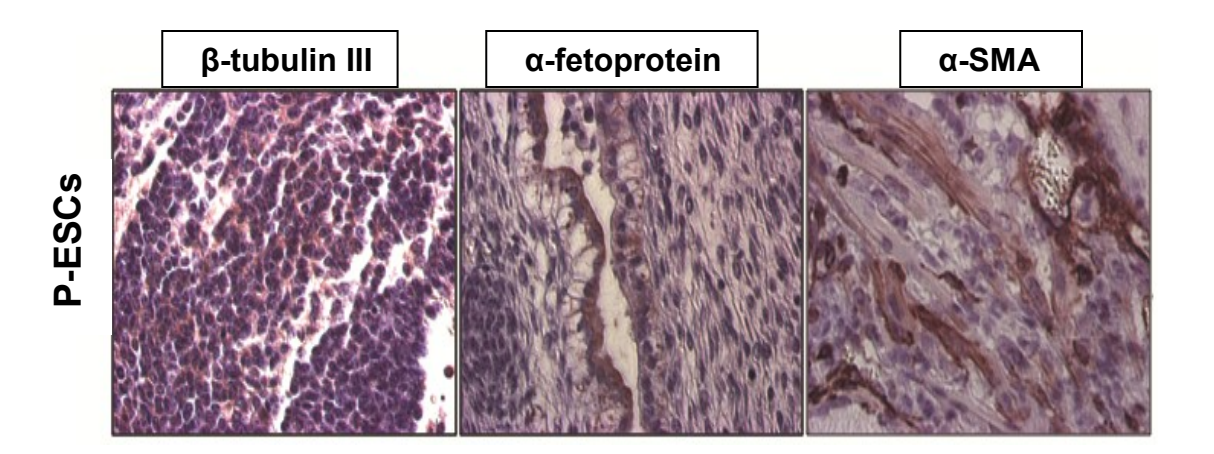
Supplemental Figure 3.3 Hematoxylin-Eosin (H&E) staining of mouse B-ESCs and P-ESCs (P-ESCs 1 and P-ESCs 2) derived teratomas indicating the ability of these cells to give rise to all three germ layers when differentiated *in vivo*.



Supplemental Figure 3.4 Immunohistochemical staining of teratoma sections derived from mouse Rosa 26 B-ESC and P-ESC lines confirming the identity of the germ layer derivatives. (A) β -galactosidase, (B) α -fetoprotein, α -SMA, β -tubulin III.

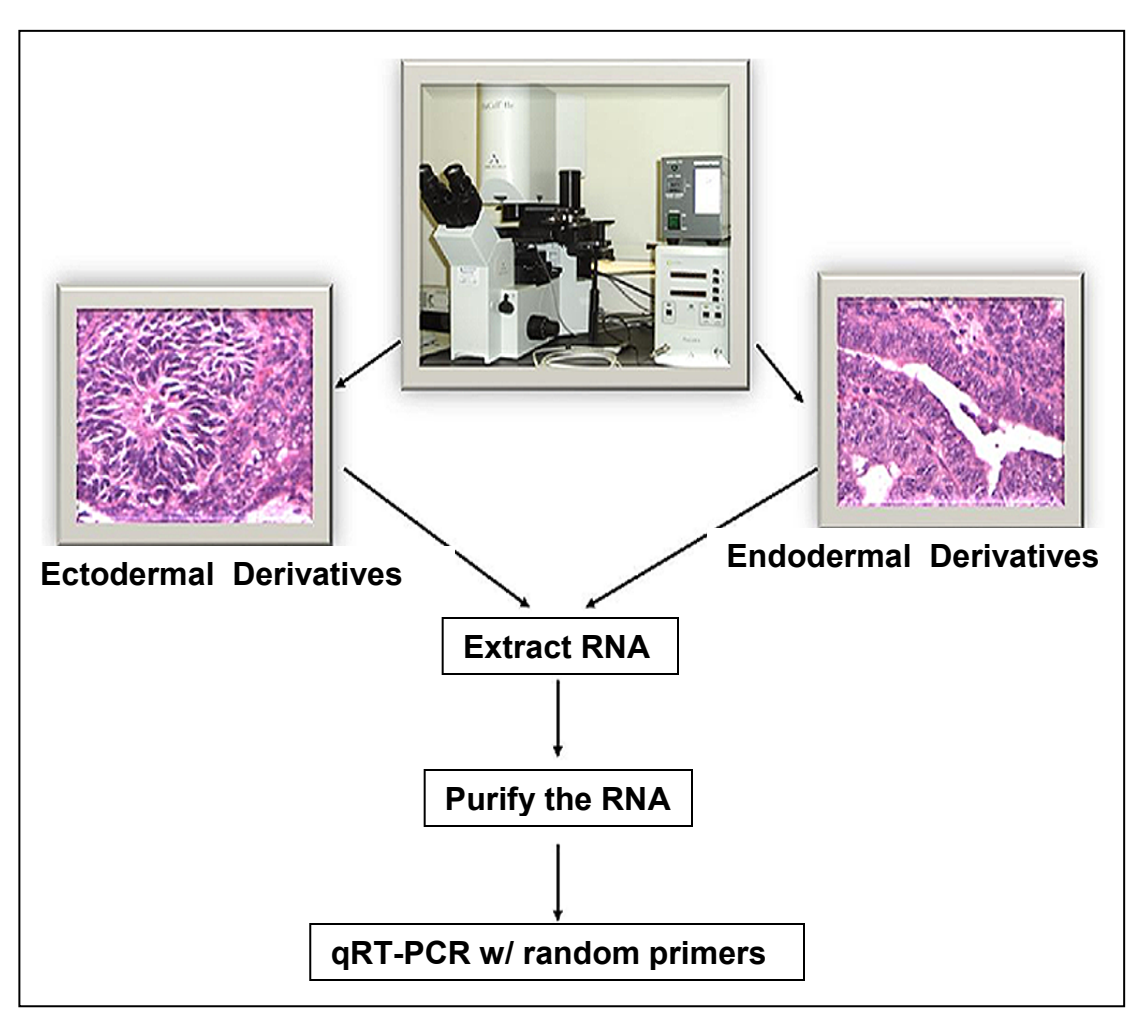


B

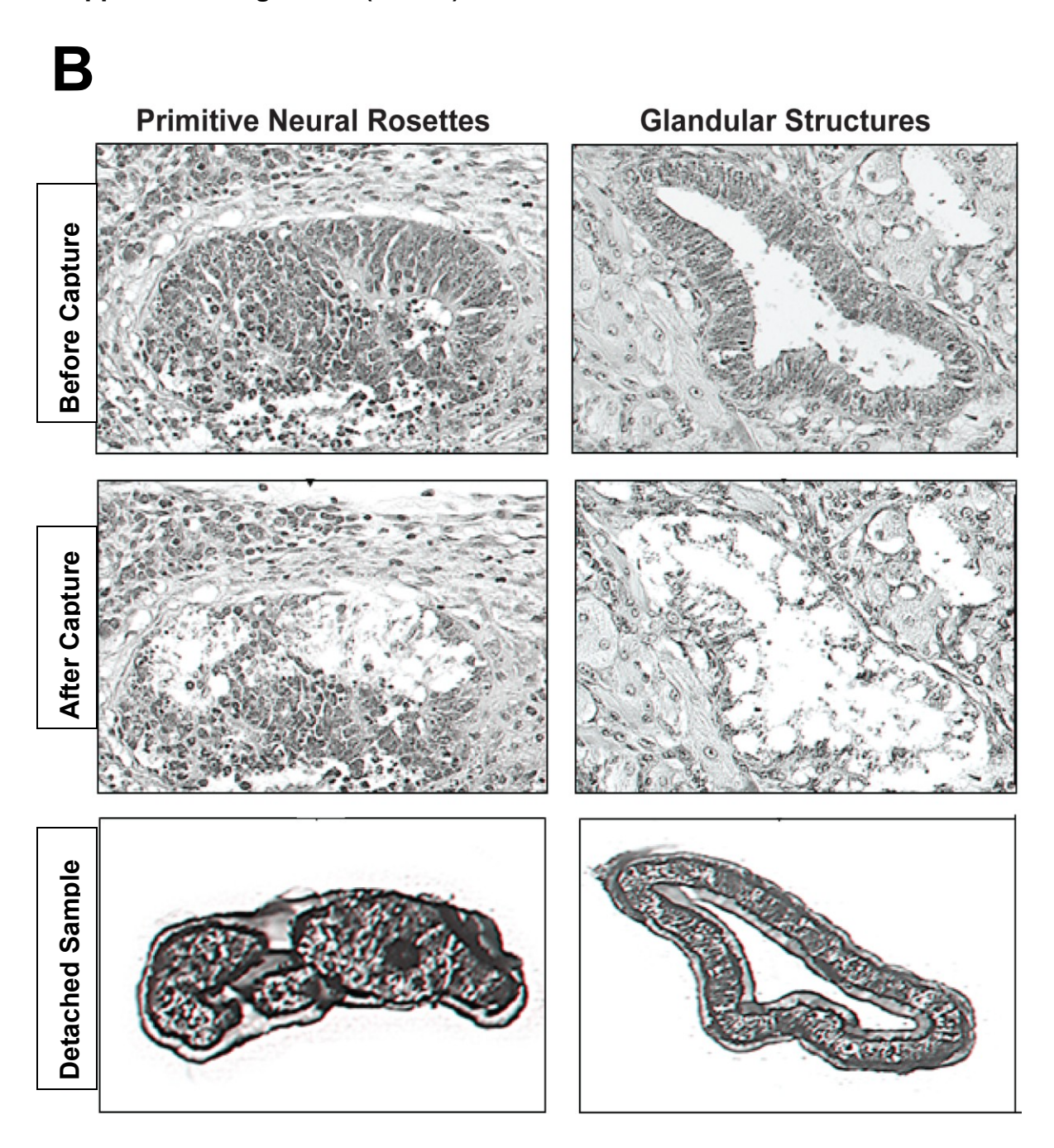


Supplemental Figure 3.5 Laser Capture Microdisection (LCM). (A) LCM experimental outline. (B) Ectoderm (primitive neural rosettes) and endoderm (glandular structures) derivatives obtained from mouse B-ESCs and P-ESCs derived teratomas before and after LCM sample acquisition.



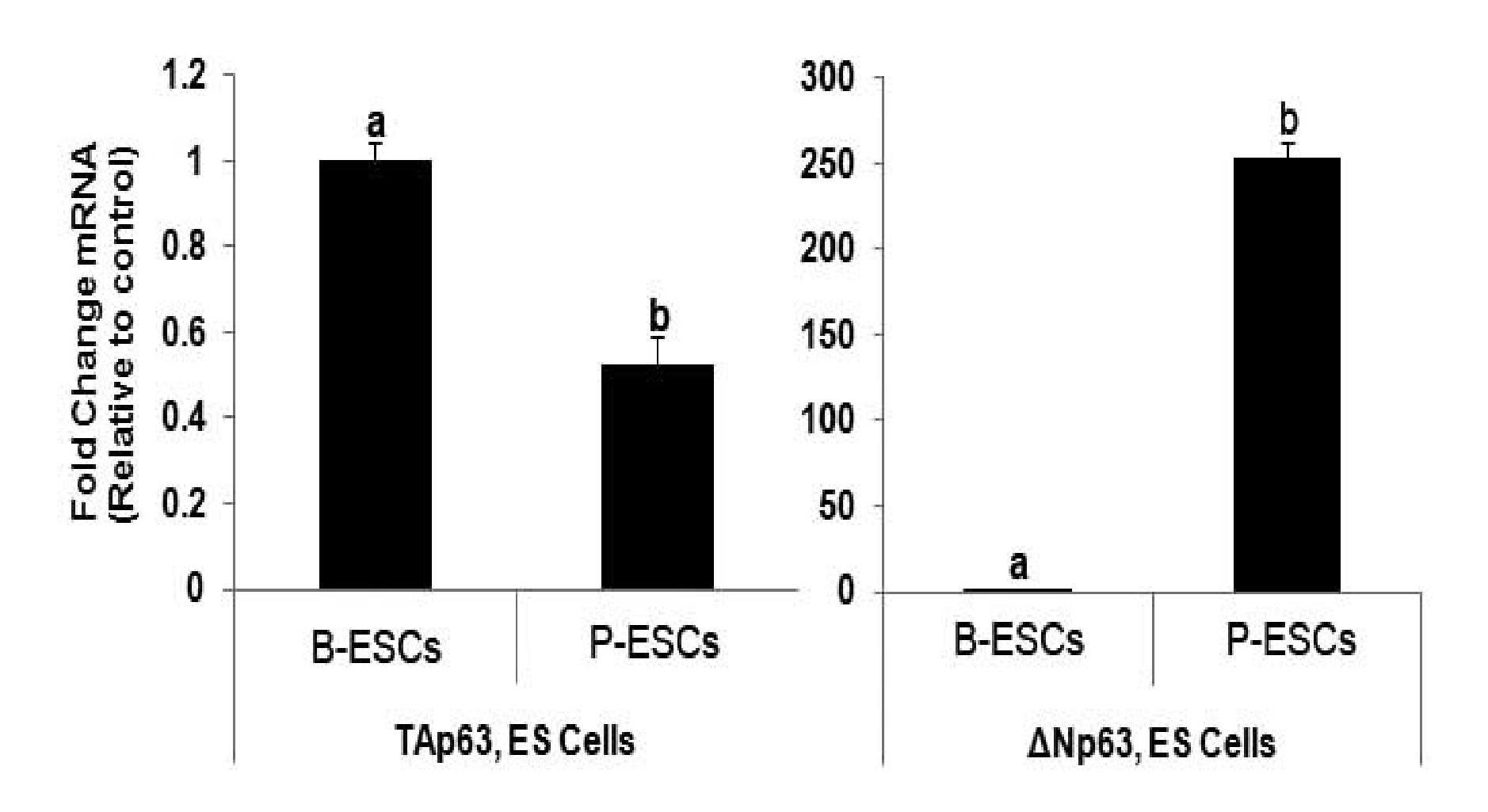


Supplemental Figure 3.5 (cont'd)

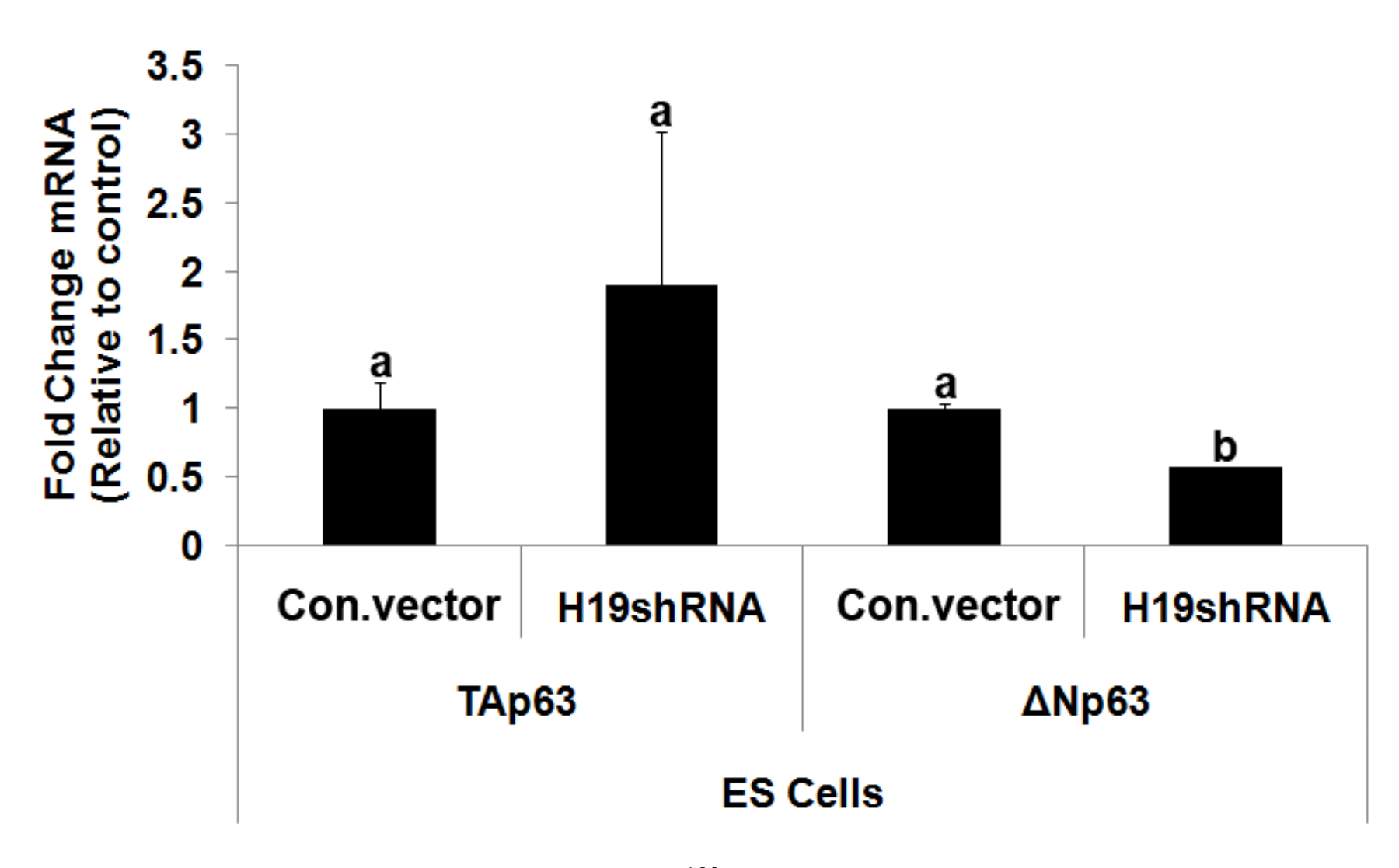


Supplemental Figure 3.6 Delta Np63 and TAp63 expression is indicative of germ layer commitment. Relative mRNA expression levels of Delta Np63 and TAp63 in ES cells (A-B) and teratomas(C-D) measured by qRT-PCR (P<0.05). For all qRT-PCR experiments three biological replicates (n=3) in three technical replicates were used in each run and a P<0.05 has been considered as statistical significant, unless stated otherwise. The bars represent standard error bars. All the letters above the error bars represent the difference between samples on the basis of standard error values (P<0.05).

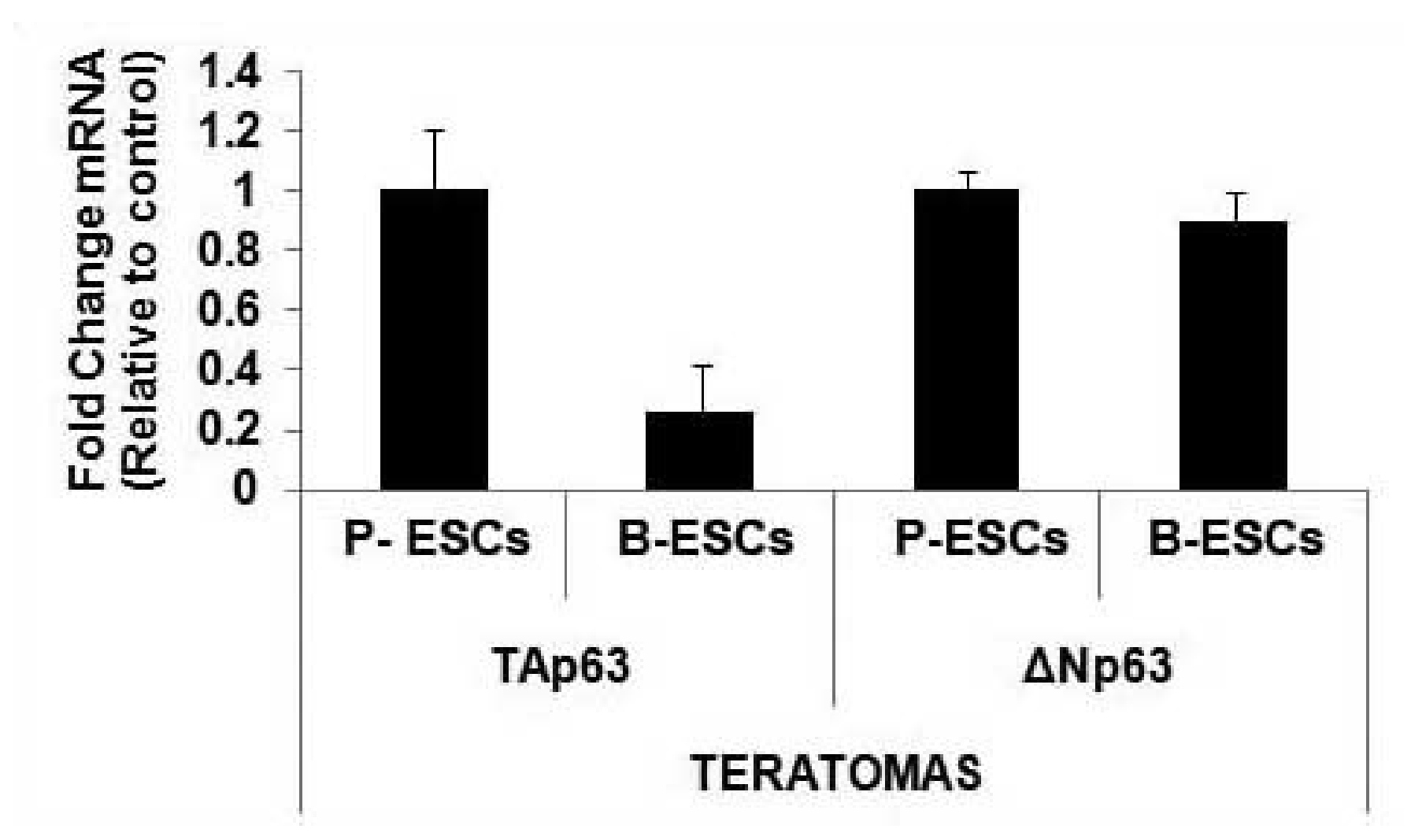
A



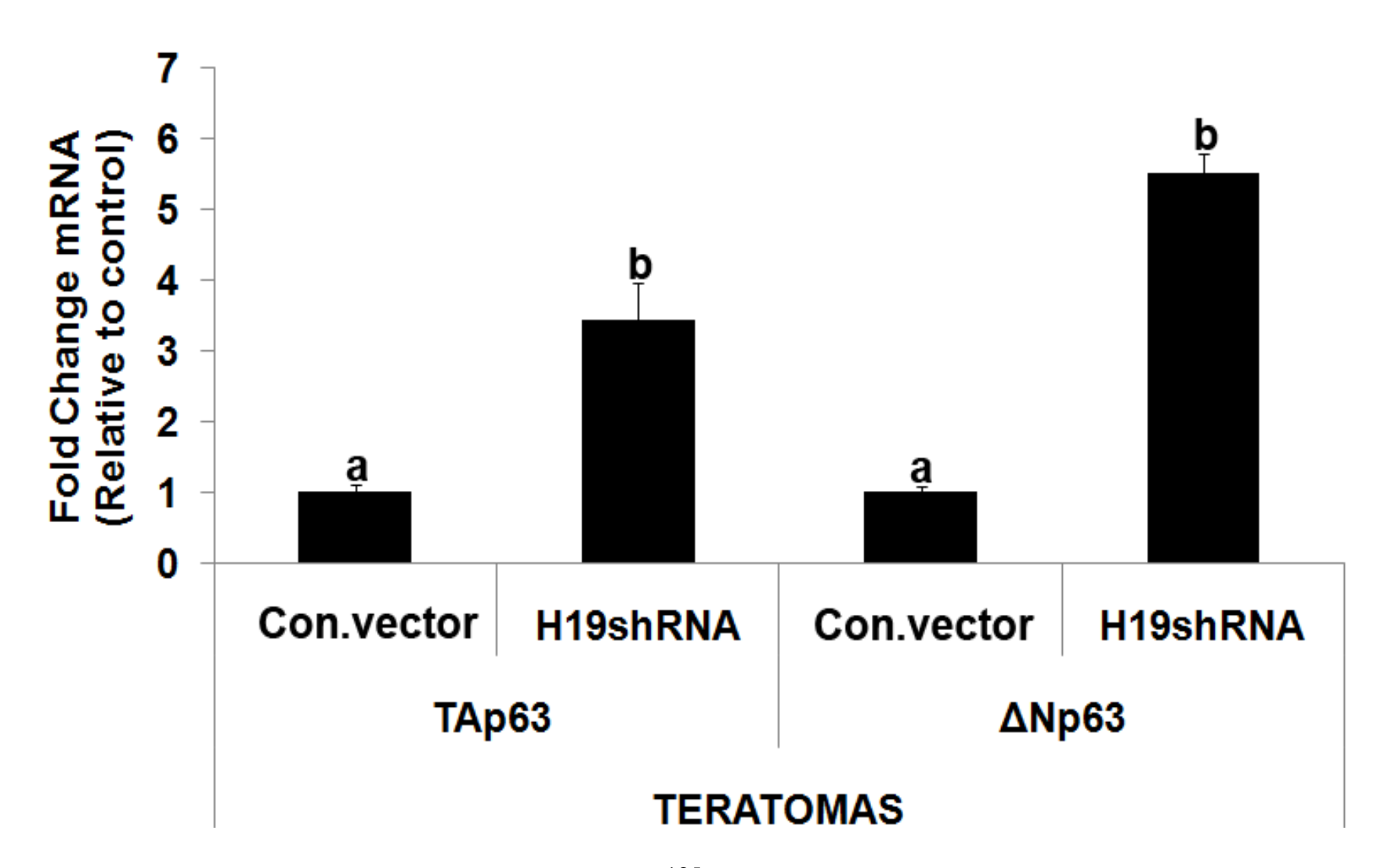
B



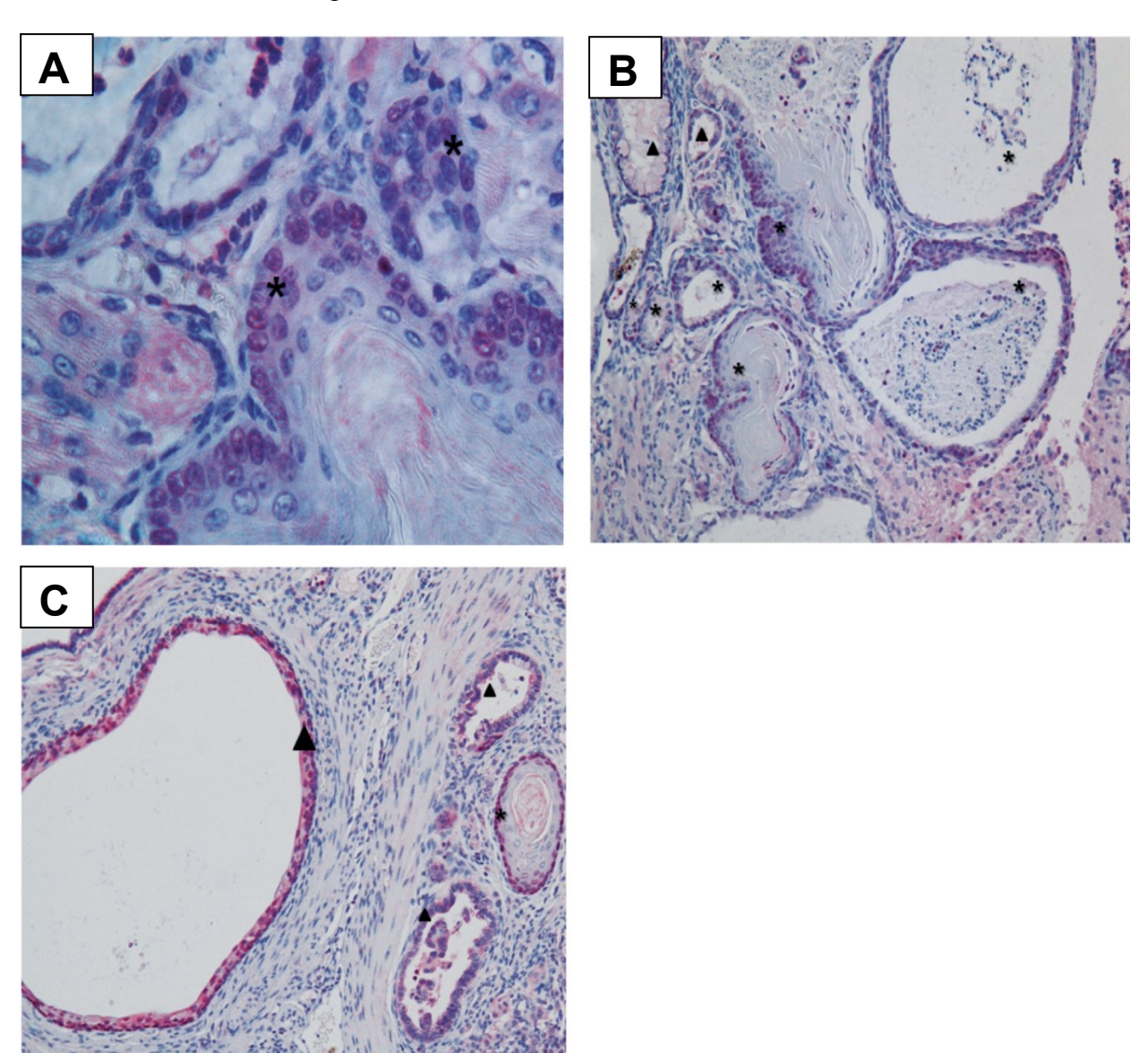
C



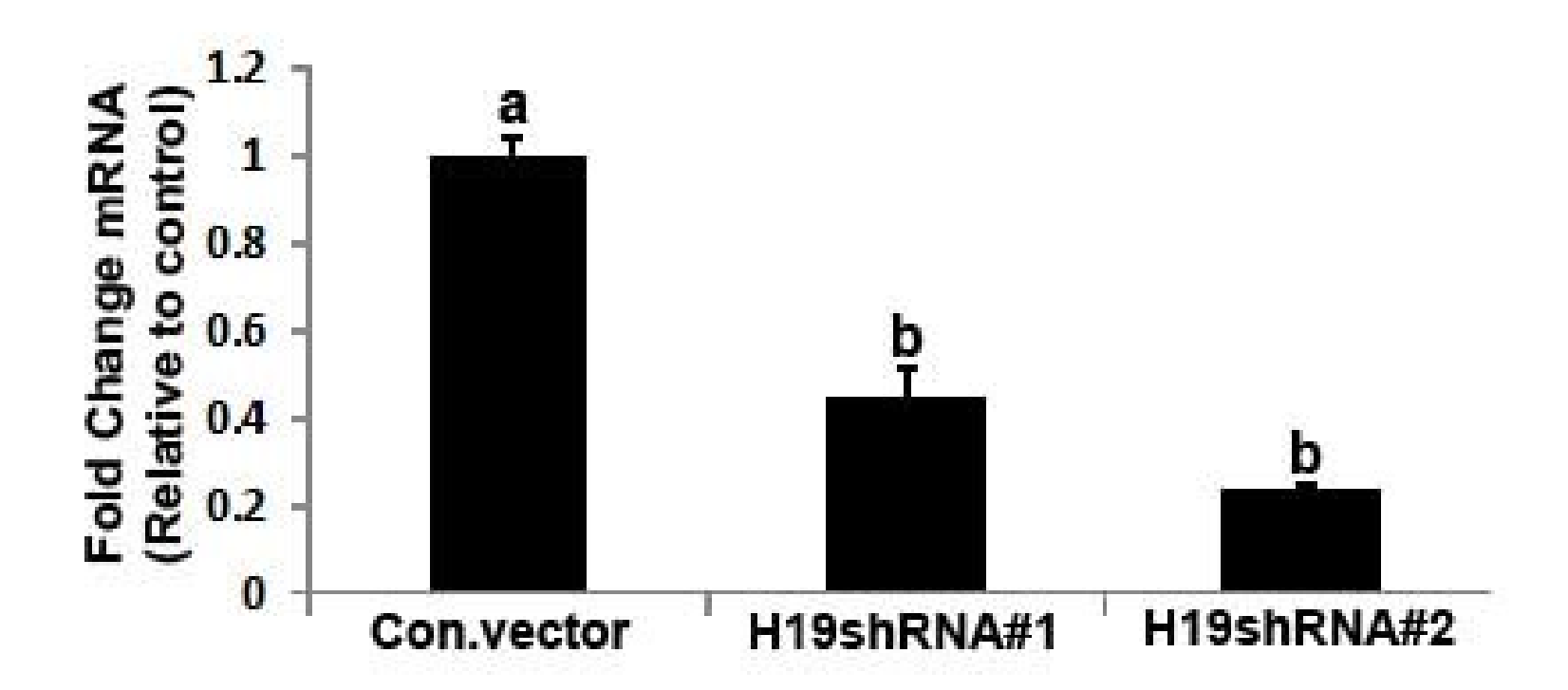
D



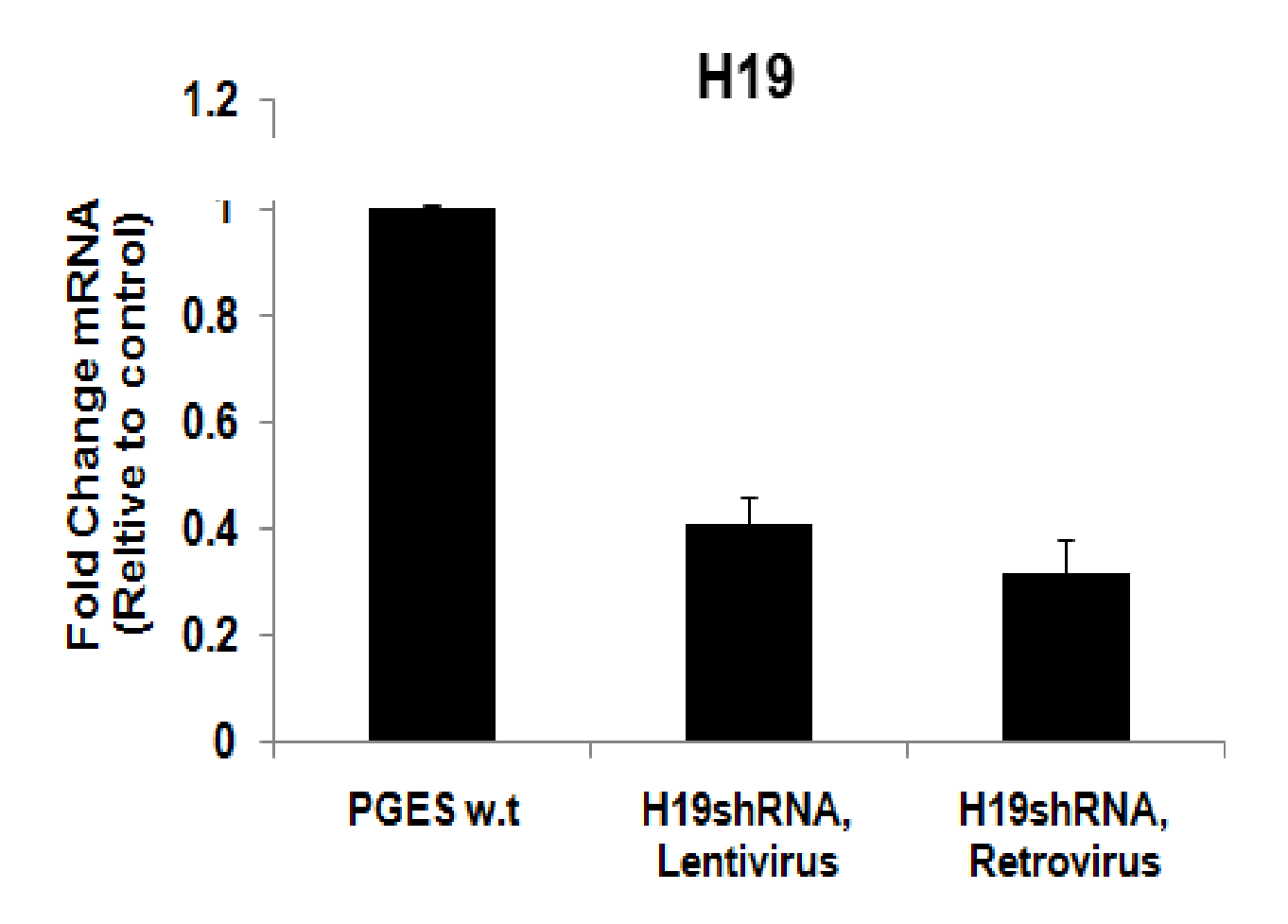
Supplemental Figure 3.7 Immunohistochemical staining for delta Np63 of mouse B-ESCs derived teratomas using conjugated Alkaline Phosphates secondary antibody (red color) (A-C). Intense nuclear staining (red) was identified in the basal cells of the epithelial structures with glandular (black arrow head) and squamous (black asterix) differentiation. There was no clear evidence of positive staining for delta Np63 seen in mesenchyme or neural tissues. The squamous epithelium structures, however, were more abundant than the glandular ones.



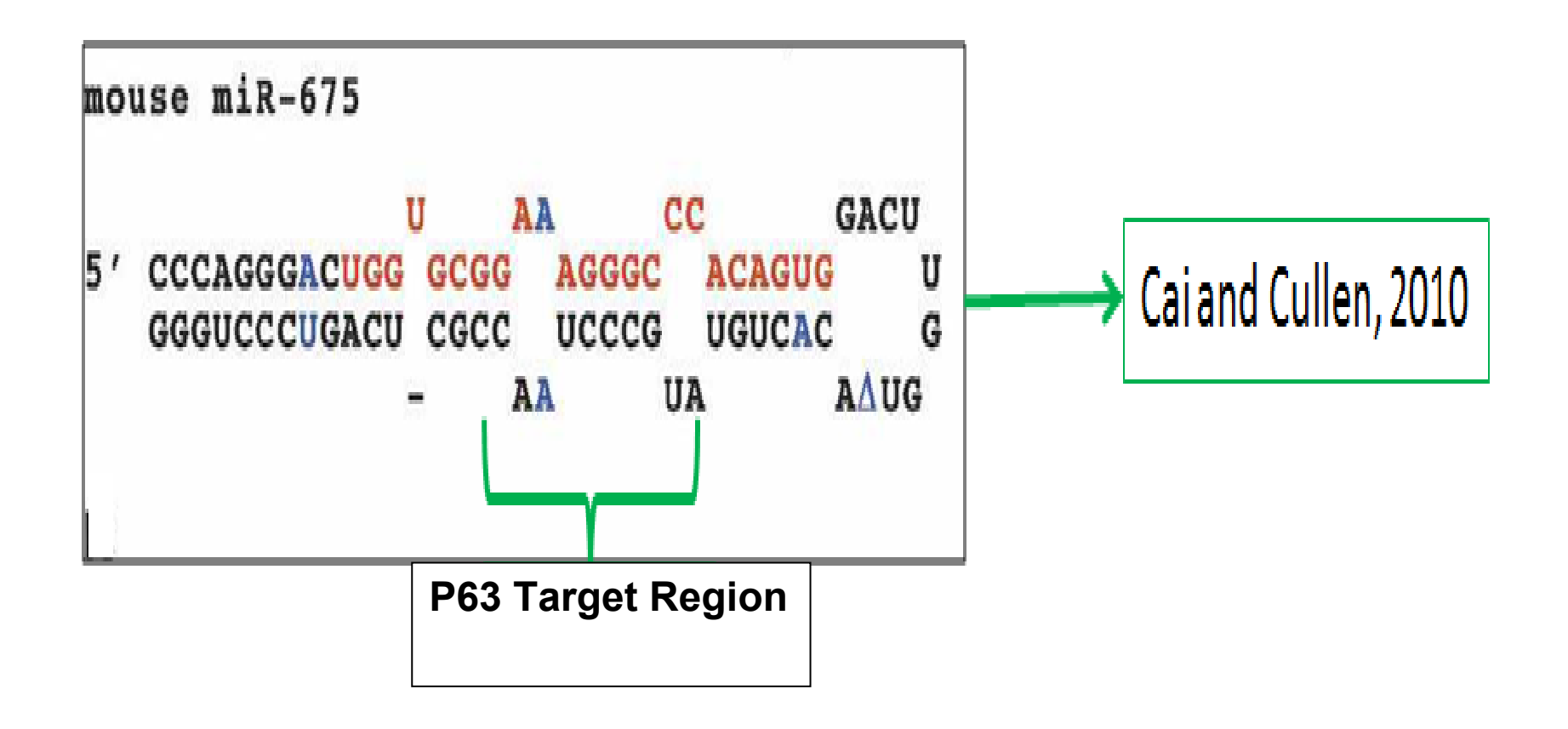
Supplemental Figure 3.8 Down-regulation of *H19* expression in Mouse Embryonic Fibroblasts (MEFs) infected with two different *H19*shRNA oligos (*H19*shRNA#1 and *H19*shRNA#2) by qRT-PCR, (P<0.05). For all qRT-PCR experiments three biological replicates (n=3) in three technical replicates were used in each run and a P<0.05 has been considered as statistical significant, unless stated otherwise. The bars represent standard error bars. All the letters above the error bars represent the difference between samples on the basis of standard error values (P<0.05). For all qRT-PCR experiments three biological replicates (n=3) in three technical replicates were used in each run and a P<0.05 has been considered as statistical significant, unless stated otherwise. The bars represent standard error bars. All the letters above the error bars represent the difference between samples on the basis of standard error values (P<0.05)



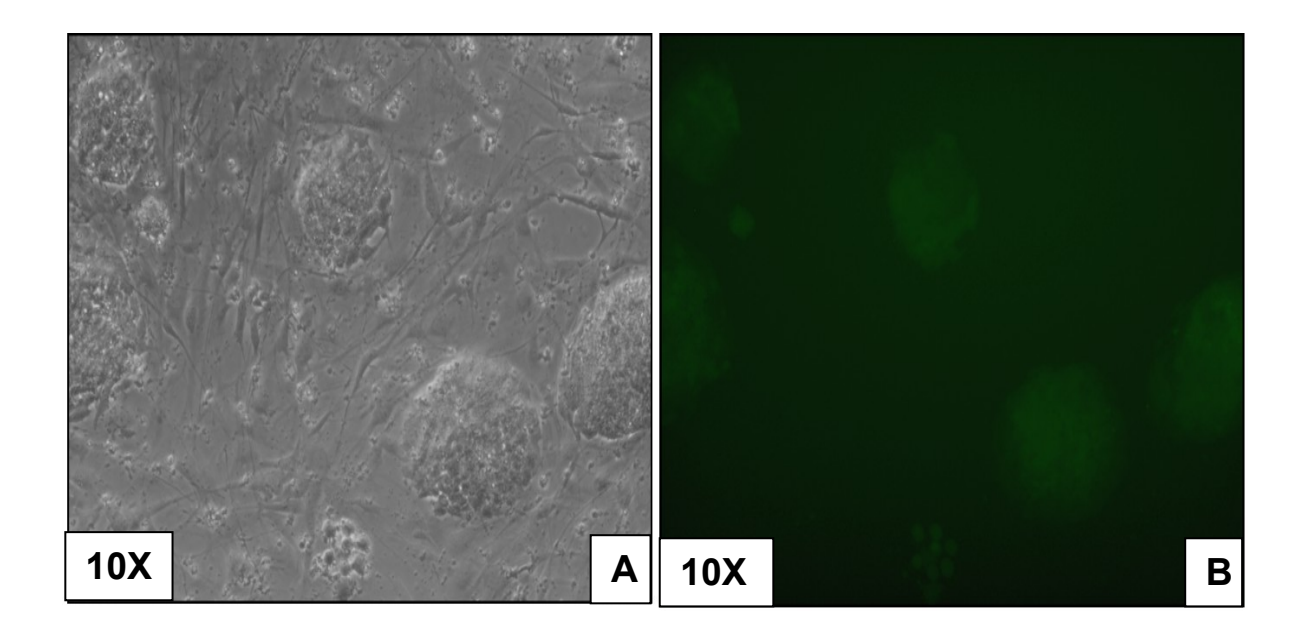
Supplemental Figure 3.9 Down-regulation of *H19* expression in mouse P-ESCs infected with two different H19 shRNA expressing pLenti-DEST/Hygro -EGFP shRNA expressing lentiviral and pMSCV-Hygro-EGFP shRNA expressing retroviral vectors (P<0.05). For all qRT-PCR experiments three biological replicates (n=3) in three technical replicates were used in each run and a P<0.05 has been considered as statistical significant, unless stated otherwise. The bars represent standard error bars. All the letters above the error bars represent the difference between samples on the basis of standard error values (P<0.05).



Supplemental Figure 3.10 Schematic representation of the mir675 region that is a perfect 11bp match to the TP63 Trans Activating (TA) domain and therefore may affect the transcription or regulate the translation of TP63 mRNA.



Supplemental Figure3.11 EGFP fluorescence (B) and bright field (A) of mouse PGES cells infected with pMSCV-Hygro-EGFP - *H19* shRNA retroviral vector.



Supplemental Table 3.1 Cytogenetic analysis of B-ESC, P-ESC, and transgenic P-ESC cell lines

Date	Cell Line	# of Metap hases	Composite	Clonal or Mixed Clones	Analyzed by
2007	mesPGES- R26-1	20	Normal Karyotype 40,XX	Clonal	Cell Line Genetics (WI, Madison)
2007	mesPGES- R26-4	20	Normal Karyotype 40,XX	Clonal	Cell Line Genetics (WI, Madison)
2007	mesPGES- R26-7	20	Normal Karyotype 40,XX	Clonal	Cell Line Genetics (WI, Madison)
10/8/20 08	mes PGES- R26-7 or CRL-08- 075 p9	20	39,XO[14] / 40,XX[6][cp20] Mosaic	Client indic ated clonal; results indic ated mixed clones	Germline Modification and Cytogenetics Laboratory
9/9/200 8	CRL-08- 105 p16	23	39~41,XO,Add(2)[3],+Der(?)T(?A1;6 D2)[9], +Der(?)T(?A1;8C1)[7],+12[8][cp23]	Mixed Clones	Germline Modification and Cytogenetics Laboratory
9/3/200 8	CRL-08- 106 p16	22	40,XO,+Der(?)T(? A1;8C1)[19],+12[2] [cp22]	Mixed Clones	Germline Modification and Cytogenetics Laboratory
7/22/20 08	08-112 clone 4	20	40,XO,+Der(?)T(? A1;8C1)[cp20]	Clonal	Germline Modification and Cytogenetics Laboratory
7/22/20 08	08-113 clone 8	20	40,XO,+Der(?)T(? A1;8C1)[cp20]	Clonal	Germline Modification and Cytogenetics Laboratory
7/13/20 08	PGES 08- 112 clone 8 p14	20	40,X,+Der(?)T(?;8 C1)[cp20]	Clonal	Germline Modification and Cytogenetics Laboratory
7/13/20 08	PGES 08- 113 clone 4 p14	20	40,X,+Der(?)T(?;8 C1)[cp20]	Clonal	Germline Modification and Cytogenetics Laboratory
7/13/20 08	PGES 08- 113 clone 10 p14	20	40,X,+Der(?)T(?;6 D2)[cp20]	Clonal	Germline Modification and Cytogenetics Laboratory
7/22/20 08	08-113 clone 10	20	40,XO,+Der(?)T(? A1;6D2)[cp20]	Clonal	Germline Modification and Cytogenetics Laboratory

Supplemental Table 3.1 (cont'd)

Supplemental Table 3.1 (cont'd)					
			41,X,+8,ins(10),+(
			12) has a missing		
			sex chromosome,		
	mesPGES-		trisomy 8, insertion		
	R26-1,		of genetic material		
	pMSCU-		into chromosome		
	Hygro-GFP		10 and an extra		
	sh#10,FAC		isochrom osome		
	s Passage		12 (resulting in a		
	#17 -		total of 4 copies of	Mixed	Cell Line Genetics (WI,
2008	Clone #1	15	chromosome 12).	Clones	Madison)
			40,X,+8,ins(10),-		
			12,+(12) has a		
			missing sex		
			chromosome,		
			trisomy 8, an		
	mesPGES-		insertion of genetic		
	R26-1,		materia I into		
	pMSCU-		chromosome 10,		
	Hygro-GFP		and an		
	sh#10,FAC		isochrom osome		
	s Passage		12.(resulting in a		
	#17 -		total of 3 copies of	Mixed	Cell Line Genetics (WI,
2008	Clone #2	3	chromosome 12).	Clones	Madison)
			40,XX, 39,X,		
			X,Der(6), Del(17),		
			39,X,-X,-7,Del(?),		
			39,X,-		
0.0.000			X,Del(6D),Der(6),		
9/8/200	PGES,	0.4	Del(?17C), 40,X,-	Mixed	Gemline Modification and
9	R26-7 sh6	21	X,+6	Clones	Cytogenetics Laboratory
			39, X, 39,X,-		
			X,Der(6), Del(?17C		
), 39,X,-X,-		
			16,+Del?, 39,X,-		
			X,Der(6), Del(14D),		
	PGES		Del(17C), 39		
9/8/200			breakage	Mixed	Germline Modification and
	R26-7	45			l .
9	sh12	15		Clones	Cytogenetics Laboratory
9/8/200	PGES				Germline Modification and
9	R26-7 K2	13	39XO	Clonal	Cytogenetics Laboratory
9/8/200	PGES				Germline Modification and
9	R26-7 K15	13	39XO	Clonal	Cytogenetics Laboratory
-			-		_,,
9/8/200	CRL-09-		30V0/40 VO 16	Mixed	Germline Modification and
1 1		10	39X0/40,XO,+6,		l I
9	240 sh9	12	Mosaic	Clones	Cytogenetics Laboratory

Supplemental Table 3.2 Mouse PCR Primer Sequences

PCR Primer Name	Forward	Reverse	Gene bank
			Acsessio
			n
			number
Mouse	CTCCTCCCCCTACCTTGA	AATGGGGAAACAGAGTC	NR 0015
H19.2	AC	ACG	92.1
Mouse Igf2	ATTCGGCCTCTGCGACT	GGAAGTACGGCCTGAGA	NM_0105
	С	GGT	<u>14</u>
Mouse Igf2R	CCACTGGTCAAGTCCAG	CATGCAGGGTAAGAAGA	<u>NM_0105</u>
	GTT	GC	<u>15</u>
Mouse P57	CTGGGACCTTTCGTTCAT	GTGGGGGCTTTTACTCA	<u>NM_0098</u>
	GT	ACA	<u>76</u>
Mouse Mkrn	GCTTTGGCATTCTTTTCA	ACCACCATCTGGTCTTG	<u>NM_0117</u>
	GC	GAG	<u>46</u>
Mouse	AGGTTTGAAGACGCAGA	TTCGAGAGATTCGAGGG	<u>NM_0167</u>
Nestin	GGA	AGA	01
Mouse	TGGTTGACACCCACTCA	GCTTTTGGGGTGTCAGT	NM 0117
Vimentin	AAA	TGT	<u>01</u>
Mouse Myf6	AGATCGTCGGAAAGCAG	TTGCTCCTCCTTCCTTAG	NM_0086
14.65	CTA	CA	<u>57</u>
Mouse Myf5	AGACGCCTGAAGAAGGT	TGGAGAGAGGGAAGCTG	NM_0086
	CAA	TGT	<u>56</u>
Mouse	CACGACTGCTTTCTTCAC	TGCTGTCTCAAAGGAGC	NM_0108
MyoD	CAACCAACCCCTCTCAA	AGA	66 NM 0074
Mouse AFP	GAAGCAAGCCCTGTGAA CTC	CCGAGAAATCTGCAGTG ACA	NM_0074
Mouse	CTGTGCCAACTGCCAGA	CTGCTGTGCCCATAGTG	<u>23</u>
GATA4	CTA	AGA	NM 0080 92
Mouse Mier2	ACACAGACAGACCCCAG	CGGCTTTTCCTGAAGTG	NM 0274
Wouse Wileiz	ACC	AAG	22
Mouse α-	CTGAGATGTCTCTCTCTC	ACAATGACTGATGAGAG	NM 0096
cardiac actin	TCTTAG	ATG	08.2
Mouse	TTCAACGGCACAGTCAA	CATGGACTGTGGTCATG	NM 0080
GAPDH	GG	AG	84
Mouse Rb	GCAAGTGATCAGCCATC	CCAGAATCAAGATGCTG	NM 0090
	AGA	CAA	<u>29</u>
Mouse	CCAAAAGCTCCTCAAAG	AAAATGAATGGGGATGG	NM 0085
Mest1	ACG	ACA	90

Supplemental Table 3.3 Mouse qRT-PCR Primer Sequences

qPCR Primer Name	Forward	Reverse	Gene bank Acsession number
Mouse retinoblastoma	5'- CGCTGTACTCCGAT	5'- GGATGTTGGGCACATCTT	NM_00902 9
1 (Rb1)	GTCAACAC-3'	TAAAG-3'	
Mouse nestin (Nes), mRNA	5'- GAGGGAGACCTGGC TCACTTT-3'	TGATGAAAACCAGGAGA CAATTGT	NM_01670 1
Mus musculus vimentin	GAAAACAGCTTTCAA GTGCCTTTAC	CAGTTGTTAAGTGCTGAG CTTCTTTCTA	NM_01170 1
Mouse myogenic factor 6 (Myf6	CGGTGCAGCAGGTC CTGTA	TGCCCAAGGTGGAGATT CTG	NM 00865 7
Mouse myogenic factor 5 (Myf5),	GACGT GATCCGATC CACAATG	AATGCATGTGCTGCAGAT AAAAG	NM 00865 6
Mouse myogenic differentiation 1 (Myod1),	TCCGGAGTGGCAGA AAGTTAA	AGAAGCTCCATATCCCAG TTCCT	NM_01086 6
Mouse alpha fetoprotein (Afp),	CAGGTTAATGAGAA GCTCTTGTTTCA	AAATTCATCTTCCACAAG GATCTGT	NM_00742 3
Mouse GATA binding protein 4 (Gata4),	CTCTTGCAATGCGG AAGGA	CTGGCGTCTTAGATTTAT TCAGGTT	NM_00809 2
Mouse mesoderm induction early response 1, family member 2 (Mier2)	GCCACAG GACGAGG TATATGG	TGGCCTCCAGCCTTTGC	NM 02742 2
Mouse, TAp63	CGCAGAGCACCCAG ACAA	CGATGGGCTGTACTGAG CATATAG	NM 00112 7259.1 NM 00112 7260
Mouse, ΔNp63	AGC CCA GCT CCA CCT TT G A	GGC CCG GGT AAT CTG TGT T	NM_01164 1.2

Supplemental Table 3.3 (cont'd)

Mouse H19	GATTCAGAACGAGA	ATGGTGCTACCCAGCTCA	NR_00159
	CGGACTTAAAG	TGT	2.1
Mouse Igf2	TGTGCTGCATCGCT	AAACTGAAGCGTGTCAAC	NM 01051
	GCTTAC	AAGCT	4.2
Mouse Nanog	GGTTGAAGACTAGC AATGGTCTGA	TGCAATGGATGCTGGGA TACTC	NM 02801

Supplemental Table 3.4 Bisulfate Sequencing Primers

H19 ICR region	Bisulfate sequencing primers	
Outside forward	GAGTATTTAGGAGGTATAAGAATT	
Inside forward	GTAAGGAGATTATGTTTATTTTTGG	
Inside reverse	CCTCATTAATCCCATAACTAT	
Outside reverse	ATCAAAAACTAACATAAACCCCT	

^{*}The primers are after Lucifero *et al.*, Methylation Dynamics of Imprinted Genes in mouse germ cells, Genomics, April 2002.

Supplemental Table 3.5 H19 small hairpin RNA (shRNA) sequence information

H19shRN	Accessio	Top strand	Bottom strand
Α	n		
	number		
H19shRNA	NR 0015	5'-	5'-
,1	<u>92</u>	CACCGCAGGTGAGTCTCCT	AAAAGCAGGTGAGTC
		TCTTCTCGAAAGAAGAAGGA	TCCTTCTTCTTCGAG
		GACTCACCTGC-3'	AAGAAGGAGACTCAC
			CTGC-3'
H19shRNA	NR 0015	5'-	5'-
,2	92	CACCGCAGAATGGCACATA	AAAAGCAGAATGGCA
		GAAAGGCGAACCTTTCTATG	CATAGAAAGGTTCGC
		TGCCATTCTGC-3'	CTTTCTATGTGCCATT
			CTGC-3'

REFERENCES

REFERENCES

- 1. Sheehy, E., et al., *Estimating the number of potential organ donors in the United States.* N Engl J Med, 2003. **349**(7): p. 667-74.
- 2. Network, N.Y.O.D., http://www.donatelifeny.org/index.asp, 2010.
- 3. Coombes, J.M. and J.F. Trotter, *Development of the allocation system for deceased donor liver transplantation*. Clin Med Res, 2005. **3**(2): p. 87-92.
- 4. Sasazuki, T., et al., Effect of Matching of Class I HLA Alleles on Clinical Outcome after Transplantation of Hematopoietic Stem Cells from an Unrelated Donor. New England Journal of Medicine, 1998. **339**(17): p. 1177-1185.
- 5. Flomenberg, N., et al., Impact of HLA class I and class II high-resolution matching on outcomes of unrelated donor bone marrow transplantation: HLA-C mismatching is associated with a strong adverse effect on transplantation outcome. Blood, 2004. **104**(7): p. 1923-1930.
- 6. Petersdorf, E.W., et al., *Major-Histocompatibility-Complex Class I Alleles and Antigens in Hematopoietic-Cell Transplantation.* New England Journal of Medicine, 2001. **345**(25): p. 1794-1800.
- 7. Ishikawa, K., et al., *The innate immune system in host mice targets cells with allogenic mitochondrial DNA.* J Exp Med, 2010.
- 8. Petersdorf, E.W., et al., *Major-Histocompatibility-Complex Class I Alleles and Antigens in Hematopoietic-Cell Transplantation*. 2001. p. 1794-1800.
- 9. Hipp, J. and A. Atala, *Tissue engineering, stem cells, cloning, and parthenogenesis: new paradigms for therapy.* J Exp Clin Assist Reprod, 2004. **1**(1): p. 3.
- 10. Kaufman, M.H., et al., *Establishment of pluripotential cell lines from haploid mouse embryos.* J Embryol Exp Morphol, 1983. **73**(1): p. 249-261.

- 11. Robertson, E.J., M.J. Evans, and M.H. Kaufman, *X-chromosome instability in pluripotential stem cell lines derived from parthenogenetic embryos.* J Embryol Exp Morphol, 1983. **74**: p. 297-309.
- 12. Cibelli, J.B., et al., *Parthenogenetic stem cells in nonhuman primates*. Science, 2002. **295**(5556): p. 819.
- 13. Mitalipov, S.M., K.D. Nusser, and D.P. Wolf, *Parthenogenetic Activation of Rhesus Monkey Oocytes and Reconstructed Embryos.* Biology of Reproduction, 2001. **65**(1): p. 253-259.
- 14. Fang, Z.F., et al., *Rabbit embryonic stem cell lines derived from fertilized,* parthenogenetic or somatic cell nuclear transfer embryos. Exp Cell Res, 2006. **312**(18): p. 3669-82.
- 15. Dighe, V., et al., *Heterozygous embryonic stem cell lines derived from nonhuman primate parthenotes.* Stem Cells, 2008. **26**(3): p. 756-66.
- 16. Revazova, E.S., et al., *Patient-Specific Stem Cell Lines Derived from Human Parthenogenetic Blastocysts.* Cloning Stem Cells, 2007. **9**(3): p. 432-49.
- 17. Onodera, Y., et al., *Differentiation diversity of mouse parthenogenetic embryonic stem cells in chimeric mice.* Theriogenology, 2010. **74**(1): p. 135-45.
- 18. Jagerbauer, E.M., et al., *Parthenogenetic stem cells in postnatal mouse chimeras*. Development, 1992. **116**(1): p. 95-102.
- 19. Fundele, R.H., et al., *Temporal and spatial selection against parthenogenetic cells during development of fetal chimeras.* Development, 1990. **108**(1): p. 203-211.
- 20. Kono, T., et al., *Epigenetic modifications during oocyte growth correlates with extended parthenogenetic development in the mouse.* Nat Genet, 1996. **13**(1): p. 91-4.

- 21. Barton, S.C., M.A.H. Surani, and M.L. Norris, *Role of paternal and maternal genomes in mouse development.* Nature, 1984. **311**(5984): p. 374-376.
- 22. Karin S. Sturm, M.L.F.R.A.P., *Abnormal development of embryonic and extraembryonic cell lineages in parthenogenetic mouse embryos.* Developmental Dynamics, 1994. **201**(1): p. 11-28.
- 23. Park, J.I., et al., Differentiative potential of a mouse parthenogenetic embryonic stem cell line revealed by embryoid body formation in vitro. Jpn J Vet Res, 1998. **46**(1): p. 19-28.
- 24. Sturm, K.S., et al., *Unrestricted lineage differentiation of parthenogenetic ES cells*. Development Genes and Evolution, 1997. **206**(6): p. 377-388.
- 25. Allen, N., et al., *A functional analysis of imprinting in parthenogenetic embryonic stem cells*. Development, 1994. **120**(6): p. 1473-1482.
- Sotomaru, Y., et al., Unregulated Expression of the Imprinted Genes H19 and Igf2r in Mouse Uniparental Fetuses
 J. Biol. Chem., 2002. 277(14): p. 12474-12478.
- 27. Kono, T., et al., *Birth of parthenogenetic mice that can develop to adulthood.* Nature, 2004. **428**(6985): p. 860-864.
- 28. Kawahara, M., et al., *High-frequency generation of viable mice from engineered bi-maternal embryos.* Nat Biotechnol, 2007. **25**(9): p. 1045-50.
- 29. Ogawa, H., et al., *Disruption of parental-specific expression of imprinted genes in uniparental fetuses.* FEBS Lett, 2006. **580**(22): p. 5377-84.
- 30. Ogawa, H., et al., *Disruption of parental-specific expression of imprinted genes in uniparental fetuses.* FEBS Letters, 2006. **580**(22): p. 5377-5384.
- 31. Liu, J.-H., et al., *Diploid parthenogenetic embryos adopt a maternal-type methylation pattern on both sets of maternal chromosomes*. Genomics, 2008. **91**(2): p. 121-8.

- 32. Schoenfelder, S., et al., *Non-coding transcripts in the H19 imprinting control region mediate gene silencing in transgenic Drosophila*. EMBO Rep, 2007. **8**(11): p. 1068-73.
- 33. Berteaux, N., et al., A novel H19 antisense RNA overexpressed in breast cancer contributes to paternal IGF2 expression. Mol Cell Biol, 2008. **28**(22): p. 6731-45.
- 34. Platonov, E.S., L.I. Penkov, and D.A. New, [Effects of growth factors FGF2 and IGF2 on the development of parthenogenetic mouse embryos in utero and in vitro]. Ontogenez, 2002. **33**(1): p. 60-7.
- 35. Kono, T., *Genomic imprinting is a barrier to parthenogenesis in mammals.* Cytogenet Genome Res, 2006. **113**(1-4): p. 31-5.
- 36. Kono, T., et al., *Paternal dual barrier by Ifg2-H19 and Dlk1-Gtl2 to parthenogenesis in mice.* Ernst Schering Res Found Workshop, 2006(60): p. 23-33.
- 37. Wu, Q., et al., Regulated expression of two sets of paternally imprinted genes is necessary for mouse parthenogenetic development to term. Reproduction, 2006. **131**(3): p. 481-488.
- 38. Hikichi, T., et al., Functional full-term placentas formed from parthenogenetic embryos using serial nuclear transfer. Development, 2010. **137**(17): p. 2841-7.
- 39. Zambrowicz, B.P., et al., Disruption of overlapping transcripts in the ROSA beta geo 26 gene trap strain leads to widespread expression of beta-galactosidase in mouse embryos and hematopoietic cells. Proc Natl Acad Sci U S A, 1997. **94**(8): p. 3789-94.
- 40. Kono, T., et al., A cell cycle-associated change in Ca2+ releasing activity leads to the generation of Ca2+ transients in mouse embryos during the first mitotic division. J Cell Biol, 1996. **132**(5): p. 915-23.
- 41. Hikichi, T., et al., *Differentiation Potential of Parthenogenetic Embryonic Stem Cells Is Improved by Nuclear Transfer.* Stem Cells, 2007. **25**(1): p. 46-53.

- 42. Abbondanzo, S.J., I. Gadi, and C.L. Stewart, *Derivation of embryonic stem cell lines*. Methods Enzymol, 1993. **225**: p. 803-23.
- 43. Bettegowda, A., et al., Quantitative analysis of messenger RNA abundance for ribosomal protein L-15, cyclophilin-A, phosphoglycerokinase, beta-glucuronidase, glyceraldehyde 3-phosphate dehydrogenase, beta-actin, and histone H2A during bovine oocyte maturation and early embryogenesis in vitro. Mol Reprod Dev, 2006. **73**(3): p. 267-78.
- 44. Whelan, J.A., N.B. Russell, and M.A. Whelan, *A method for the absolute quantification of cDNA using real-time PCR*. Journal of Immunological Methods, 2003. **278**(1-2): p. 261-269.
- 45. Li, X. and X. Wang, Application of real-time polymerase chain reaction for the quantitation of interleukin-1[beta] mRNA upregulation in brain ischemic tolerance. Brain Research Protocols, 2000. **5**(2): p. 211-217.
- 46. Norris, H.J., H.J. Zirkin, and W.L. Benson, *Immature (malignant) teratoma of the ovary: a clinical and pathologic study of 58 cases.* Cancer, 1976. **37**(5): p. 2359-72.
- 47. O'Connor, D.M. and H.J. Norris, *The influence of grade on the outcome of stage I ovarian immature (malignant) teratomas and the reproducibility of grading.* Int J Gynecol Pathol, 1994. **13**(4): p. 283-9.
- 48. Steeper, T.A. and K. Mukai, *Solid ovarian teratomas: an immunocytochemical study of thirteen cases with clinicopathologic correlation.* Pathol Annu, 1984. **19 Pt 1**: p. 81-92.
- 49. Lucifero, D., et al., *Methylation dynamics of imprinted genes in mouse germ cells.* Genomics, 2002. **79**(4): p. 530-8.
- 50. Friedman, R.C., et al., *Most mammalian mRNAs are conserved targets of microRNAs.* Genome Res, 2009. **19**(1): p. 92-105.

- 51. Yuasa, S., et al., *Transient inhibition of BMP signaling by Noggin induces cardiomyocyte differentiation of mouse embryonic stem cells.* Nat Biotechnol, 2005. **23**(5): p. 607-11.
- 52. Dean, W., et al., Altered imprinted gene methylation and expression in completely ES cell-derived mouse fetuses: association with aberrant phenotypes. Development, 1998. **125**(12): p. 2273-2282.
- 53. Horii, T., et al., Loss of genomic imprinting in mouse parthenogenetic embryonic stem cells. Stem Cells, 2008. **26**(1): p. 79-88.
- 54. Jiang, H., et al., *Activation of paternally expressed imprinted genes in newly derived germline-competent mouse parthenogenetic embryonic stem cell lines.* Cell Res. **17**(9): p. 792-803.
- 55. Bibikova, M., et al., *Human embryonic stem cells have a unique epigenetic signature.* Genome Res, 2006. **16**(9): p. 1075-83.
- 56. Sasaki, H., K. Ishihara, and R. Kato, *Mechanisms of Igf2/H19 imprinting: DNA methylation, chromatin and long-distance gene regulation.* J Biochem, 2000. **127**(5): p. 711-5.
- 57. Tsang, W.P., et al., *Oncofetal H19-derived miR-675 regulates tumor suppressor RB in human colorectal cancer.* Carcinogenesis, 2010. **31**(3): p. 350-358.
- 58. Onodera, Y., et al., *Differentiation diversity of mouse parthenogenetic embryonic stem cells in chimeric mice.* Theriogenology. **In Press, Corrected Proof**.
- 59. Kono, T., et al., *Birth of parthenogenetic mice that can develop to adulthood.* Nature, 2004. **428**(6985): p. 860-4.
- 60. Kono, T., et al., *Mouse parthenogenetic embryos with monoallelic H19 expression can develop to day 17.5 of gestation*. Dev Biol, 2002. **243**(2): p. 294-300.

- 61. Milligan, L., et al., *H19 gene expression is up-regulated exclusively by stabilization of the RNA during muscle cell differentiation.* Oncogene, 2000. **19**(50): p. 5810-6.
- 62. Chung, S., et al., Analysis of different promoter systems for efficient transgene expression in mouse embryonic stem cell lines. Stem Cells, 2002. **20**(2): p. 139-45.
- 63. Varrault, A., et al., *Zac1 Regulates an Imprinted Gene Network Critically Involved in the Control of Embryonic Growth.* Developmental Cell, 2006. **11**(5): p. 711-722.
- 64. Lengerke, C., et al., *Differentiation potential of histocompatible parthenogenetic embryonic stem cells.* Annals of the New York Academy of Sciences, 2007. **1106**(1): p. 209-18.
- 65. Thuan, N.V., S. Kishigami, and T. Wakayama, *How to improve the success rate of mouse cloning technology.* J Reprod Dev, 2010. **56**(1): p. 20-30.
- 66. Kim, K., et al., *Histocompatible embryonic stem cells by parthenogenesis*. Science, 2007. **315**(5811): p. 482-6.
- 67. Hao, J., et al., *Human parthenogenetic embryonic stem cells: one potential resource for cell therapy.* Sci China C Life Sci, 2009. **52**(7): p. 599-602.
- 68. Honeycutt, K.A., M.I. Koster, and D.R. Roop, *Genes involved in stem cell fate decisions and commitment to differentiation play a role in skin disease.* J Investig Dermatol Symp Proc, 2004. **9**(3): p. 261-8.
- 69. Senoo, M., et al., *p63 Is Essential for the Proliferative Potential of Stem Cells in Stratified Epithelia*. Cell, 2007. **129**(3): p. 523-536.
- 70. Yang, A., et al., *p63 is essential for regenerative proliferation in limb, craniofacial and epithelial development.* Nature, 1999. **398**(6729): p. 714-8.

- 71. Barrandon, C., B. Spiluttini, and O. Bensaude, *Non-coding RNAs regulating the transcriptional machinery.* Biol Cell, 2008. **100**(2): p. 83-95.
- 72. Koster MI, K.S., Mills AA, DeMayo FJ, Roop DR, *p63 is the molecular switch for initiation of an epithelial stratification program.* Genes Dev. , 2004 **18**(2): p. 126-31.
- 73. Roop, M.I.K.a.D.R., *Transgenic Mouse Models Provide New Insights into the Role of p63 in Epidermal Development*. CellCycle, 2004. **3**(4): p. 409 411.
- 74. Gaudet, F., et al., *Induction of tumors in mice by genomic hypomethylation*. Science, 2003. **300**(5618): p. 489-92.
- 75. Zvetkova, I., et al., *Global hypomethylation of the genome in XX embryonic stem cells*. Nat Genet, 2005. **37**(11): p. 1274-1279.
- 76. Izadpanah, R., et al., Long-term in vitro expansion alters the biology of adult mesenchymal stem cells. Cancer Res, 2008. **68**(11): p. 4229-38.
- 77. Cimini, D. and F. Degrassi, *Aneuploidy: a matter of bad connections*. Trends Cell Biol, 2005. **15**(8): p. 442-51.
- 78. Cheng, L., *More new lines of human parthenogenetic embryonic stem cells.* Cell Res, 0000. **18**(2): p. 215-217.
- 79. Sun, X., et al., Two active X Chromosomes and methylation of the imprinted gene in human parthenogenetic embryonic stem cell line. Cell Res, 0000. **18**(S1): p. S35-S35.
- 80. Park JI, Y.I., Tada T, Takagi N, Takahashi Y, Kanagawa H., *Trisomy 8 does not affect differentiative potential in a murine parthenogenetic embryonic stem cell line*. Jpn J Vet Res., 1998 **46**(1): p. 29-35.
- 81. Epstein, C.J., Mouse monosomies and trisomies as experimental systems for studying mammalian aneuploidy. Trends in Genetics, 1985. 1: p. 129-134.

- 82. Gropp, A., U. Kolbus, and D. Giers, *Systematic approach to the study of trisomy in the mouse. II.* Cytogenet Cell Genet, 1975. **14**(1): p. 42-62.
- 83. Gropp, A., et al., *Murine trisomy: developmental profiles of the embryo, and isolation of trisomic cellular systems.* J Exp Zool, 1983. **228**(2): p. 253-69.
- 84. Gropp, A., D. Giers, and U. Kolbus, *Trisomy in the fetal backcross progeny of male and female metacentric heterozygotes of the mouse. i.* Cytogenet Cell Genet, 1974. **13**(6): p. 511-35.
- 85. Longo, L., et al., *The chromosome make-up of mouse embryonic stem cells is predictive of somatic and germ cell chimaerism.* Transgenic Research, 1997. **6**(5): p. 321-328.
- 86. Inoue, K., et al., *Sex-Reversed Somatic Cell Cloning in the Mouse.* The Journal of Reproduction and Development, 2009. **55**(5): p. 566-569.
- 87. Sanchez-Pernaute, R., et al., *Parthenogenetic dopamine neurons from primate embryonic stem cells restore function in experimental Parkinson's disease*. 2008. p. 2127-2139.
- 88. Sanchez-Pernaute, R., et al., Long-Term Survival of Dopamine Neurons Derived from Parthenogenetic Primate Embryonic Stem Cells (Cyno-1) After Transplantation. 2005. p. 914-922.
- 89. Ferrari, D., et al., *Transplanted dopamine neurons derived from primate ES cells preferentially innervate DARPP-32 striatal progenitors within the graft.* Eur J Neurosci, 2006. **24**(7): p. 1885-96.

DISSERTATION CHAPTER 4

TITLE CONCLUSIONS, FUTURE DIRECTIONS AND PRELIMINARY RESULTS

DISSERTATION CONCLUSIONS

The study of P-ESCs and PgEs has been of high interest in the area of stem cells and developmental biology primarily for three reasons: the potential application of P-ESCs in transplantation medicine, the role of imprinted genes in stem cell differentiation and embryo development, and third, their homozygosity, as it relates to fetal and stem cell viability and tumor formation.

P-ESCs used in our studies were derived from three different species -human (LLC-6p), primate (Cyno1) and mouse. We focused primarily on the deregulation of a specific set of imprinted genes, their impact on cell differentiation and potential regulation. Morphologically all the P-ESCs were indistinguishable from their respective biparental ES cells. The P-ESCs were propagated for long period of time while maintaining their undifferentiated ES cell morphology. Mouse, primate and human P-ESCs stain positive for the pluripotency markers OCT4, SOX2, SSEA1, and SSEA4 similar to their biparental counterparts. That the P-ESCs were pluripotent was revealed by an in vivo assay where the cells were injected subcutaneously into immune compromised Nude-SCID mice and were able to give rise to teratomas consisting of derivatives of all three germ layers- ectoderm, endoderm and mesoderm. Moreover, the teratomas formed on the site of injection, and no metastatsis were discovered. In this study we developed a method for quantification of germ layer derivatives based on morphological evaluation of consecutive sections of paraffin fixed formalin embedded teratoma sample. We modified the well established Tumberlek-Skully grading system, which is approved by the College of American pathologists (CAP) and highly used in clinics for determining

the tumor grade of solid ovarian teratomas, in order to account for the heterogeneous nature of our teratomas [136-138]. By using this method we determined that P-ESCs teratomas consisted of mostly terminally differentiated tissues of ectoderm, endoderm and mesoderm origin. These studies indicated that the P-ESCs are indistinguishable from normal biparental ES cells in terms of pluripotency and morphology, and can be induced to give rise to derivatives of all three germ layers –ectoderm, mesoderm and endoderm when differentiated *in vivo* but unlike teratomas derived from fertilized B-ESCs, mouse, primate and human P-ESCs derived teratomas showed restricted developmental potential towards endoderm derivatives. Mouse and primate P-ESCs also exhibited less potential to give rise to mesoderm muscle derivatives.

Numerous reports have identified *H19* gene as critical for proper PgE development [2, 55, 72, 107-108]. *H19* is an imprinted gene that codes for an untranslated mRNA molecule. *H19* is maternally expressed i.e. paternally imprinted gene. Recently it was found that *H19* and other imprinted genes form an imprinted gene network whereby even a slow alteration of an imprinted gene of the hub effects the expression of the imprinted genes in the network [36, 169]. Therefore one can assume that modulating *H19* gene expression may affect the expression of other imprinted genes and ultimately can change the differentiation potential of the cells since one of the main function of *H19* and other imprinted genes in the network such as *IGF2*, *DIO3*, *DLK1*, *IGF2R* is to control embryo and cell growth and differentiation.

H19 expression in the cell is coordinately regulated with the expression of the paternally expressed gene Insulin Growth Factor 2(IGF2) which resides around 70kb upstream of

H19 [144]. The coordinate expression of H19 and IGF2 is mainly under the control of a DMR region located upstream of H19. Our data revealed that H19 was highly overexpressed in P-ESC cell lines derived from mouse, primate and human parthenogenetic blastocysts. We were also able to detect expression of paternally expressed genes which normally are expected to be silent in P-ESCs. These findings were consistent with reports coming from other groups, pointing out that the imprinting maintenance is unstable in P-ESCs during passaging [72, 76, 83, 87]. The same phenomenon has been found to be the case in normal fertilized B-ESCs revealing that the expression pattern of the imprinted genes changes upon in vitro culturing and propagation [24, 142, 170]. For example gene expression data from our P-ESC lines indicated that *lgf2* was expressed in all mouse, primate and human P-ESCs. The expression of *Igf2* in mouse P-ESCs did not correlate with the methylation of the DMR region which remained partially methylated in the two mouse P-ESC lines; P-ESC-1 and P-ESC-2 tested. Other paternally expressed genes whose expression was detected in P-ESCs were *PEG10* and *SNRPN* in primate P-ESCs, *DIO3* in human P-ESCs and Mest1 and Mkrn in mouse P-ESCs.

We focused our study on evaluating the effect of *H19* on P-ESCs differentiation plasticity because *H19* was highly overexpressed in all P-ESC cell lines tested and second because a huge body of literature has revealed that *H19* is critical for PgE development to term. We and other groups have also observed that P-ESCs with *H19* overexpression give rise to mostly ectodermal derivatives when introduced into chimeric animals *in vivo* [79-81, 146].

We used small hairpin RNA (shRNA) plasmid and retroviral vector system to chronically suppress the H19 expression in mouse, primate and human P-ESCs. We followed the developmental potential of mouse P-ESCs with suppressed H19 expression and found that these cells were more prone to give rise to endoderm and mesoderm derived muscle compare to P-ESC control cells (there was a 15% increase in endoderm and 11% increase in mesoderm derived muscle in mouse P-ESCs with suppressed H19 compare to control P-ESCs). By using our modified Tumberleck –Skully method for quantification of germ layer derivatives, we estimated the percentage of endoderm and mesoderm muscle tissues in H19 downregulated P-ESCs derived teratomas to be similar to that observed in B-ESC control cells. The increase of mesoderm derived muscle correlated with a statistical significant increase (P<0.05) in the expression of the muscle specific genes Myf5, Myf6, MyoD and an increase in the early mesoderm promoting marker *Mier2*. Moreover, we found that the expression of the ectoderm promoting gene $\Delta Np63$ was significantly down regulated in the mouse P-ESCs with suppressed H19 expression which may account for the decrease of the ectoderm derived tissues in teratomas. We also performed a functional study where we induced the mouse P-ESCs with downregulated H19 to differentiate into beating EBs following a very well established protocol [141]. Our data revealed that P-ESCs with suppressed H19 give rise to more beating EBs compare to P-ESC control cells and more similar to normal B-ESCs.

All together these results suggest that P-ESCs are amenable to genetic modification and that downregulation of *H19* can bring them functionally closer to normal B-ESCs.

Improving the differentiation plasticity of P-ESCs towards endoderm and mesoderm muscle derivatives will aid towards a potential application of these cells for stem cell therapy. Another advantage of the P-ESCs for transplantation application is that these cells are isogenic with the oocyte donor i.e. a perfect match for the tissue rejection antigens of the major histocompatible complex loci [98, 171].

Unfortunately we found that P-ESCs are very prone, probably due to their monoparental genomic complement, to accumulate cytogenetic abnormalities. This may be avoided if an early passage (not later than passage 6) P-ESCs are used. The maternal-only genomic complement also carries some risk for failure of the P-ESCs derived tissues and organs due to genetic homozygosity for deleterious mutations. The "1000 genomes" project" estimated that on average, in a heterozygous genome, there are 50-100 variants classified by the Human Gene Mutation Database (HGMD) as causing inherited disorders in humans [172]. Assuming random recombination among the chromatids prior to meiotic reduction and division as demonstrated by Kim et al., we can presume that a human parthenote would, on average, be homozygous for half the number of the deleterious alleles annotated by The "1000 genomes project" mentioned above [172]. However, it is not known if these deleterious alleles are disadvantageous for specific tissues and organs or only for the whole individual. Therefore, more data is needed to reveal the impact these allele variants may have on the use of P-ESCs for tissue replacement.

In conclusion, despite the pitfalls outlined above, P-ESCs can give rise to functional tissues such as those already reported and exhibited long term survival and function

upon grafting into animal models [17-18, 106]. Also P-ESCs bypass the ethical issues associated with destruction of viable embryos which the fertilized B-ESCs face. Future pre-clinical studies on the safety and efficiency of P-ESCs during engraftment and tissue regeneration will help us determine the real potential of these cells for clinical application.

FUTURE DIRECTIONS

The data presented here suggests that *H19* expression affects the differentiation potential of mouse P-ESCs towards endoderm and mesoderm germ layers.

Future studies would need to focus on the mechanism through which *H19* exerts its action. We now know that *H19* codes for an antisense (AS) RNA molecule as well as for a microRNA (mir675). We also identified through Target Scan software that *Mier2* is a potential target of mir675. Therefore a possible way for *H19* mode of action can be affecting the mesoderm and/or the endoderm differentiation by using the miRNA pathways. It has been already reported that mir675 targets the 3'UTR region of the Retinoblastoma (RB) transcript and suppresses *RB* expression in different carcinoma cell lines [145]. Another mechanism can be that the H19asRNA is the molecule that targets transcriptional or post transcriptional silencing of candidate genes and thus modulates the developmental program. This can be tested *in vitro* by over expressing the H19AS RNA followed by a microarray experiment looking for global changes in gene expression.

It has been reported that suppression of *H19* is critical for PgEs development to term.

These studies were based on genetically modifying the PgE genome so that the *H19* coding and upstream DMR region is deleted from one of the maternal chromosomes [55, 107]. An elegant experiment to look at the role of *H19* in PgE development to term would be to incubate a PgE at 2-cells or blastocyst stage in the supernatant of our packaged shRNA expressing retroviral vector. Then the PgE can be transferred to a pseudopregnanat surrogate mother and the development of the embryo can be followed and analyzed to term.

A more sophisticated modification of the experiment proposed above is to use our *H19*shRNA viral vector construct which is also Tetracycline off vector i.e. the *H19* is expressed unless tetracycline is added. After infection of the PgE at blastocyst stage and transfer to surrogate mother, the mother can be fed tetracycline and the H19 shRNA expression can be regulated on timely manner at different stages of embryo development – implantation, gastrulation, and organogenesis.

Recent studies in PgE development revealed that when passed through serial nuclear transfers, the parthenogenetic genome can be partially reprogrammed so that the PgE development can be prolonged as a result of improvement in placental development [84, 110]. This study showed that as the placental formation and embryo development improved the levels of *H19* expression decreased. Therefore, it would be of great scientific value if we use our transgenic P-ESC lines with suppressed *H19* gene expression for nuclear transfer experiment. We would expect that the nuclear transfer

PgEs would exhibit prolong embryo development, placental formation even after the first round of nuclear transfer.

Finally, we are currently applying the knowledge on *H19* down regulation gained from in mouse P-ESCs studies on modulating the differentiation potential of human P-ESCs – LLC-6p. Primates and rodents are far in the tree of evolution; however the imprinting pattern of most of the imprinted genes such as *H19* has been conferred. We have constructed an *H19*shRNA and *H19*asRNA expressing vectors to study the effect of downregulation of *H19* on the differentiation plasticity of the human P-ESCs. The preliminary results are outlined below.

HUMAN PARTHENOGENETIC EMBRYONIC STEM CELLS (P-ESCS) PRELIMINARY RESULTS

AIMS

- A. To study the differentiation potential of human B-ESCS and P-ESCs in vivo, by teratoma formation
- B. To analyze the expression of set of maternally and paternally imprinted genes as well as the expression pattern of DNA Methyl transferase enzymes (DNMTs) in different passages of human B-ESCs and P-ESCs.
- C. To design expression vectors for stable downregulation of *H19* gene expression in human B-ESCs and P-ESCs

MATERIALS AND METHODS

Embryonic Stem Cell Culturing and Propagation

Human Biparental Embryonic Stem cells(H1) (WiCell Institute, Wisconsin, USA) and Human Parthenogenetic Embryonic Stem (LLC-6p) (International Stem Cells Corporation, California, USA) cells with a stable, normal (46, XX) karyotype, were cultured on mitotically inactivated feeder layer of mouse embryonic fibroblast cells as described by *Zhang et al.*, 2001. The culture media consisted of Dulbecco's Modified Eagle's Medium (DMEM/F12; Invitrogen), 20% knock out serum replacement

(Invitrogen), 0.1mM β-mercaptoethanol, 4ng/ml FGF-2 (Invitrogen), 1% nonessential amino acids (Invitrogen), and 2mM L-glutamine (Invitrogen). The embryonic stem (ES) cells were cultured and maintained in humidified incubator with 5% CO₂ at 37°C.

Immunocytochemistry

Cells were washed 3 times, each time 5 minutes with washing buffer (DPBS, 0.1% TX100 (Triton 100X) and incubated with Permeabilization Buffer (DPBS, 1% TX100) for 10min. Subsequently, the cells were washed once more with washing buffer, then blocked with blocking buffer (DBPS + 0.1%TX100 + 1%BSA + 10%NGS) for 1-2 hours. OCT4 antibody (sc8628, Santa Cruz Biotechnology, Inc.) in dilution 1:300 and SSEA4 antibody (DSHB at the University of Iowa, mc813-70), in 1:500 dilution, NANOG (sc33759, Santa Cruz Biotechnology, Inc.), LIN28 (sc67266, Santa Cruz Biotechnology, Inc.), and SOX2 (ab5603, Abcam) was added to the cells and incubated for 3 hours to overnight at 4°C. Cells were washed 6 times each time 10 minutes. Then secondary Ab (Abcam) was added in 1:500 dilutions following the manufacturer's recommendations.

RNA isolation and cDNA synthesis from ES cells

Total mRNA from human H1 and LLC-6p embryonic stem (ES) cells was isolated using the RNeasy Isolation Mini Kit (Qiagen) following the manufacturer's instructions and strict RNAse and DNAse free procedures. Total mRNA amount was measured using Nanodrop. One ug of total RNA with OD260/280 > 2.1 was used for first strand cDNA synthesis. cDNA was synthesized with Superscript II (Invitrogen) using anchored Oligo (dT₁₂₋₁₈) primers (Invitrogen) and following the manufacturer's instructions.

Quantitative real time RT-PCR

The quantification of all gene transcripts was performed by reverse transcription of total RNA followed by absolute real-time quantitative RT-PCR using SYBR Green PCR Master Mix (Applied Biosystems). Absolute quantification using this method is described elsewhere (Li and Wang, 2000; Whelan et al., 2003). Primers for absolute real time PCR were designed using Primer Express program (Applied Biosystems) and derived from human sequences found in GeneBank (Table4.1). A primer matrix was performed for each gene tested to determine optimal concentrations. Each reaction mixture consisted of 2 µl of cDNA, optimum concentration of each forward and reverse primer, nuclease free water, and 12.5 µl of SYBR Green PCR Master Mix in a total reaction volume of 25 µl (96well plates). Reactions were performed in triplicate for each sample using an ABI Prism 7000 Sequence Detection System (Applied Biosystems). The thermal cycle consisted of 40 cycles of 95°C for 15sec and 60 °C for 1min. Standard curves for each gene and controls were constructed using tenfold serial dilution and run on sample plates as standards. For gene expression normalization expression levels of β -actin mRNA was used. Copies of β -actin RNA in each pool were determined using standard curves constructed from the plasmid PCR2.1 Topo containing partial β -actin cDNA sequence (Bettegowda et al. 2006). Partial cDNA sequences for β -actin, H19, *IGF2* and the other genes tested, were amplified from human H1 ES cells, cloned into pCR2.1 Topo vector (Invitrogen), and subjected to fluorescent dye primer sequencing to confirm identity. Resulting plasmids were used to construct standard curves. Representative R^2 for β -actin, H19 and the rest of the genes were estimated and only

the one ≥ 0.98 used. For each measurement, threshold lines were adjusted to intersect amplification lines in exponential portion of amplification curve (Bettegowda et al).

Teratoma formation

For all teratoma experiments, a suspension of around 1x10⁶ H1 HES cells and LLC-6p ES cells were injected subcutaneously (s.c.) into immunodeficient Nude mice-CD-1 (Charles River Laboratories). Mice were euthanized around eight weeks after injection or when tumors had grown to about 1cm in diameter, whichever came first. Teratomas were then isolated, fixed in paraformaldehyde, embedded in paraffin and stained with hematoxilin eosin.

Quantification of Endoderm, Ectoderm and Mesoderm derivatives in teratomas

Teratomas from H1 HES cells and LLC-6p ES cells were derived by subcutaneous
injection into immune-deficient Nude mice, CD-1 (Charles River Laboratories). The
teratomas were formalin fixed sectioned and embedded in paraffin blocks; each was
entirely submitted for histological analysis. One to three gross tissue samples per tumor
were obtained for this study. The College of American Pathologists (CAP) guidelines for
gross sampling of solid tumors state that one sample for each centimeter of tumor or
three samples, whichever is greater, should be used for tumor grading. Histological
grading was performed utilizing the modified Thurlbeck-Scully histological grading
system for solid ovarian teratomas proposed by Norris et al [136] and successfully
implemented by O'Conner et al[137] and Steeper and Mukai [138]. This system which is
widely employed clinically, estimates percentage of neuro epithelium in the total tumor
mass by counting the number of microscopic 10x Low Power Fields (LPFs) to

differentiate between tumors grades I, II, and III. We estimated that from our teratoma samples about 12-16 LPFs could be evaluated per full tissue section on one glass microscopic slide and that 3 tissue sections would yield approximately 36-48 LPFs for examination, and thus comply with the modified Thurlbeck-Scully histological grading system.

H19 shRNA and H19asRNA expressing vectors

For downregulation of *H19* in human P-ESCs (LLC-6p) we used shRNA and asRNA approach. For expression of *H19*shRNA we used pRNAT-U6.1 plasmid (GenScript, cat#SD1211) and a pMSCV-Hygro retroviral vector (Clontech Laboratories, Inc.). The pMSCV-Hygro vector (Clontech Laboratories, Inc.) was used for *H19* shRNA delivery into humanLLC-6p cells with the following modifications: Chicken b-promoter CMV-IE Enhancer fragment was derived from plasmid pCX-EGFP without PolyA signal by digestion with Sal-I and Bgl-II. The pMSCV-Hygro retroviral vector was digested with Sal1 and the Chicken b-promoter CMV-IE Enhancer-Intron-EGFP and introduced by T4 DNA ligation reaction into the Sal1 site. The cassette H1/TO promoter -H19 shRNA – Pol III termination site was released from plasmid pENTR/H1/TO plasmid (Invitrogen) by digestion with BamHI (NEB) and cloned into unique Xho1 site of the pMSCV-Hygro retroviral vector. The so modified pMSCV-Hygro retroviral vector was called pMSCV-Hygro-EGFP-*H19* shRNA retroviral vector (Figure4.8).

The packaging and transduction of pMSCV-Hygro-EGFP-*H19*shRNA vector was done following the manufacturer's recommendations (Clontech, Cat# 634401) in human LLC-6p. For negative control, non specific shRNA sequence derived from plant genome and

called *NDR1* was used. The *NDR1*shRNA was plant specific (*Arabidopsis Thaliana*) and did not match to any human coding region. The cells were subjected to Hygromyocin selection two days post-viral infection.

For the plasmid shRNA delivery, pRNAT- U6.1/Neo vector was used (GenScript, cat#SD1211). In this vector system the *H19* shRNA was expressed from U6 promoter and GFP and Neomycin expression are driven by CMV promoter. The pRNAT- U6.1/Neo *H19* shRNA vector was linearized by using a unique Scal (NEB) restriction site and transformed into human Hela cell line by using Amaxa[™] Nucleofector machine (Lonza, USA), Amaxa Cell Nucleofector Kit V (Lonza, USA), program A-030 and following the manufacturer's recommendation (Figure4.9). *H19* antisense RNA (asRNA) was amplified from human LLC-6p and sublconed into

SCNT-ES Competent –Tet Regulated retroviral vector. Yellow fluorescent protein (YFP) sequence was subcloned into the SCNT-ES Competent –Tet Regulated vector (Figure 4.8). The H19shRNA and H19as sequences are based on sequence accession number NR 002196.1 derived from GenBank. The sequences are provided below:

H19homo, shRNA#1

5'-GGCAGGAGAGTTAGCAAAGGT-3'

H19homo, shRNA#2

5-GAAGCGGGTCTGTTTCTTTAC-3'

H19homa Anti Sense RNA

5'-

Statistics

qRT-PCR experimental data and teratoma quantification data were analyzed by analysis of variance (ANOVA). Differences of p < 0.05 were considered statistically significant.

RESULTS AND DISCUSSION

Human parthenogenetic cell line LLC-6p was obtained from International Stem Cells Corporation, California, USA. LLC-6p cell line was morphologically indistinguishable

from normal biparental human ES cell line H1 and also expressed the pluripotency markers OCT4, SOX2, NANOG, LIN28, and SSEA4(Figure 4.1). Both LLC-6p and H1 ES cell lines were able to expand *in vitro* for prolong period of time without changing their ES cell morphology. Both H1 and LLC-6p cell line were able to give rise to teratomas when injected subcutaneously into immune deficient Nude-SCID mice which consisted of derivatives of all three germ layer – endoderm, ectoderm and mesoderm (Figure 4.2 and Figure 4.3). There was a difference in the endoderm derivatives between LLC-6p and H1 HES cells teratomas (Figure 4.4). Teratomas derived from human H1 ES cells gave rise to 39% endoderm derivatives compared to only 9% in LLC-6p derived ones. We did not find skeletal or smooth muscle tissue neither in the H1 ES cells nor in the LLC-6p ES cells derived teratomas. There was however, a significant amount of mesoderm-derived connective tissue in the LLC-6p teratomas (58%) compare to the connective tissue abundance in H1 HES teratomas (3%). There was less cartilage and adipose tissue, a mesoderm derived lineages, and in the LLC-6p teratomas compare to H1 HES cells derived teratomas (Figure 4.4). It has been reported that mitochondrial function is essential for proper differentiation of ES cells [173-174]. An increase of apoptosis in the ES cell culture due to impaired mitochondria function may alter the developmental potential of the ES cells. We measured apoptosis in H1 and LLC-6p ES cells by analyzing the Annexin V expression on the cell surface using FACs analysis. Annexin V is an apoptotic marker for cells in early and late apoptosis. Our results revealed that there was no statistical significant difference in apoptotic cells expressing Annexin V between H1 and LLC-6p cells (Figure 4.5). Therefore the difference in germ

layer derivatives may not be due to differences in apoptotic cells between H1 and LLC-6p ES cells during *in vivo* differentiation.

We also analyzed the expression levels of a set of imprinted genes, paternally imprinted i.e. maternally expressed genes H19 and UBE3A (Ubiquitin protein ligase E3A) and the maternally imprinted genes *IGF2* (insulin-like growth factor 2 (somatomedin A), *DIO3* (deiodinase, iodothyronine, type III) and NDN (Necdin homolog), in human H1 and LLC-6p ES cells by qRT-PCR (Figure 4.6). Multiple studies as well as data coming from studies of mouse P-ESCs in our laboratory have revealed that the levels of H19 gene can influence the differentiation potential of mouse P-ESCs towards endoderm and mesoderm derivatives. As expected, the expression level of H19 gene was significantly upregulated in LLC-6p cells (p<0.05) compare to biparental H1 ES cells (Figure 4.6). We also found that IGF2 and DIO3, maternally imprinted genes, were expressed in LLC-6p ES cells at levels similar (Figure 4.6C) or even higher (Figure 4.6B) than that of biparental H1 human ES cells. NDN, another paternally expressed gene, was not expressed in LLC-6p ES cells at least by the qRT-PCR method used (Figure 4.6E). UBE3A, another maternally expressed genes, known to be imprinted specifically in the brain, was expressed at similar levels between biparental H1 and parthenogenetic LLC-6p ES cells, suggesting that this gene may not be imprinted in ES cells (Figure 4.6D).

We next looked at the expression of the imprinted genes tested above in two different passages of human H1 and LLC-6p ES cells. We did not found a significant difference, between two different passages of H1 and LLC-6p cell lines, in the expression of the imprinted genes tested except *DIO3* gene whose expression varied statistically between

earlier and later passage of human H1 ES cells (Figure 4.7A-D, K-N). We also found that after five passages the expression of *H19* also changes a finding that is in agreement with reports coming from other groups in which gene expression of imprinted genes can change during prolonged culture in vitro. We did find alterations in the genes; *DIO3* and *H19*, in particular. We also looked at the gene expression of the major DNA methyltransferase enzymes – *DNMT1*, *DNMT3A* and *DNMT3B* in H1 and LLC-6p Es cells during passaging. There was no difference in the expression of the de novo *DNMT3A* and *DNMT3B* methyl transferase enzymes in H1 human ES cells of different passages (Figure 4.7G, I). However the levels of *DNMT1* in H1 ES cells were increasing with the increase in passage number (Figure 4.7E). On the contrary, in two different passages of LLC-6p ES cells, we observed that the levels of *DNMT1* did not differ, however the expression of the de-novo methyl transferases *DNMT3A* and *DNMT3B* had a statistical significant decrease in later passage compare to early passage (Figure 4.7 F, H, J).

In conclusion, we found, *H19* gene to be highly over expressed in human LLC-6p cells compare to normal biparental H1 ES control cells. Our data also suggest that gene expression profile should be evaluated between cell lines of the same type with no more than five passages difference. We found that the levels of DNA methyltransferases change during passage, with *DNMT1* levels were increasing in H1 HES cells and DNMT3A and 3B levels decreasing with increase of the LLC-6p passage number. Further studies are needed to correlate the changes of expression of DNMT enzymes with the expression of the imprinted genes in HES and LLC-6p cells.

Bisulfate sequencing analysis of the *H19* and *DIO3* is necessary to evaluate if the changes in the methylation of the imprinted domains underlies the changes of gene expression observed in our study and suggested by reports coming from other groups.

Next we wanted to examine if downregulation of H19 can alter the *in vivo* differentiation phenotype of human LLC-6p ES cells. We previously found that downregulation of H19 in mouse P-ESCs increase the developmental plasticity of the cells towards mesoderm and endoderm germ layer derivatives. In order to test that, we employed a small hairpin (sh) and an anti sense (as) RNA expressing vector system to stably downregulate *H19* in LLC-6p ES cells (Figure4.8). We designed a plasmid and a retroviral (pMSCV-Hygro –EGFP) *H19* shRNA expressing retroviral vector system to suppress H19 gene expression. We also designed an H19 antisense overexpressing retroviral vector system (SCNT-ES competent Tetracyclin off) which is an alternative way to suppress *H19* gene expression using a long non coding *H19* anti sense RNA instead of shRNA (Figure4.8).

In our preliminary study we utilized the pRNAT-U6.1 *H19*shRNA expressing vector. The vector was linearized and transfected into Hela cells by electroporation. We used Hela cells for our preliminary study because this cell line is very easy to transfect, grow and propagate (Figure 4.9 A, B).

We used *NRD1* (Arabidopsis thaliana Non Race-specific Disease resistance 1) cDNA sequence as a non specific RNA control that was also transfected into Hela cells. Hela cells transfected with the *H19*shRNA or Control vector were subjected to 500ug/ml G418 for 14 days. Total RNA was extracted from the *H19*shRNA and Control vector cell

lines and subjected to polymerase chain reaction to test for suppression of *H19* gene expression. The PCR results clearly revealed that *H19* was efficiently down regulated in the Hela cells transfected with the H19shRNA expressing vector (Figure 4.10). Next we attempted to transfect by electroporation the *H19*shRNA expressing pRNAT-U6.1 expressing viral vector into LLC-6p ES cells (Figure 4.9 C-E). Figure 4.9E represents a green fluorescent expression in LLC-6p cells infected with *H19*shRNA expressing vector. Unfortunately after selection with 300-400ug/ml Neomycin we lost all GFP fluorescent expressing cells i.e. we were not able to get a transgenic cell line stably expressing *H19*shRNA. We were also not able to get stable transgenic cell line from the LLC-6p infected with the *H19*asRNA expressing retroviral vectors as well. We are currently optimizing the infection conditions in order to obtain stable transgenic cell lines and evaluate the developmental potential of LLC-6p cell lines with suppressed *H19* expression either using *H19*shRNA or *H19*AS RNA expressing vector systems.

Once stable transgenic LLC-6p cell lines are selected, we will proceed evaluating their differentiation potential by teratoma formation into immune compromised Nude SCID mice. We hope to observe a change in the *in vivo* differentiation potential of LLC-6p ES cells. Furthermore, a microarray analysis will reveal the gene expression changes that underlie any change in the developmental plasticity of LLC-6p ES cells upon downregulation of *H19* gene.

FIGURES AND TABLES

Figure 4.1 Immunocytohemistry for the pluripotency markers NANOG (NAN), LIN28, SSEA4, SOX2, and OCT4 in human ES cells H1 and in human P-ESCS (LLC-6P). R-Red, G-Green.

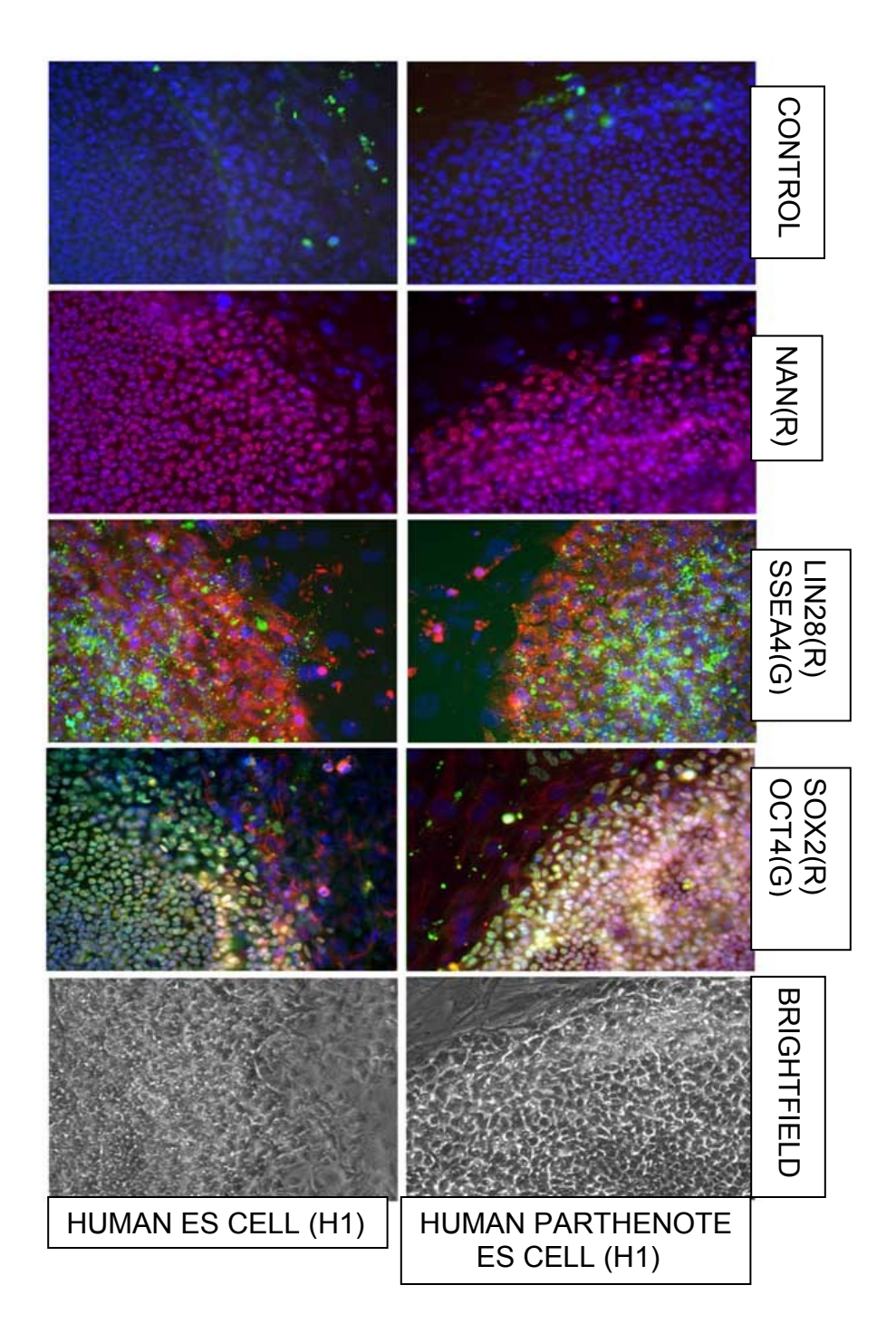


Figure 4.2 Hematoxylin-Eosin (H&E) staining of human HES H1 derived teratomas indicating the ability of these cells to give rise to all three germ layers when differentiated *in vivo*. A and D – squamos epithelium (10X and 40X respectively), B. Neuroepithelium (10X), E. Primitve neural rosette (40X), C and F- glandular structures (endoderm) (10X and 40X respectively) G and H- connective tissue (10X and 40X respectively).

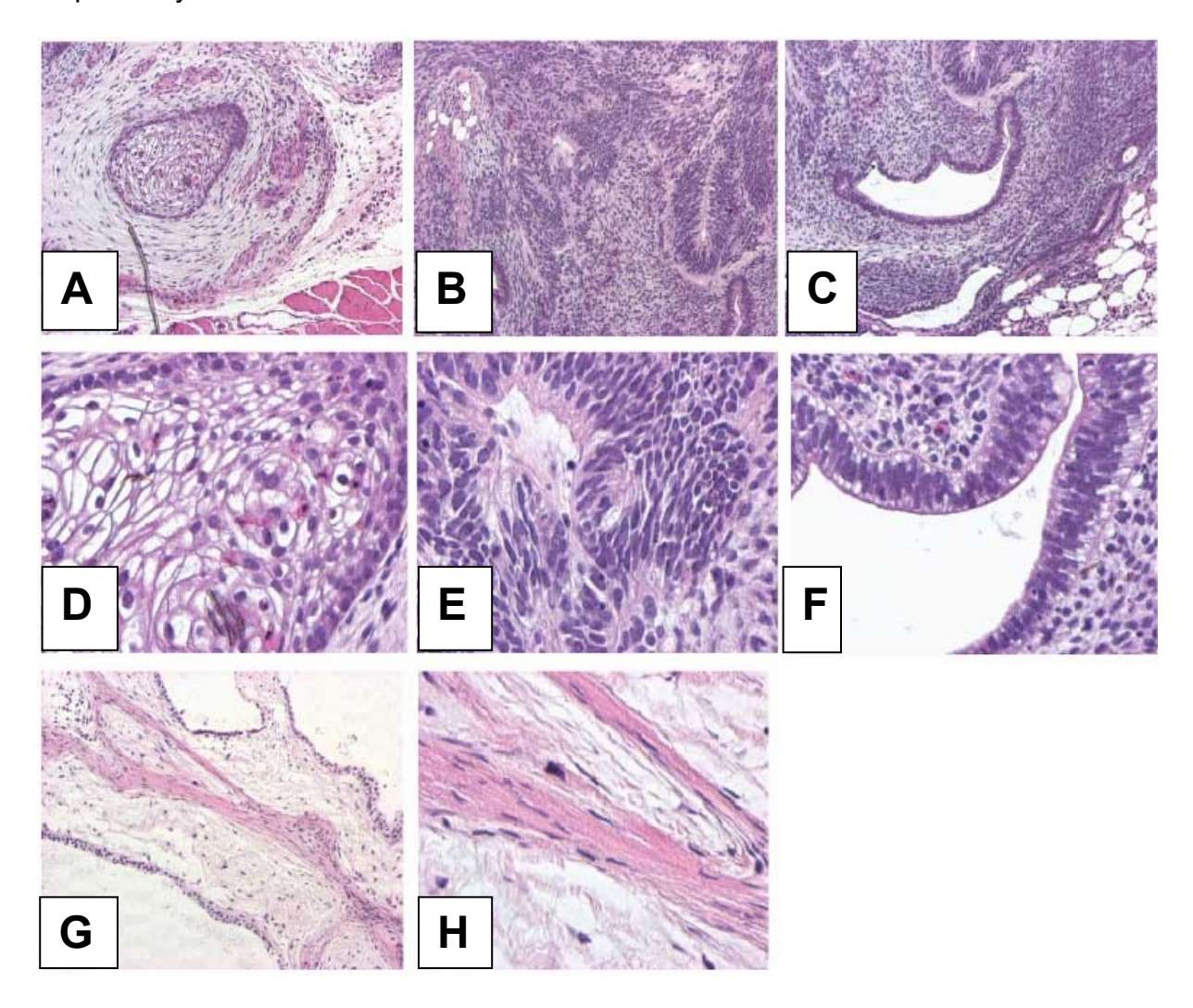


Figure 4.3 Hematoxylin-Eosin (H&E) staining of human LLC-6p cells derived teratomas indicating the ability of these cells to give rise to all three germ layers when differentiated *in vivo*. A Neural Ectoderm (10X), B. Connective tissue (40X), C. Glandular structure (10X) D. Neural ectoderm (40X).

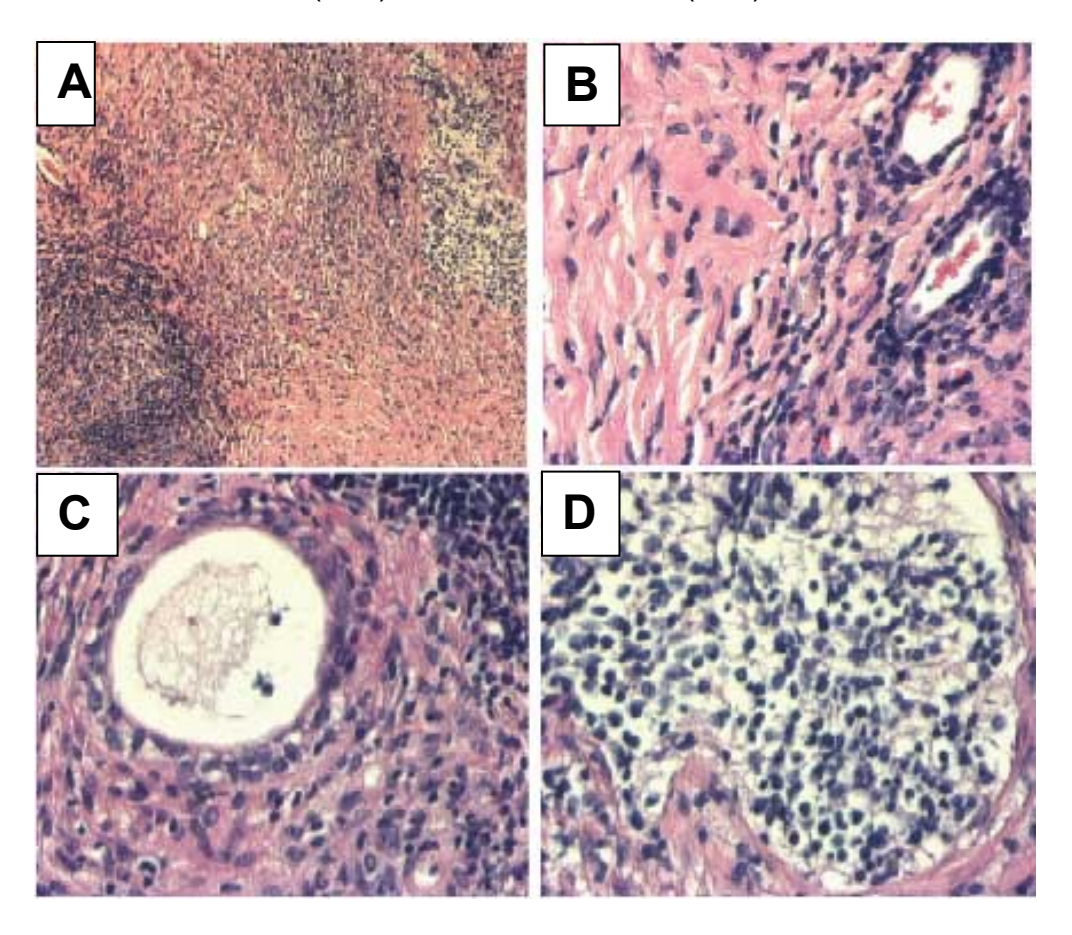


Figure 4.4 Quantification (%) of germ layer derivatives: ectoderm, endoderm and mesoderm in teratomas derived from wild type HES, H1 cells and in human P-ESCs (LLC-6p). Two LLC-6p and three H1 HES cells derived teratomas were used for quantification (See Materials and Methods section).

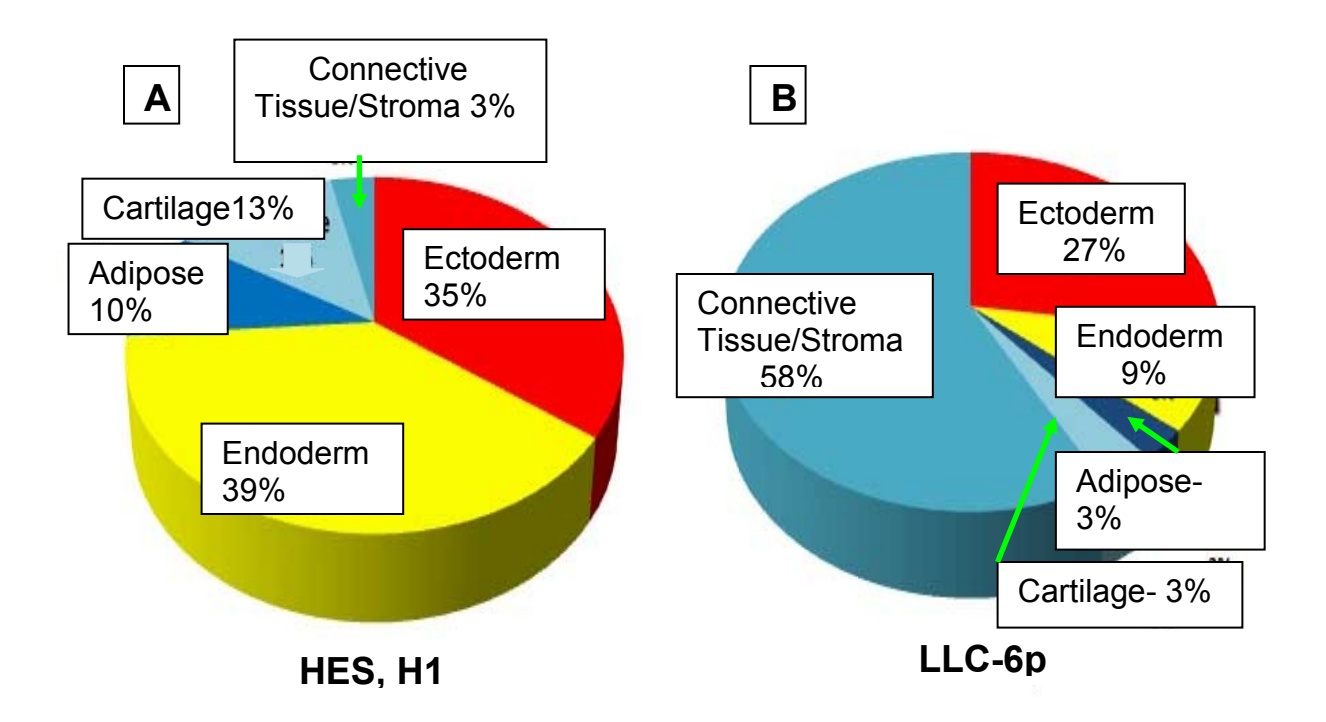


Figure 4.5 Fluorescent Activated Cell Sorting analysis (FACS) on the apoptotic rate of HES H1 and human LLC-6p cells measured by Annexin V expression. Three six well plates from each cell line have been used. The bars represent standard error bars (P<0.05).

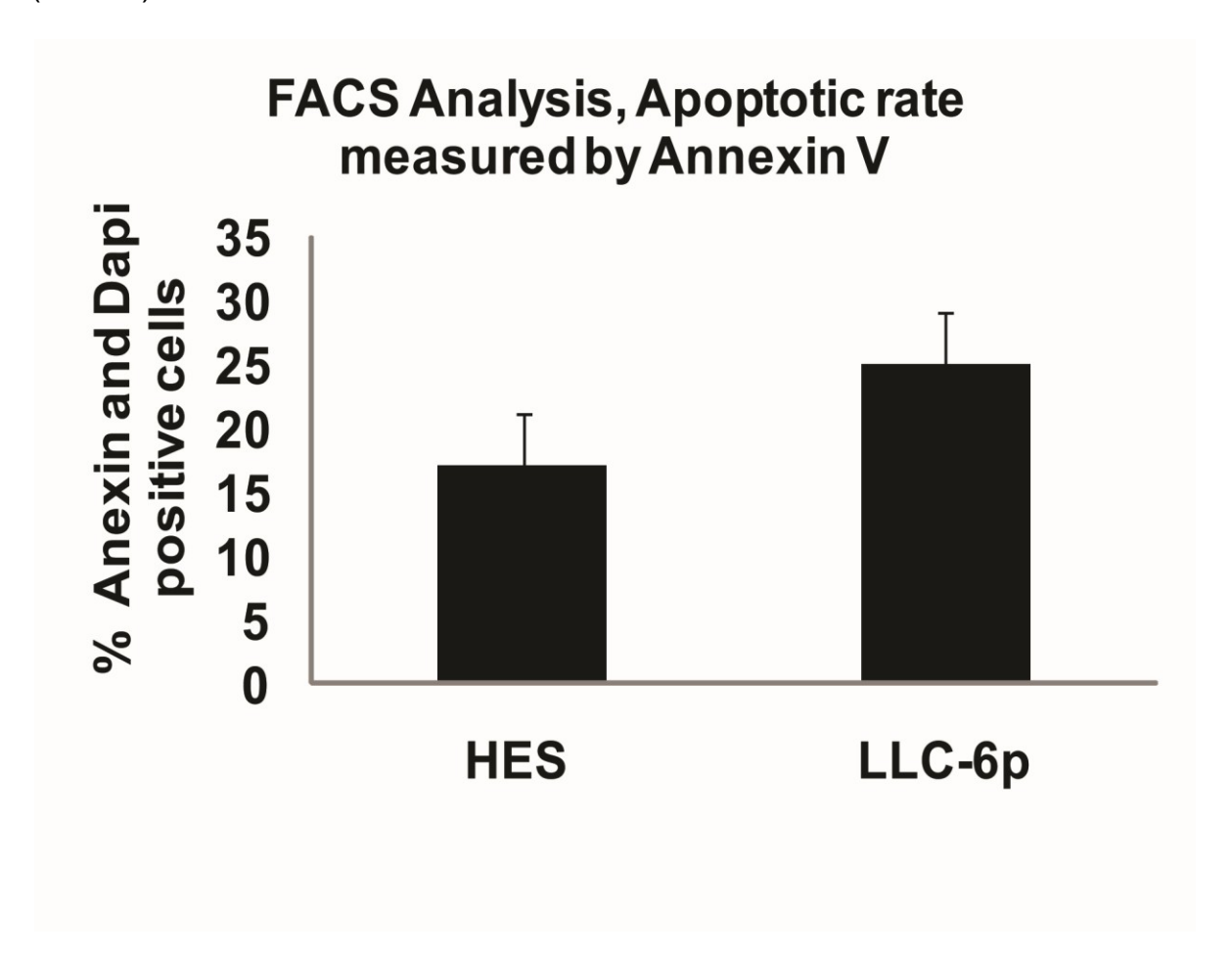


Figure 4.6 Quantification of mRNA abundance of the maternally expressed *H19* and *UBE3A* and the paternally expressed *IGF2*, *DIO3* and *NDN* in HES H1 and LLC-6p cells by qRT-PCR. For all qRT-PCR experiments three biological replicates (n=3) in three technical replicates were used in each run and a P<0.05 has been considered as statistical significant, unless stated otherwise. The bars represent standard error bars. All the letters above the error bars represent the difference between samples on the basis of standard error values (P<0.05).

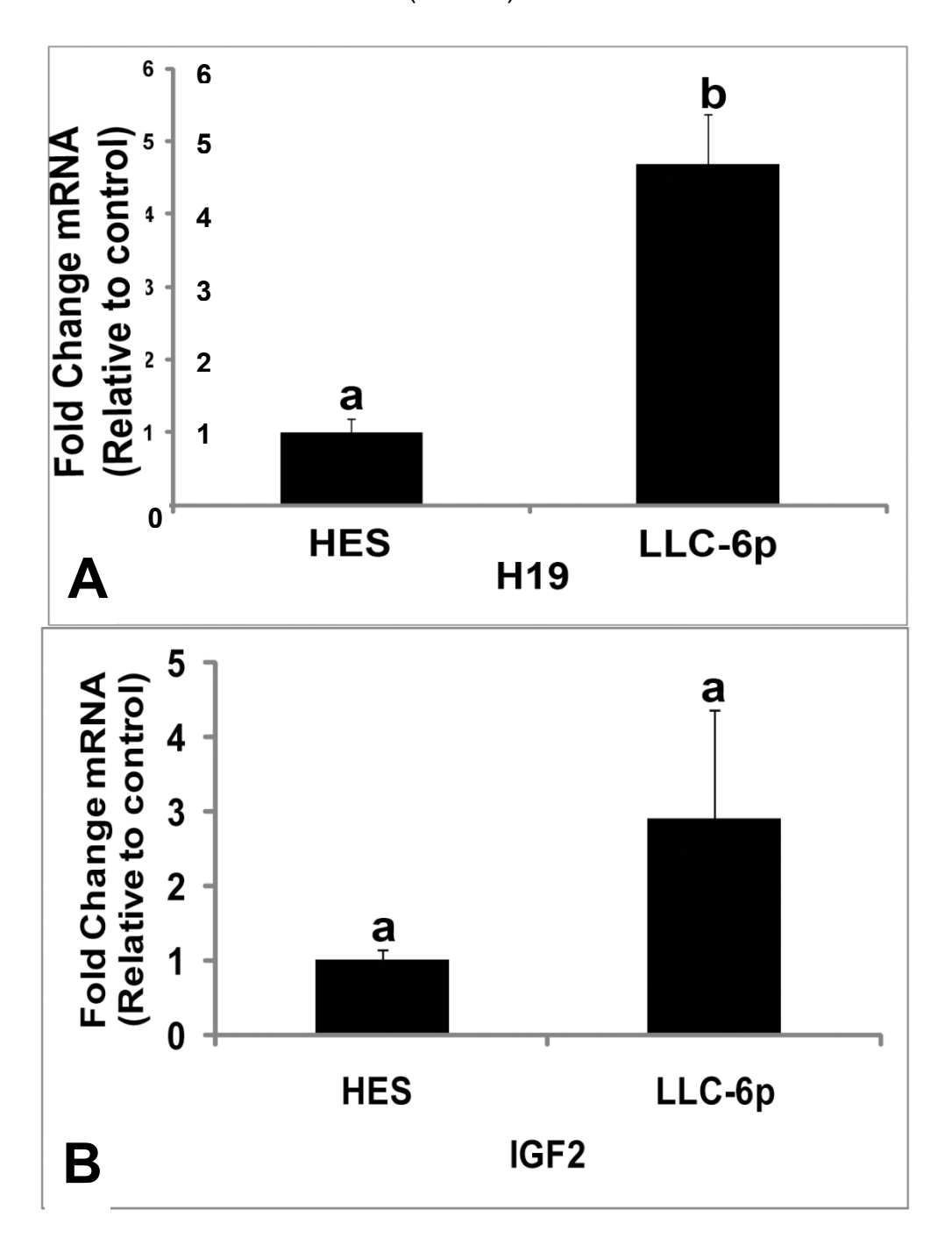


Figure 4.6 (cont'd)

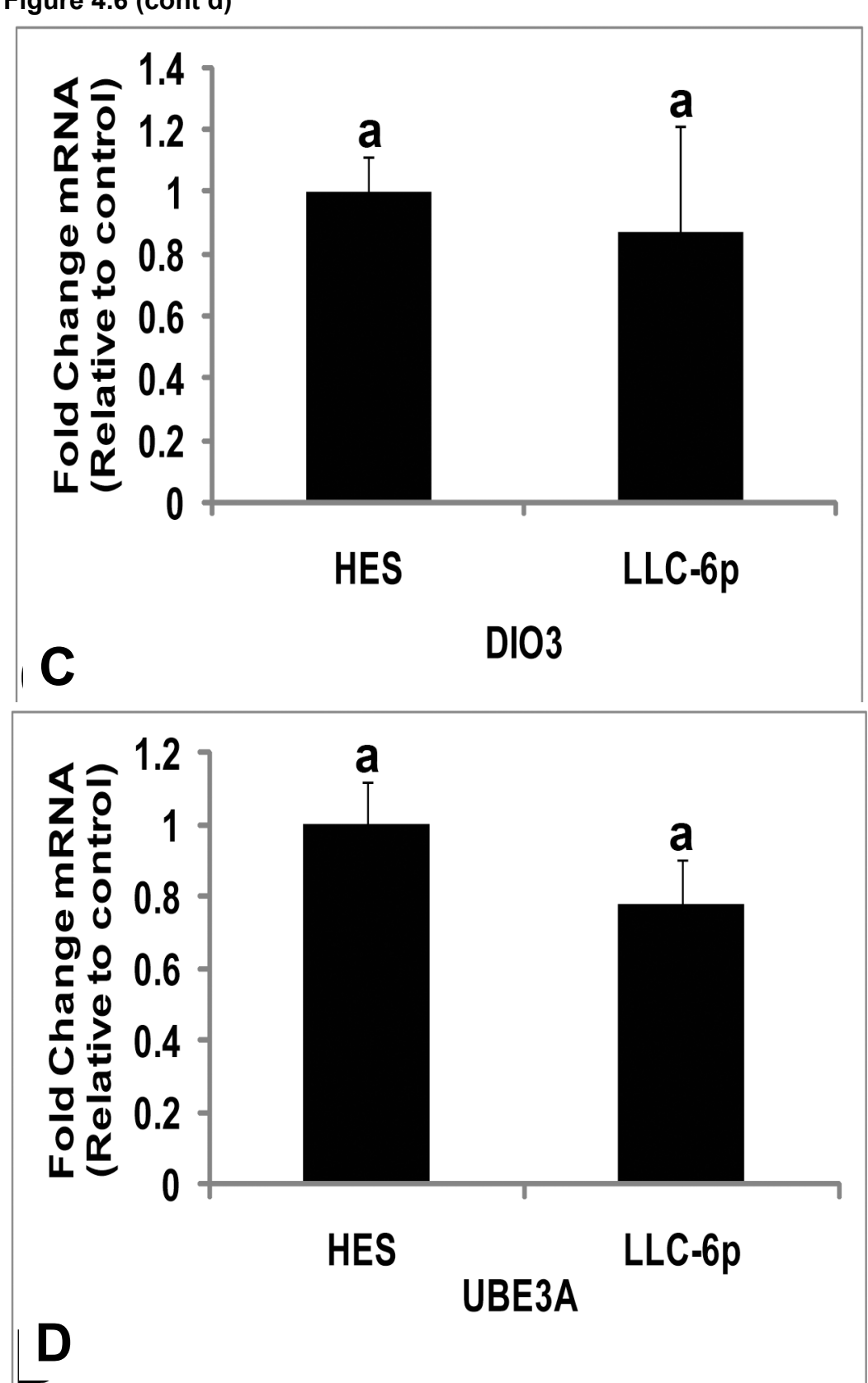


Figure 4.6 (cont'd)

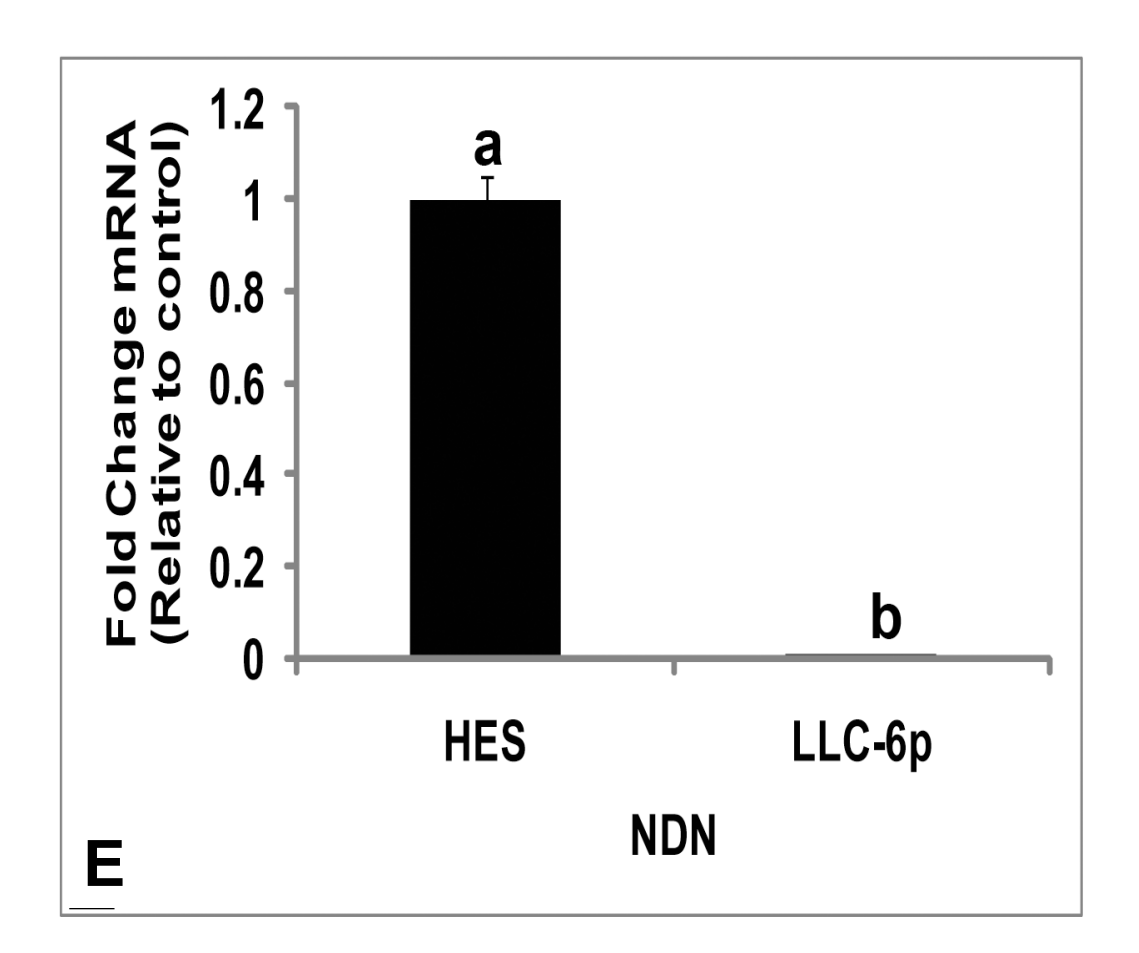


Figure 4.7 Quantification of mRNA abundance of the maternally expressed *H19* (A, B), *UBE3A* (K, L) and the paternally expressed *IGF2* (C, D), *DIO3* (M, N), DNA Methyltransferase1 (*DNMT1*) (E, F), DNA Methyltransferase3A (*DNMT3A*) (G, H) and DNA Methyltransferase3B (*DNMT3B*) (I, J) in HES H1 and LLC-6p cells from different passages by qRT-PCR. The qRT-PCR expression data was normalized towards beta actin housekeeping gene expression (O). For all qRT-PCR experiments three biological replicates (n=3) in three technical replicates were used in each run and a P<0.05 has been considered as statistical significant, unless stated otherwise. The bars represent standard error bars. All the letters above the error bars represent the difference between samples on the basis of standard error values (P<0.05).

Figure 4.7 (cont'd)

В

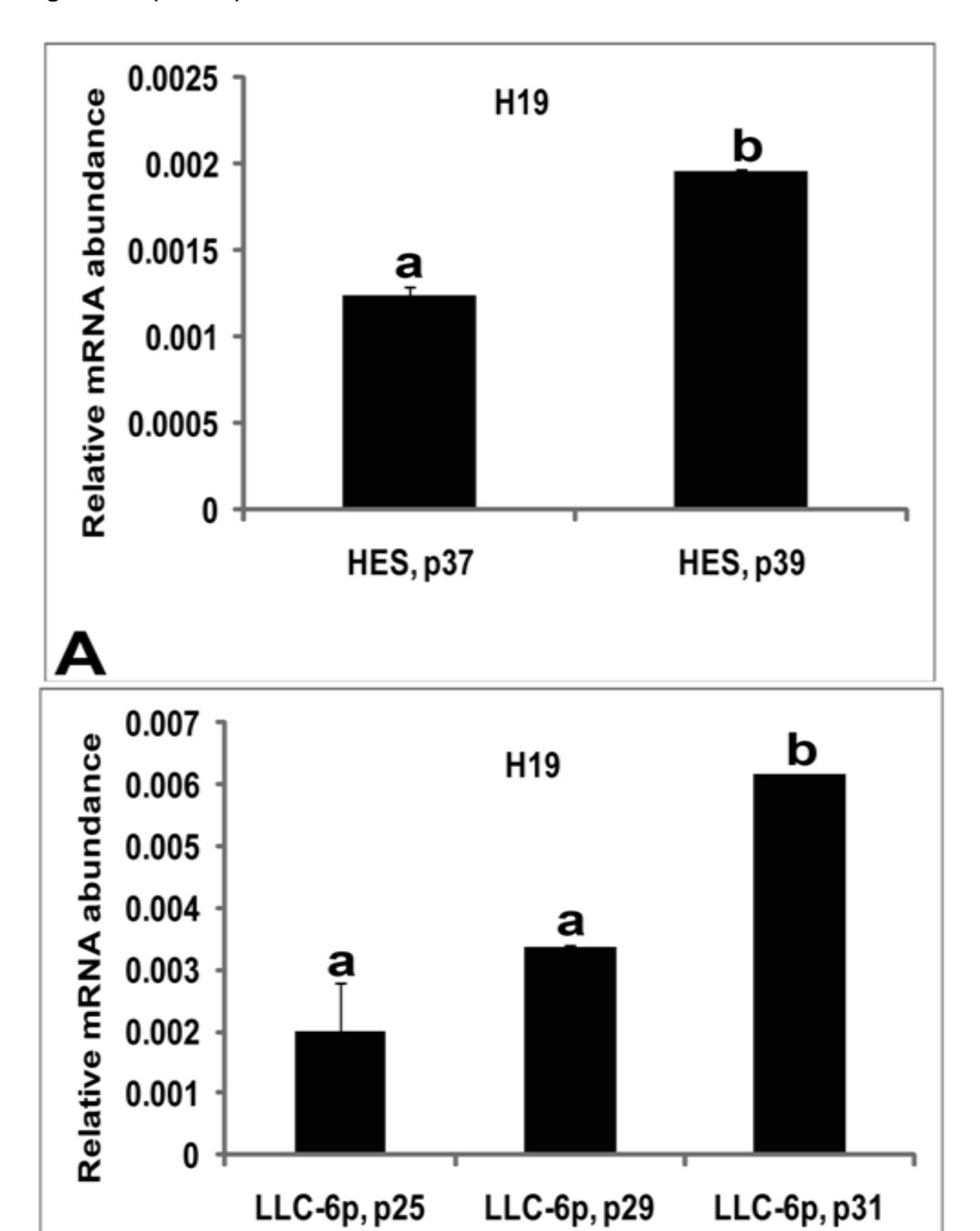
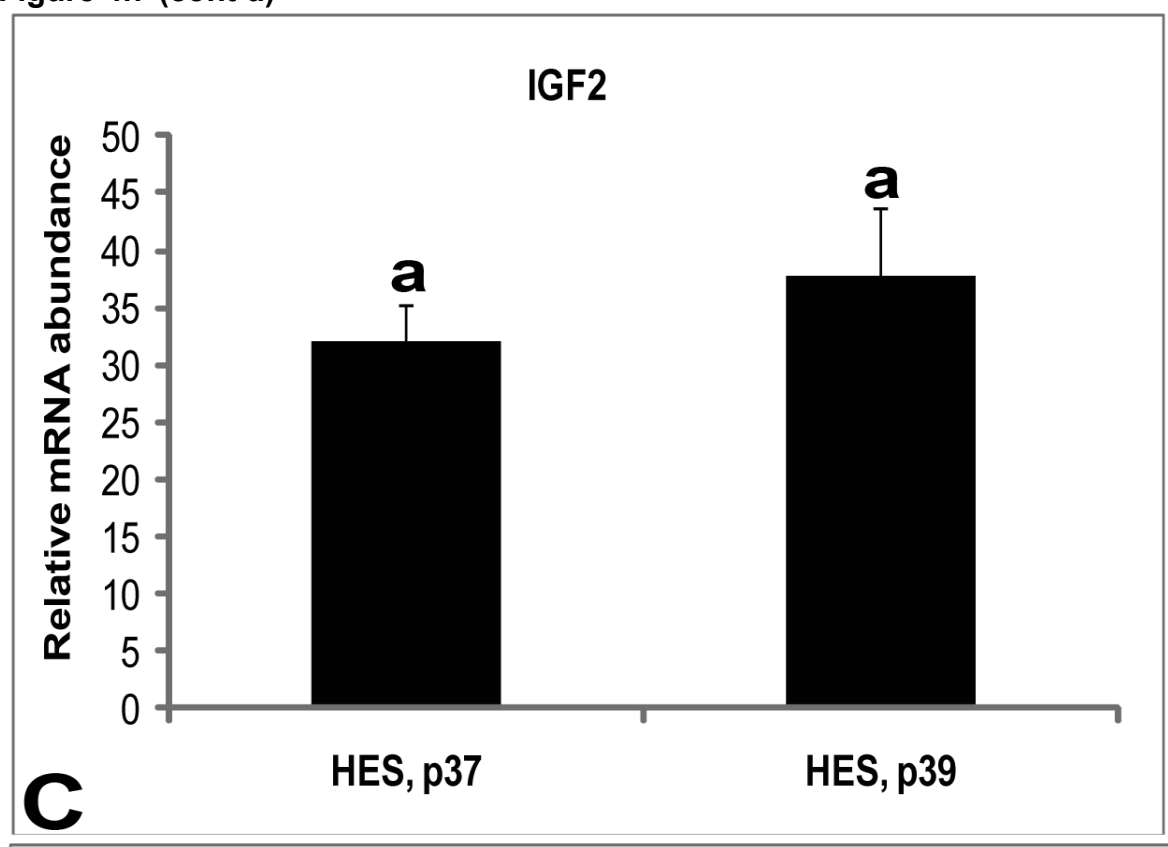


Figure 4.7 (cont'd)



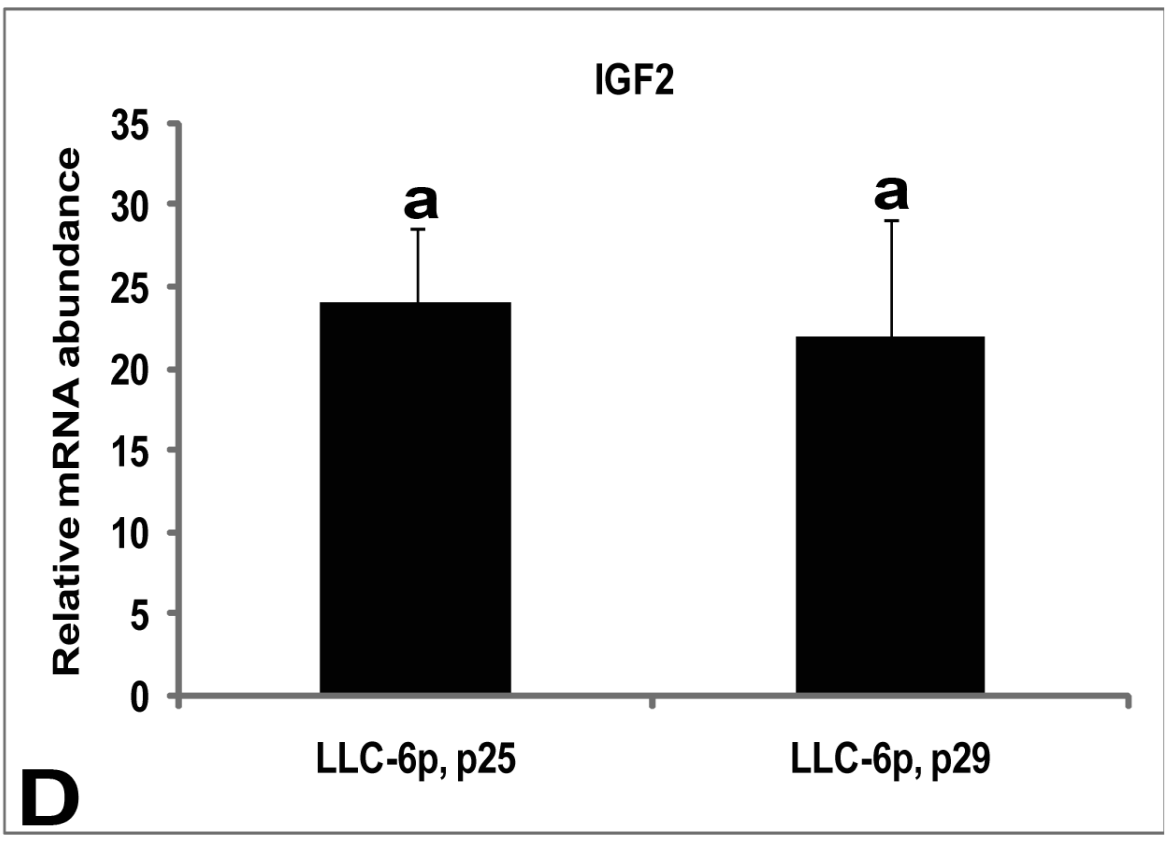
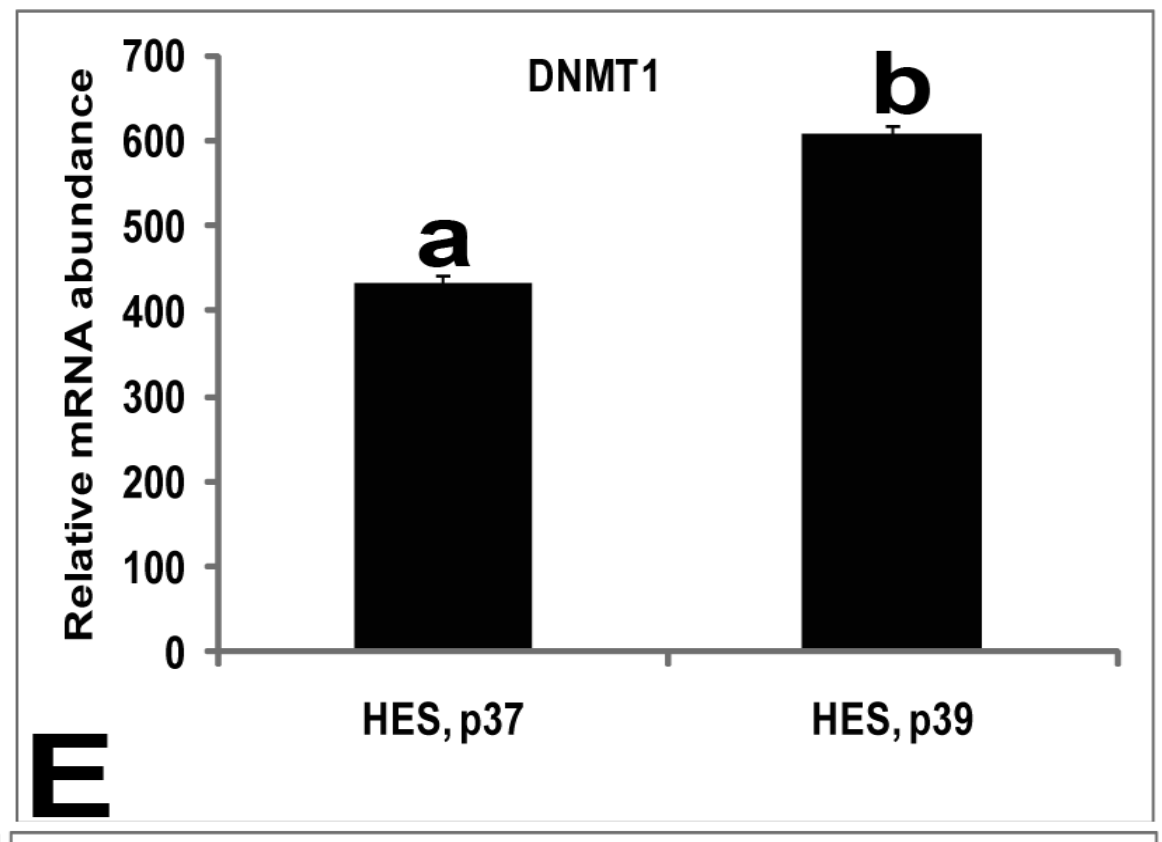


Figure 4.7 (cont'd)



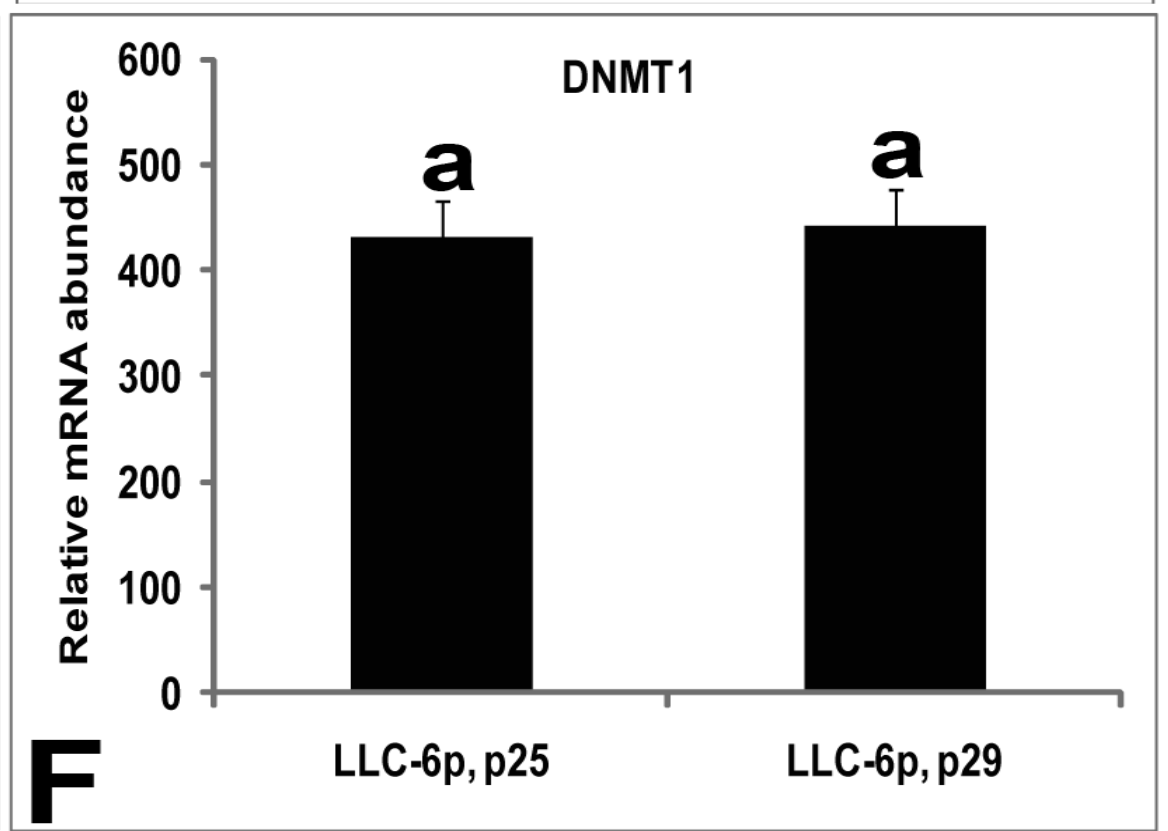


Figure 4.7 (cont'd)

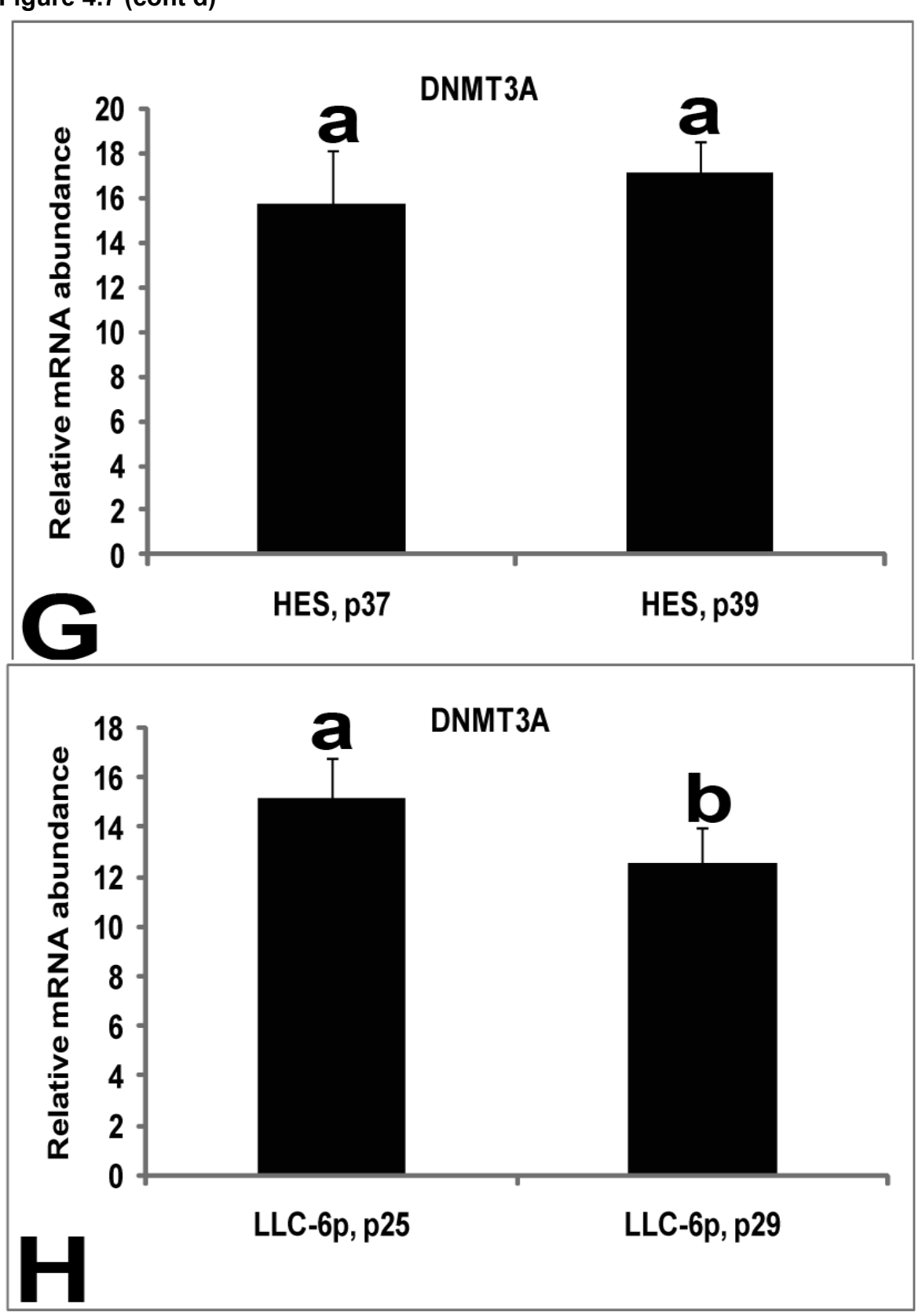
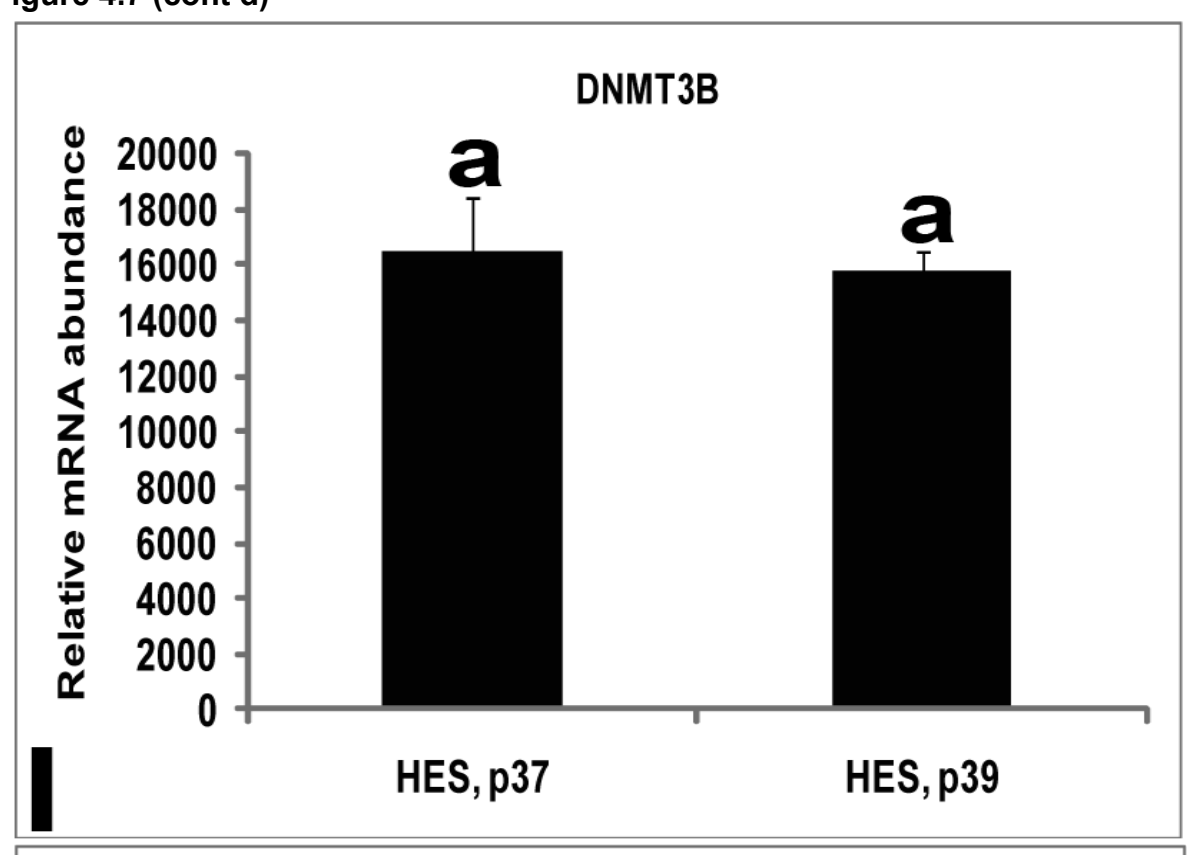


Figure 4.7 (cont'd)



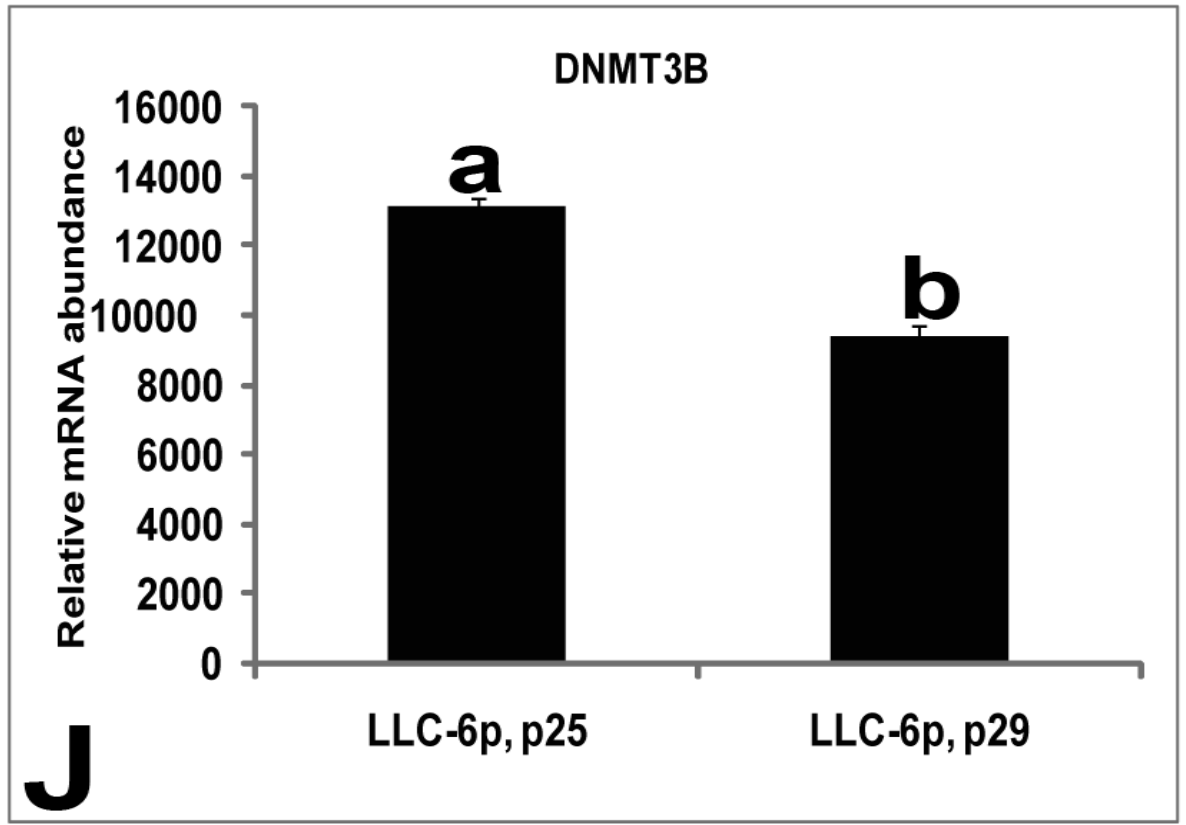
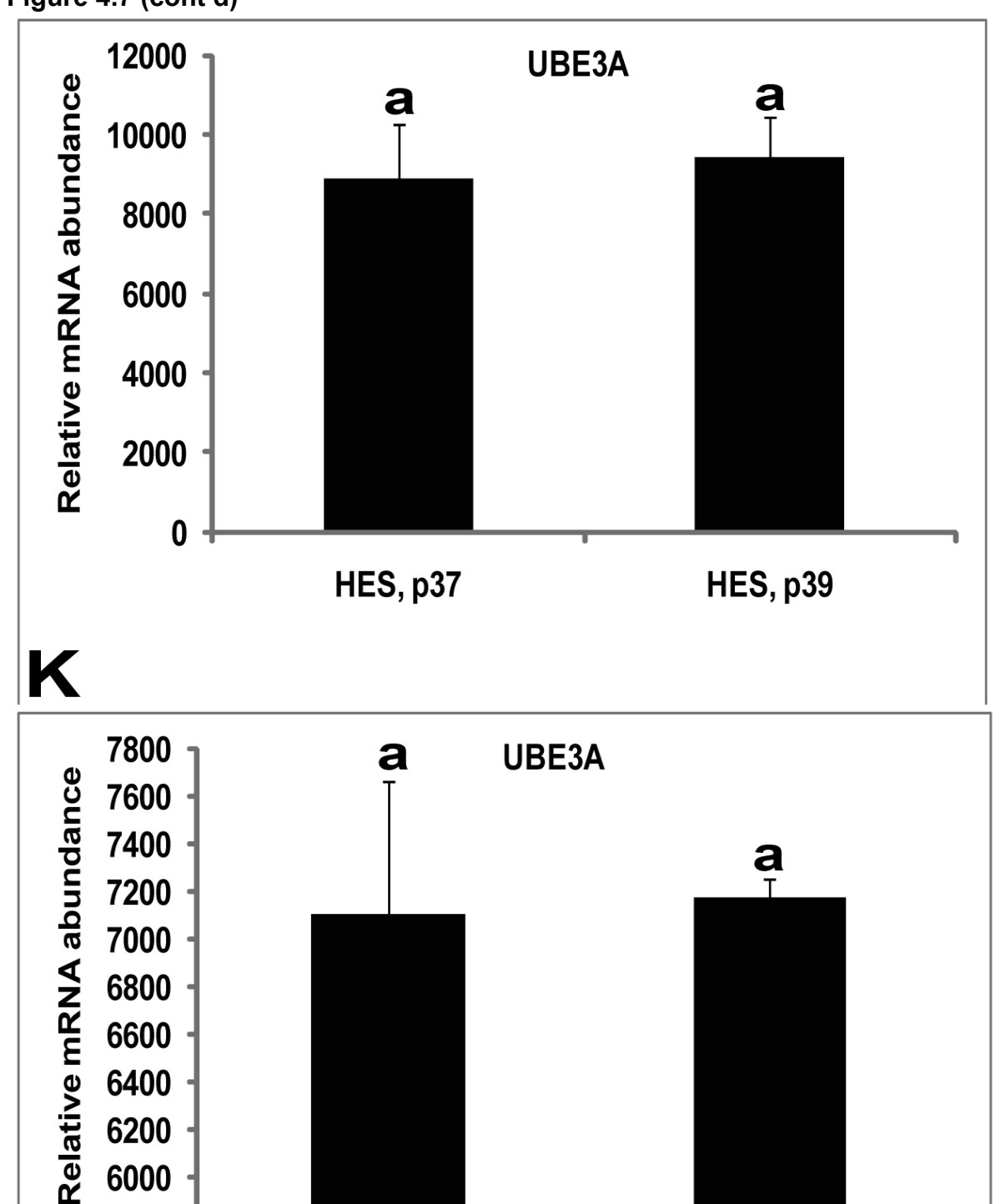


Figure 4.7 (cont'd)

6200

6000

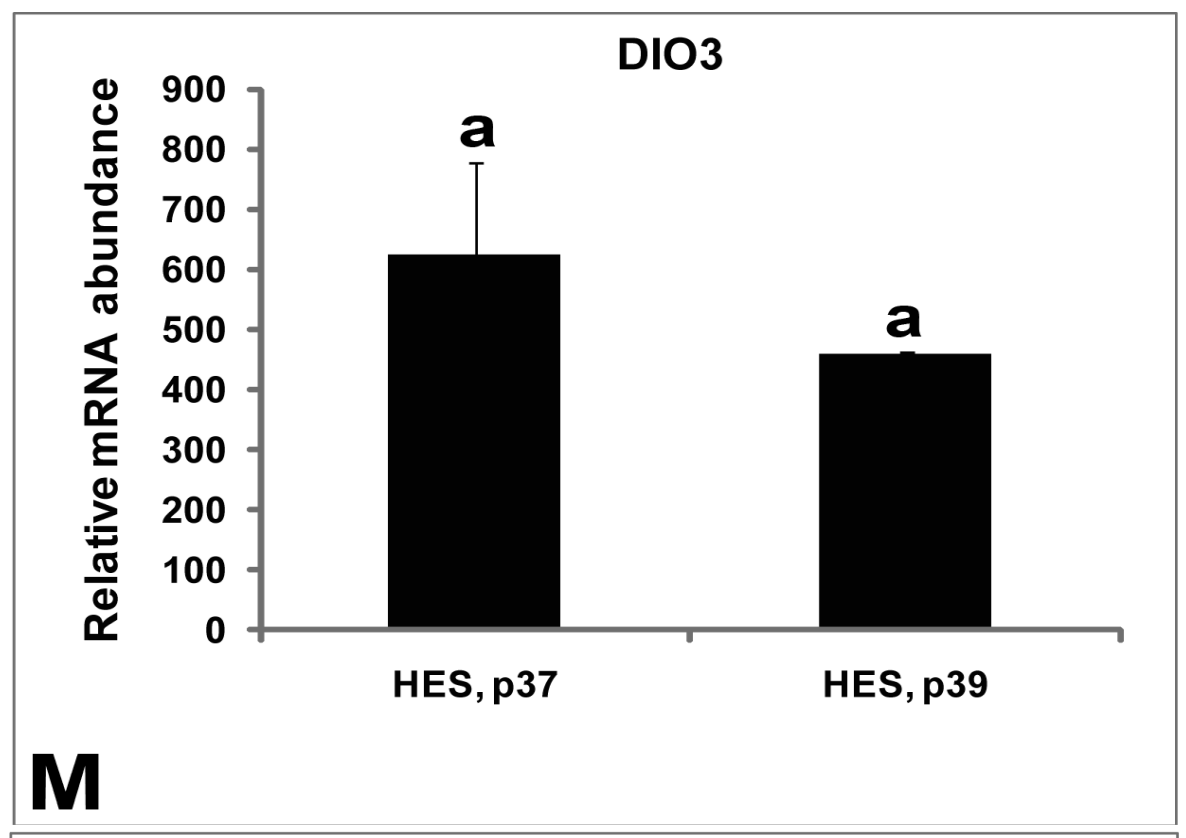
5800



LLC-6p, p29

LLC-6p, p25

Figure 4.7 (cont'd)



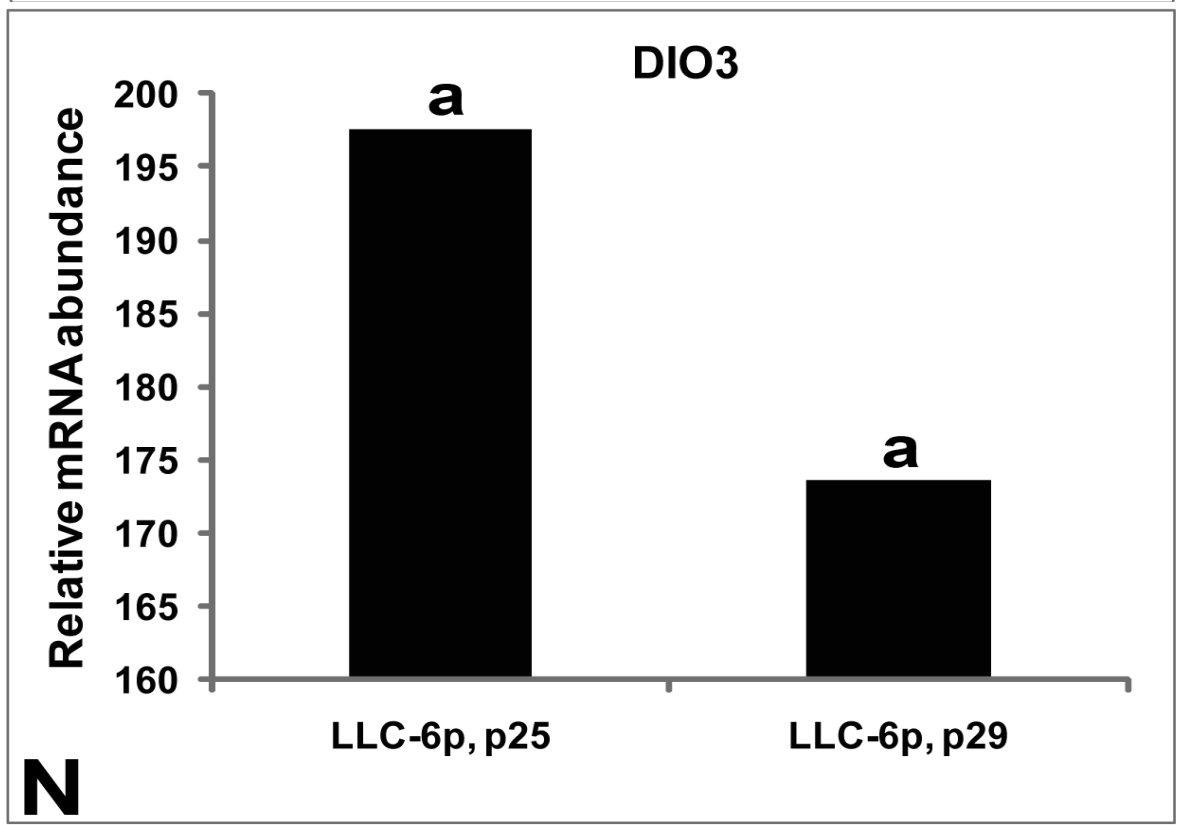


Figure 4.7 (cont'd)

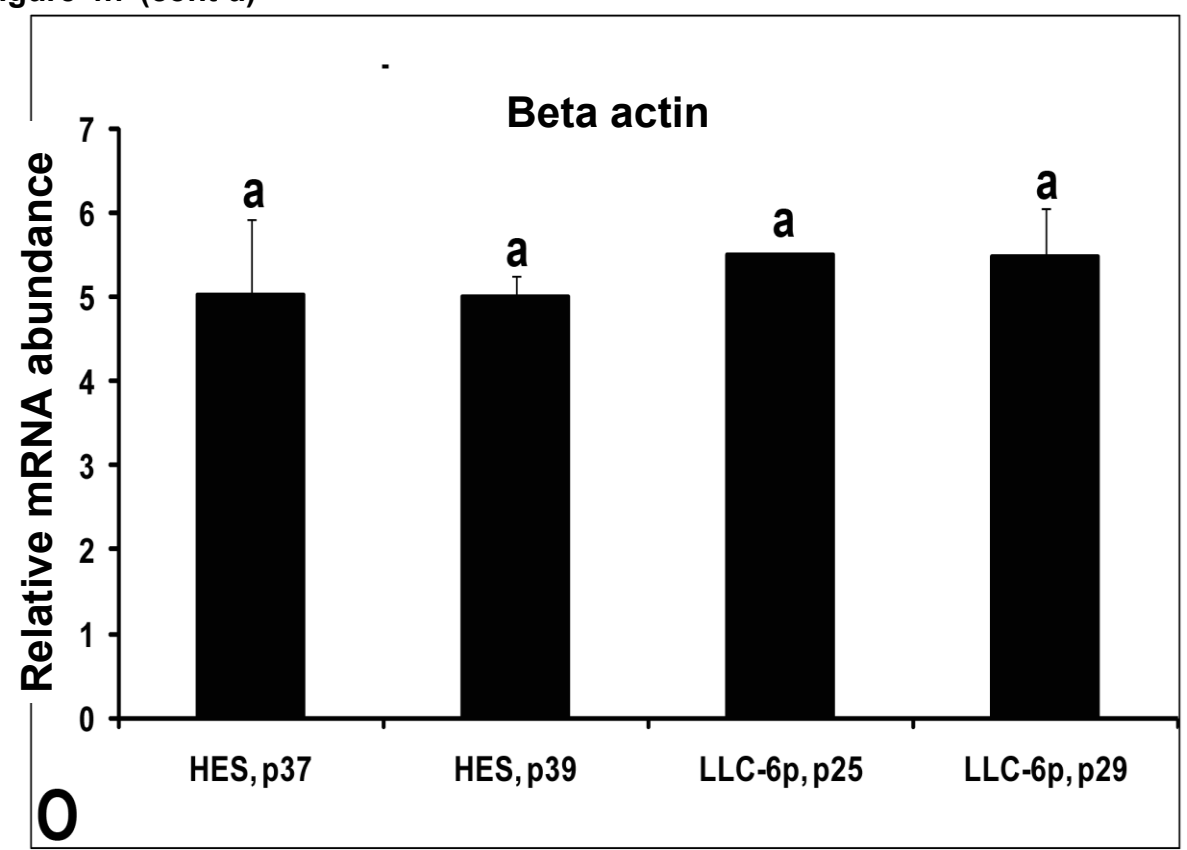


Figure 4.8 Schematic representation of H19shRNA and H19asRNA expressing plasmid (A) and Retroviral (B-E) vector constructs.

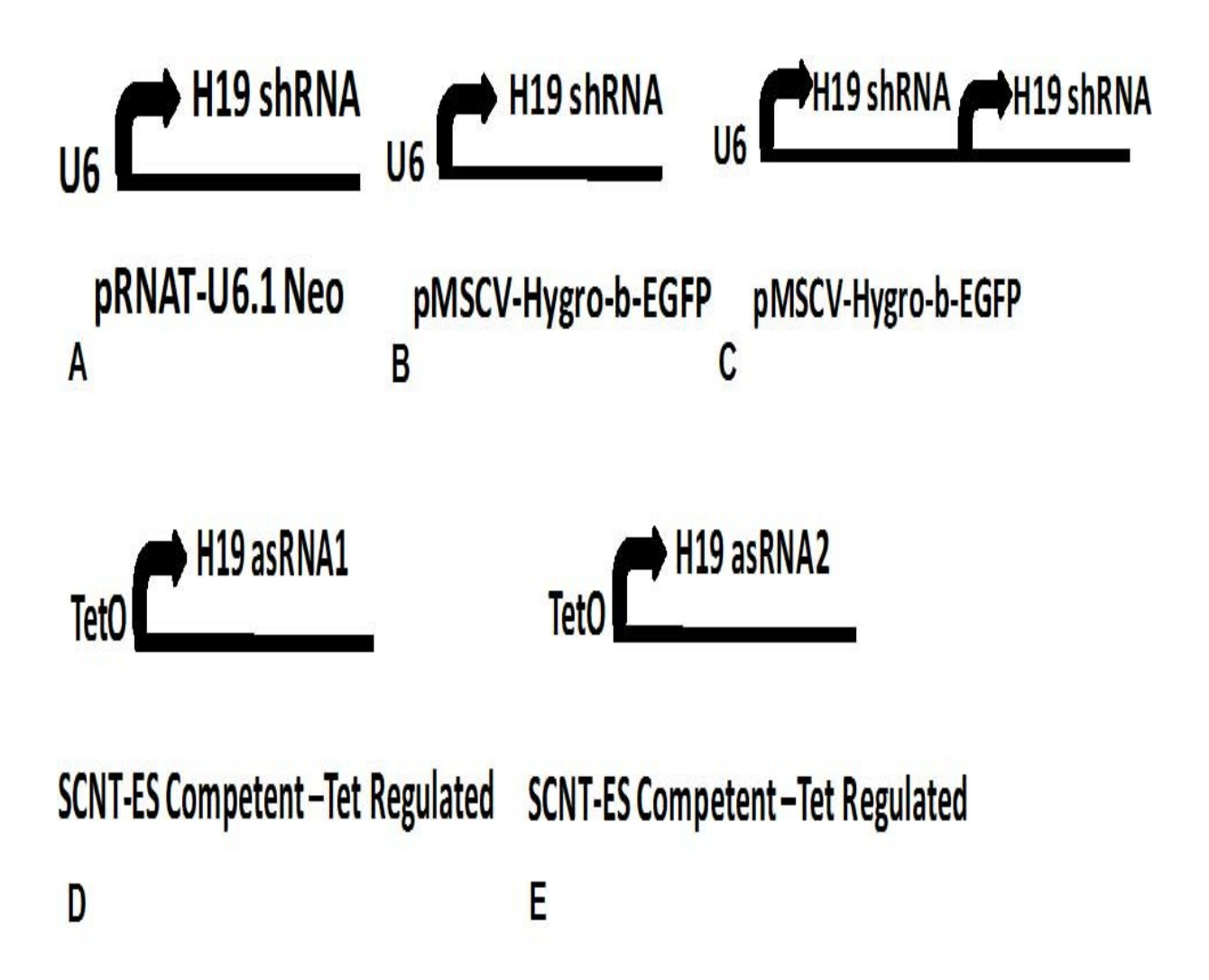


Figure 4.9 *H19*shRNA delivery in Hela cells. A, B, Hela cells transfected with *H19*shRNA pRNAT-U6.1, A-bright field, B-GFP Fluorescence. C-E, LLC-6p transfected with *H19*shRNA pRNAT-U6.1 vector, C-bright field, D-bright field fluorescence, E-EGFP fluorescence.

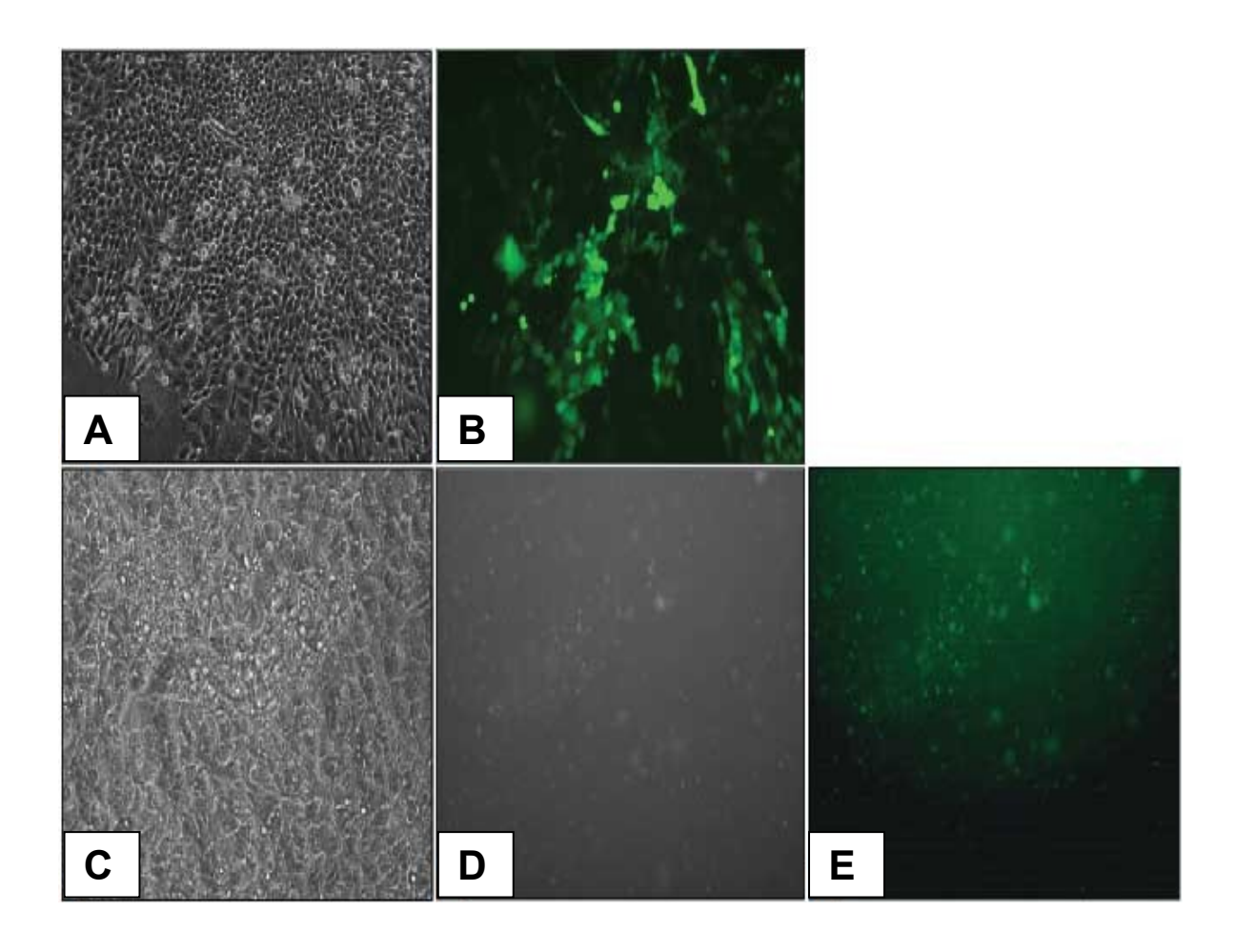


Figure 4.10 PCR-Agarose Gel Electrophoresis on *H19* expression in Hela cells transfected with two different *H19*shRNAs (human *H19*shRNA1 and human *H19*shRNA2) –Lanes 2-5, and Hela cells transfected with control unspecific shRNA (lanes 6-9). Lane1, 1kb marker, Lane 10, RT-; Two biological replicates for each treatment have been used for detection of *H19* expression.

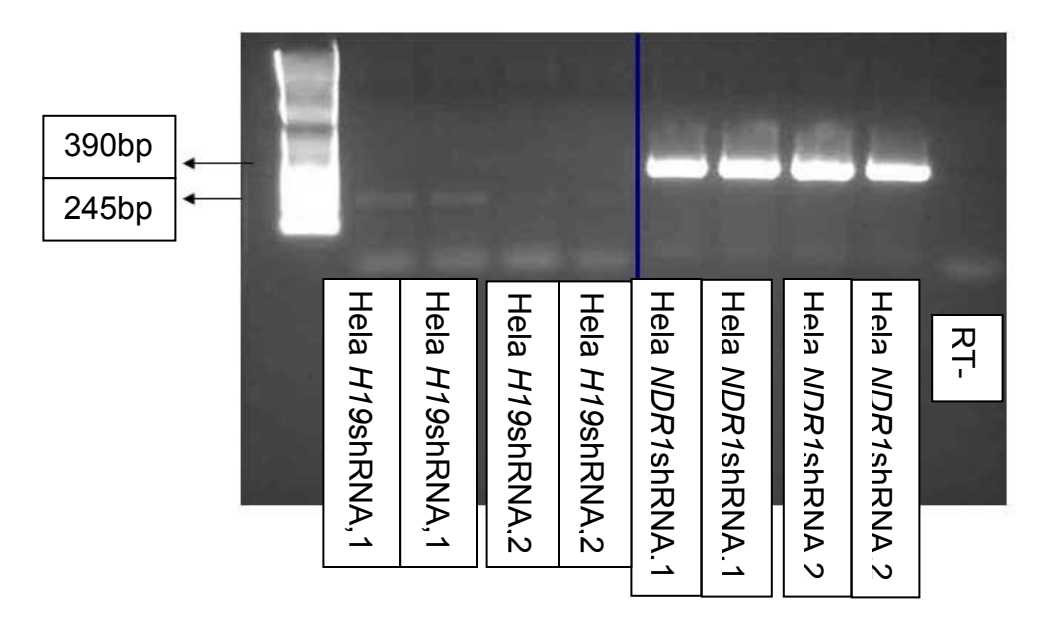


Table 4.1 Human qPCR Primers

Primer	Forward	Reverse	Gene bank
Name	0.00000		Accession
			number
H19	CTCGAGGCTCCGGCA	CCACCGCAATTCATTTAGT	NR_002196.
	TAG	AGCA	<u>1</u>
	CCTCACTCCCTTTTCC	TGTCCTCCCTCCTTTGG	NM 000612.
IGF2	ATCACT	TT	<u>4</u>
NDN	TGCACTGTAAATCCTG	GGAGGCAGATGAATGGTT	NM 002487.
	AATACTATAATGAC	TCTG	<u>2</u>
UBE3A	CACATTCCACGTTAGG	GGGTCTACACCAGATTGC	NM 130838.
	TGACAAA	TCTCTAAT	<u> 1</u>
DIO3	TCCCCCCACCTCTCTT	GCCCCAGGGAGAGAA	NM_001362.
	TCC	AAA	<u>3</u>
DNMT1	GGCCGCTGCACCGTG	CTGGCCGCGGAGTTGG	NM_001130
	GAGTATGG	TGGTC	<u>823.1</u>
DNMT3A	CAAGTCCCCATTGGG	GATCTCCAAGTCCCCATC	NM 175630.
	TAATAGC	CA	<u>1</u>
DNMT3B	CCAAGCGCCTCAAGA	TTGTTCTCGGCTCTGATCT	NM_175850.
	CAAA	TCA	<u> 1</u>
β- Actin	ATGATGGAGTTGAAG	GGCACTCTTCCAGCCTTC	NM_001101.
	GTAGTT TCGT	CT	<u>3</u>

REFERENCES

REFERENCES

- 1. Norris, H.J., H.J. Zirkin, and W.L. Benson, *Immature (malignant) teratoma of the ovary: a clinical and pathologic study of 58 cases.* Cancer, 1976. **37**(5): p. 2359-72.
- 2. O'Connor, D.M. and H.J. Norris, *The influence of grade on the outcome of stage I ovarian immature (malignant) teratomas and the reproducibility of grading.* Int J Gynecol Pathol, 1994. **13**(4): p. 283-9.
- 3. Steeper, T.A. and K. Mukai, *Solid ovarian teratomas: an immunocytochemical study of thirteen cases with clinicopathologic correlation.* Pathol Annu, 1984. **19 Pt 1**: p. 81-92.
- 4. Kono, T., et al., *Birth of parthenogenetic mice that can develop to adulthood.* Nature, 2004. **428**(6985): p. 860-864.
- 5. Sotomaru, Y., et al., *Unregulated Expression of the Imprinted Genes H19 and Igf2r in Mouse Uniparental Fetuses*
- J. Biol. Chem., 2002. **277**(14): p. 12474-12478.
- 6. Kono, T., *Genomic imprinting is a barrier to parthenogenesis in mammals.* Cytogenet Genome Res, 2006. **113**(1-4): p. 31-5.
- 7. Kono, T., et al., *Paternal dual barrier by Ifg2-H19 and Dlk1-Gtl2 to parthenogenesis in mice.* Ernst Schering Res Found Workshop, 2006(60): p. 23-33.
- 8. Hikichi, T., et al., Functional full-term placentas formed from parthenogenetic embryos using serial nuclear transfer. Development, 2010.
- 9. Varrault, A., et al., *Zac1 Regulates an Imprinted Gene Network Critically Involved in the Control of Embryonic Growth.* Developmental Cell, 2006. **11**(5): p. 711-722.

- 10. Fauque, P., et al., *Modulation of imprinted gene network in placenta results in normal development of in vitro manipulated mouse embryos.* Hum Mol Genet, 2010. **19**(9): p. 1779-90.
- 11. Sasaki, H., K. Ishihara, and R. Kato, *Mechanisms of Igf2/H19 imprinting: DNA methylation, chromatin and long-distance gene regulation.* J Biochem, 2000. **127**(5): p. 711-5.
- 12. Allen, N., et al., *A functional analysis of imprinting in parthenogenetic embryonic stem cells.* Development, 1994. **120**(6): p. 1473-1482.
- 13. Horii, T., et al., Loss of genomic imprinting in mouse parthenogenetic embryonic stem cells. Stem Cells, 2008. **26**(1): p. 79-88.
- 14. Jiang, H., et al., *Activation of paternally expressed imprinted genes in newly derived germline-competent mouse parthenogenetic embryonic stem cell lines.* Cell Res. **17**(9): p. 792-803.
- 15. Dean, W., et al., Altered imprinted gene methylation and expression in completely ES cell-derived mouse fetuses: association with aberrant phenotypes. Development, 1998. **125**(12): p. 2273-2282.
- Marina Bibikova, E.C., 1 Bonnie Wu,1 Lixin Zhou,1 Eliza Wickham Garcia,1 Ying Liu,2,12 Soojung Shin,2,12 Todd W. Plaia,3 Jonathan M. Auerbach,3 Dan E. Arking,4 Rodolfo Gonzalez,5 Jeremy Crook,6 Bruce Davidson,6 Thomas C. Schulz,7 Allan Robins,7 Aparna Khanna,8 Peter Sartipy,9 Johan Hyllner,9 Padmavathy Vanguri,10 Smita Savant-Bhonsale,10 Alan K. Smith,11 Aravinda Chakravarti,4 Anirban Maitra,4 Mahendra Rao,2,12 David L. Barker,1 Jeanne F. Loring,5 and Jian-Bing Fan1,13, Human embryonic stem cells have a unique epigenetic signature. Genome Research, 2006. 16(9): p. 1075–1083.
- 17. Fujimoto, A., et al., *Aberrant genomic imprinting in rhesus monkey embryonic stem cells*. Stem Cells, 2006. **24**(3): p. 595-603.
- 18. Jagerbauer, E.M., et al., *Parthenogenetic stem cells in postnatal mouse chimeras*. Development, 1992. **116**(1): p. 95-102.

- 19. Fundele, R.H., et al., *Temporal and spatial selection against parthenogenetic cells during development of fetal chimeras.* Development, 1990. **108**(1): p. 203-211.
- 20. Fundele, R., et al., *Systematic elimination of parthenogenetic cells in mouse chimeras*. Development, 1989. **106**(1): p. 29-35.
- 21. Onodera, Y., et al., *Differentiation diversity of mouse parthenogenetic embryonic stem cells in chimeric mice.* Theriogenology.
- 22. Yuasa, S., et al., *Transient inhibition of BMP signaling by Noggin induces cardiomyocyte differentiation of mouse embryonic stem cells.* Nat Biotechnol, 2005. **23**(5): p. 607-11.
- 23. Kim, K., et al., *Histocompatible embryonic stem cells by parthenogenesis*. Science, 2007. **315**(5811): p. 482-6.
- 24. Kim, K., et al., Recombination signatures distinguish embryonic stem cells derived by parthenogenesis and somatic cell nuclear transfer. Cell Stem Cell, 2007. **1**(3): p. 346-52.
- 25. Durbin, R.M., et al., *A map of human genome variation from population-scale sequencing.* Nature, 2010. **467**(7319): p. 1061-73.
- 26. Sanchez-Pernaute, R., et al., *Parthenogenetic dopamine neurons from primate embryonic stem cells restore function in experimental Parkinson's disease*. 2008. p. 2127-2139.
- 27. Sanchez-Pernaute, R., et al., Long-Term Survival of Dopamine Neurons Derived from Parthenogenetic Primate Embryonic Stem Cells (Cyno-1) After Transplantation. 2005. p. 914-922.
- 28. Ferrari, D., et al., *Transplanted dopamine neurons derived from primate ES cells preferentially innervate DARPP-32 striatal progenitors within the graft.* 2006. p. 1885-1896.

- 29. Tsang, W.P., et al., *Oncofetal H19-derived miR-675 regulates tumor suppressor RB in human colorectal cancer.* Carcinogenesis, 2010. **31**(3): p. 350-358.
- 30. Hikichi, T., et al., Functional full-term placentas formed from parthenogenetic embryos using serial nuclear transfer. Development, 2010. **137**(17): p. 2841-7.
- 31. Hikichi, T., et al., *Differentiation Potential of Parthenogenetic Embryonic Stem Cells Is Improved by Nuclear Transfer.* Stem Cells, 2007. **25**(1): p. 46-53.
- 32. Crespo, F.L., et al., *Mitochondrial reactive oxygen species mediate* cardiomyocyte formation from embryonic stem cells in high glucose. Stem Cells, 2010. **28**(7): p. 1132-42.
- 33. Zhu, D.Y., et al., *PPAR-beta facilitating maturation of hepatic-like tissue derived from mouse embryonic stem cells accompanied by mitochondriogenesis and membrane potential retention.* J Cell Biochem, 2010. **109**(3): p. 498-508.